SAMSO-TR-72-22
APL/JHU TG 1197
AUGUST 1972

Prediction Techniques for the Effect of the Ionosphere on Pseudo-Ranging from Synchronous Altitude Satellites

V. L. PISACANE
M. M. FEEN
M. STURMANIS
The Johns Hopkins University
Applied Physics Laboratory

USAF MIPR FY 7616-70-00325
Space and Missile Systems Organization
Los Angeles, California 90045

280

UNCLASSIFIED
Security Classification

DOCUMENT CONTROL DATA - R & D

(Security classification of title, body of abstract and indexing annotation must be entered when the overall report is classified)

1. ORIGINATING ACTIVITY (Corporate author) The Johns Hopkins University Applied Physics Laboratory Silver Spring, Maryland 20910	2a. REPORT SECURITY CLASSIFICATION UNCLASSIFIED 2b. GROUP

3. REPORT TITLE
Prediction Techniques for the Effect of the Ionosphere on Pseudo-Ranging from Synchronous Altitude Satellites

4. DESCRIPTIVE NOTES (Type of report and inclusive dates)
Final Report

5. AUTHOR(S) (First name, middle initial, last name)
Vincent L. Pisacane
Michael M. Feen
Martins Sturmanis

6. REPORT DATE	7a. TOTAL NO. OF PAGES	7b. NO. OF REFS
April 1972	274	29

8a. CONTRACT OR GRANT NO. MIPR FY 7616-70-00325 b. PROJECT NO. c. d.	9a. ORIGINATOR'S REPORT NUMBER(S) APL/JHU TG-1197 9b. OTHER REPORT NO(S) (Any other numbers that may be assigned this report) SAMSO TR-72-22

10. DISTRIBUTION STATEMENT

Approved for public release; distribution unlimited

11. SUPPLEMENTARY NOTES	12. SPONSORING MILITARY ACTIVITY
	Space and Missile Systems Organization (XRLO) AF Unit Post Office Los Angeles, California 90045

13. ABSTRACT
This study is directed toward defining and evaluating prediction techniques for the influence of the ionosphere on pseudo-range observations from a satellite navigation system. The synchronous satellite navigation system for which the study was intended is discussed and the limitations imposed on the correction technique by its characteristics and the proposed navigation equipment are described. The salient features of an operational correction system are defined. Alternatives for the content format and method of conveyance of the information from which the corrections are to be made are discussed. Three distinct algorithms that can be utilized to predict the ionospheric induced time (or range) error are defined and evaluated. One algorithm is capable of long-term predictions while the other two are dedicated to near real-time predictions. Data accumulated over several years at several locations form the basis of the evaluation of the three algorithms.

UNCLASSIFIED
Security Classification

14. KEY WORDS	LINK A		LINK B		LINK C	
	ROLE	WT	ROLE	WT	ROLE	WT
System 621B						
Navigation Satellites						
Ionosphere						
Model Ionospheres						
Ionospheric Group Time Delay Predictions						
Faraday Rotation Observation						

UNCLASSIFIED
Security Classification

SAMSO-TR-72-22
APL/JHU TG 1197
AUGUST 1972

Prediction Techniques for the Effect of the Ionosphere on Pseudo-Ranging from Synchronous Altitude Satellites

V. L. PISACANE
M. M. FEEN
M. STURMANIS
The Johns Hopkins University
Applied Physics Laboratory

Supported by USAF under
MIPR FY 7616-70-00325

THE JOHNS HOPKINS UNIVERSITY • APPLIED PHYSICS LABORATORY
8621 Georgia Avenue ∘ Silver Spring, Maryland ∘ 20910
Operating under Contract N00017-72-C-4401 with the Department of the Navy

FOREWORD

This report was prepared by the Johns Hopkins University Applied Physics Laboratory (JHU/APL) for the Air Force Space and Missile Systems Organization (SAMSO) under Contract Number MIPR FY 7616-70-00325.

SAMSO report number is TR-72-22.
JHU/APL report number is TG-1197.

The principal investigators involved in this work were V.L. Pisacane, M.M. Feen, and M. Sturmanis. L.A. Dreiling developed the software for the statistical evaluation of the study results and together with M.J. O'Neill prepared the graphs and tables presenting the results. I.J. Hamil prepared the manuscript. The Air Force Project Officers of the study were Capt. L.J. Plotkin and Maj. R.H. Jessen. Technical assistance to the Applied Physics Laboratory was provided by R.L. Dutcher of the Aerospace Corporation.

The Faraday rotation data used in the study were provided by Air Force Cambridge Research Laboratories, Stanford Electronics Laboratories, University of Hawaii, and the University of Illinois.

Publication of this report does not constitute Air Force approval of the report's findings or conclusions. It is published only for the exchange and stimulation of ideas.

Paul S. Deem

PAUL S. DEEM, Lt. Col., USAF

Chief, Orbital Systems Branch

ABSTRACT

This study is directed toward defining and evaluating prediction techniques for the influence of the ionosphere on pseudo-range observations from a satellite navigation system. The synchronous satellite navigation system for which the study was intended is discussed and the limitations imposed on the correction technique by its characteristics and the proposed navigation equipment are described. The salient features of an operational correction system are defined. Alternatives for the content, format and method of conveyance of the information from which the corrections are to be made are discussed. Three distinct algorithms that can be utilized to predict the ionospheric induced time (or range) error are defined and evaluated. One algorithm is capable of long-term predictions while the other two are dedicated to near real-time predictions. Data accumulated over several years at several locations form the basis of the evaluation of the three algorithms.

Preceding page blank

CONTENTS

Preceding page blank

CONTENTS (contd)

CONTENTS (contd)

ILLUSTRATIONS

Preceding page blank

TABLES

Preceding page blank

1. INTRODUCTION

Recent studies of navigation by means of satellites have emphasized the passive approach in which there is no active radio participation by the navigator. The Air Force currently has under development a synchronous satellite navigation system which would be capable of simultaneous and near instantaneous determination of a navigator's position and velocity [Miller, 1970]. To navigate, the user would utilize observations from four geographically distinct satellites whose locations must be made known to him. As described in more detail in Section 3.4, the observations on which the navigation is to be based are the times of reception of signals that are radiated from each satellite. Since nominal times of transmission are known, it is possible to compute the transit time of each signal and consequently an estimate of range. This technique is generally referred to as pseudo-ranging because of the uncertainty in the navigator's estimate of the times of transmission. Errors in making the measurements, predicting the ephemerides and in estimating the velocity of propagation of the satellite signal at each point along the ray path will contribute to reduced navigation accuracy.

For accurate navigation the influence of both the neutral and ionized atmosphere must be accounted for in the estimation of the propagation velocity of the pseudo-ranging signal. The neutral atmosphere of interest is known as the troposphere of which 97 percent is below an altitude of 24 km. The vertical transmission of a signal through this region would induce an apparent increase in the range measurement of from 2.3 to 2.6 meters if the vacuum speed of light were to be used [Hopfield, 1971]. This effect is independent of the frequency of the signal up to about 15 GHz. For other than vertical incidence the range error introduced by the troposphere could be appreciably larger. For example, at a zenith angle of 85 degrees a typical value would be in the neighborhood of 26 meters [Hopfield, 1972]. By utilizing surface weather data it is possible to estimate the tropospheric induced range error for vertical incidence with an rms error of only a few millimeters [Hopfield, 1971].

The electronic component of the upper atmosphere is known as the ionosphere. The velocity of propagation for electromagnetic radiation in this region is different than for propagation in a vacuum. For propagation at the

group velocity, the measured range would be increased if the vacuum velocity were used, which is similar to the influence of the troposphere. Both the group and phase velocities can be adequately approximated for propagation in an ionized medium as a function of the electron density and transmission frequency. For propagation at a frequency at VHF or higher the error in range can be approximated as being proportional to the electron density integrated along the propagation path divided by the square of the transmitter frequency [Budden, 1961]. During periods of maximum solar activity, the vertical range error that could be expected at low latitudes should be no larger than 150 meters at 1600 MHz [Burns and Fremouw, 1970]. The 1600 MHz is used as a reference because it is the carrier frequency of interest in the succeeding study. At incidence other than vertical, the ionospheric range error can be appreciably higher.

There are three alternatives by which the influence of the ionosphere on the navigation accuracy can be minimized. A first alternative is suggested from the fact that the magnitude of the apparent range (or timing) error in any observation is inversely proportional to the square of the transmitter frequency. In principle then, it is possible to select a frequency high enough that the errors will be reduced to acceptable levels. A second alternative would be to utilize the frequency dependence of the induced error by radiating two distinct coherent frequencies from each satellite. From the difference in the apparent range to each satellite, the major influence of the ionosphere could be eliminated. This is the technique used in the operational Navy Navigation Satellite System where only one satellite at a time is observed. Unfortunately, both of these alternatives have the same deficiency although not to the same degree, i.e., an increase in the complexity of the equipment for both the satellites and in particular the navigators. Since any navigation system must serve a broad class of users, the development of reliable and low cost navigation equipment is a most important consideration. If a single frequency, e.g., 8000 MHz, were to be used without any additional attempt to account for the ionosphere, the 150 meter vertical range error at 1600 MHz referred to above would be reduced to 6 meters. However, several studies, discussed by Keane [1969], have shown that operating at a frequency above L-band (1000 to 2000 MHz) is inadvisable principally because of power limitations and the need for high gain antennae. The utilization of two frequencies from each satellite would necessitate a receiver capable of

receiving eight distinct signals simultaneously. However, this approach becomes practical if a five-channel receiver is utilized in which one channel is time shared among the different satellites for the sole purpose of obtaining the ionospheric refraction correction. The third alternative is to correct for the ionospheric effect numerically, based on predictions of the characteristics of the ionosphere. For precision navigation a correction will have to be made by the navigator for the influence of the troposphere. At the same time it would also be possible to computationally make a correction for the influence of the ionosphere. Unfortunately, the electron density distribution of the ionosphere is characterized by great variations in magnitude which makes the task of effecting a correction more difficult than for the troposphere.

If it were possible to predict accurately the ionospheric characteristics and be able to convey this information to the navigator, the third alternative would be most attractive. It would result in less complex electronics for both the navigator and the satellites. Consequently, this paper is directed toward defining and then evaluating prediction algorithms which could be utilized to estimate the ionospheric correction for a high-altitude pseudo-ranging satellite navigation system.

2. SUMMARY OF RESULTS

The study undertook the development of computational techniques and algorithms that could be used in the world-wide prediction of the ionospheric induced time (or range) error that would be experienced by satellite pseudo-ranging signals. Several alternatives are discussed for the transfer of the ionospheric correction to the navigators. These include tables or charts based on long-term predictions and a series or matrix approach for the dissemination of the real-time corrections.

Three distinct algorithms that predict the characteristics of the ionosphere that are needed to estimate the time (or range) corrections have been defined and evaluated. The first, Algorithm I, provides long-term (on the order of 2 weeks to 5 months) predictions while the second (Algorithm II) and the third (Algorithm III) are capable of near real-time predictions.

The data base provided for the study consisted of Faraday rotation observations obtained at nine sites in North America, one site in Puerto Rico and one site in Hawaii. The time intervals over which the data was obtained were during 1965, a period of low solar activity, and during 1968 and 1969, a period of moderate to high solar activity. The ionospheric induced time delays inferred from this data were used in the real-time predictions and as the basis for the evaluation.

Summarizing the results of the study over the data base for both daytime and nighttime conditions indicates that Algorithm I is able to predict in an rms sense about 58 percent of the range error while Algorithms II and III are able to predict about 72 percent. The maximum error observed in each of the algorithms occurred for the same datum in which the vertical time delay induced by the ionosphere was 86 ns (at 1600 MHz). Algorithms I, II and III predicted values of 54, 50 and 43 ns too low. Because of the somewhat limited extent of the data base, restraint should be exercised in attempting to interpret these values in a global sense.

The above figures represent the prediction ability on an individual range measurement. However, the navigation error is sensitive only to the uncorrelated errors that appear in four near-simultaneous measurements made by a

navigator from geometrically distinct satellites. For this reason, the above figures would represent a worse case situation if, when utilized in an error analysis, they are assumed to be uncorrelated.

In general, the results indicate an ability to make predictions of the ionospheric range error which would be useful to some classes of navigators. Further improvements in the algorithms would expand the user base. However, at the present state-of-the-art, a dual frequency system would appear to be advisable for users requiring high precision navigation fixes at all times.

3. DESCRIPTION OF THE HIGH ALTITUDE NAVIGATION SATELLITE SYSTEM

3.1 INTRODUCTION

As discussed in Section 1, a navigation satellite system is being developed by the Air Force Space and Missile System Organization (SAMSO) to enable military users to obtain fast and precise position and velocity information. This high altitude satellite system is the candidate of the Air Force for the Defense Navigation Satellite System which is a proposed tri-service satellite network to meet the navigation requirements of a broad spectrum of military users. These users range from high performance strike and reconnaissance aircraft to ships, helicopters, vehicles and foot-soldiers. System accuracy is projected to be on the order of tens of feet in position and fractions of a foot per second in velocity. Details of the proposed Air Force system are given by Dept. of Air Force [1970] and Miller [1970]. These unclassified documents are by nature abbreviated and do not totally characterize the Air Force system. In any event, the design of such a complex system is naturally in a continual state of evolution. Consequently, it is impossible at this time to present a definitive description of what the final design may be. However, for completeness and to facilitate discussion and design of the ionospheric correction system, a navigation system is postulated here which is a composite of the information given in the above referenced documents. It should be carefully noted that the postulated navigation system should not be interpreted as the final Air Force candidate. When the design becomes frozen, any differences with the postulated design should be studied with respect to their influence on the ionospheric correction system.

3.2 SATELLITE CONSTELLATIONS

The satellite network is to consist of constellations of spacecraft in which each constellation would appear to an observer on the ground to be either in a rotating "X" configuration of five spacecraft or a rotating "Y" configuration of four [Miller, 1970]. Both of these geometrical constellations can be achieved with a center satellite in a synchronous, near-circular and equatorial orbit and peripheral satellites in inclined and elliptic orbits with the same mean altitude as the central spacecraft. In each case,

the three or four peripheral spacecraft would describe, relative to an observer on the earth, essentially a circle about the centrally located satellite. A single constellation would provide coverage to a region just under one-third of the earth's surface. The coverage contours and satellite ground track for a typical "X" configuration are given in Figs. 3.1 and 3.2 which are taken from Woodford et al. [1969]. Three similar constellations of the "X" configuration properly spaced in longitude would provide continuous coverage anywhere north of 45 degrees south latitude.

3.3 NAVIGATION SYSTEM SUPPORT

The satellite navigation system, apart from the user equipment and spacecraft, is to consist of from three to six ground stations constrained to possessions of the United States, computational centers and possibly area calibration stations. The ground stations are necessary to obtain tracking data so that the ephemeris of each satellite, which is required by the navigator, can be extrapolated into the future with sufficient accuracy. For orbit determination, two-way (closed loop) range and range-rate data is to be obtained at each tracking site for all spacecraft above the horizon. With a knowledge of the positions of the tracking stations, a model of the geopotential and models for effects such as the luni-solar gravitational effect and solar radiation forces, the spacecraft ephemerides can be extrapolated in time. The area calibration stations are to consist of navigators at known locations. From their measurements it would be possible to estimate systematic errors in their vicinity. This information would then be made available for use by nearby navigators.

3.4 NAVIGATION OBSERVATIONS

To eliminate active radio participation of the navigator, each satellite is to transmit an identifiable range code modulation on an L-band carrier (approximately 1600 MHz). These transmissions will also contain the ephemerides of the spacecraft and any additional information that may be needed by the navigator for calibration or effecting corrections to the observations. The measurement that is made is the interval between the time of reception of the range code signal and the nominal time of transmission as given by the navigator's clock. The estimate of the time of reception is to be accomplished by means of a correlation detector.

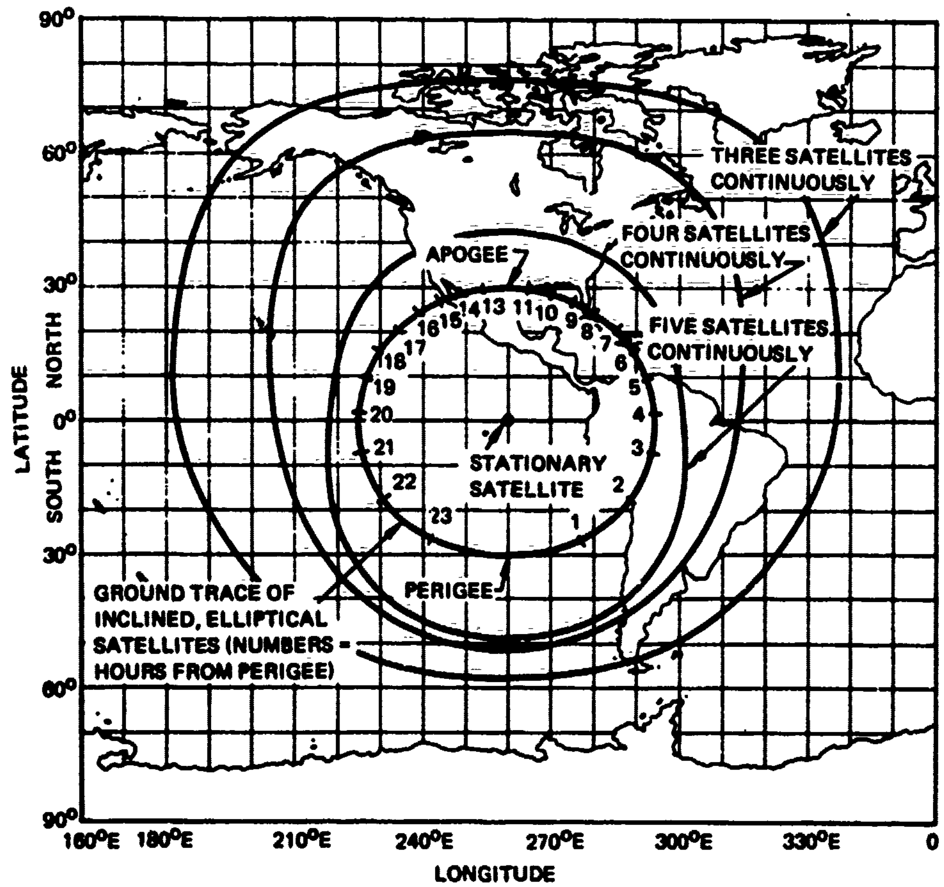

Fig. 3.1 COVERAGE CONTOURS AND SATELLITE GROUND TRACK FOR THE "X" TYPE CONFIGURATION [WOODFORD et al., 1969]

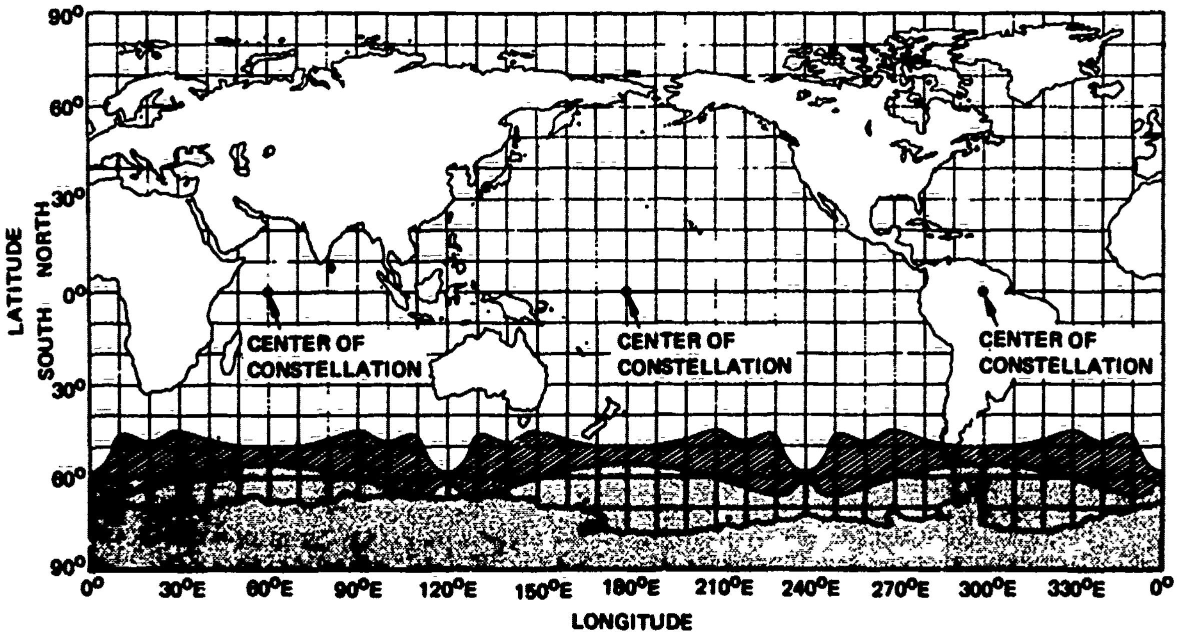

CODE	SATELLITES CONTINUOUSLY VISIBLE	NAVIGATION PROVIDED
(hatched)	3	2-DIMENSIONS
(white)	4 TO 7	3-DIMENSIONS
(black)	INTERMITTENT COVERAGE	

COVERAGE FOR i = 30 DEGREES, e = 0.30
MINIMUM ELEVATION ANGLE = 5 DEGREES
THREE CONSTELLATIONS OF FIVE SATELLITES EACH

Fig. 3.2 COVERAGE FOR FIFTEEN DEPLOYED SYNCHRONOUS SATELLITES [WOODFORD et al., 1969]

The time interval measurement can be thought of as being partitioned into three components

$$T_j = \tau_{\rho j} + \tau_d + \tau_{ej} \quad , \quad j = 1 \text{ to } 4 \qquad (3.1)$$

where

$\tau_{\rho j} \equiv \rho_j/c$, is the vacuum propagation time from the predicted position of the j^{th} spacecraft to the navigator

$\rho_j \equiv$ range from the predicted position of the j^{th} spacecraft to the navigator

$c \equiv$ speed of light in a vacuum

$\tau_d \equiv$ navigator's clock offset

$\tau_{ej} \equiv$ time delay arising from various error sources

$T_j \equiv$ the measurements, which are the time intervals from the navigator's clock epoch

The navigator's clock offset, τ_d , is the difference between the epochs of his clock and the clocks of the spacecraft if the latter are assumed to be synchronized among themselves. The error sources, τ_e , are several in number, such as: lack of synchronization among the satellite clocks, time delays in the transmitters and receiver, errors in the predicted ephemerides and the ionospheric and tropospheric effects on the propagation velocity. If the error sources are small enough so that they can be ignored, $\tau_{ej} \approx 0$, and the offset of the navigator's clock is unknown, then four observations are necessary to utilize Eq. (3.1) to effect a position estimation. With the four observations, it is possible to eliminate τ_d and obtain three equations in terms of either range differences or time differences. Consequently, the satellite navigation system is conceptually similar to ordinary hyperbolic radio navigation in which the role of the fixed network of transmitting stations is replaced by the satellite constellation. Through normal doppler extraction techniques, it is also possible to measure the range-rate between the user and each spacecraft from which an estimate of the velocity of the navigator can be inferred [Miller, 1970].

3.5 PRINCIPAL OBSERVATIONAL ERRORS

Two of the major sources of navigation error are the inaccuracies in the predicted ephemerides and the influence of the medium on the propagation velocity. The accuracy to which the satellite ephemerides must be estimated is within the state-of-the-art [Melton, 1971]. The influences of the troposphere and the ionosphere have been discussed in detail in Section 1. However, it should be noted that because of the hyperbolic nature of the navigation solution, all of the errors introduced by the troposphere and ionosphere do not propagate into the solution for the navigator's position. This point is discussed in more detail in Section 5.2.5.

4. IONOSPHERIC EFFECTS

4.1 EFFECT OF THE IONOSPHERE ON SATELLITE RANGING

In the proposed high-altitude navigation system, the satellite-to-navigator geometric range is to be inferred from a measurement of the satellite-to-navigator propagation time of an identifiable range code modulation (hereafter, ranging signal) on an L-band carrier (at 1600 MHz).

At VHF and above, the time of propagation of the satellite ranging signal between satellite and navigator, assuming group velocity, is shown in Appendix G to be given to first order (in rationalized mks units) as

$$\tau(G,t) = \frac{\rho(t)}{c} + \frac{1.34 \times 10^{-7}}{f^2} \int_{G(t)} N(\vec{r},t)\, ds \qquad (4.1)$$

where

$\tau(G,t)$ = time of propagation of the ranging signal between satellite and navigator along the geometric path $G(t)$

$\rho(t)$ = satellite-navigator geometric range at time t

c = speed of light

f = carrier frequency, Hz

$G(t)$ = geometric range path at time t

$N(\vec{r},t)$ = electron density at $\vec{r}$ and t

$\vec{r}$ = position vector to a point on $G(t)$ from a geocentric coordinate system

ds = differential element of arc along $G(t)$

As shown by Eq. (4.1), the effect of the ionosphere on the ranging signal is to increase the propagation time of the signal over its free space value, $\rho(t)/c$. If this ionospheric induced propagation time error were neglected, the effect would be to increase the apparent range between the satellite and navigator. The ionospheric contribution to the propagation time is proportional to the integrated electron content along the range. Thus from a knowledge of the electron density distribution, $N(\vec{r},t)$ as a function of

space and time, for given positions of the spacecraft and navigator, it is possible to determine the ionospheric group time delay.

4.2 FARADAY ROTATION OF SATELLITE SIGNALS

The quantity on which the evaluation of the algorithms was to be based in the present study is the equivalent vertical ionospheric group time delay obtained from synchronous altitude satellites. At the present time a large enough body of direct measurements of the time delay does not exist. However, there does exist a significant amount of Faraday rotation data from both low and high altitude satellites. From Faraday rotation data it is possible to infer equivalent vertical integrated electron content (hereafter EVIC) data. In this study, Faraday rotation data were used to infer the EVIC from which equivalent vertical group time delay values were obtained.

The term Faraday rotation refers to the phenomenon of rotation of the plane of polarization of a linearly polarized electromagnetic wave as a result of the birefringent property of the ionosphere in the presence of the earth's magnetic field.

At VHF and above, the amount of Faraday rotation occurring between the satellite and observer is given to first order (in rationalized mks units) as

$$\Omega(G,t) = \frac{2.97 \times 10^{-2}}{f^2} \int_{G(t)} N(\vec{r},t)H(\vec{r})\cos\theta(G,\vec{r})\sec\chi(G,\vec{r})\,dh \text{ (radians)} \tag{4.2}$$

where

$\Omega(G,t)$ = Faraday rotation along $G(t)$ at time t

$H(\vec{r})$ = magnetic field strength at $\vec{r}$

$\theta(G,\vec{r})$ = angle between $G(t)$ and the magnetic field vector $(\vec{H}(\vec{r}))$ at $\vec{r}$

$\chi(G,\vec{r})$ = vertical angle of $G(t)$ at $\vec{r}$

dh = differential element of altitude

In order to obtain EVIC data from the Faraday rotation measurements, Eq. 4.2 is rewritten as

$$\Omega(G,t) = K\,M(G,t) \int_{G(t)} N(\vec{r},t)dh \tag{4.3}$$

where

$$M(G,t) \equiv \frac{\int_{G(t)} N(\vec{r},t)\,H(\vec{r})\cos\theta(G,\vec{r})\sec\chi(G,\vec{r})dh}{\int_{G(t)} N(\vec{r},t)dh}$$

and

$$K = \frac{2.97 \times 10^{-2}}{f^2}$$

then

$$\frac{\Omega(G,t)}{K\,M(G,t)} = \int_{G(t)} N(\vec{r},t)dh \equiv I_v(G,t) \tag{4.4}$$

Note that, strictly speaking, $I_v(G,t)$ is the integral of the vertical component of $N(\vec{r},t)$ integrated along the geometric path.

The equivalent ionospheric vertical group time delay, $\tau_v(G,t)$, is then obtained from $I_v(G,t)$ using Eq. (4.1) as

$$\tau_v(G,t) = \frac{1.34 \times 10^{-7}}{f^2} I_v(G,t) = 4.51 \times 10^{-6} \frac{\Omega(G,t)}{M(G,t)} \tag{4.5}$$

The value of $M(G,t)$ is a function of the "shape" of the electron density distribution and thus will exhibit both diurnal and geographical variations. In order to simplify calculations, it is common practice in many quarters to approximate $M(G,t)$ by a constant value obtained by evaluating $H(\vec{r})\cos\theta(G,\vec{r})\sec\chi(G,\vec{r})$ at an altitude of 300 to 450 km along the geometric path [Yeh and Gonzales, 1960]. The approximate value of $M(G,t)$ obtained in this manner, using a constant altitude for all locations without resorting to the explicit introduction of an electron density distribution, becomes independent of time but will vary geographically.

Using either $M(G,t)$ or its approximation which is denoted by M_h, where h represents the height used, "experimental" values of EVIC can be obtained from Eq. (4.4). The use of the approximation ignores the diurnal variations of $M(G,t)$ and the EVIC obtained using M_h can differ by as much as a factor of two from that using $M(G,t)$. Figs. 4.1a and 4.1b show comparison of M_{350} and $M(G,t)$ for the Faraday rotation observation stations at Arecibo and Sagamore

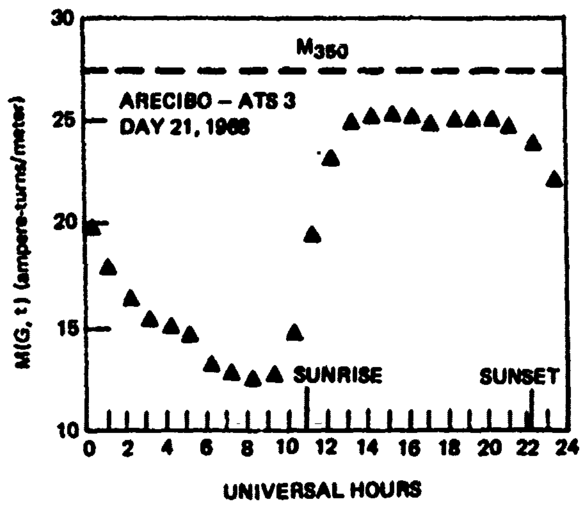

Fig. 4.1a DIURNAL VARIATION OF M (G,t)

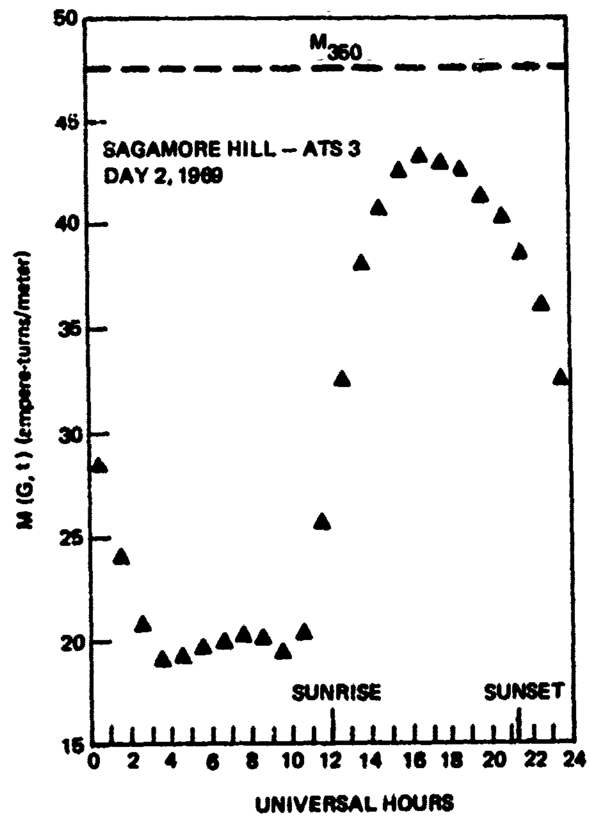

Fig. 4.1b DIURNAL VARIATION OF M (G,t)

Hill. These curves are representative of the type of differences to be found at other locations. Figs. 4.2a and 4.2b show the comparison of the $\tau_V(G,t)$ inferred using the M_{350} and $M(G,t)$ of Figs. 4.1a and 4.1b respectively. Because of the strong diurnal variations of $M(G,t)$ as well as the magnitude of the differences of the means, it was concluded that this approximation to the M-factor was not adequate for the purposes of this study. Consequently, the value of $M(G,t)$ was computed for each data point at the time of the data point.

It is important to note that because of the $|\vec{r}|^{-3}$ fall-off of the geomagnetic field, the Faraday rotation is sensitive to the electron density in the lower ionosphere and relatively insensitive to the electron density in the higher ionosphere. In order to infer EVIC data from the Faraday data, as discussed above, a normalized profile <u>must</u> be introduced. Electron density distributions which are similar in the lower ionosphere and depart widely in the upper ionosphere would yield the same measure of Faraday rotation but different EVIC data. A measure of the significance of this is given by the fact that totally ignoring the upper ionosphere in the determination of EVIC data from Faraday rotation data can result in errors of the order of 20 percent.

The Faraday rotation data used in this study were measurements obtained at VHF (nominally 137 MHz) from geostationary satellites. These data were scaled to the frequency of interest (1600 MHz) by the $1/f^2$ frequency dependence shown in Eq. (4.2). However, it should be noted that due to the possible existence of sharp gradients of electron density in the ionosphere, this scaling procedure could result in differences in the inferred EVIC from that actually observed at L-band [<u>Guier</u>, 1963] and [<u>Kelso</u>, 1964]. This concern is discussed in Section 10.7 as an area for further study.

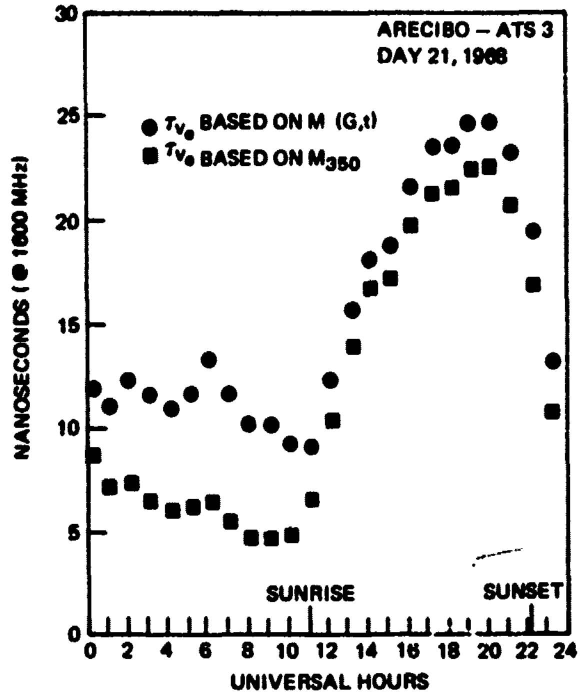

Fig. 4.2a DIURNAL VARIATION OF VERTICAL TIME DELAY BASED ON M (G,t) AND M_{350}

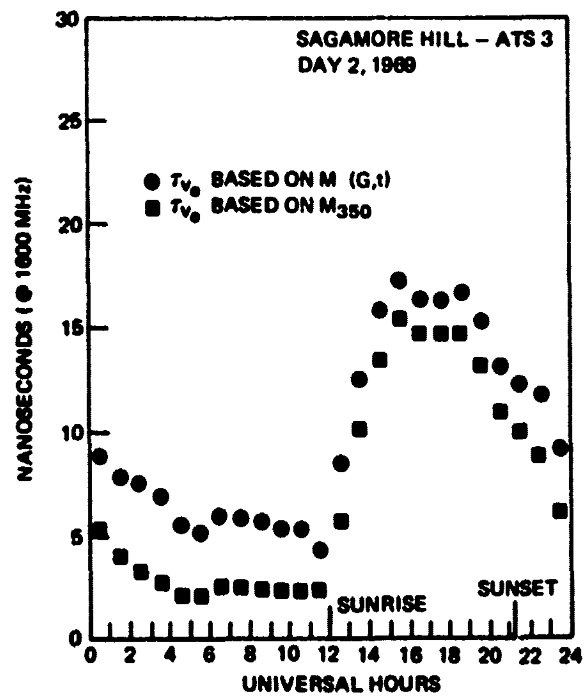

Fig. 4.2b DIURNAL VARIATION OF VERTICAL TIME DELAY BASED ON M (G,t) AND M_{350}

5. PROPOSED OPERATIONAL IONOSPHERIC CORRECTION SYSTEM

5.1 INTRODUCTION

This section is devoted to delineating an operational computational system by which the ionospheric corrections can be estimated and forwarded to the navigators. The computations are discussed apart from the prediction techniques that must be utilized to estimate the electron density distribution of the ionosphere. Discussion of the details of the prediction techniques are given in Section 6.

5.2 CONSTRAINTS ON THE OPERATIONAL IONOSPHERIC CORRECTION SYSTEM

There are several important factors and constraints that must be reflected in the synthesis of such a system. These are:

5.2.1 Geometrical Characteristics of the Satellite Constellation

The geometrical characteristics of the candidate constellations have been discussed in Section 3. Ground tracks and coverage contours for the "X" type configuration are displayed in Figs. 3.1 and 3.2. In both the "X" and "Y" constellations, the peripheral spacecraft rotate about the geostationary central spacecraft such that their nominal positions repeat themselves every 24 hours. Departures from the nominal orbit arise principally from the luni-solar gravitational effects and the influence of solar radiation pressure. By periodically adjusting the orbits, the magnitude of the departures could be minimized. This attribute of a repeating ground track correlated with the solar day is emphasized because it is demonstrated in Section 5.4 how this can be utilized to advantage in implementing the ionospheric correction.

5.2.2 Spacecraft Hardware Limitations

A description of the spacecraft hardware limitations as regards the ionospheric correction is given by Dept. of Air Force [1970]. Real-time transfer of information from which the correction can be made is to be accomplished by utilizing a portion of the message content of the L-band ranging signal. This link is also utilized to transfer

spacecraft ephemerides and ranging signal time synchronization data. For the purposes of this study, a maximum continuous data rate of 10 bits per second per spacecraft was allowed for the ionospheric correction.

5.2.3 User Hardware Limitations

Because of the large number of potential users of the navigation system, a significant portion of the overall cost will be the navigation equipment. Consequently, there is a strong desire to minimize the cost of the navigation equipment. The navigator is envisioned to have a digital computer in order to compute his position from the satellite observations. This device can also be used to compute the ionospheric (as well as the tropospheric) corrections. The significant limitation on the computer is the maximum memory that can be allocated for the ionospheric correction which was tentatively limited for this study to 2000 24-bit words [Dept. of Air Force, 1970].

5.2.4 User Accuracy and Operational Requirements

The user population constitutes a broad spectrum of accuracy requirements and operational characteristics which impacts significantly in the design of the operational correction scheme. Because of this, several levels of ionospheric correction accuracy should be made available, each being suited to the particular needs of a class of navigators. There will be those whose accuracy requirements will be such that they will not require any correction. Because of this, the correction system must be implemented in a manner in which it is transparent to these users. In some instances a user may have such lax operational requirements that he may be able to schedule his observations during the evening hours. The influence of the ionosphere is usually significantly less in the evening hours than during daylight. In this case, the navigator may need only very approximate estimates of the correction, if any at all. There will also be users whose interest will be in position determination as opposed to navigation. For these, it would be possible to effect an ionospheric correction well after the navigation observations are obtained. Then, these corrections could be estimated based on ionospheric data accumulated before, during, and after the observation period.

The bulk of the users will be those interested in navigation in which it is necessary to effect corrections in real time. For discussion purposes it is convenient to arbitrarily categorize these users into three groups of distinct accuracy requirements characterized by their desire to utilize: (a) long-term predictions generated 3 to 6 months in advance, (b) short-term predictions generated 1 to 14 days in advance and (c) real time estimates. Whereas high performance aircraft might require the best estimate possible (i.e., a real-time prediction), a merchant ship may be satisfied with a less accurate estimate (i.e., long-term prediction) if the cost is appreciably less.

5.2.5 Nature of the Influence of the Ionosphere on Navigation

The nature of the influence of the ionosphere on navigation is important in the development of an operational correction system. The effect on the group time delay can be conveniently discussed by utilizing Eq. (3.1) which represents the measurement made by a navigator as

$$T_j = \tau_{\rho j} + \tau_d + \tau_{ej} \quad , \quad j = 1 \text{ to } 4$$

To eliminate the effect of the navigator's clock offset it is necessary to difference the members of a set of four observations obtaining three equations of the form

$$(T_j - T_i) = (\tau_{\rho j} - \tau_{\rho i}) + (\tau_{ej} - \tau_{ei}) \ , \ j=1 \text{ to } 4 \text{ and } i=1,2,3 \text{ or } 4 \quad (5.1)$$

In this context, it is clear that it is the differences of the errors which propagate into the navigation solution, not the individual errors. If all the τ_{ek} (k=i,j) had the same magnitude, the navigation solution would be unaffected. In general, this will not be the case. As discussed in Section 4, the ionospheric induced error is proportional to the integrated electron content along the path from the navigator to the spacecraft. The differences in the ionospheric errors will be a function of the horizontal gradient of the electron density distribution and the differences in the elevation angles of the spacecraft with respect to the navigator.

5.3 NAVIGATOR'S COMPUTATION OF IONOSPHERIC CORRECTION

There are several alternatives to the computation that the navigator can make to infer the correction, depending on the form and substance of the information that is transmitted to him. The major constraints on effecting the

correction are the maximum allowed real-time data rate discussed in Section 5.2.2 and the maximum user computer capability discussed in Section 5.2.3. Naturally, the most desirable computation would entail the minimum cost associated with both.

In order to carry out a navigation solution, a user requires besides the observational data, the ephemerides of the spacecraft. In principle then, a user need only be additionally supplied with the electron density distribution as a four dimensional function of space and time. Given the position of the spacecraft, the electron density distribution and an assumed navigator's position, the computation is direct-being given to sufficient accuracy by integration of the electron density along the geometrical range path as discussed in Section 4.

An alternative technique introduced here would minimize the users' computational burden relative to the direct approach discussed above. The central theme to this alternative approach is that at a central computing facility the range or time corrections be computed for every potential location of a navigator for each satellite once the electron density distribution has been predicted. The maximum electron density occurs at an altitude of about 350 km. The difference in the geographical position of the geometrical path to a synchronous satellite at this altitude for an observer on the surface of the earth and one at 20,000 ft. varies from zero for a satellite overhead to 10 minutes of arc for a satellite on the horizon. For an observer at 60,000 ft. the difference increases to only 30 minutes of arc for a satellite on the horizon. It is doubtful that the electron density distribution as modelled over the coverage region of the satellite would be sensitive to positional differences of these magnitudes. Consequently, the computation of the ionospheric correction is insensitive to the navigator's height so that the correction for each satellite can be expressed as a three-dimensional function of the navigator's geographic location and time. This function, which will be referred to as the ionospheric correction function, would be supplied to each navigator rather than a description of the electron density distribution from which the range or time correction would have to be computed. To give an intuitive appreciation for this approach it is instructive to consider a hypothetical ionosphere in which the electron density distribution is radially symmetric. In this case, the contours of constant magnitude correction would be concentric circles about the

subsatellite point in which the magnitudes associated with the contours increase with distance from the subsatellite point.

5.4 TRANSFER OF IONOSPHERIC CORRECTION

There are several possible ways by which the ionospheric correction function can be transmitted to the navigator. The alternatives depend on both his operational and accuracy requirements.

As discussed in Section 5.2.4, there are users for whom long-term predictions (3-6 months) may be adequate. It would be possible to supply these corrections to the navigator before a mission is undertaken. An estimate of the volume of a priori information that a navigator must have access to can be obtained as follows. The satellite constellations under consideration, as discussed in Section 5.2.1, are such that the ephemeris for each satellite nearly repeats itself every day. Suppose that a monthly median electron density distribution given as a function of time of day and geographic location is estimated by the computational center. Then, the ionospheric correction functions based on this electron density distribution for one day would be valid for every other day of that month. The assumption that the ionospheric correction function need be determined every two hours in order to provide adequate interpolation within the day, would result in the need of 12 such functions per spacecraft per month. A constellation of 5 spacecraft for a period of 6 months would require a total of 360 ionospheric correction functions. Further economy could be obtained by displaying only the differences in the correction for the most desirable four satellites in view. This would result in a total of 216 ionospheric correction functions. By having this a priori information, any navigator would have available a backup capability to a real-time scheme. It should be noted here that it would be most efficient to include as part of the correction the influence of the troposphere. The long-term predictions would be most useful to those who desire navigation at minimum cost and where extreme accuracy is not important. These correction functions could be provided in graphical form either in a book or on microfilm, for easy use.

Short-term estimates, made available 1 to 14 days in advance, can be transferred by several means. For example, overall corrections to the long-term estimates comprising just a few numbers possibly transferred along with the spacecraft ephemeris may be adequate.

It is the real-time estimates of the corrections that are to be transmitted through the L-band ranging signal that are of prime importance and will dictate the design of the operational correction system. It should be noted that in an operational system it would be a straightforward matter to include in the corrections for the ionosphere the influence of the troposphere. There are at least two forms by which it would be possible to transfer the ionospheric correction function to the navigator in real time. The first consists of representing the function as a series expansion. An estimate of the data rate can be obtained by assuming that the structure of the correction contours closely resemble the monthly median values of the critical frequency of the F2 region. In such a case it should take no more than 52 coefficients to represent the ionospheric correction at each instant of time as a function of geographic longitude and latitude [Davies, 1965]. Assuming an additional 18 words for identifiers and a precision of seven bits, for a range of 0 to 127, gives a total of 490 bits. For a linear interpolation or extrapolation in time, a total of 980 bits must be transferred. At the maximum allowed data rate of 10 bits/sec discussed in Section 5.2.2, 98 sec would be required to transfer the corrections which should be valid for at least an hour. The frequency at which the correction information is updated would be dependent on the capriciousness of the ionosphere and should be under the control of the ground command facility. The 98 seconds establishes a lower bound to the updating interval.

At any one time, the navigator would require about 4000 bits of computer storage to be able to correct the observations from all four satellites. This is considerably less than the allowed maximum of 48,000 bits discussed in Section 5.2.3. The ability to obtain powers of the sine and

cosine functions of the nominal latitude and longitude and the ability to multiply and sum which would be needed to perform the computation should exist in the software capability required to perform the navigation solution independent of the presence of a numerical ionospheric correction.

The alternative approach which could be used in place of or in addition to the series representation would be to divide the viewing region of each spacecraft into a matrix and to transmit individually the correction averaged over each element of the matrix. In such a case, each navigator need only determine in which region he is located and recover only that particular number from the satellite transmission. The received data would represent the time error or range error itself so that no processing of the received information would be necessary. An estimate of the data rate in this case can be obtained in the following manner. Each spacecraft has a viewing region of approximately 40 percent of the earth's surface. For elements of 5 degrees by 5 degrees, 1040 words would be required. If 210 identifier words are assumed needed then a total of 1250 words must be transmitted. For a word length of seven bits and a data rate of 10 bits per second it would take 875 seconds (14.6 min) to transmit the correction function from each spacecraft.

5.5 IONOSPHERIC CORRECTION COMPUTATIONAL SYSTEM

A schematic of a suggested computational system is given in Fig. 5.1. The system is constructed in a manner such that long-term, short-term and real-time estimates of the corrections are obtained. In each case the estimates are meant to be either the ionospheric correction function itself or adjustments to the function. It is doubtful that real-time orbit data need be used to improve the ephemeris for the purpose of computing the ionospheric correction. Ephemerides generated several weeks in advance will probably suffice. In an operational system it is anticipated that the tropospheric corrections would be determined in a similar manner and combined with the ionospheric corrections. Consequently, a navigator would be able to correct for both effects by making a single computation.

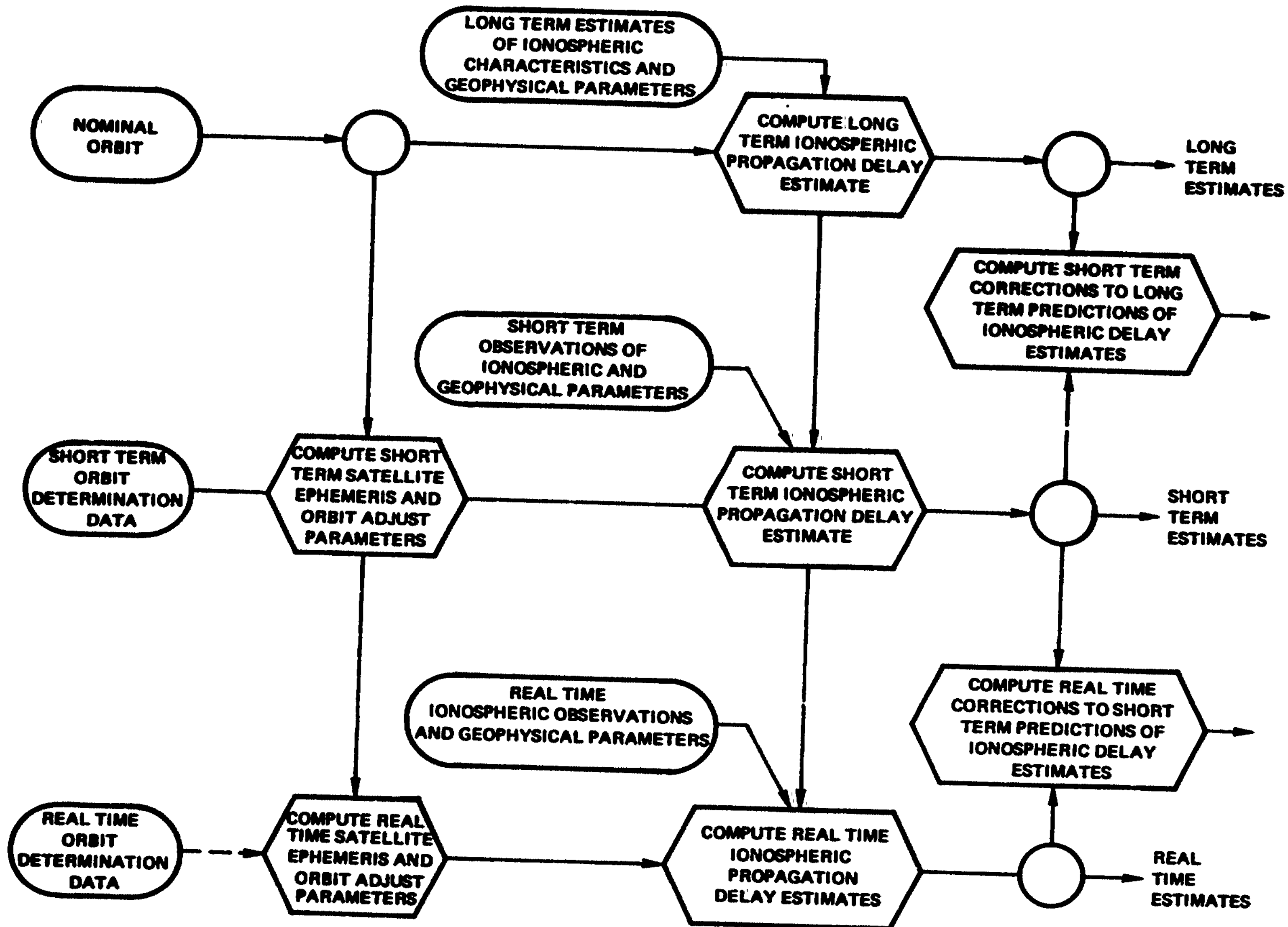

Fig. 5.1 SCHEMATIC OF THE OPERATIONAL IONOSPHERIC CORRECTION COMPUTATIONAL SYSTEM

6. GENERAL APPROACH TO THE PREDICTION ALGORITHMS

6.1 INTRODUCTION

The purpose of this section is to delineate the thought that went into defining the prediction algorithms that were ultimately evaluated. As described in the previous sections, both the satellite ephemerides and the global electron density distribution, or its equivalent, must be predicted into the future. The accuracy to which the satellite ephemerides must be estimated is within the state-of-the-art, as discussed in Section 3.5. The difficult aspect of the ionospheric prediction algorithm will be the estimation of the ionospheric characteristics. For this reason it will be instructive to begin with a concise description of the state of knowledge of the ionosphere that is relevant to the estimation of the ionospheric group velocity.

6.2 STATE OF KNOWLEDGE OF THE IONOSPHERE

The ionosphere may be defined as that portion of the earth's upper atmosphere where ions and electrons are present in quantities sufficient to affect the propagation of radio waves. It extends upwards from about 50 km with no well-defined upper boundary. The ionosphere is characterized by several regions which are designated as D, E, F1 and F2. Since the early years of ionospheric research, theoretical models starting with the well-known Chapman model have been developed to attempt to understand the mechanisms involved. More complex theoretical models consist of numerically solving simultaneously the time-dependent coupled chemical, dynamical and thermodynamical partial-differential equations for a multiconstituent ionosphere in a multiconstituent neutral atmosphere, e.g. King and Ruster [1971]. Their solutions are hindered by many uncertainties such as the time and spatial distribution of the constituents, neutral gas temperatures, ion and electron velocities, neutral wind velocities, production and loss mechanisms, electric field intensity, geomagnetic field intensity and in the boundary conditions. In spite of this, theoretical models provide useful tools for research into the physical concepts of ionospheric behavior. Unfortunately, the departure of observations from the model results are generally the rule rather than the exception.

Paralleling the development of theoretical ionospheric models has been the development of what are known as model

ionospheres which are dedicated toward providing representative characteristics for given conditions and locations. Though they draw heavily on theoretical modeling, model ionospheres are usually empirical in nature. The Institute of Telecommunications Sciences (ITS) of the Office of Telecommunications, U.S. Department of Commerce, has developed extensive capabilities in the predictions of global ionospheric characteristics. Their estimates are given as functions of the geographic location, season, time of day, geomagnetic characteristics and the 12-month running average of the smoothed Zurich sunspot number (R_{12} or SSN) [Jones and Gallet, 1962] and [Jones et al., 1969]. The basis of these estimates is the fitting of world-wide experimental data obtained over daily, seasonal and solar cycles. For example, the critical frequencies of the F2 layer, foF2, which define the maximum electron densities are derived from data that was obtained from a world-wide network of stations over a span of several years. The number of different geographic locations for which data was available varied from year to year, averaging about 160. The data was reasonably well distributed geographically, including such areas as Europe, Africa, North and South America, Asia, Australia, the Pacific, Russia and mainland China. A typical global prediction of the foF2 available from ITS is given in graphical form in Fig. 6.1.

Predictions of the ionospheric characteristics that are available from ITS are:

1. critical frequency of the F2 layer, foF2
2. maximum usable frequency factor, M(3000) F2
3. maximum usable frequency, MUF(0) F2
4. maximum usable frequency at 4000 km, MUF(4000) F2
5. critical frequency of the E layer, foE
6. height to semi-thickness ratio of F2 region, hmF2/ymF2
7. semimonthly revision factors to correct the MUF(0) F2

These predictions are in use by several communities. For example, they are currently used in the estimation of high-frequency telecommunication parameters which are published regularly by the Office of Naval Research for use by the fleet.

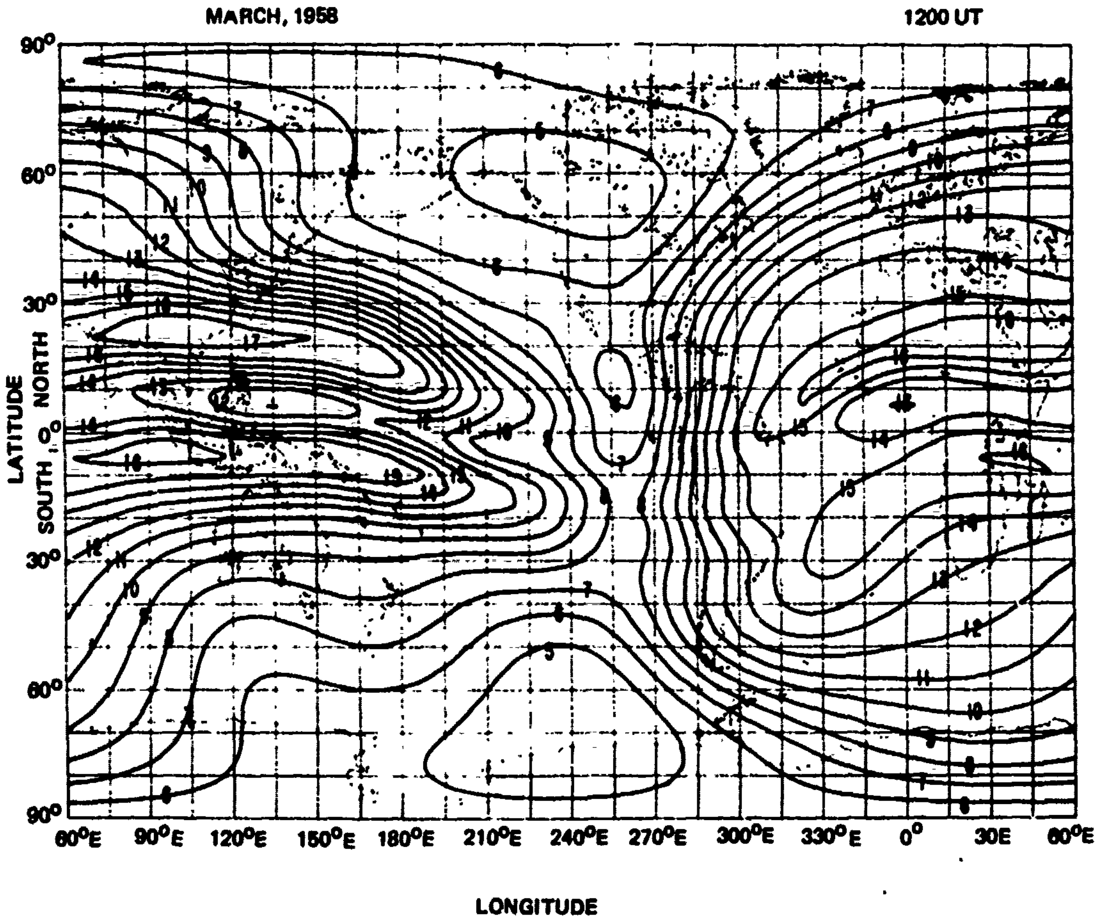

Fig. 6.1 DISTRIBUTION OF foF2 MEDIAN (MHz) [JONES et al., 1969]

6.3 METHODOLOGY OF THE PREDICTION ALGORITHMS

Several alternative approaches exist in developing the methodology of the prediction algorithms. In this section two distinct approaches are discussed and contrasted. In the first approach the vertical group time delay itself forms the basis of the prediction in a manner by which it is possible to completely avoid the explicit introduction of the electron density distribution. To facilitate discussion, it is appropriate to introduce two terms. Imagine the point on the position vector from a navigator to a satellite at which the electron density is a maximum. Denote this point as the "ionospheric point" and its projection on the ground as the "ionospheric geographic location" of the navigator. Denote, also, the angle between the intersection of the position vector with the geometrical vertical at the ionospheric point as the "ionospheric zenith angle". In principle it would be possible to obtain a prediction algorithm with the ionospheric geographical location of the navigator, the ionospheric zenith angle and time as the independent variables and with the season, solar and magnetic activity, etc. as parameters. This approach becomes more attractive by introducing the notion that the significant portion of the electron density distribution is confined to a narrow vertical region. For satellites above this region it is possible to approximately characterize the total group time delay by the vertical group time delay at the ionospheric geographic location of the navigator. The total time delay for propagation through this point at other than vertical incidence could then be inferred; possibly by just multiplying the vertical time delay by the secant of the ionospheric zenith angle. With this, the prediction algorithm reduces to a prediction of the vertical time delay with the ionospheric geographic location of the navigator and time as the independent variables. Real-time predictions can be achieved by using real-time measurements of the model parameters and the group time delays obtained at various sites. The basis of the second approach is the prediction of the electron density distribution from which the group time delay or equivalent range error can be determined in a separate step. The time delay would be computed utilizing Eq. (4.1) in which $N(\vec{r},t)$ is given by the predicted electron density distribution.

The distinction between the two approaches, while seemingly subtle, is nevertheless significant. It is our belief that this latter approach is superior to the former. Consequently, the algorithms developed here predict the electron density distribution as a function of space and time. Once this has been achieved it is straightforward to compute the total time delay for each satellite as a

function of time and the actual geographic location of potential navigators as discussed in detail in Sections 5.3 and 5.4.

The decision to predict the electron density distribution instead of the total vertical time delay has important consequences and is clearly in need of additional discussion. It is our contention that in the implementation of the ionospheric correction system, the electron density distribution should be introduced for several reasons. If this is true, then rather than introduce it implicitly, it would be superior to treat it explicitly in the prediction algorithm. The following constitutes several of the advantages of this approach:

6.3.1 Increased Accuracy in Estimation of the Total Time Delay

Once the electron density distribution is predicted, it is possible, as explained in Section 5.3, to determine directly the total time delays and equivalent range errors once the position of the spacecraft has been estimated. This procedure inherently takes into account the horizontal and vertical gradients of the electron density distribution. If only the vertical time delay is predicted then it will be necessary to infer from this the total time delay between the observer and each satellite. The uncertainty in this process has been investigated by Woodford and Dutcher [1970] who found that for an elevation angle of 5 degrees errors as large as ± 25% are possible. To investigate this point further, a limited study was undertaken. It consisted of the computation of the total time delay for several navigators whose geographic locations were different but whose ionospheric geographic locations were identical. Comparisons were then made of the vertical time delay and the equivalent for oblique incidence which was obtained by dividing the total oblique delay by the secant of the ionospheric zenith angle. The model used for the electron density distribution is described in detail in Section 6.4. For an elevation angle of 5 degrees, errors as large as 44% during the evening and 24% during the day were frequently observed. For an elevation angle of 30 degrees these errors reduce to 34% and 12% respectively.

6.3.2 Greater Theoretical Background

A wealth of theoretical studies already exist which can be utilized in the estimation of the electron density distribution. In addition, there is considerable interest in understanding and in predicting the state of the ionosphere,

i.e., the numbers of free electrons and the various ionic species, from many different viewpoints. As discussed in Section 6.2, besides the theoretical ionospheric models that have been defined, several semiempirical model ionospheres exist which characterize the ionosphere as a function of geographic location and time [Bauer, 1971].

6.3.3 Greater Utility

There would be many potential uses, besides navigation, of estimates of the electron density distribution. These include use for over-the-horizon radar as well as the avoidance of detection by this technique and the estimation of high frequency communication parameters. A significant number of the navigators may have need for ionospheric information for purposes other than navigation.

6.3.4 Greater Experimental Background

The development of techniques to estimate the electron density distribution has had stimuli other than satellite navigation systems. The utilization of the semiempirical model ionospheres that have already been developed is straightforward. These models have been developed on the basis of many different types of data over many decades over all parts of the earth. At the present time, there is no existing world-wide model for the vertical integrated electron content which is needed to determine the vertical time delays directly. Since the launching of satellites, it has been possible in principle to obtain the integrated electron content along the path from the observer to the spacecraft. Differential time delay on coherently related frequencies would be the most direct method but little of this data is available. There has been considerable effort expended in the measurement of Faraday rotation data from which it is possible to infer the integrated electron content by using normalized models of the electron density distribution as discussed in Section 4.2. Unfortunately, the observations that have been obtained have been over limited regions of the earth. To develop a world-wide capability, it would be necessary to collect data over long periods of time over all parts of the earth. This task, aside from its magnitude, would be difficult because of the inaccessibility of certain regions because of geographical or political impediments.

6.3.5 Increased Confidence in the Validity of an Evaluation

Care must be taken in performing any evaluation in order for it to be meaningful. A most important consideration is to ensure that the data utilized to make predictions are completely distinct from the data utilized to perform the evaluation. In the prediction of the electron density distribution this poses no problem since the ionospheric models can be based on distinctly different types of data than those supplied for use in the evaluation. However, difficulty is encountered in performing a nonprejudiced evaluation when estimating directly the vertical time delay. In the absence of vertical integrated columnar content data, Faraday rotation observations from high altitude satellites can be utilized to determine empirical models of the vertical time delay as discussed by Da Rosa [1969]. The body of data, described in Section 7, that was provided to perform the evaluation was Faraday rotation data. This data set constitutes a significant portion of the total body of data that is available to obtain empirical model parameters in the prediction of the vertical time delay.

6.3.6 Increased Real-Time Updating Capability

Real-time updating of either approach is possible by using the range residuals obtained at sites of known location. To attempt to utilize Faraday rotation, differential doppler, topside and bottomside sounding data, etc. would require the introduction of the electron density distribution. Consequently, it would be most desirable to adopt an approach which can directly utilize many types of data, some of which is already being obtained for other purposes, for both increased accuracy, lower operating costs and for a backup capability.

6.4 ALGORITHM I

The philosophy behind this algorithm was to utilize the best available long-term a priori predictions of ionospheric characteristics in order to predict an electron density distribution. Then the ionospheric group time delay would be computed as in Eq. (4.1) where $N(\vec{r},t)$ is given by the predicted electron density distribution. The predicted values of group time delay obtained in this way would establish a basis for comparison for both short-term and real-time predictions and indicate a measure of the extent to which either is needed. To assist in characterizing the electron density distribution a vertical electron density profile was utilized. The model adopted is that defined by Haydon and Lucas [1968] which is depicted in Fig. 6.2. The vertical profile is characterized by eleven parameters each of which can be a function of geographic location, time, solar activity, etc. The validity of the

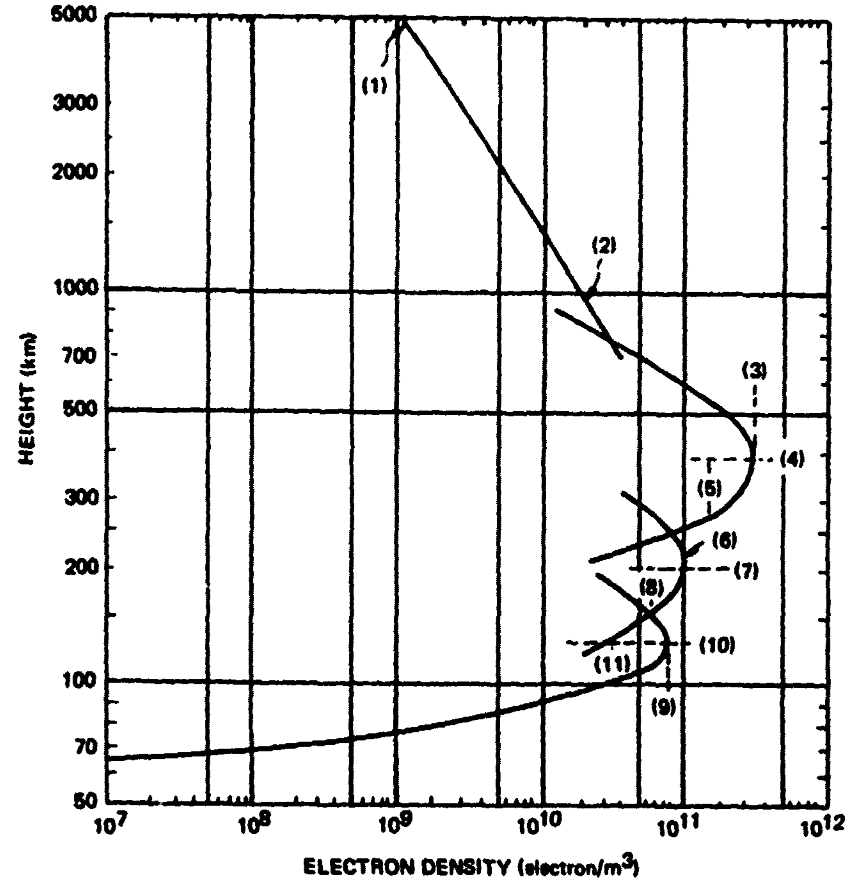

Fig. 6.2 ELEVEN PARAMETER VERTICAL ELECTRON DENSITY PROFILE [HAYDON AND LUCAS, 1968]

model has been established by the realization of good agreement between virtual height computations obtained using the model with experimentally determined values [Haydon and Lucas, 1968]. Typical comparisons for several different conditions are given in Fig. 6.3. In this algorithm, of the eleven parameters that are required to define the vertical electron density, four are obtained through the predictions available from ITS. Of these four, three define the F2 region which is dominant in the determination of the integrated electron content along the propagation path. The eleven parameters are determined for Algorithm I in the following manner, where the item numbers correspond to the numbers on Fig. 6.2:

(1) Density at 5000 km - an analytical function of the month of the year and the gyrofrequency [Smith, 1961].

(2) Density at 1000 km - an analytical function of magnetic dip and solar zenith angle [Chandra and Ragaswamy, 1967].

(3) Maximum electron density of the F2 region - obtained as a function of R_{12}, geographic location, month and time of day from predictions of foF2 which are available monthly from ITS [Jones and Gallet, 1962].

(4) Height of the maximum of the F2 region - obtained as a function of R_{12}, geographic location, month and time of day from predictions of M(3000)F2 which are available monthly from ITS [Jones and Gallet, 1962].

(5) Semithickness of the F2 region - obtained as a function of R_{12}, geographic location, month and time of day from predictions of hmF2/ymF2 which are available monthly from ITS [Jones and Gallet, 1962].

(6) Maximum electron density of the F1 region - obtained as a function of R_{12}, month and time of day from an empirical formula [AVCO, 1963].

(7) Height of maximum of the F1 region - obtained as a function of time of day [AVCO, 1963].

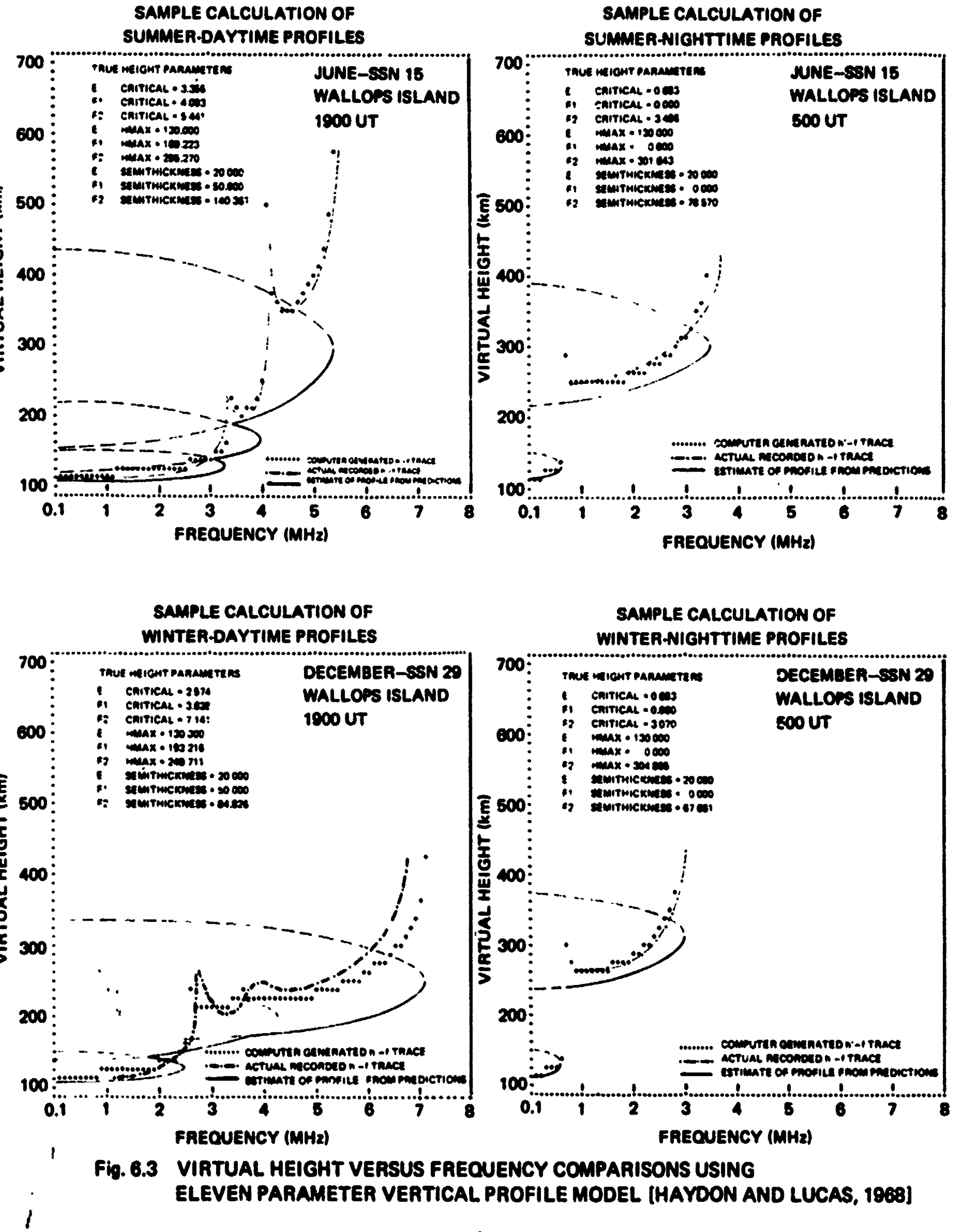

Fig. 6.3 VIRTUAL HEIGHT VERSUS FREQUENCY COMPARISONS USING ELEVEN PARAMETER VERTICAL PROFILE MODEL [HAYDON AND LUCAS, 1968]

(8) Semithickness of the F1 region - constant at 50 km.

(9) Maximum electron density of the E region - obtained as a function of R_{12}, geographic location, month and time of day from predictions of foE which are available monthly from ITS [Jones and Gallet, 1962].

(10) Height of maximum of the E region - constant at 130 km.

(11) Semithickness of the E region - constant at 20 km.

6.5 ALGORITHM II

Algorithm II was devoted to the capability of effecting a real-time ionospheric correction. The most desirable approach would have been to utilize one of the several rather sophisticated theoretical ionospheric models that are available. With such a model as a basis, the philosophy of the updating scheme would be rather straightforward. It would be possible to determine some of the more uncertain model parameters as a function of time by "fitting" the model to whatever experimental ionospheric data is available. Prediction of the parameters and integration of the system of nonlinear time-dependent partial differential equations would then result in the determination of the electron density distribution at any time in the future.

The evaluation of the performance of any of the algorithms developed in this study was to be achieved by processing a large amount of Faraday rotation data obtained over several years. This data set and the evaluation plan is defined in detail in Sections 7 and 8. Preliminary estimates for the cost of processing even only a minimum definitive subset of data indicated that the computational complexities had to be minimized. Consequently, in order to perform a meaningful evaluation of the algorithm a less sophisticated approach had to be adopted.

The a priori predictions of Algorithm I, as described in the previous section, constitute in themselves a rather sophisticated model. The predicted electron density distribution has considerable geographical structure as evidenced by a typical map of the foF2 distribution (which is proportional to the square root of the maximum electron density)

given in Fig. 6.1. Because of this, it was concluded that rather than attempt to model the electron density distribution itself it would be more expeditious to model the differences between the actual electron density distribution and the estimates obtained from the a priori predictions of Algorithm I. The basis for this approach is the anticipation that the a priori estimates will adequately reflect the detailed structure and that a correction which is slowly varying in both space and time would be adequate.

The adjunct model developed for the electron density distribution is distinguished by being an analytic model consisting of distinct daytime and nighttime functions. The daytime model was obtained from a first order perturbation solution to the continuity equation in which the production is given by the Chapman function, the loss mechanism assumed as a linear function of the electron density and where transport phenomena are neglected. Under these conditions, the electron density at the height of maximum production, which is assumed to be the height of the maximum density, is given by

$$N_d' = \alpha \cos \chi + \beta\, \omega \cos \lambda_n \cos \lambda_s \sin \omega(t-12) + \gamma \quad (6.1)$$

where

α, β, γ = parameters, m^{-3}

χ = solar zenith angle at "ionospheric point"

λ_n = "ionospheric latitude" of navigator

λ_s = latitude of sun

ω = earth's rotation rate, rad/hour

t = local time, hour

N_d' = maximum daylight electron density, m^{-3}

This expression for the maximum electron density exhibits some of the more typical characteristics that have been observed. The first term alone would give an electron density that is a maximum at the subsolar point and decreases with increasing solar zenith angle. The second term introduces a phase (or time) lag in the appearance of the maximum which conforms with observations. One effect that this expression does not introduce is diffusion of the electrons along the geomagnetic field lines. This phenomenon is discussed by Rastogi [1959] who demonstrated that it is signifi-

cant in the vicinity of the geomagnetic equator but can be neglected at the middle latitudes. The magnitude of the effect is shown to be correlated with both magnetic dip angle and solar activity. In order to account for this phenomenon the following approximation was used which reasonably fits the experimental data given by Rastogi [1959]:

$$N_d = K(D)\, N_d' \tag{6.2}$$

where

$$K(D) = \begin{cases} 1 & , |D| \geq \pi/4 \\ (1-0.305 \cos 6\,D) & , |D| < \pi/4 \end{cases}$$

D = magnetic dip at a height of 350 km,rad

N_d = maximum daylight electron density, m^{-3}

The nighttime model that was utilized represents a solution to the continuity equation which consists of a linear loss mechanism and no production mechanism. The maximum nighttime electron density is then just simply

$$N_n = N_d(t_{ss})\, e^{-\delta(t-t_{ss})} + N_\infty(1-e^{-\delta(t-t_{ss})}) \tag{6.3}$$

where

N_n = nighttime maximum electron density, m^{-3}

N_∞ = parameter to be determined, m^{-3}

$N_d(t_{ss})$ = maximum electron density at sunset, m^{-3}

t = local time, hour

t_{ss} = time of sunset, hour

δ = effective recombination coefficient, 12/day

This solution represents an exponential decay of the maximum density from sunset to sunrise.

Now that the maximum electron density as a function of time and geographical location has been specified, it is necessary to define the vertical profile as a function of this single variable. Let

$$N(h) = \begin{cases} N_d \; w(h) \\ \\ N_n \; g(h) \end{cases} \tag{6.4}$$

where h is the height above the earth's surface and $w(h)$ and $g(h)$ represent normalized vertical profiles. There are many alternatives available for both $w(h)$ and $g(h)$ but, as will be shown later in Section 8.5.2, they will not have to be explicitly defined for this particular study.

In summary, an analytic model for the electron density distribution has been specified as a function of geographic location, local time and magnetic dip. The model is a linear function of the parameters $\alpha, \beta, \gamma, N_\infty$ which are to be determined from real-time observations and other measures of the ionosphere. Because of the linearity of the model, it is possible to utilize these functions to model directly the difference between the observed ionosphere and the a priori predictions of Algorithm I.

6.6 ALGORITHM III

To further explore the potential of a real-time ionospheric correction an alternative approach to Algorithm II was explored. In Algorithm II the basis of the correction was the development of a theoretical ionospheric model. In contrast, the basis of Algorithm III is the utilization of an empirically developed model ionosphere. At any geographic location the vertical electron density profile is taken to be that utilized in Algorithm I and depicted in Fig. 6.2. As described in Section 6.4, five of the eleven parameters used to define the profile for any specific geographic position are functions of the predicted R_{12}. Most significant are the three parameters defining the F2 region which contributes overwhelmingly to the total group time delay. These are functions of geographic location, time, season, and R_{12}. World-wide predictions of each of the parameters can be obtained from ITS as discussed in Section 6.3. With this background it is now possible to describe the central theme of Algorithm III.

The R_{12} used in the ITS predictions represent the predicted 12-month running average of the smoothed Zurich sunspot number determined from optical observations of the sun. Suppose this interpretation is changed so that the R_{12} were to simply represent a number, or parameter,

on which the electron density distribution is dependent. Given ionospheric data for some interval of time, then, it would be possible to determine an effective R_{12} (designated by R) such that the modeling electron density distribution best represents the observed data. Then by using this R, or a value predicted from a sequence of such numbers, a real-time prediction of the electron density distribution can be obtained.

Inherent to this approach are the spatial and time correlations which have been determined experimentally and reside in the sets of coefficients which form the basis of the ITS predictions. One concern in this approach is that the ITS model ionosphere represents monthly median values and the same correlation may not exist for the instantaneous electron density distribution. Utilizing data over a period of one to several days should minimize any difficulty induced by this inconsistency. The implementation of this approach is discussed in detail in Section 8.5.3.

7. EVALUATION DATA

7.1 INTRODUCTION

The experimental data provided for use in the study were Faraday rotation observations obtained from VHF (nominally 137 MHz) transmissions from near-synchronous satellites. From this type of data it is possible to "infer" an "experimental" vertical ionospheric group time delay, τ_{v_e}. The τ_{v_e} data obtained in this manner was to be used for updating and evaluation of the prediction algorithms. In Section 4.2 theoretical expressions for converting the experimental Faraday rotation data to τ_{v_e} data are given and the approximations in these expressions, which would result in errors in τ_{v_e}, are discussed. In this section, the errors in τ_{v_e} resulting from experimental errors in the Faraday rotation and the deficiencies of the data base as regards its use in verification of algorithms for use in a navigation context, are discussed.

7.2 EXPERIMENTAL ERRORS

The experimental errors in the Faraday rotation data result from uncertainties in

a) the initial polarization of the satellite radiated signal

b) the measurement of the polarization of the received signal

c) resolution of the $n\pi$ uncertainty inherent to any polarization measurement.

Together, a) and b) have been estimated by the experimenters to amount to about $\pm 15^{\circ}$ which at 1600 MHz would range from ± 0.2 to ± 0.8 ns depending on station location and time of day. The time of day dependence arises through the diurnal variation of $M(G,t)$, as discussed in Section 4.2. As regards c), it is usually assumed that the $n\pi$ ambiguity has been successfully resolved. However, the existence of negative values of rotation in the data make the assumption suspect. An error of $\pm \pi$ in resolving this ambiguity can lead to errors in the range ± 2 to ± 4 nsec at 1600 MHz for daylight periods, depending on station location. In this study it has been assumed that the values of the Faraday

Preceding page blank

rotation data that have been supplied are correct. Thus the inferred τ_{v_e} data are subject to the experimental error in the Faraday rotation measurement.

7.3 LIMITATIONS OF THE DATA BASE

One of the deficiencies of the data base in providing a meaningful evaluation of ionospheric prediction algorithms in a navigation environment is its limited geographic and geomagnetic coverage. Table 7.1 gives a list of the data provided for use in the study. Table 7.2 gives the geographic coordinates and geomagnetic dip angles of each of the measurement sites. Fig. 7.1 is a world map depicting the measurement sites. Since the satellites were in equatorial orbits with slow drift rates, the data was confined to a limited geographic area. With the exception of Honolulu, Cold Bay, and Arecibo, the remaining stations are in the continental United States and at Edmonton. It is already known that there exists a high degree of correlation in the behavior (magnitude and local temporal dependence) of the data at the mid-latitude stations. Moreover, as is clear from Fig. 7.1 and Table 7.2 for all stations except Honolulu, the geomagnetic dip angles of the ionospheric points fall in the range of 50°N to 72°N; Honolulu is at 37.5°N. On the basis of the behavior of the ionospheric electron density as a function of geomagnetic dip, one would expect that the magnitudes and local temporal dependence of τ_{v_e} at all stations except Honolulu would be similar. It would be expected that the magnitudes of τ_{v_e} at Honolulu would be higher than all other stations. These expectations were borne out as evidenced by the cumulative frequency distributions of the vertical time delay, τ_{v_e}, discussed later.

Another problem with the data was that the satellites were always south of the measurement stations. In an actual navigation system, a navigator would in general be looking at satellites north, east, south, and west from his location. The high degree of correlation exhibited by the data as discussed above would then tend to obscure the validity of the evaluation.

TABLE 7.1

DURATIONS, OBSERVATION STATIONS, SATELLITES AND SOURCES OF FARADAY ROTATION DATA. (AFCRL, SEL, UH and UI represent Air Force Cambridge Research Laboratories, Stanford Electronics Laboratories, University of Hawaii and University of Illinois, respectively.)

Duration	Location	Satellite	Source
1 Jan 1965	Stanford, Ca.	SYNCOM3	SEL
to 31 Dec 1965	Honolulu, Hi.	SYNCOM3	SEL
1 Dec 1967	Arecibo, P.R.	ATS1	SEL
to 18 Apr 1968	Honolulu, Hi.	ATS1	SEL and UH
	Sagamore Hill, Ma.	ATS3	AFCRL
	Stanford, Ca.	ATS1	SEL
	Stanford, Ca.	ATS3	SEL
	Urbana, Il.	ATS3	UI
1 Jan 1968	Honolulu, Hi.	ATS1	UH
to 31 Dec 1968	Sagamore Hill, Ma.	ATS3	AFCRL
	Stanford, Ca.	ATS1	SEL
1 Dec 1968	Arecibo, P.R.	ATS3	SEL
to 13 Nov 1969	Clark Lake, Ca.	ATS1	SEL
	Cold Bay, Ak.	ATS1	UI
	Edmonton, Can.	ATS1	SEL
	Fort Collins, Co.	ATS1	SEL
	Honolulu, Hi.	ATS1	UH
	Rosman, N.C.	ATS3	SEL
	Sagamore Hill, Ma.	ATS3	AFCRL
	Stanford, Ca.	ATS1	SEL
	Stanford, Ca.	ATS3	SEL
	Urbana, Il.	ATS3	UI

TABLE 7.2

GEOMAGNETIC DIP AND GEOGRAPHIC COORDINATES OF THE "IONOSPHERIC GEOGRAPHIC LOCATION" OF THE FARADAY ROTATION MEASUREMENT STATIONS
(Epoch January 15, 1969)

Station	Satellite	Geomagnetic Dip degrees north	Latitude degrees north	Longitude degrees east
Edmonton	ATS1	71.3	48.1	239.5
Sagamore Hill	ATS3	70.6	39.3	289.4
Urbana	ATS3	68.7	37.0	273.8
Rosman	ATS3	65.2	32.6	278.4
Cold Bay	ATS1	64.0	49.8	199.5
Fort Collins	ATS1	63.6	37.0	248.5
Stanford	ATS1	58.4	34.6	234.8
Clark Lake	ATS1	55.6	30.9	240.1
Arecibo	ATS3	50.0	17.3	293.1
Honolulu	ATS1	37.5	19.9	202.7

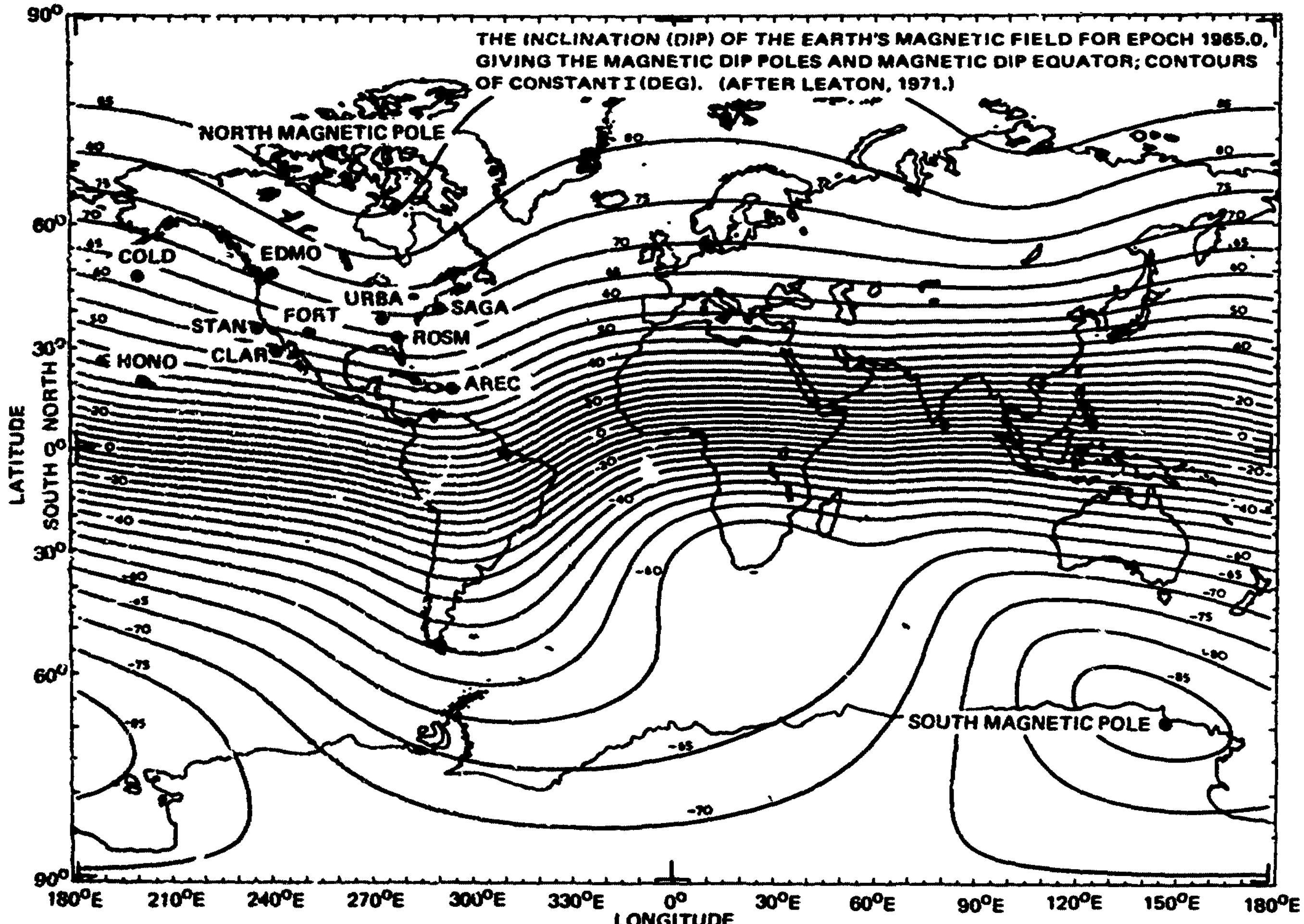

EDMO - EDMONTON – ATS 1
COLD = COLD BAY – ATS 1
SAGA = SAGAMORE HILL – ATS 3
URBA = URBANA – ATS 3
ROSM = ROSMAN – ATS 3
FORT = FORT COLLINS – ATS 1
STAN = STANFORD – ATS 1
CLAR = CLARK LAKE – ATS 1
AREC = ARECIBO – ATS 3
HONO = HONOLULU – ATS 1

Fig. 7.1 WORLD MAP SHOWING GEOGRAPHIC AND MAGNETIC DIP COORDINATES OF THE "IONOSPHERIC GEOGRAPHIC LOCATION" OF THE FARADAY ROTATION MEASUREMENT STATIONS (EPOCH JANUARY 15, 1969)

8. EVALUATION PHILOSOPHY

8.1 EVALUATION CONDITIONS

In order to simulate the application of the algorithm in a navigation system the Faraday rotation data provided for the study and listed in Table 7.1 was subsetted into five so-called "evaluation conditions" [Dept. of Air Force, 1970]. The five evaluation conditions are described in Table 8.1. In an evaluation condition, the stations listed as "observation stations" correspond to the system ground stations whose data is to be used in the updating process. The stations listed as "evaluation stations" correspond to navigators. Their data is to be used for comparison with the predictions and thus forms the basis of the evaluation of the algorithms.

8.2 CRITERIA FOR EVALUATING THE ALGORITHMS

In Section 6.3.5 attention was directed to the care that must be exercised in performing the evaluation of the prediction algorithms. The algorithms developed in this study are truly prediction algorithm for use in a navigation system. This point is emphasized by two important criteria that have been observed in their evaluation:

1) none of the experimental data provided for evaluation of the prediction algorithms at stations designated as evaluation stations (navigators) were used in any way to make the predictions of the time delays at an evaluation station

2) the experimental data from the stations designated as observation stations (system ground stations) were used in a prediction sense rather than a filtering or smoothing sense (the terms prediction, filtering and smoothing being used in their technical estimation theory sense).

The first criterion indicates that it was not appropriate to derive any correlations between observation and evaluation stations and then use these correlations in the evaluation of the algorithms. The implication of such an approach in a navigation system is knowledge of the correlations between observation stations and any geographic

TABLE 8.1

EVALUATION CONDITIONS

EVALUATION CONDITION 1: Day 342-67 to Day 109-68

Observation Stations

Arecibo ATS3
Honolulu ATS1

Evaluation Stations

Stanford ATS1
Stanford ATS3
Urbana ATS3
Sagamore Hill ATS3

EVALUATION CONDITION 2: Day 342-67 to Day 109-68

Observation Stations

Sagamore Hill ATS3
Arecibo ATS3
Honolulu ATS1

Evaluation Stations

Stanford ATS1
Stanford ATS3
Urbana ATS3

EVALUATION CONDITION 3: Day 1-65 to Day 365-65

Observation Station

Stanford SYNCOM 3

Evaluation Station

Honolulu SYNCOM 3

EVALUATION CONDITION 4: Day 1-68 to Day 366-68

Observation Station

Stanford ATS1

Evaluation Station

Sagamore Hill ATS3
Honolulu ATS1

TABLE 8.1 (cont'd)

EVALUATION CONDITION 5: Day 336-68 to Day 317-69

<u>Observation Stations</u>

Edmonton ATS1
Sagamore Hill ATS3
Honolulu ATS1

<u>Evaluation Stations</u>

Stanford ATS1
Stanford ATS3
Clark Lake ATS1
Fort Collins ATS1
Urbana ATS3
Rosman ATS3
Arecibo ATS3
Cold Bay ATS1

location and the temporal variations (diurnal, seasonal, solar cycle) of these correlations.

The second criterion indicates that in the real-time updating (Algorithms II and III), the observation station data is used only up to some time prior to the time of interest at evaluation stations (prediction) rather than up, including, and beyond (filtering and smoothing) the time of use at an evaluation station. Thus the algorithms truly represent the navigation situation.

8.3 UPDATING DATA

As was indicated in the general discussion in Section 6.3, a major virtue of the estimation of the electron density distribution approach that was adopted in this study, is the diverse body of data which could be utilized for the near real-time updating of Algorithms II and III. Such data as

1) integrated electron content
2) ground based vertical and oblique soundings
3) topside vertical and oblique soundings
4) geomagnetic activity
5) ionospheric refraction data available from other systems (e.g., Navy Navigation Satellite System)
6) Faraday rotation

could easily be utilized for purposes of updating.

An updating scheme using some or all of the above data naturally partitions itself into three types of updating:

1) global
2) regional
3) local

In global updating, data from a specified geographic region would be used to update and predict the ionospheric time delay at other geographic locations, both within and outside the region. In an operational system this must correspond to having the system ground stations confined to the territory of the United States and using data collected by these stations for world-wide predictions.

In a regional updating, where the interest is confined to the cover region of a single satellite constellation,

data collected at system ground stations within the region would be used to update the algorithms in order to predict the ionospheric time delays within the entire region.

A local updating would be similar to the regional updating in which both the system ground stations and navigators are confined to a limited area within the region.

Each of the algorithms proposed in this study has inherent to it a global capability. However, in performing the study, only the integrated electron content, inferred from the provided data base, was used as a data source for updating. Thus given the limitations of the data base as discussed in Section 7, the evaluation of the algorithms was necessarily local.

8.4 WEIGHTING

A considerable effort was expended in considering whether or not a weighting scheme should be implemented as part of the algorithms. When one considers weighting it is for the reasons of:

1) data of distinct differences in quality (precision and accuracy)

2) deficiencies in the model with regard to the intended use of the model.

In this study all the data furnished was assumed to be of equal quality. This assumption is somewhat suspect due to the existence of negative Faraday rotation values in the Honolulu data. However, without the proper means of assessing the quality of all the data provided, it is the only reasonable assumption.

All models suffer from some deficiencies and one might want to weight the observation station data so as to improve the predictions at some specified sites. This was particularly true of the Honolulu data which was of a distinctly different character when compared with the data from all other stations. One might wish to deweight the Honolulu data when Honolulu appeared as an observation station along with other observation stations.

The development of weighting schemes is not a trivial matter of geographic or relative distance weighting but involves complex considerations. This is made apparent

in evaluation condition 5, when one notes that the character of the ionospheric time delay data at Arecibo is much more like that at Cold Bay than is the Honolulu data, (see Fig. 7.1) Yet a simple relative distance weighting scheme would tend to inappropriately deweight Arecibo relative to Honolulu. From our knowledge of the correlation of ionospheric electron densities with geomagnetic dip, Section 6.5, it is apparent that any weighting scheme would necessarily involve geomagnetic parameters.

Limited comparisons of the Algorithm II capability with and without Honolulu observation data were made for January 1969 from evaluation condition 5. The results are given in Table 8.2. The results indicate that if Honolulu data were not used, the rms of the residuals averaged over the evaluation stations are about 12 percent less than when Honolulu data were used.

In order to avoid creating a false impression by developing a weighting scheme peculiar to the given regional character of the data base, it was decided to give all observation station data equal weight. This was consistent with the desire to interpret the results of the evaluation in a world-wide context.

8.5 EVALUATION DETAILS

8.5.1 Algorithm I

The basic features of Algorithm I were given in Section 6.4. Therein it was pointed out that the underlying philosophy behind this algorithm was the use of the best available long-term estimates of ionospheric characteristics needed to define the electron density distribution. One of the best long-term predictions of ionospheric characteristics presently available are provided by ITS as discussed in Section 6.2. Of the predictions available, Algorithm I uses

1) E-layer, maximum electron density
2) F-layer, maximum electron density
3) F-layer, height to semi-thickness ratio
4) F-layer, M(3000) factor from which height can be inferred

with which to obtain four of the eleven required parameters. The long-term predictions of the above characteristics are prepared by ITS five months prior to the month of prediction. Use of these predictions in Algorithm I would enable one to provide a priori estimates of world-wide ionospheric time delay five months in advance of use. Such estimates would

TABLE 8.2

COMPARISON OF ALGORITHM II PREDICTION CAPABILITY WITH AND WITHOUT HONOLULU OBSERVATION DATA

January 1969 Evaluation Condition 5

Evaluation Station	Number of Points	RMS of the Residuals (ns) With Honolulu Data	RMS of the Residuals (ns) Without Honolulu Data
Stanford-ATS1	2021	3.42	3.69
Clark Lake-ATS1	477	3.47	3.14
Fort Collins-ATS1	2084	3.62	2.81
Urbana-ATS3	2137	3.86	3.10
Rosman-ATS3	2039	3.30	3.22
Arecibo-ATS3	1847	5.47	4.13
Cold Bay-ATS1	2105	2.21	2.26
Mean over all stations	--	3.62	3.19

be useful to certain classes of navigators, to whom they could be provided in advance as discussed in Section 5.4.

In addition to the long-term predictions, ITS also provides the so-called Semi-monthly Revision Factors as described in Zacharisen, Ostrow and Huang [1969]. These factors apply only to the F-layer critical frequency and can be used to provide corrections to the long-term estimates of the F-layer maximum electron density. They are prepared by subjective methods of comparison of the long-term predictions of the MUF (3000) F2 with experimentally determined values of MUF (3000) F2 from a small set of ionosonde stations. The comparisons are based on experimental data available one to two weeks prior to the half-month of application.

The implementation of Algorithm I has included the use of these revision factors. This was in keeping with the desire to provide the best possible estimates of the ionospheric characteristics. Since the revision factors are available about two weeks prior to use, Algorithm I as implements is, strictly speaking, a two-week prediction. However, comparisons of Algorithm I predictions with and without the revision factors showed little substantial differences.

To investigate the significance of the semi-monthly revision factors, a compilation of their statistics for a representative sample of the data supplied, with which to perform the evaluation, is given in Table 8.3. (The indicated months actually represent those which formed the subset of data ultimately used in the evaluation as discussed in Section 9.1.) The mean and both rms' are obtained by summing over time throughout the day and over space over the entire globe. The rms' of the semi-monthly revision factor over all the months is six percent, i.e., a six percent correction to the critical frequency of the F2 region. What is of interest however, is the influence on the vertical ionospheric time delay which is proportional to the integrated electron density. It is not unreasonable to assume that the vertical time delay is proportional to the maximum electron density which is itself proportional to the square of the critical frequency of the F2 region. For this reason the rms of the deviation from unity of the square of the semi-monthly revision factor is given for each month. The rms is 12 percent over all the data.

Based on this discussion, it is possible to make a statement as to the maximum benefit incurred by utilizing the semi-monthly revision factors; or alternately to estimate

TABLE 8.3

STATISTICS OF SEMI-MONTHLY REVISION FACTORS

432 Data Points Per Month

Month	Year	Mean	RMS from Unity	RMS of the Square from Unity
January	65	0.99	0.06	0.12
April	65	1.00	0.08	0.16
July	65	1.01	0.09	0.19
January	68	1.03	0.05	0.11
February	68	1.05	0.07	0.15
March	68	1.05	0.06	0.13
April	68	1.03	0.05	0.11
October	68	0.99	0.05	0.09
January	69	1.02	0.06	0.10
April	69	1.00	0.04	0.07
July	69	1.00	0.02	0.04
October	69	0.98	0.04	0.07

the maximum degradation to be expected were Algorithm I utilized without them. The degradation would have been no greater than 12 percent. Consequently, to a precision better than 12 percent, it is possible to interpret the results of Algorithm I as a five month prediction.

8.5.2 Algorithm II

Algorithm II constitutes a real-time updating of the a priori estimates provided by Algorithm I. The details of the algorithm are given in Section 6.5. Briefly, the algorithm consists of a parameterized analytic model which describes the electron density distribution as a function of geographic location, local time, and magnetic dip.

Using Eq. (6.4) the vertical ionospheric time delay at local hour t is given as

$$\tau_{v_d}(t) = C \int N_d(t)\, w(h)dh \quad , \text{ for daytime} \qquad (8.1a)$$

and

$$\tau_{v_n}(t) = C \int N_n(t)\, g(h)dh \quad , \text{ for nighttime} \qquad (8.1b)$$

where $C = 1.34 \times 10^{-7}/f^2$, rationalized mks units where f is the carrier frequency of the ranging signal in Hz. Inserting Eqs. (6.2) and (6.3) into the above yields

In the implementation of the algorithm, a simplification was introduced which allowed the use of the Algorithm I results and thereby removed the need for additional ray tracing. The simplification is based on the fact that the major contribution to τ_v comes from the F2-layer of the ionosphere. It is then possible to write that

$$\tau_v(\lambda,\theta,t,R) \approx C\, N_{max}(\lambda,\theta,t,R) \int W(\lambda,\theta,t,h)\, dh \qquad (8.5)$$

where

$C = 1.34 \times 10^{-7}/f^2$ mks units where f is the carrier frequency of the ranging signal in Hz.

λ = ionospheric geographic latitude of the observation station (in fitting) or the evaluation station (in predicting)

θ = ionospheric geographic longtidue of the observation station (in fitting) or the evaluation station (in predicting)

t = UT time

R = effective value of R_{12}

$N_{max}(\lambda,\theta,t,R)$ = maximum electron density of the F2 layer at $\lambda,\theta,t,$ and R , given explicitly as a function of R

$W(\lambda,\theta,t,h)$ = normalized electron density profile at $\lambda,\theta,$ and t; independent of R

Strictly speaking, the normalized vertical profile, W , should be a function of R . The independence of R is introduced here only as a simplification, as discussed above, so that the value of $\int W(\lambda,\theta,t,h)dh$ may be obtained from the Algorithm I results. The value of $\int W(\lambda,\theta,t,h)dt$ is then given as

$$\int W(\lambda,\theta,t,h)dh = \frac{\tau_v(\lambda,\theta,t,R_{12,a})}{C\, N_{max}(\lambda,\theta,t,R_{12,a})} \qquad (8.6)$$

where $R_{12,a}$ is the value of R_{12} used in making the Algorithm I predictions.

From Eqs. (8.5) and (8.6) the fitting function is given as

$$\tau_v(\lambda,\theta,t,R) = \left\{\frac{\tau_v(\lambda,\theta,t,R_{12,a})}{N_{max}(\lambda,\theta,t,R_{12,a})}\right\} N_{max}(\lambda,\theta,t,R) \quad (8.7)$$

where R is the fitting parameter and the functional form taken for $N_{max}(\lambda,\theta,t,R)$ is that utilized by ITS in their predictions of the critical frequency of the F-layer, foF2 [Jones and Obitts, 1970].

The fitting function Eq. 8.7 was then least squares fitted to the experimental τ_v (i.e., τ_{v_e}) values obtained at the observation stations. The fitted value of R thus obtained, when used in Eq. (8.7) at the evaluation stations, gives the updated prediction at the evaluation station.

The fitting span in this algorithm, unlike the case in Algorithm II, has no defined minimum length. However, to provide a meaningful estimate of R, it was felt that the fitting span should be at least 24 UT hours. As in Algorithm II this was taken as the span length so as to make the model responsive to daily variations. Longer fitting spans would make the model more sluggish in its response. The time between the end of the fitting span and the beginning of the prediction time was, as in Algorithm II, taken as 1/2 hour. A prediction span of 3 hours, as in Algorithm II, was found to be suitable. Shorter spans did not show any improvement in the results.

$$\tau_{v_d}(t) = \{\alpha\, C \int w(h)\, dh\}\, K(D) \cos\chi$$

$$+ \{\beta\, C \int w(h)\, dh\}\, K(D)\omega \cos\lambda_n \cos\lambda_s \sin\omega(t-12)$$

$$+ \{\gamma\, C \int w(h)\, dh\}\, K(D) \qquad (8.2a)$$

and

$$\tau_{v_n}(t) = \{N_d(t_{ss})\, C \int g(h)\, dh\}\, e^{-\delta(t-t_{ss})}$$

$$+ \{N_\infty\, C \int g(h)\, dh\}\, (1-e^{-\delta(t-t_{ss})}) \qquad (8.2b)$$

Imposition of the continuity criteria

$$\tau_{v_d}(t_{ss}) = \tau_{v_n}(t_{ss})$$

restricts

$$N_d(t_{ss})\, C \int g(h)\, dh = \tau_{v_d}(t_{ss})$$

In the study, updating was effected using only vertical time delay data, τ_v . In this case there is no need to explicitly define the profiles $w(h)$ and $g(h)$. By defining

$$\begin{aligned} \alpha' &= \alpha\, C \int w(h)\, dh \\ \beta' &= \beta\, C \int w(h)\, dh \\ \gamma' &= \gamma\, C \int w(h)\, dh \\ N_\infty' &= N_\infty\, C \int g(h)\, dh \end{aligned} \qquad (8.3)$$

then Eqs. (8.2) yield

$$\tau_{v_d}(t) = \alpha' K(D)\cos\chi + \beta' K(D)\, \omega \cos\lambda_n \cos\lambda_s \sin\omega(t-12)$$

$$+ \gamma' K(D) \qquad (8.4a)$$

for the daytime

and

$$\tau_{v_n}(t) = \tau_{v_d}(t_{ss}) + N'_\infty (1-e^{-\delta(t-t_{ss})}) \qquad (8.4b)$$

for the nighttime.

Thus a fit is made directly for α', β', γ', and N'_∞ without explicit definition of $f(h)$ and $g(h)$. In the implementation of the fitting process, the daytime function Eq. (8.4a) would be fit first so as to define $\tau_{v_d}(t_{ss})$ which is required for the nighttime function given by Eq. (8.4b). The fitting functions $\tau_{v_d}(t)$ and $\tau_{v_n}(t)$ as given by Eqs. (8.4) are linear in the fitting parameters α', β', γ', and N'_∞. Thus it is possible to fit this model directly to the residuals of the observation station data obtained in Algorithm I.

The minimum length of the fitting time span is dictated by the model itself. The model is a function of local time. Thus, in order to obtain both day and night estimates at any observation station, allowing for the varying longitudes of the stations, the minimum fitting time span is 24 hours or less. The length of the span that was chosen for the study was taken as 24 hours to be consistent with our attempt to track the daily variations expected in the residuals. A suitable prediction span (that is, the time span over which the fitted parameters are used for updating) for purposes of making the model responsive to fluctuations in the residuals was found to be 3 hours. The time between the end of the fitting span and the beginning of the prediction span was taken to be 1/2 hour. In an operational system this would correspond to the time required for a central ground facility to

1) gather data from the system ground stations
2) perform the computations
3) inject corrections into the satellite memory

8.5.3 Algorithm III

Algorithm III is an alternative approach to a real-time updating scheme. The fundamentals of the algorithm are given in Section 6.6.

9. EVALUATION RESULTS

9.1 INTRODUCTION

In Section 8.1, the general outline of the evaluation of the algorithms in terms of evaluation conditions was discussed and the particulars involved in the implementations of each of the algorithms were given in Sections 8.5.1, 8.5.2, 8.5.3. The basis of the evaluation of each algorithm was the difference in nanoseconds referenced to 1600 MHz between the predicted vertical group time delay and the group time delay as inferred from the experimental Faraday rotation data, τ_{v_e} . This difference, denoted as $\delta\tau_v$, is termed the residual.

Due to constraints imposed on the study and the expense of numerical integrations inherent to the algorithms, it was necessary to pick from each evaluation condition a representative data rate and subset of days on which to base the evaluation. The data rate was taken as one data point per 20 minute interval. The representative subset of days for each evaluation condition is called the subsetted evaluation condition and is given in Table 9.1. In future references, the term evaluation condition will mean the subsetted evaluation condition.

The results presented for each of the evaluation conditions to the extent permitted by the Faraday rotation data are:

1) Plots of the monthly rms of τ_{v_e} and $\delta\tau_v$ (for each algorithm) for each one hour (UT) interval, for each station (both evaluation and observation), for each month of the evaluation condition, together with the rms value of τ_{v_e} and $\delta\tau_v$ over the month and the number of residuals used in computing these values (Appendices A and B).

2) Plots of the cumulative frequency distributions of the τ_{v_e} and $\delta\tau_v$ (for each algorithm) over the entire span of months of the evaluation condition together with the rms value of τ_{v_e} and $\delta\tau_v$ over the entire span and the number of residuals used in computing these values (Appendix C).

TABLE 9.1

SUBSETTED EVALUATION CONDITIONS

Evaluation Condition	Subset of Data Used in Study
1	Day 1 to 91 - 1968 (January, February, March)
2	Day 1 to 91 - 1968 (January, February, March)
3	Days 1 to 31, 91 to 120, 182 to 212 - 1965 (January, April, July)
4	Days 1 to 31, 92 to 121, 183 to 213, 275 to 305 - 1968 (January, April, July, October)
5	Days 1 to 31, 91 to 120, 182 to 212, 274 to 304 - 1969 (January, April, July, October)

3) Tables of the values of the correlation coefficient of the $\delta\tau_v$ residuals (for each algorithm) for each of the station pairs designated in Table 9.2, for each hour (UT) interval over the month of the evaluation condition, together with the number of residuals used in computing each correlation coefficient (Appendix D).

4) Tables of the values of the correlation coefficient of the $\delta\tau_v$ residuals (for each algorithm) for each of the station pairs designated in Table 9.2 over the entire span of months of the evaluation condition and the number of residuals used in computing these values (Appendix E).

5) Tables of the cumulative frequency distribution of the daily correlation coefficient of the $\delta\tau_v$ residuals (for each algorithm) for each of the station pairs designated in Table 9.2 over the entire span of months of the evaluation condition and the number of residuals used (Appendix F).

On each of the cumulative frequency plots, Appendix C, a table has been added which summarizes the plot by giving percentage of τ_{v_e} and $\delta\tau_v$ values which fall in the four intervals, ± 3 ns, ± 9 ns, ± 18 ns, and ± 27 ns. (Note that 1 ns $\simeq$ 1 foot.) The plots are given on a probability grid with the ordinate range 0.01 percent to 99.99 percent and the abscissa range -70 ns to +110 ns in 1 ns steps. To determine 0 percent subtract 1 ns from the left-most abscissa point of the curve and to determine 100 percent add 1 ns to the right-most abscissa point of the curve. The residual pairs used in computing the correlation coefficients were separated by a time interval of not more than 15 minutes. A given residual was not used in more than one residual pair for a given correlation coefficient evaluation pair.

9.2 DISCUSSION

The results of the study are given in detail in the figures and tables located in the appendices. In this section we wish to bring out some of the salient features of the results.

Table 9.3 summarizes the rms of the $\delta\tau_v$ residuals over evaluation conditions for the evaluation stations. Table 9.4 summarizes the rms of the $\delta\tau_v$ residuals over

TABLE 9.2

CORRELATION COEFFICIENT EVALUATION PAIRS

Evaluation Condition	Station Pair
1	Stanford ATS3 - Stanford ATS1 Stanford ATS3 - Urbana ATS3 Urbana ATS3 - Sagamore Hill ATS3
2	Stanford ATS3 - Stanford ATS1
5	Stanford ATS1 - Stanford ATS3 Stanford ATS1 - Clark Lake ATS1 Stanford ATS1 - Fort Collins ATS1 Rosman ATS3 - Urbana ATS3 Arecibo ATS3 - Cold Bay ATS1

TABLE 9.3

SUMMARY OF RMS VALUES OVER EVALUATION CONDITIONS FOR EVALUATION STATIONS

Station	E.C.	τ_{v_e} (ns)	$\delta\tau_v$ Alg. I(ns) ($\delta\tau_v/\tau_{v_e}$)	$\delta\tau_v$ Alg. II(ns) ($\delta\tau_v/\tau_{v_e}$)	$\delta\tau_v$ Alg. III(ns) ($\delta\tau_v/\tau_{v_e}$)	Number of Residuals Used In Computation of RMS
Stanford ATS1	1	15.06	5.41 (0.36)	4.63 (0.31)	3.24 (0.22)	5776
Stanford ATS3	1	15.35	5.72 (0.37)	4.81 (0.31)	3.61 (0.24)	5782
Urbana ATS3	1	15.67	6.87 (0.44)	4.07 (0.26)	4.00 (0.26)	5110
Sagamore Hill ATS3	1	15.41	7.20 (0.47)	4.71 (0.31)	4.65 (0.30)	5391
Stanford ATS1	2	15.23	5.50 (0.36)	4.01 (0.26)	3.14 (0.21)	5978
Stanford ATS3	2	15.48	5.73 (0.37)	4.13 (0.27)	3.53 (0.23)	5980
Urbana ATS3	2	15.67	6.87 (0.44	3.38 (0.22)	3.85 (0.25)	5168
Honolulu SYNCOM3	3	9.92	3.37 (0.34)	3.14 (0.32)	3.16 (0.32)	4154
Sagamore Hill ATS3	4	13.35	5.97 (0.45)	4.23 (0.32)	3.99 (0.30)	5960
Honolulu ATS1	4	25.77	10.1 (0.39)	6.68 (0.26)	8.72 (0.34)	5963
Stanford ATS1	5	14.33	6.11 (0.43)	3.48 (0.24)	3.52 (0.25)	8301
Stanford ATS3	5	17.61	7.59 (0.43)	4.37 (0.25)	4.99 (0.28)	1898
Clark Lake ATS1	5	19.17	8.50 (0.44)	3.81 (0.20)	4.19 (0.22)	3928
Cold Bay ATS1	5	11.58	5.55 (0.48)	3.83 (0.33)	3.75 (0.32)	5636
Fort Collins ATS1	5	14.38	7.19 (0.50)	3.88 (0.27)	4.17 (0.29)	6276
Urbana ATS3	5	14.57	7.20 (0.49)	3.65 (0.25)	4.71 (0.32)	8522
Rosman ATS3	5	13.27	5.75 (0.43)	3.36 (0.35)	4.12 (0.31)	5652
Arecibo ATS3	5	15.38	6.56 (0.43)	5.44 (0.35)	4.70 (0.31)	1894
ALL	ALL	15.68	6.60 (0.42)	4.27 (0.27)	4.38 (0.28)	97369

TABLE 9.4

SUMMARY OF RMS VALUES OVER
EVALUATION CONDITIONS FOR OBSERVATION STATIONS

Station	E.C.	τ_{v_e} (ns)	$\delta\tau_v$ Alg. I(ns) ($\delta\tau_v/\tau_{v_e}$)	$\delta\tau_v$ Alg. II(ns) ($\delta\tau_v/\tau_{v_e}$)	$\delta\tau_v$ Alg. III(ns) ($\delta\tau_v/\tau_{v_e}$)	Number of Residuals Used in Computation of RMS
Arecibo ATS3	1	19.35	8.13 (0.42)	4.53 (0.23)	4.89 (0.25)	5180
Honolulu ATS1	1	28.13	11.73 (0.42)	7.88 (0.28)	10.70 (0.38)	5632
Sagamore Hill ATS3	2	15.30	7.12 (0.47)	4.01 (0.26)	4.47 (0.29)	5607
Arecibo ATS3	2	19.46	8.14 (0.42)	4.17 (0.21)	4.75 (0.24)	5294
Honolulu ATS1	2	28.34	11.81 (0.42)	7.79 (0.27)	10.73 (0.38)	5717
Stanford SYNCOM 3	3	5.62	1.47 (0.26)	1.32 (0.23)	1.43 (0.25)	4401
Stanford ATS1	4	14.06	4.79 (0.34)	2.59 (0.18)	3.11 (0.22)	6305
Sagamore Hill ATS3	5	12.99	6.18 (0.48)	4.01 (0.31)	4.57 (0.35)	8538
Edmonton ATS1	5	13.90	7.70 (0.55)	5.10 (0.37)	5.06 (0.36)	7582
Honolulu ATS1	5	24.41	9.78 (0.40)	5.33 (0.22)	7.68 (0.31)	8236
ALL	ALL	19.53	8.29 (0.42)	5.09 (0.26)	6.43 (0.33)	62492

evaluation conditions for the observation stations. These tables also include a column for the rms τ_{v_e} values to provide a basis for measuring the performance of each of the algorithms. The τ_{v_e} is the experimentally determined vertical time delay induced by the ionosphere. The $\delta\tau_v$ is the vertical time delay remaining after making a correction. Thus $\delta\tau_v/\tau_{v_e}$, which have been included parenthetically under the time value for each algorithm, give a measure of the performance of the algorithm.

In general, as indicated in Table 9.3, the prediction abilities of Algorithms II and III are about the same, the relative prediction ability varying from case to case. In the case of Honolulu, Algorithm II is superior to Algorithm III as can be seen in both Tables 9.3 and 9.4. In Evaluation Condition 3, a period of low solar activity, the difference is negligible.

Summarized, over all evaluation stations and over all evaluation conditions, the rms value of τ_{v_e} is 15.68 ns. The rms of the residuals $\delta\tau_v$ for Algorithms I, II, and III, are respectively 6.60 ns, 4.27 ns, and 4.38 ns. Using these rms values, the ratio $\delta\tau_v/\tau_{v_e}$ for each algorithm is respectively 0.42, 0.27, 0.28. These results indicate that at the present time long-term predictions (3-6 months) of the rms vertical time delay can be made to within 42 percent and real-time predictions to within 27 or 28 percent. As pointed out in Section 8.3, the only data used in the present study for updating in Algorithms II and III were the τ_{v_e} values at the stations designated as observation stations.

Overall, the long-term predictions of Algorithm I tend to be low (i.e., Algorithm I tended to under predict τ_{v_e}). The Algorithm II and III residuals are more normally distributed about zero than are the Algorithm I residuals. A more detailed picture of the distribution of the errors is given in Appendix C.

The extreme values of τ_{v_e} and $\delta\tau_v$ observed in the study occurred at Honolulu in Evaluation Conditions 1 and 2. The values were 86 ns in τ_{v_e}, -54 ns in $\delta\tau_v$ Alg. I, -50 ns in $\delta\tau_v$ Alg. II, and -43 ns in $\delta\tau_v$ Alg. III.

10. FUTURE EFFORTS

10.1 INTRODUCTION

The study described above represents a first attempt to synthesize a prediction technique to estimate the ionospheric induced group time delay. Because of this, its scope had to be constrained so that several important areas of interest could not be explored. The evaluation of the two real-time algorithms described in Section 8 indicated that, while both were acceptable from a statistical viewpoint, periods of time did exist when further improvements would be necessary in order to meet the navigation accuracy requirements. In addition, several fundamental questions have arisen during the development of the algorithms that need be answered to substantiate the validity of the prediction methods. Consequently, it is suggested that extension or continuance of this study be directed to the following items.

10.2 ADDITIONAL TEST FOR REGIONAL PREDICTIONS

In any future studies, efforts should be made to obtain an expanded data base giving adequate coverage in longitude, latitude and geomagnetic dip along with solar activity. In particular, it would be useful to obtain data at a given location from two or more satellites so as to obtain a data base which represented a navigation situation. Due to inherent limitations of Faraday rotation data in providing the expanded geographic coverage just mentioned, other sources of data will be required. One such source presently available would be the U.S. Navy Navigation Satellite System. Ionospheric refraction data which is presently available as a by-product of both the tracking and navigation process could be used to help establish a base to permit a world-wide evaluation. The only limitation of the data would be that it would provide only a measure of the ionospheric time delay to 1000 km (the nominal altitude of a satellite in the system). However, this would measure about 80 percent of the time delay to synchronous altitude satellites. One advantage of the ionospheric data obtained from the U.S. Navy Navigation Satellite System would be the measurement of the ionospheric induced range error over a large region of the sky during a transit of the satellite over a station. This would provide a measure of the correlation of the ionospheric range error from near-simultaneous observations which is the quantity of interest because of the hyperbolic nature of the pseudo-ranging system.

Preceding page blank

10.3 GLOBAL PREDICTIONS

It would be instructive to broaden the region over which the evaluation is made to determine the true global capability of the current technology. Each of the algorithms proposed in the study has inherent to it a global prediction capability. A priori estimates of the group time delay obtained through Algorithm I, which does not require real-time data, can be made for anywhere in the world subject only to specification of the predicted solar activity and the locations of the navigator and navigation satellite. The data base on which the a prior estimates are based consists of data from all parts of the world including such areas as Africa, Europe, Russia and mainland China. The real-time predictions, Algorithm II and III, can also be used in their current state to estimate the group time delay anywhere in the world. The information required to effect a real-time prediction is the position of the navigator and the navigation satellite and real-time data taken anywhere in the world.

It is important to note that all the algorithms utilized in this study are already defined in a global sense so that the only data that would be required is that on which the evaluation is to be based.

10.4 IMPROVEMENTS IN MODEL IONOSPHERES

The model ionospheres utilized in the study to represent the electron density as a function of space and time represent only a first attempt as discussed in Section 6. More detailed models do exist which could be adapted for utilization in the prediction algorithms [King and Ruster, 1971]. Improvements in the prediction accuracy are to be expected if more detailed model ionospheres are exploited.

10.5 UTILIZATION OF OTHER DATA IN THE PREDICTIONS

In the completed study, the data on which the real-time predictions were based were solely the group time delay inferred from Faraday data measured at the observation stations. There is a significant number of other types of data that could be used in the prediction algorithms. Some of these are: geomagnetic and solar indices, satellite observations such as the UV intensity and ionosonde data. These should be explored for their effectiveness in the predictions of the group time delay.

10.6 VALIDITY OF GROUP TIME DELAYS INFERRED FROM FARADAY ROTATION DATA

As discussed in Section 4, the group time delays were inferred from Faraday rotation data. This data, because of the $1/r^3$ (where r is geocentric distance) fall-off of the geomagnetic field, is sensitive to the lower ionosphere and insensitive to the higher ionosphere. Consequently, group time delays inferred from Faraday observations could be in significant error because of the uncertainties in the upper atmosphere. It is important that the group time delays as inferred from Faraday data be compared with simultaneous measurements of the group time delay itself. An experimental study directed to this end would establish a confidence in the Faraday data which does not currently exist.

10.7 EFFECT OF MEASUREMENT FREQUENCY IN FARADAY ROTATION OBSERVATIONS

The Faraday data utilized in the study was obtained from satellite frequencies in the neighborhood of 137 MHz (VHF). The data was then scaled to the 1600 MHz frequency of interest (L-band) by use of Eq. (4.2). While this formula is appropriate for a near-homogenous medium there is some question as to its applicability in a medium with sharp gradients in the electron density distribution [Guier, 1963] and [Kelso, 1964]. Experiments should be undertaken to confirm the validity of the extrapolation of the data from the VHF band to the L-band.

10.8 SCINTILLATIONS

Scintillations are characterized by amplitude and phase variation in radio waves that pass through the ionosphere. This phenomenon arises from irregularities in the electron density distribution. There is some concern as to the depth of the scintillations at L-band and whether they would impact significantly in the navigation measurements. Consequently, a study should be made to investigate the effect of scintillations.

10.9 VELOCITY OF PROPAGATION

There are several velocities of propagation associated with the transmission of electromagnetic energy: the phase velocity, the group velocity and the signal velocity. In the measurement of limited wave motion the velocity of interest is generally the signal velocity which is the velocity with which the main part of the wave motion propagates in a dispersive medium. The signal velocity is practically the same as the group velocity whenever the wave motion proceeds without strong absorption. As discussed in Section 4, the assumption that the signal velocity is equal to the group velocity is inherent to this study. This assumption should be studied to investigate the accuracy of the approximation for the L-band ranging system proposed for the High Altitude Navigation Satellite System.

REFERENCES

AVCO, "Natural Communications Study Phase 1 - Feasibility study on a reliable polar high-frequency communications system," Technical Report RAD-TR-63-37, July 31, 1963.

Bauer, S. J., "Ionospheric models and model ionospheres," Conference on Theoretical Ionospheric Models, University Park, Penna., June 14-16, 1971.

Brillouin, L., Wave Propagation and Group Velocity, Academic Press, New York, Ch. 4, 1960.

Budden, K. G., Radio Waves in the Ionosphere, Cambridge Univ. Press, Cambridge, 1961.

Burns, A. A. and Fremouw, E. J., "A real-time correction technique for transionospheric ranging error," IEEE Trans. on Antennas and Propagation, v. AP-18, no. 6, pp. 785-790, 1970.

Chandra, S. and Ragaswamy, S., "Geomagnetic and solar control of ionization at 1000 km," Journal of Atmospheric and Terrestrial Physics, v. 29, no. 3, pp. 259-265, 1967.

Da Rosa, A. V., "Propagation errors in the VHF satellite-to-aircraft ranging," IEEE Trans. on Antennas and Propagation, v. AP-17, no. 5, pp. 628-634, 1969.

Davies, K., Ionospheric Radio Propagation, National Bureau of Standards Monograph 80, U.S. Government Printing Office, pp. 301-309, 1965.

Department of the Air Force, HQ-SAMSO, "Ionospheric prediction model study," F04701-70Q 0020, April 24, 1970.

Guier, W. H., "Ionospheric contributions to the doppler shift at VHF from near-earth satellites," Applied Physics Laboratory Report CM-1040, July 1963.

Haydon, G. W. and Lucas, D. L., "Predicting ionospheric electron density profiles," Radio Science, v. 3, no. 1, pp. 111-119, 1968.

Hopfield, H. S., "Tropospheric effect on electromagnetically measured range: Prediction from surface weather data," Radio Science, v. 6, no. 3, pp. 357-367, 1971.

Hopfield, H. S., Private communication, January 1972.

Jones, W. B. and Gallet, R. M., "The representation of diurnal and geographic variations of ionospheric data by numerical methods," Telecommunications Journal, v. 29, no. 5, pp. 129-149, 1962.

Jones, W. B., Graham, R. P. and Leftin, M., "Advances in ionospheric mapping by numerical methods," U.S. Dept. of Comm./ESSA Report ERL 107-ITS 75, May 1969.

Jones, W. B. and Obitts, D. L., "Global representation of annual and solar cycle variation of foF2 monthly median 1954-1958," U.S. Dept. of Comm./OT Report ITSSR 3, October 1970.

Keane, L. M., "A multiple user satellite system for navigation and traffic control," EASCON '69 RECORD, Electronics and Aerospace Systems, IEEE, pp. 190-197, October 1969.

Kelso, J. M., Radio Ray Propagation in the Ionosphere, McGraw-Hill Book Company, New York, 1964.

King, J. W. and Ruster, R., "Simultaneous solutions of the ionization continuity equations and the equations of motion of the atmospheric constituents in calculations of electron densities for practical purposes," Conference on Theoretical Ionospheric Models, University Park, Penna., June 14-16, 1971.

Miller B., "Satellite clusters studied for tri-service navigation," Aviation Week and Space Technology, v. 92, no. 5, pp. 20-21, 1970.

Melton, W. C., Private communication, October 1971.

Rastogi, R. G., "Geomagnetic influence in the F1- and F2-regions of the ionosphere - Effect of solar activity," Journal of Atmospheric and Terrestrial Physics, v. 14, no. 1, pp. 31-40, 1959.

Ross, W. J., "Second-order effects in high-frequency transionospheric propagation," Journal of Geophysical Research, v. 70, no. 3, pp. 597-612, 1965.

Smith, R. L., "Properties of the outer ionosphere deduced from noise whistlers," Journal of Geophysical Research, v. 65, no. 11, pp. 3709-3716, 1961.

The Johns Hopkins University Applied Physics Laboratory, "Ionosphere prediction model study," TS-2232, June 1970.

Woodford, J. B. and Dutcher, R. L., "A satellite system to support an advanced air traffic control concept," Proc. of the IEEE, v. 58, no. 3, pp. 438-447, 1970.

Woodford, J. B., Melton, W. C. and Dutcher, R. L., "Satellite systems for navigation using 24-hour orbits," EASCON '69 RECORD, Electronics and Aerospace Systems, IEEE, pp. 184-189, October 1969.

Yeh, K. C. and Gonzalez, V. H., "Note on the geometry of the earth magnetic field useful to Faraday effect experiments," Journal of Geophysical Research, v. 65, no. 10, pp. 32[illegible]-3214, 1960.

Zacharisen, D. H., Ostrow, S. M., and Huang, G. C., "Validity of revision factors in updating long-term F2-layer maximum usable frequency predictions," U.S. Dept. of Comm./ESSA Technical Report ERLTM-ITS 156, February 1969.

APPENDIX A

PLOTS OF VERTICAL TIME DELAY AND RESIDUALS – HOURLY RMS

Preceding page blank

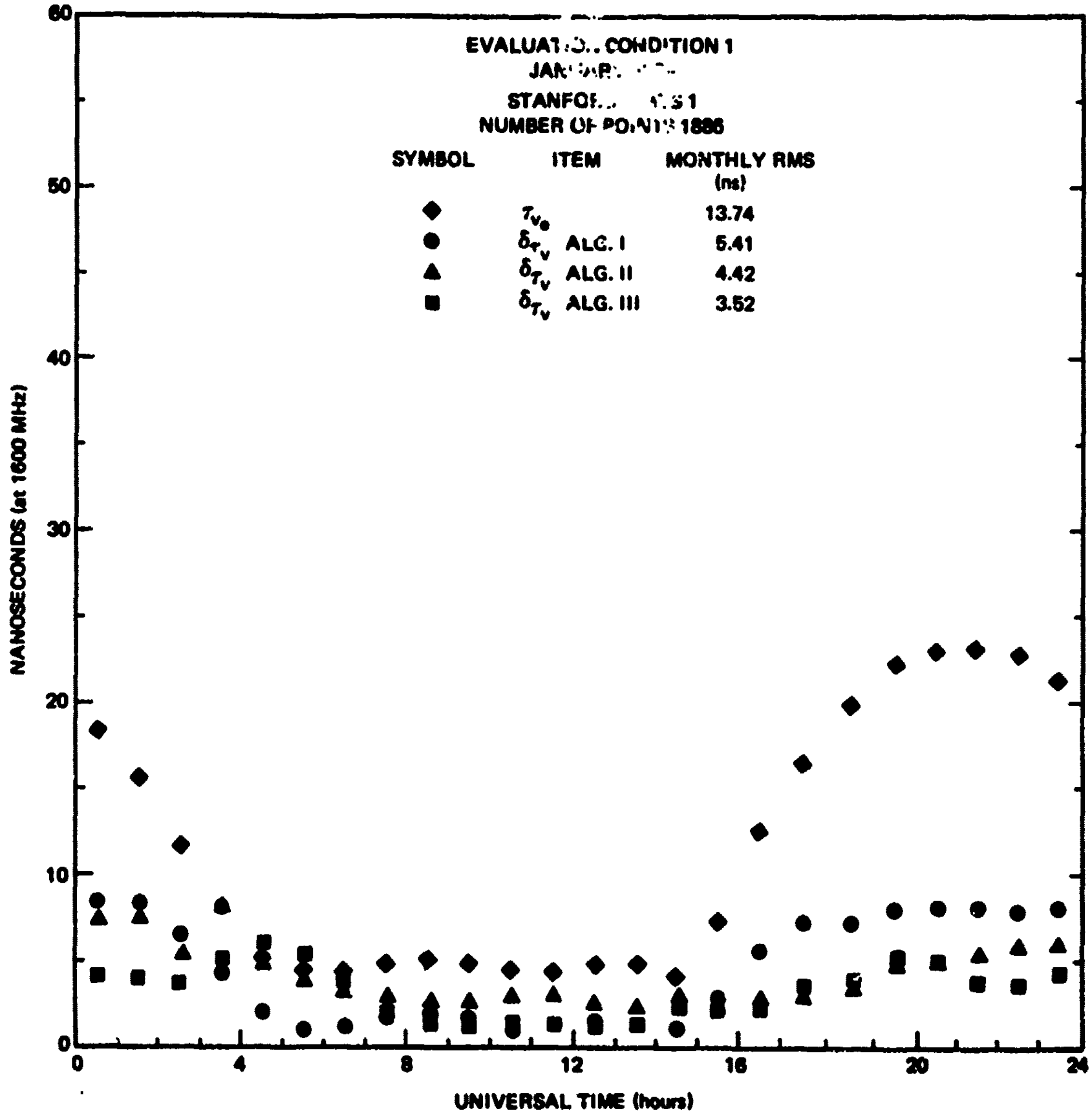

Fig. A.1 VERTICAL TIME DELAY AND RESIDUALS-HOURLY RMS OVER MONTH

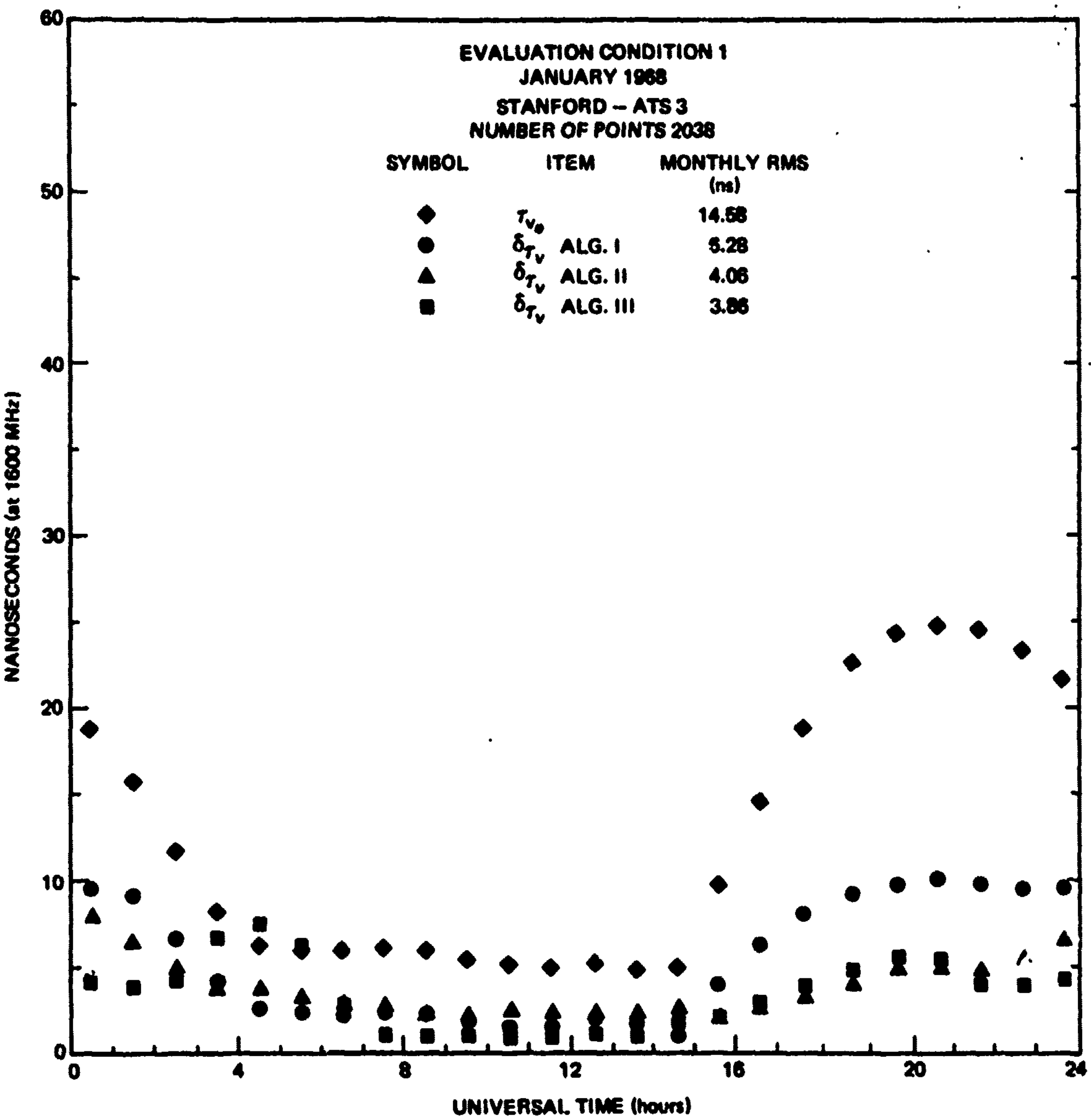

Fig. A.2 VERTICAL TIME DELAY AND RESIDUALS-HOURLY RMS OVER MONTH

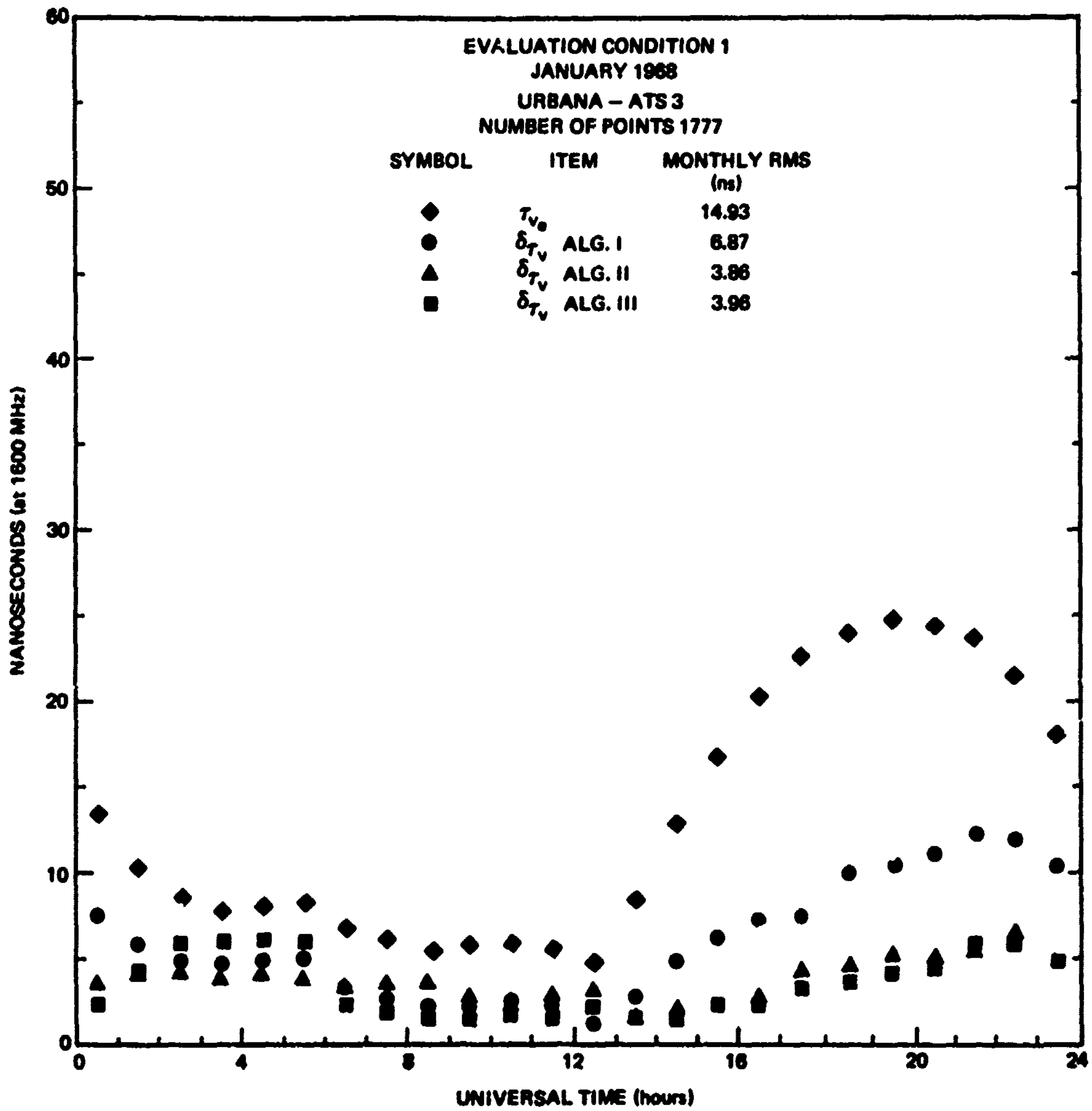

Fig. A.3 VERTICAL TIME DELAY AND RESIDUALS-HOURLY RMS OVER MONTH

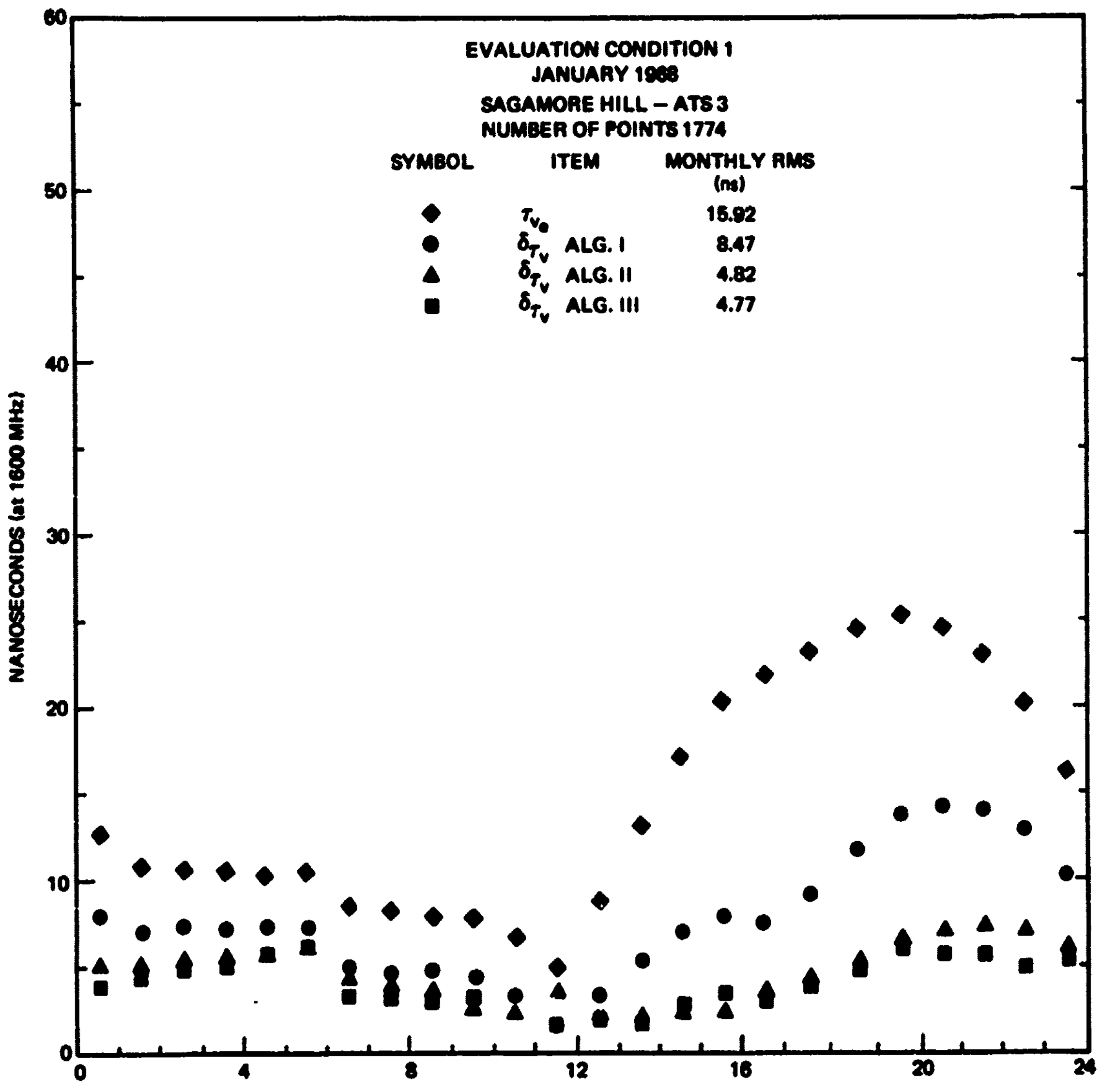

Fig. A.4 VERTICAL TIME DELAY AND RESIDUALS-HOURLY RMS OVER MONTH

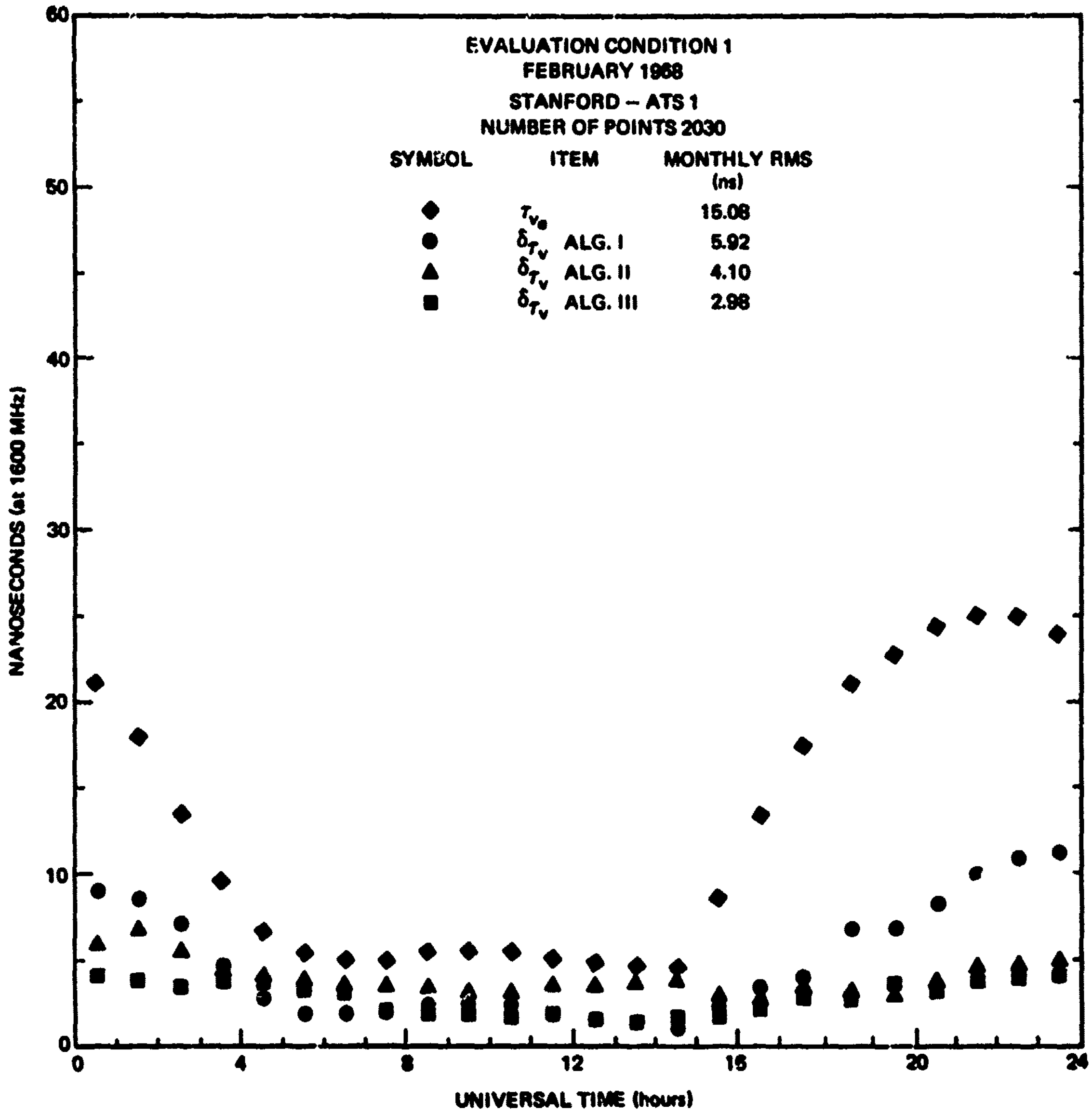

Fig. A.5 VERTICAL TIME DELAY AND RESIDUALS-HOURLY RMS OVER MONTH

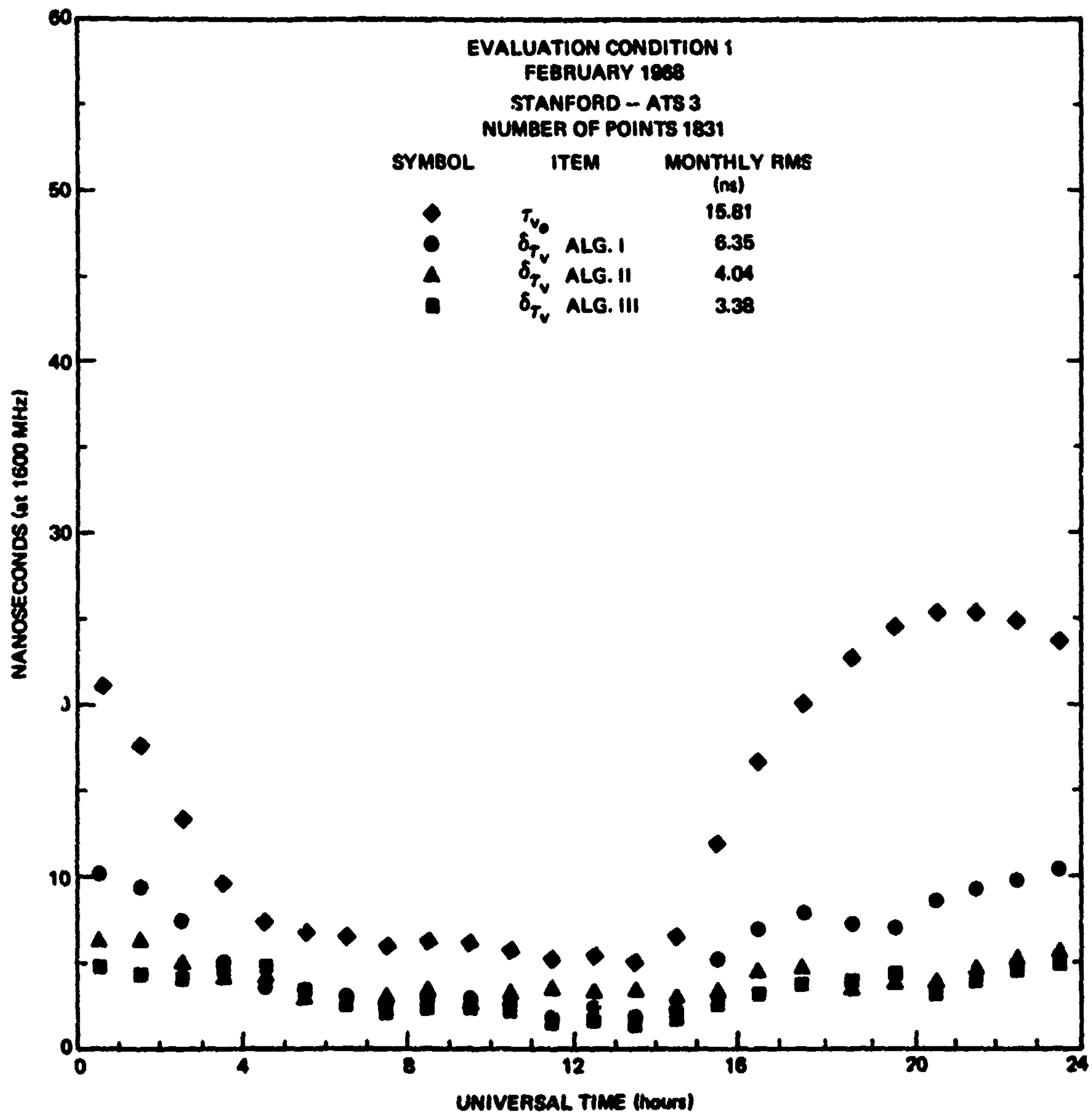

Fig. A.6 VERTICAL TIME DELAY AND RESIDUALS-HOURLY RMS OVER MONTH

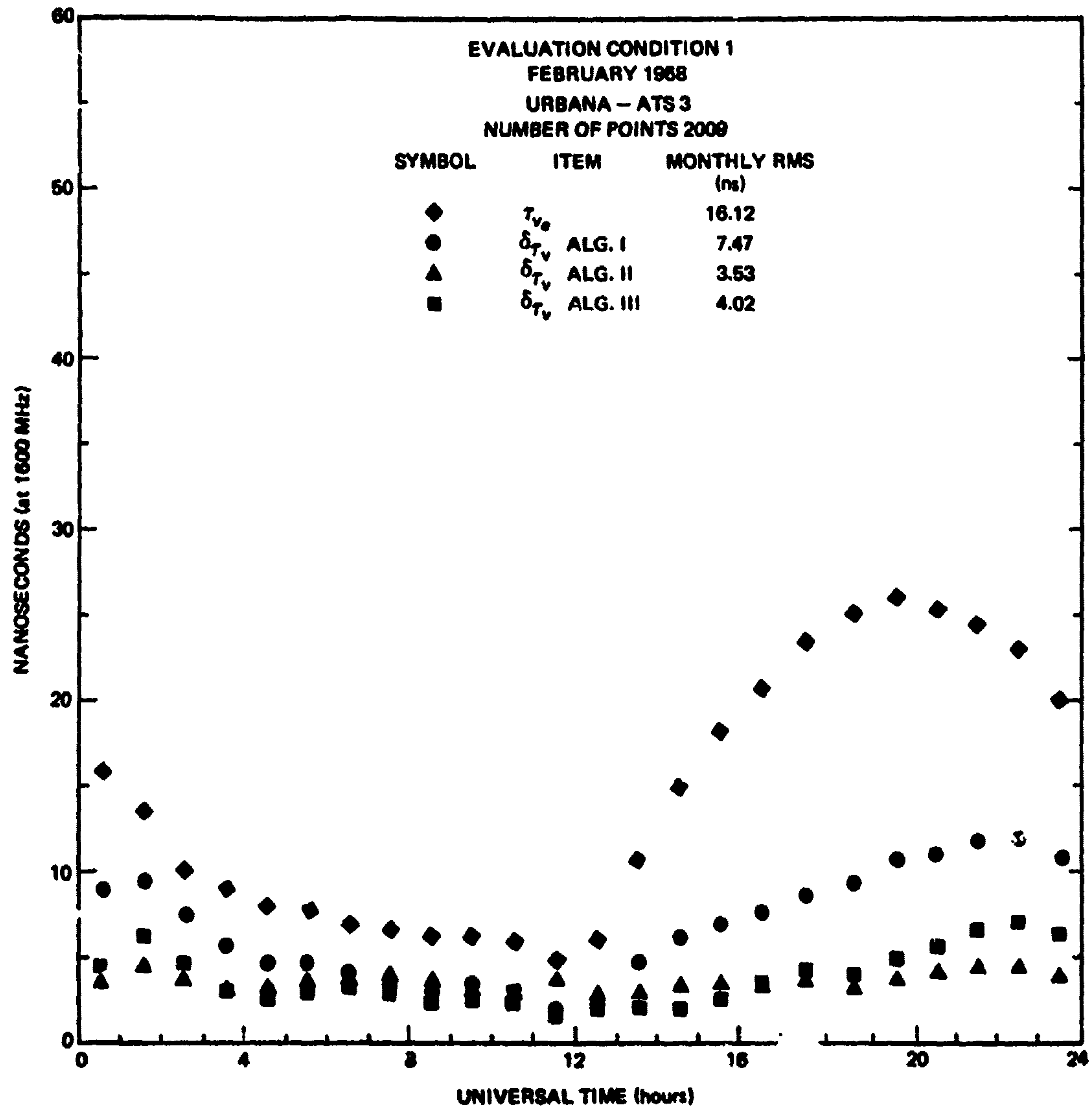

Fig. A.7 VERTICAL TIME DELAY AND RESIDUALS-HOURLY RMS OVER MONTH

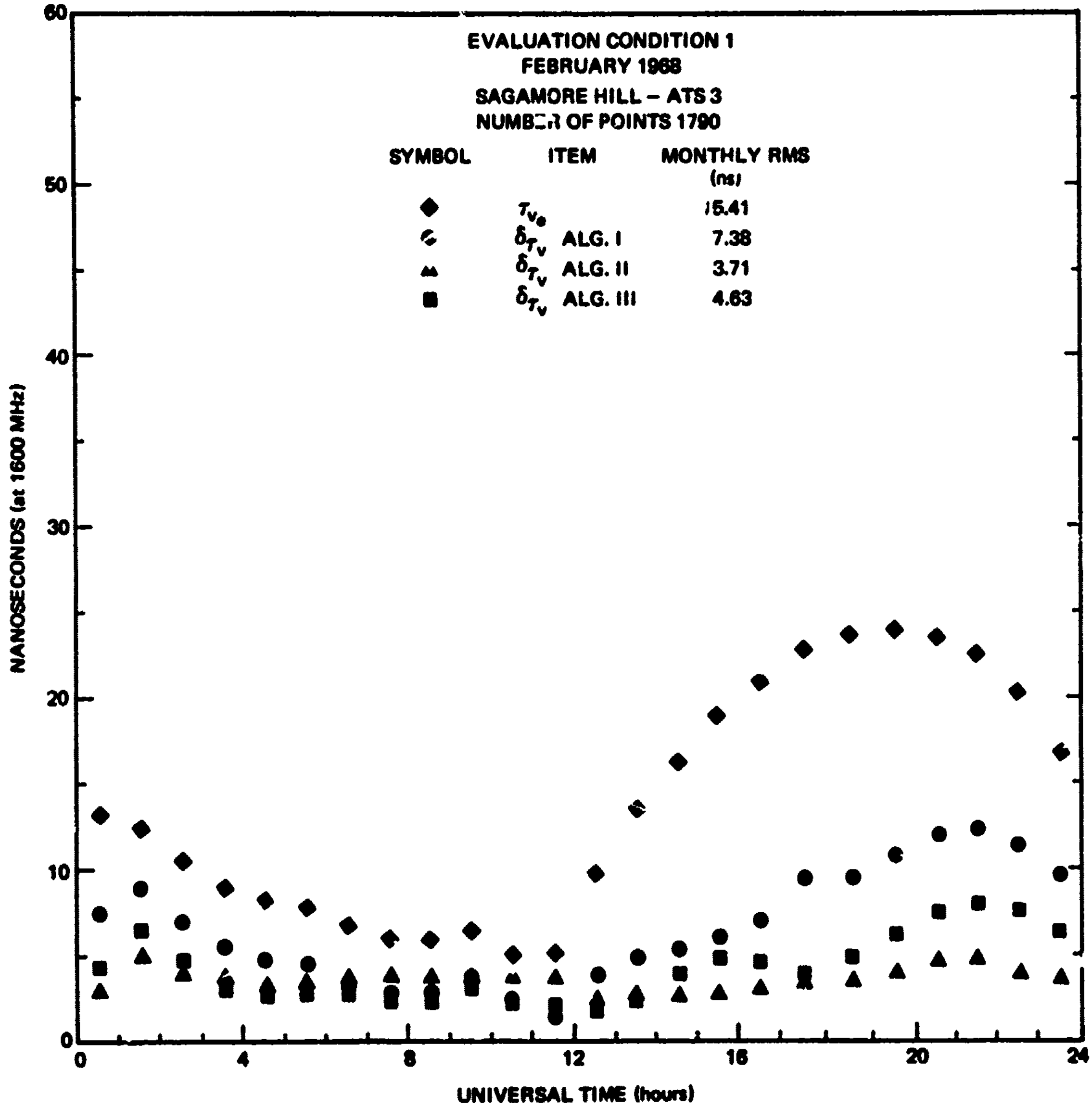

Fig. A.8 VERTICAL TIME DELAY AND RESIDUALS-HOURLY RMS OVER MONTH

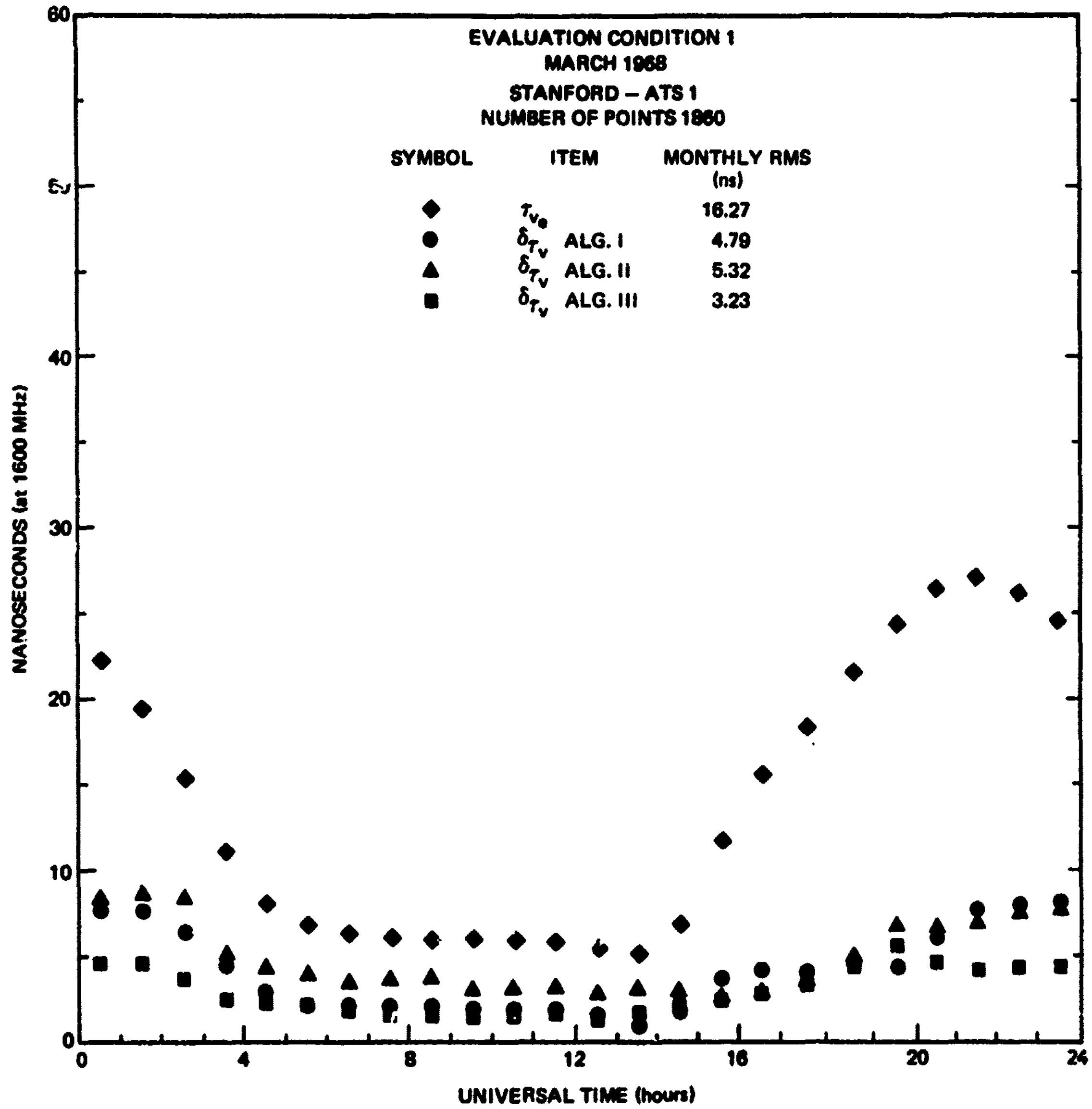

Fig. A.9 VERTICAL TIME DELAY AND RESIDUALS-HOURLY RMS OVER MONTH

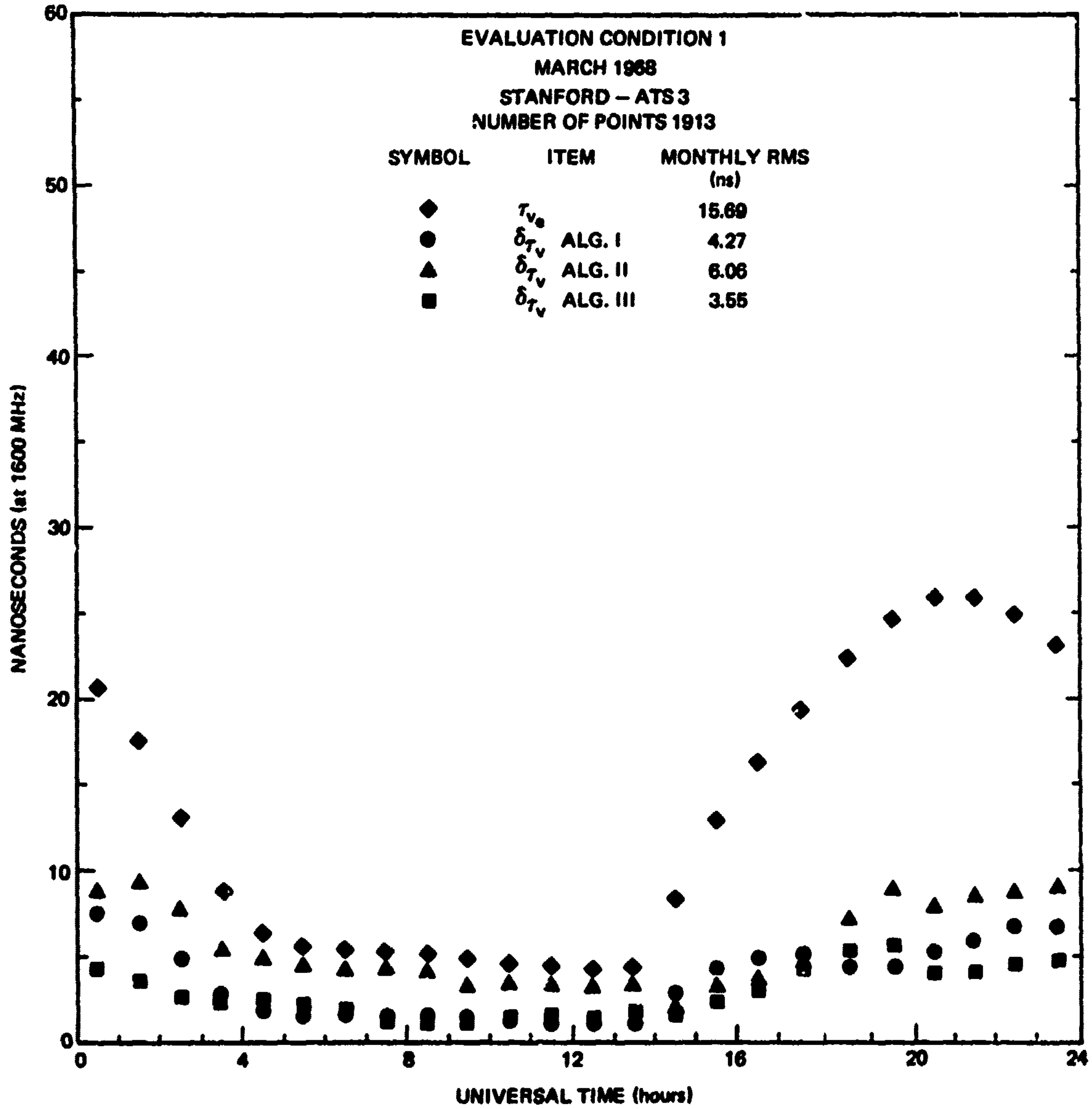

Fig. A.10 VERTICAL TIME DELAY AND RESIDUALS-HOURLY RMS OVER MONTH

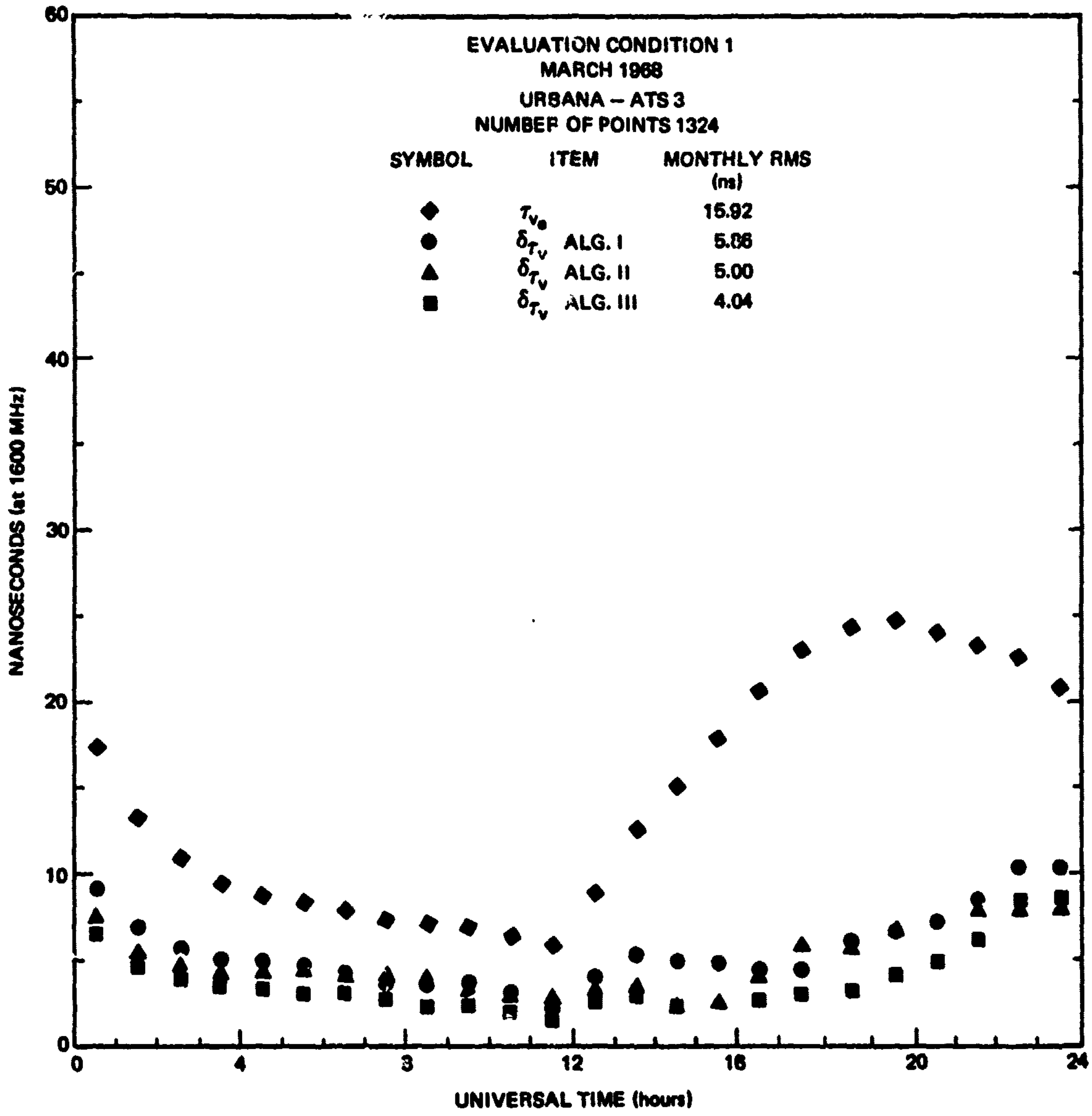

Fig. A.11 VERTICAL TIME DELAY AND RESIDUALS-HOURLY RMS OVER MONTH

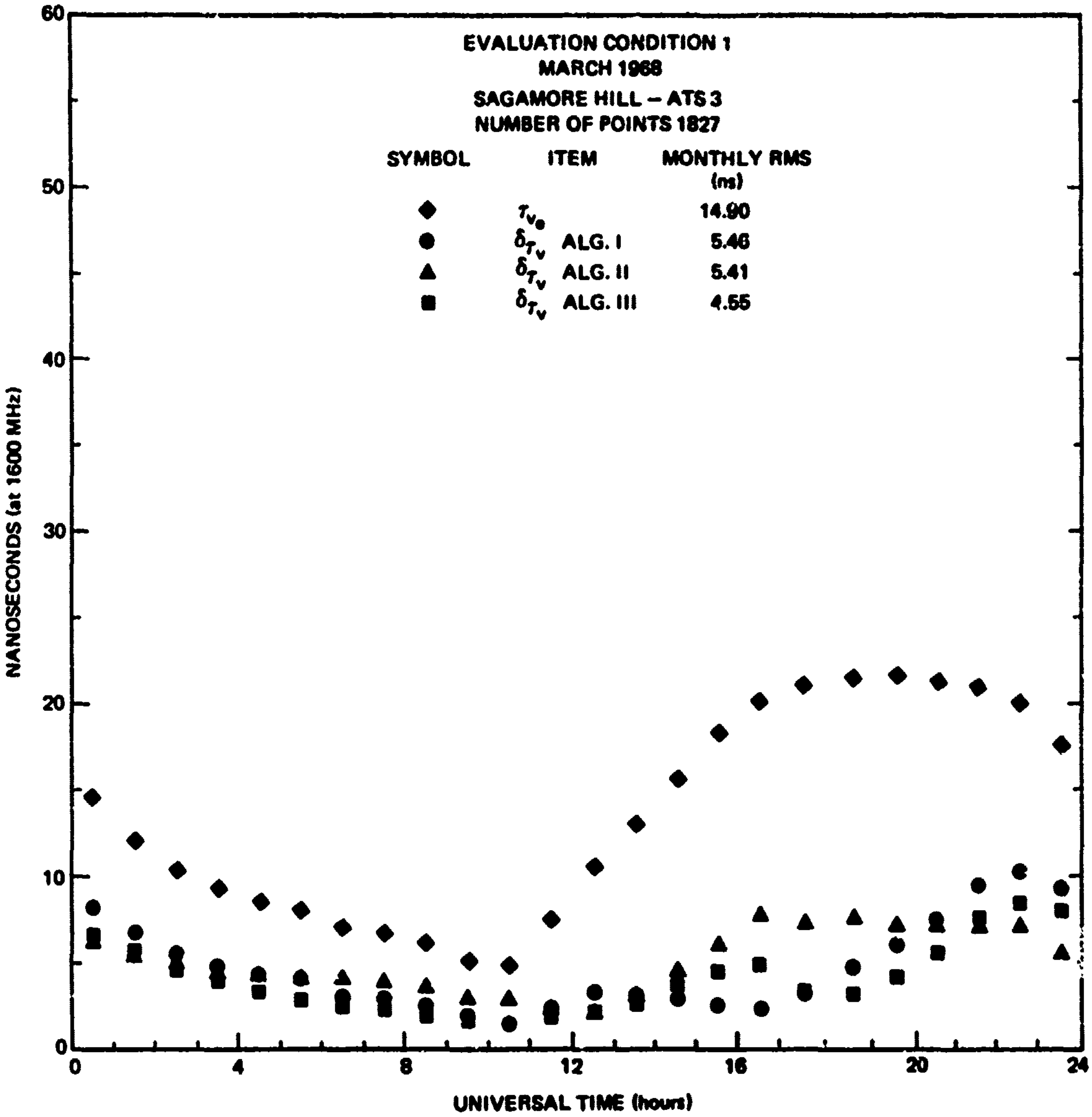

Fig. A.12 VERTICAL TIME DELAY AND RESIDUALS-HOURLY RMS OVER MONTH

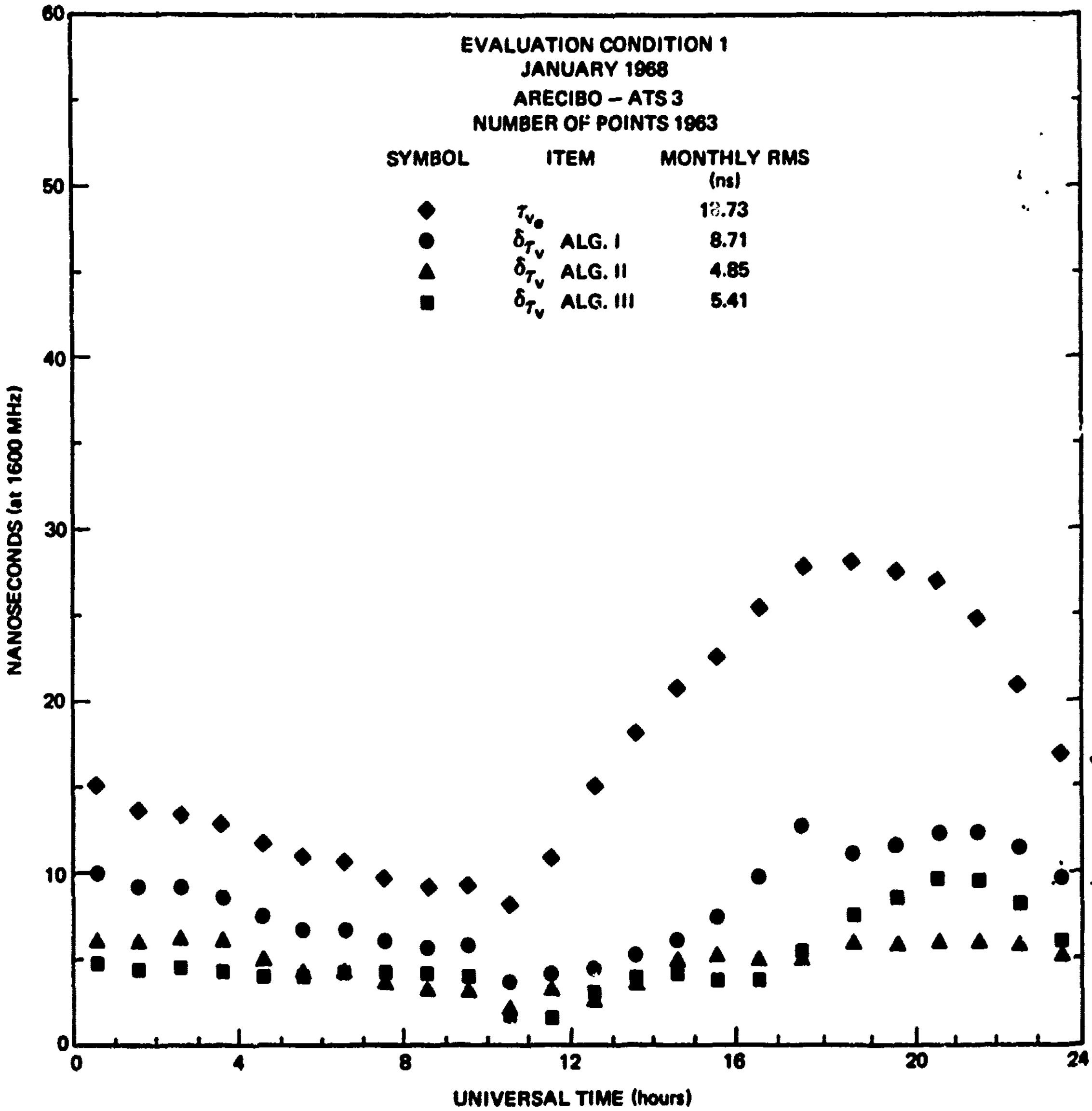

Fig. A.13 VERTICAL TIME DELAY AND RESIDUALS-HOURLY RMS OVER MONTH

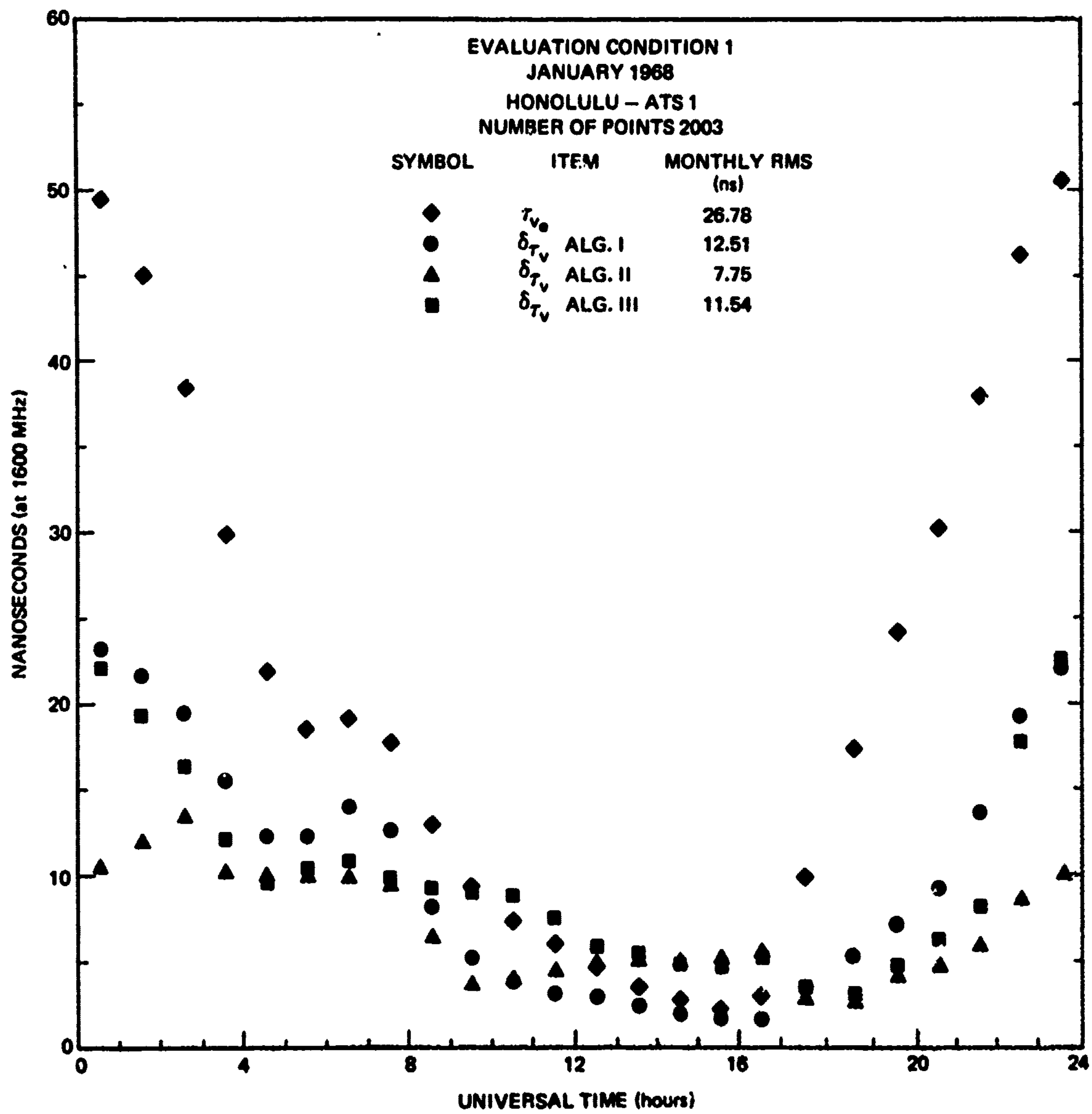

Fig. A.14 VERTICAL TIME DELAY AND RESIDUALS-HOURLY RMS OVER MONTH

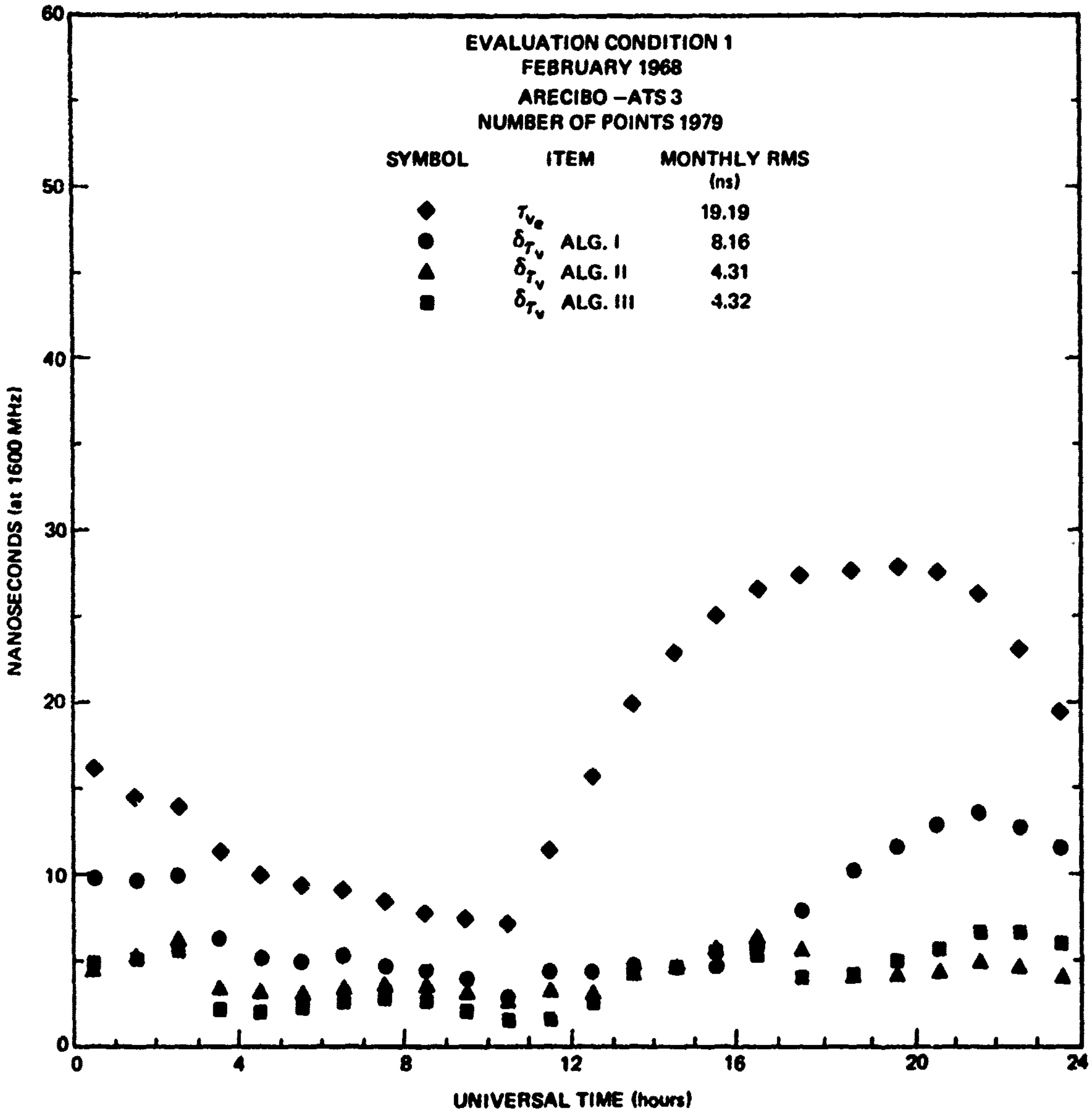

Fig. A.15 VERTICAL TIME DELAY AND RESIDUALS-HOURLY RMS OVER MONTH

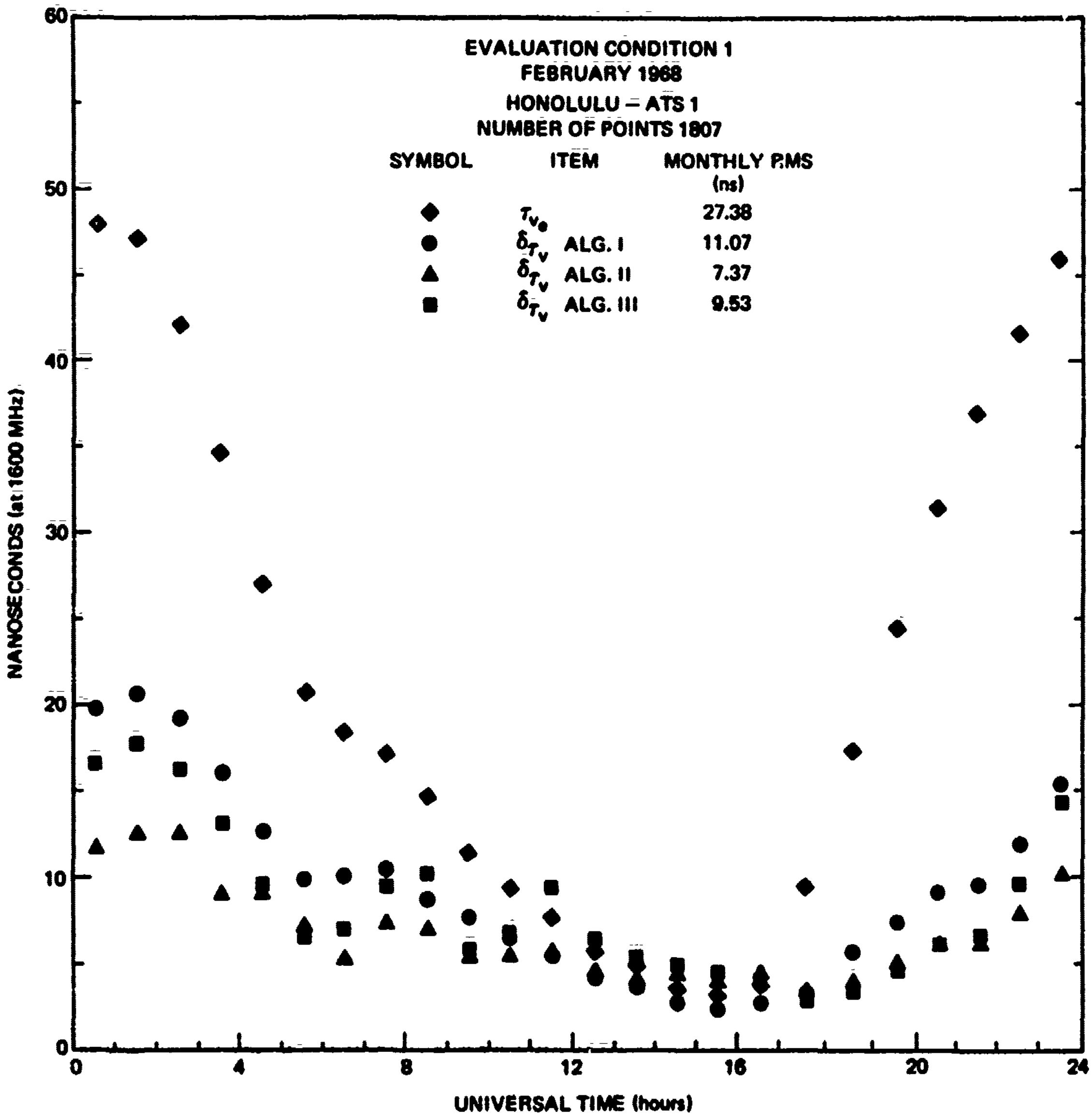

Fig. A.16 VERTICAL TIME DELAY AND RESIDUALS-HOURLY RMS OVER MONTH

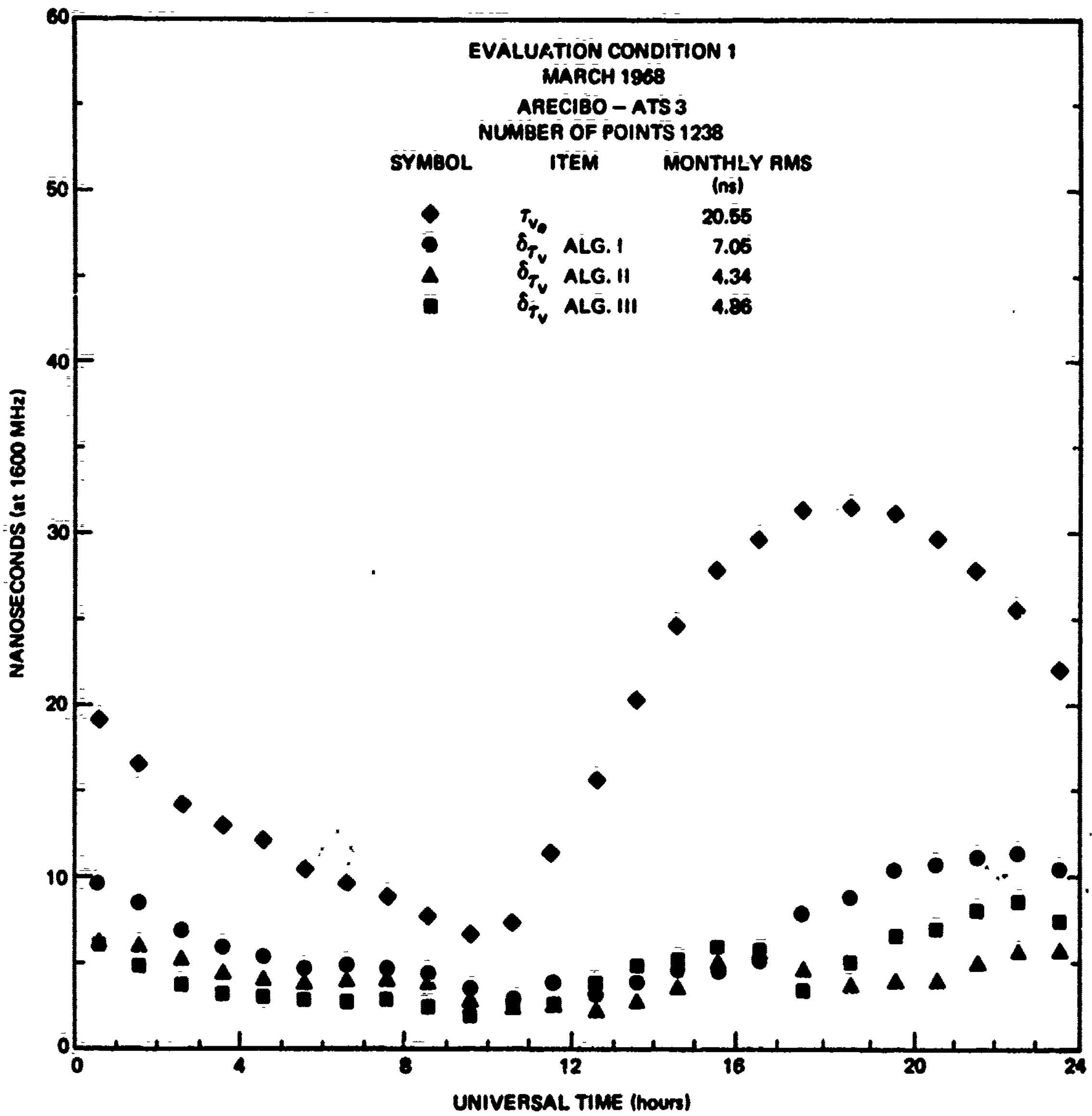

Fig. A.17 VERTICAL TIME DELAY AND RESIDUALS-HOURLY RMS OVER MONTH

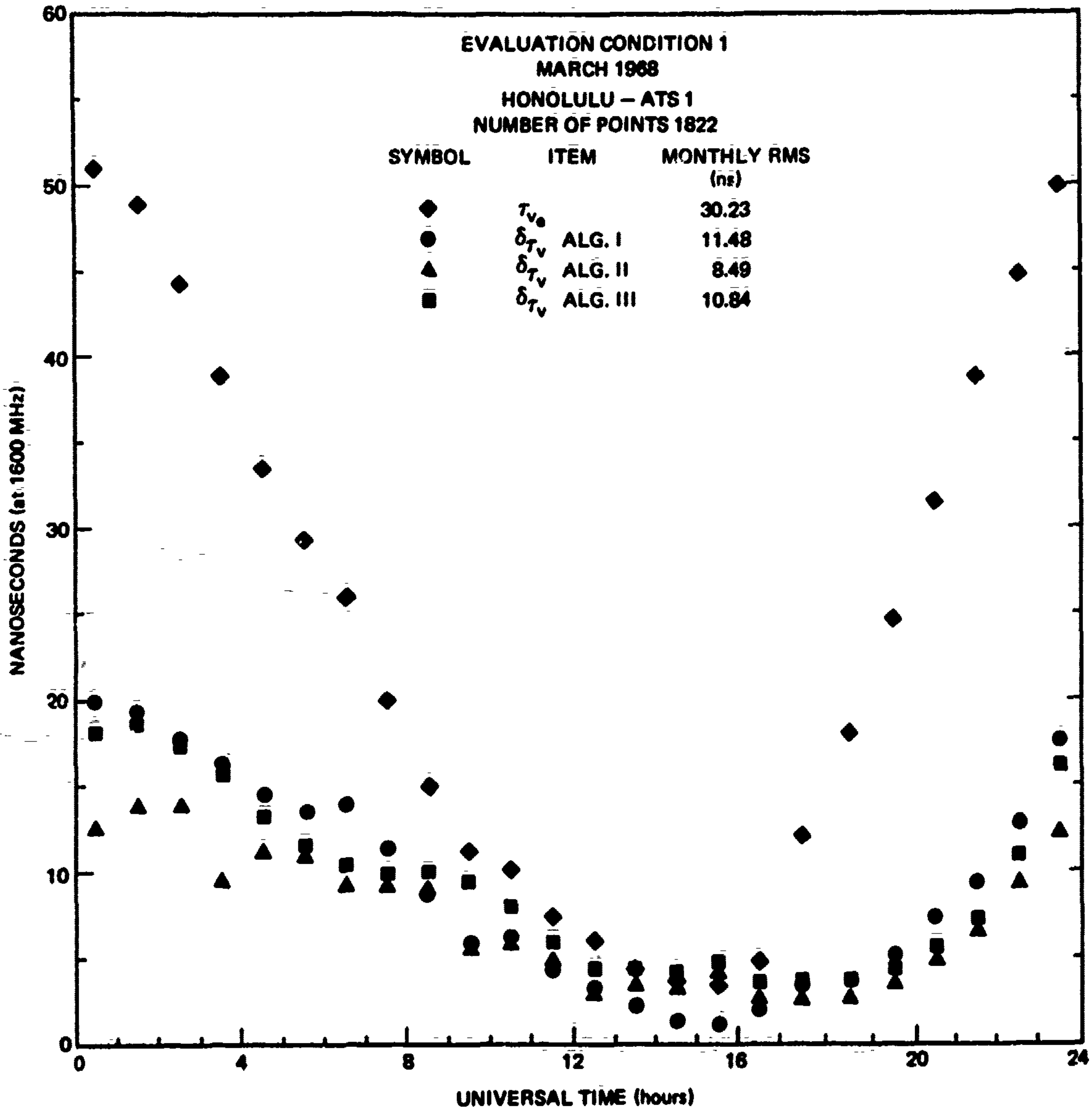

Fig. A.18 VERTICAL TIME DELAY AND RESIDUALS-HOURLY RMS OVER MONTH

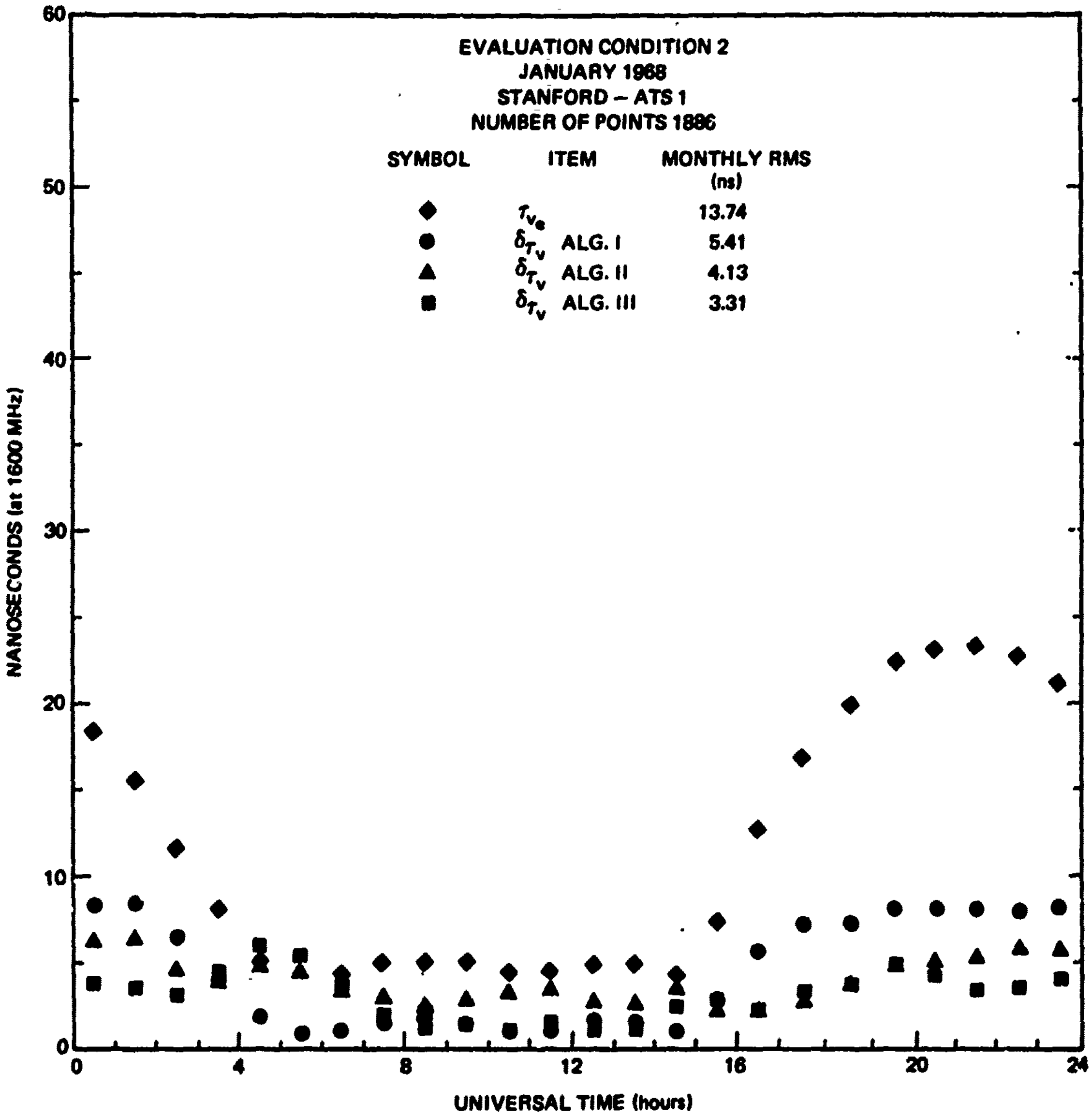

Fig. A.19 VERTICAL TIME DELAY AND RESIDUALS-HOURLY RMS OVER MONTH

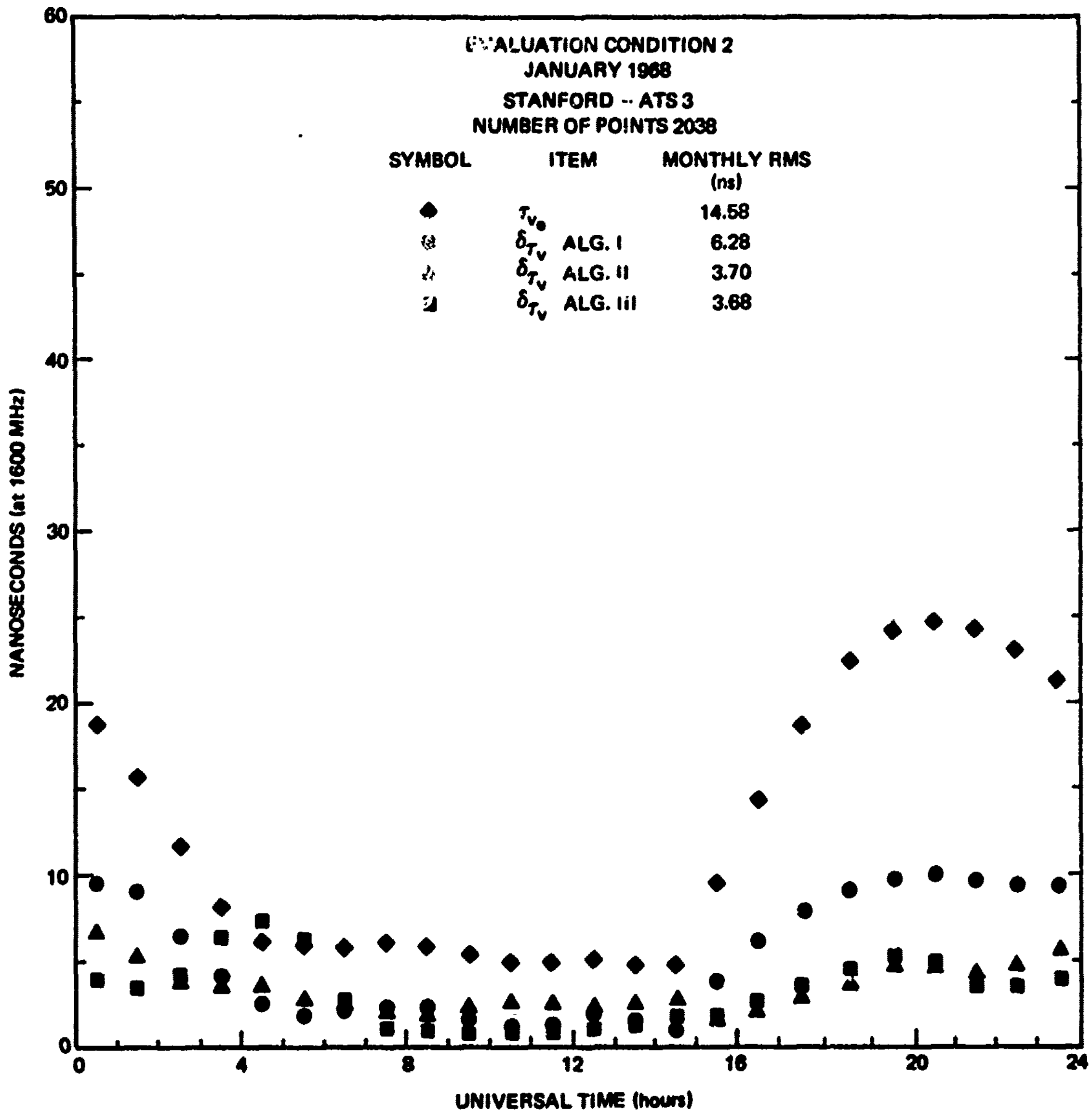

Fig. A.20 VERTICAL TIME DELAY AND RESIDUALS-HOURLY RMS OVER MONTH

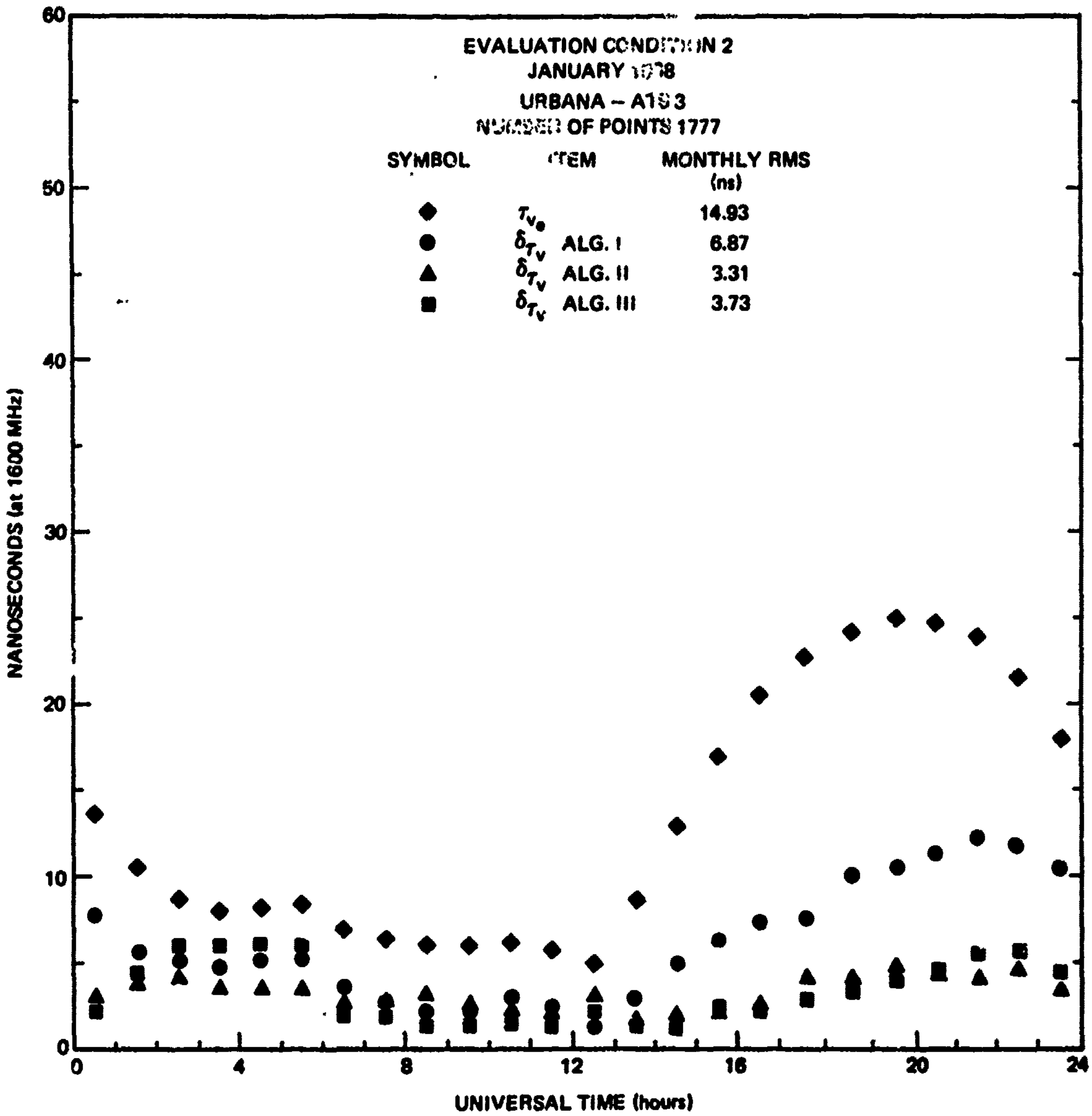

Fig. A.21 VERTICAL TIME DELAY AND RESIDUALS-HOURLY RMS OVER MONTH

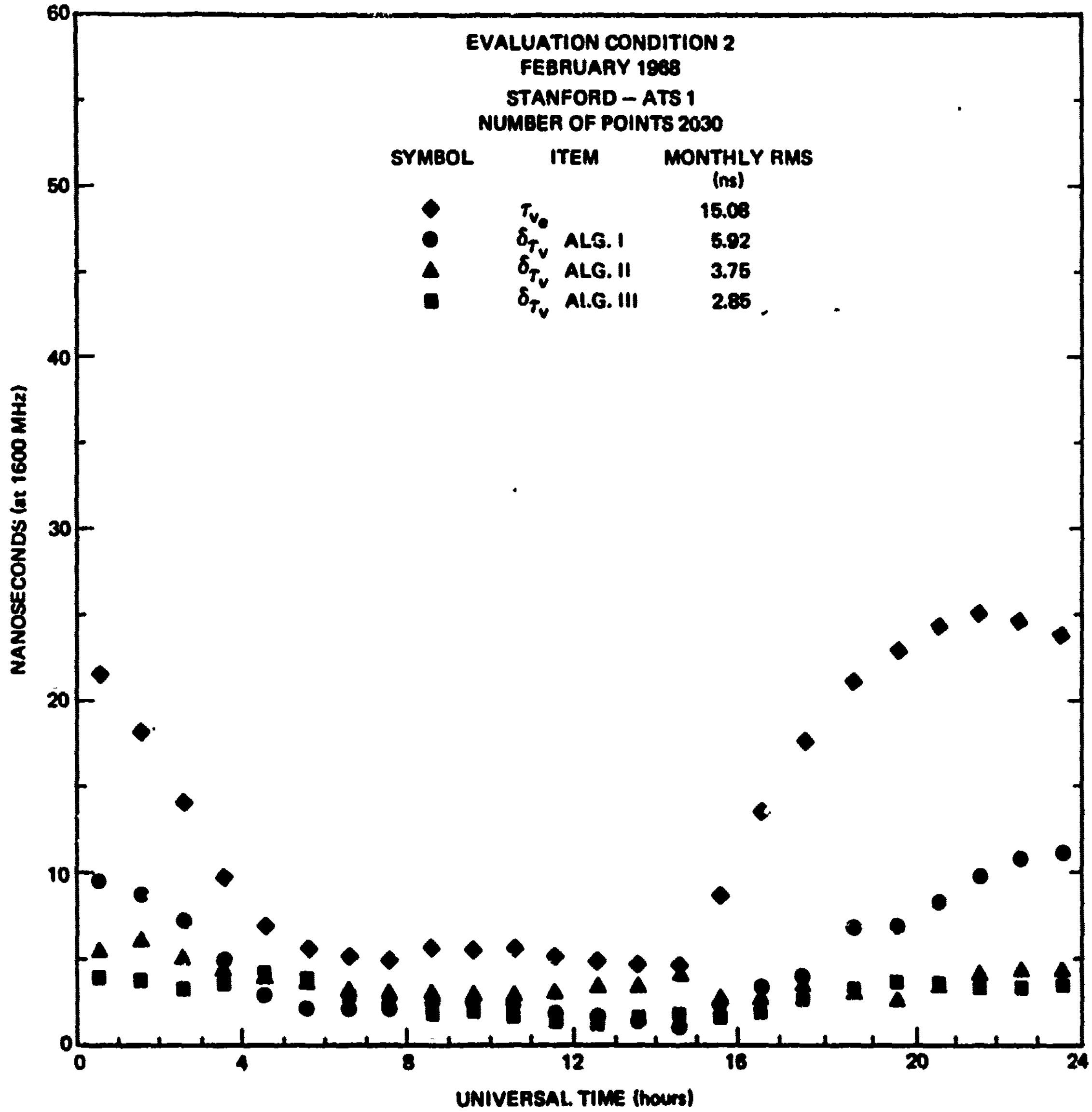

Fig. A.22 VERTICAL TIME DELAY AND RESIDUALS-HOURLY RMS OVER MONTH

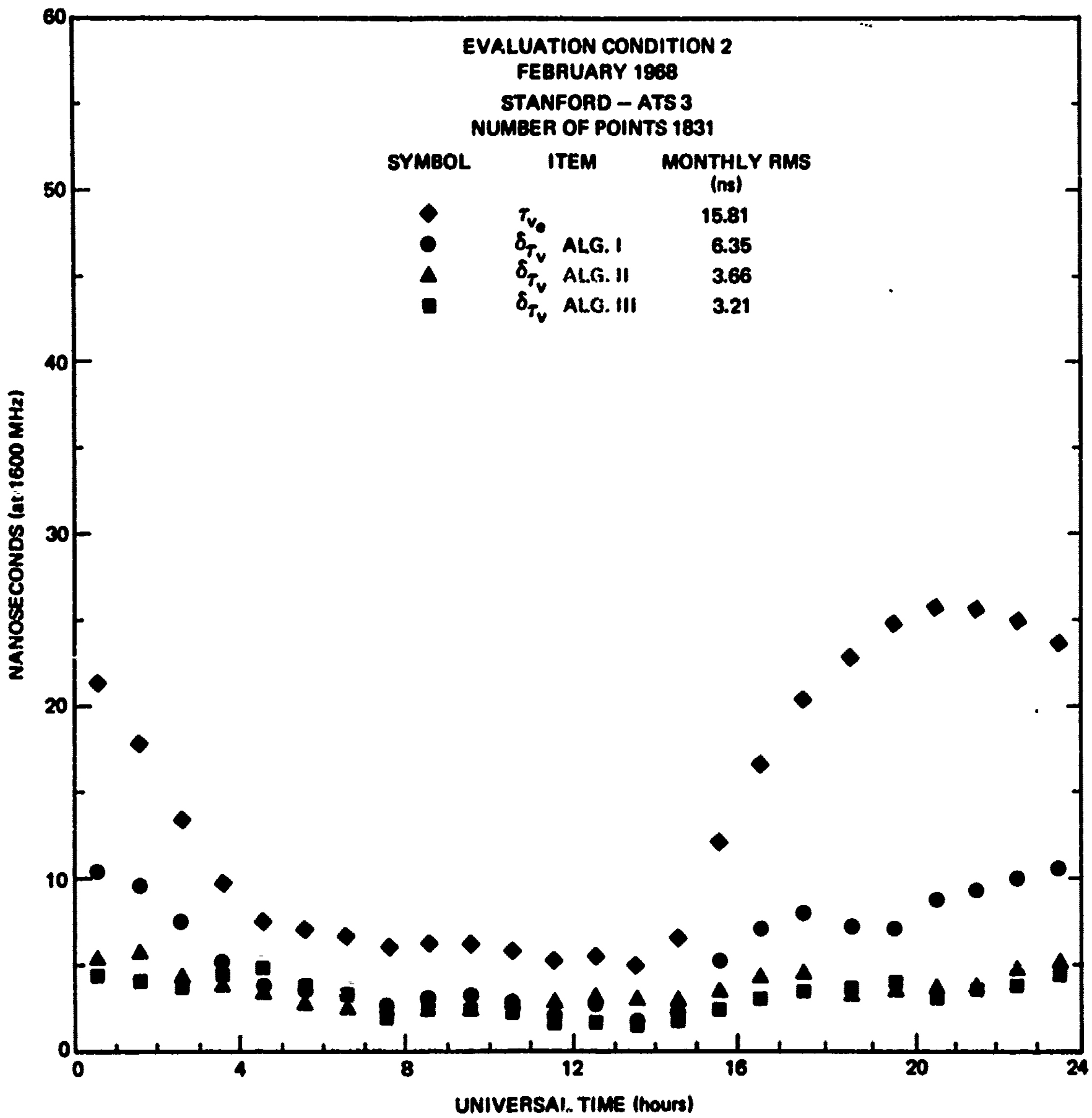

Fig. A.23 VERTICAL TIME DELAY AND RESIDUALS-HOURLY RMS OVER MONTH

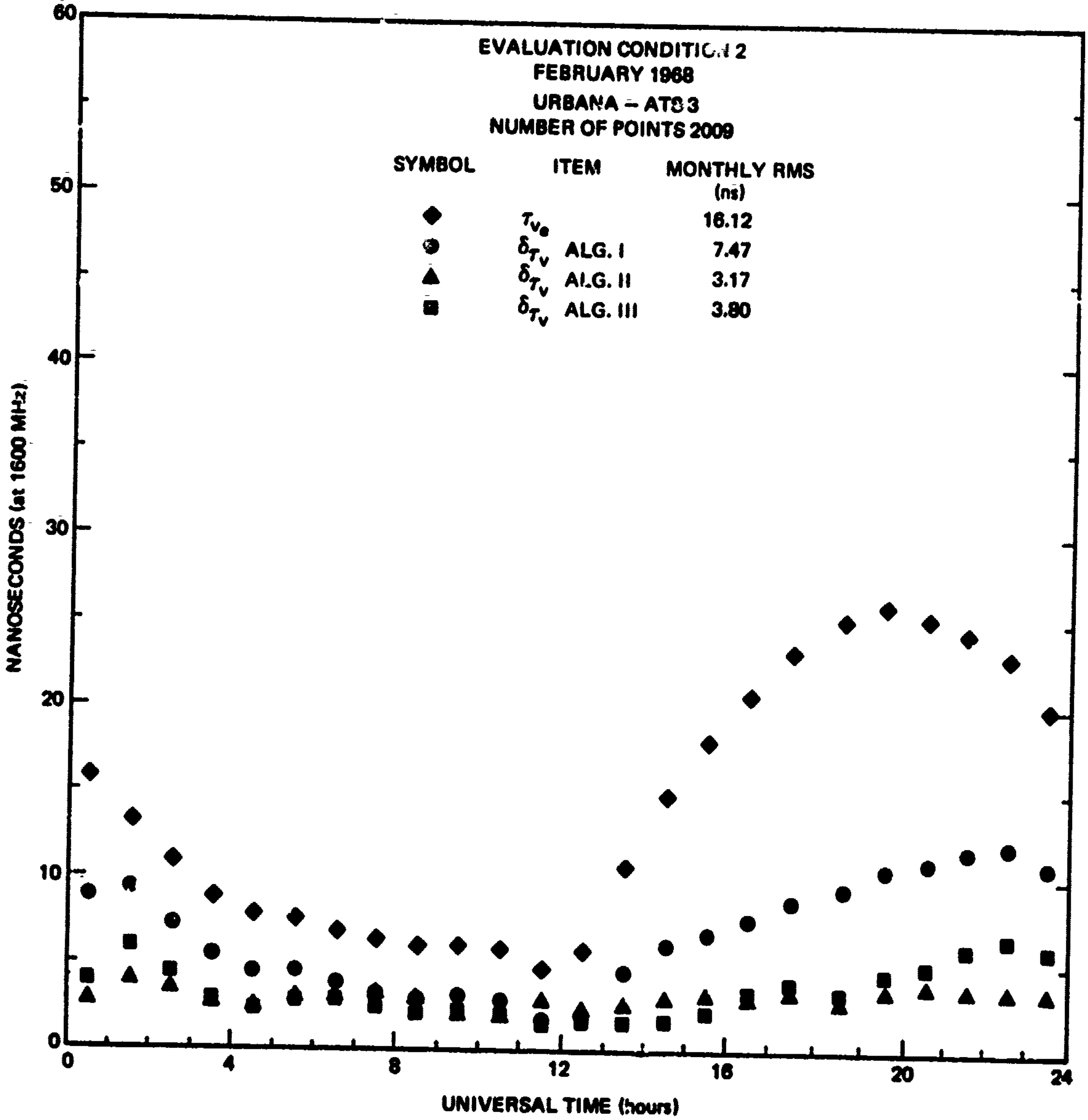

Fig. A.24 VERTICAL TIME DELAY AND RESIDUALS-HOURLY RMS OVER MONTH

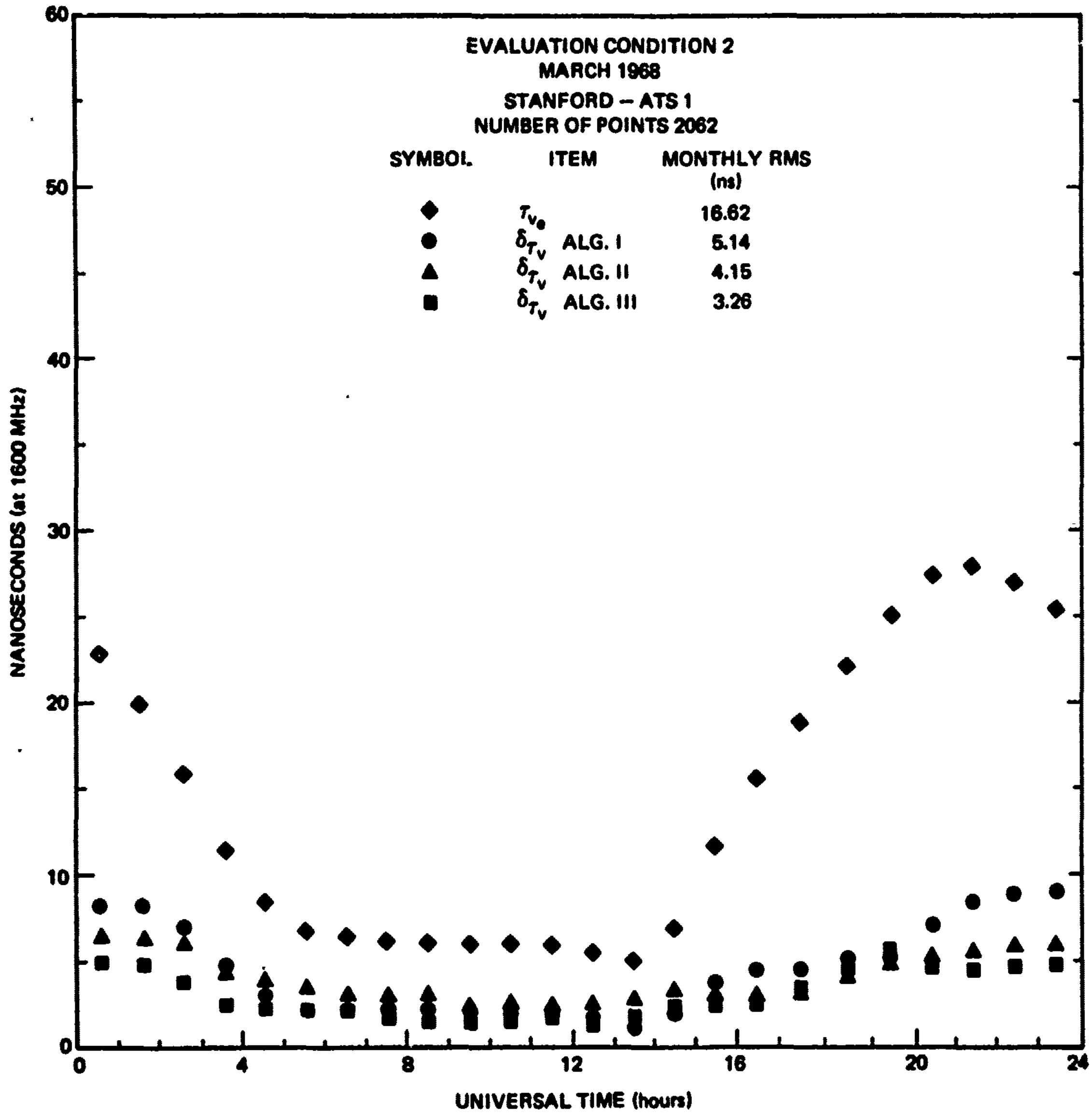

Fig. A.25 VERTICAL TIME DELAY AND RESIDUALS-HOURLY RMS OVER MONTH

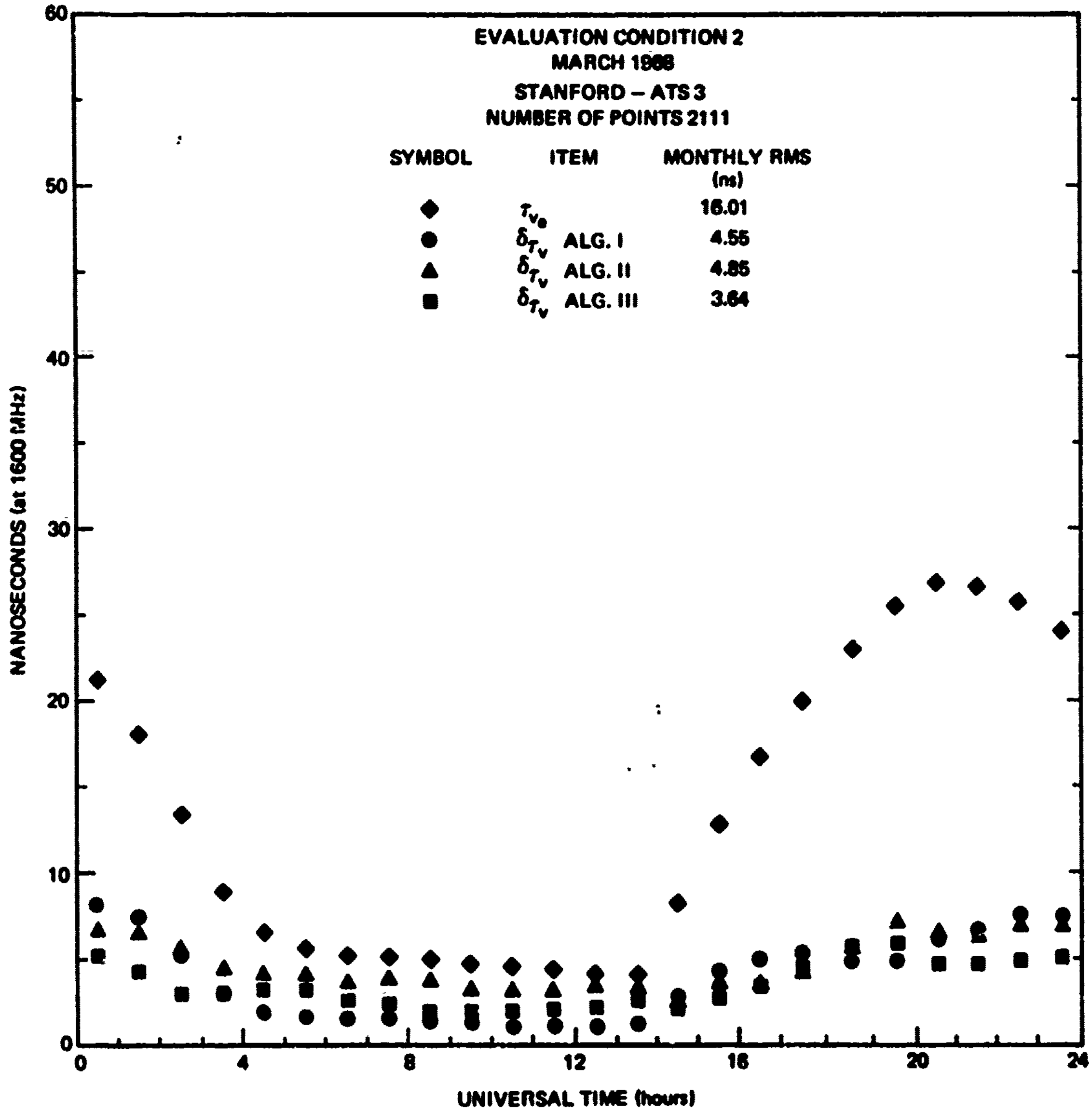

Fig. A.26 VERTICAL TIME DELAY AND RESIDUALS-HOURLY RMS OVER MONTH

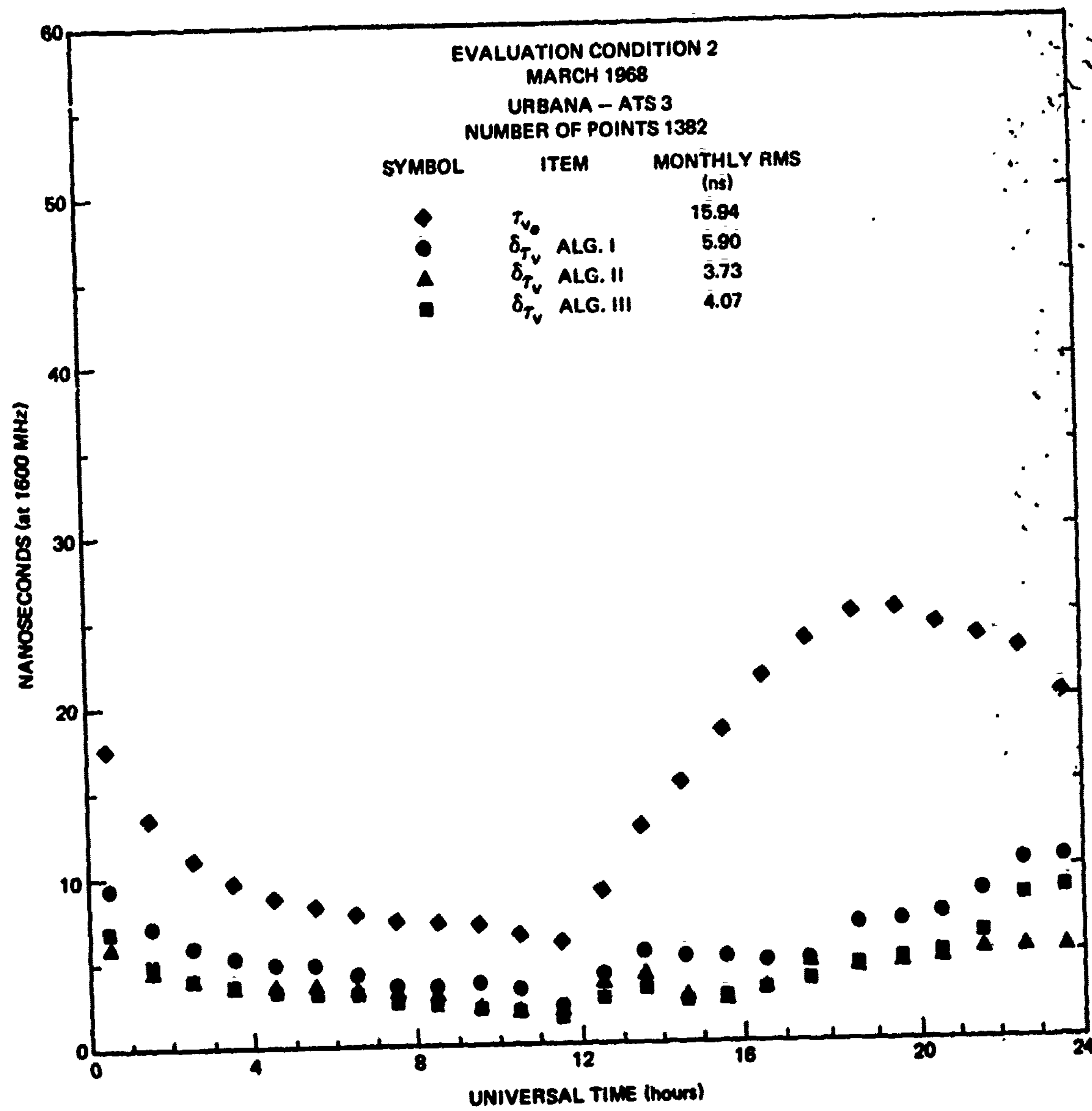

Fig. A.27 VERTICAL TIME DELAY AND RESIDUALS-HOURLY RMS OVER MONTH

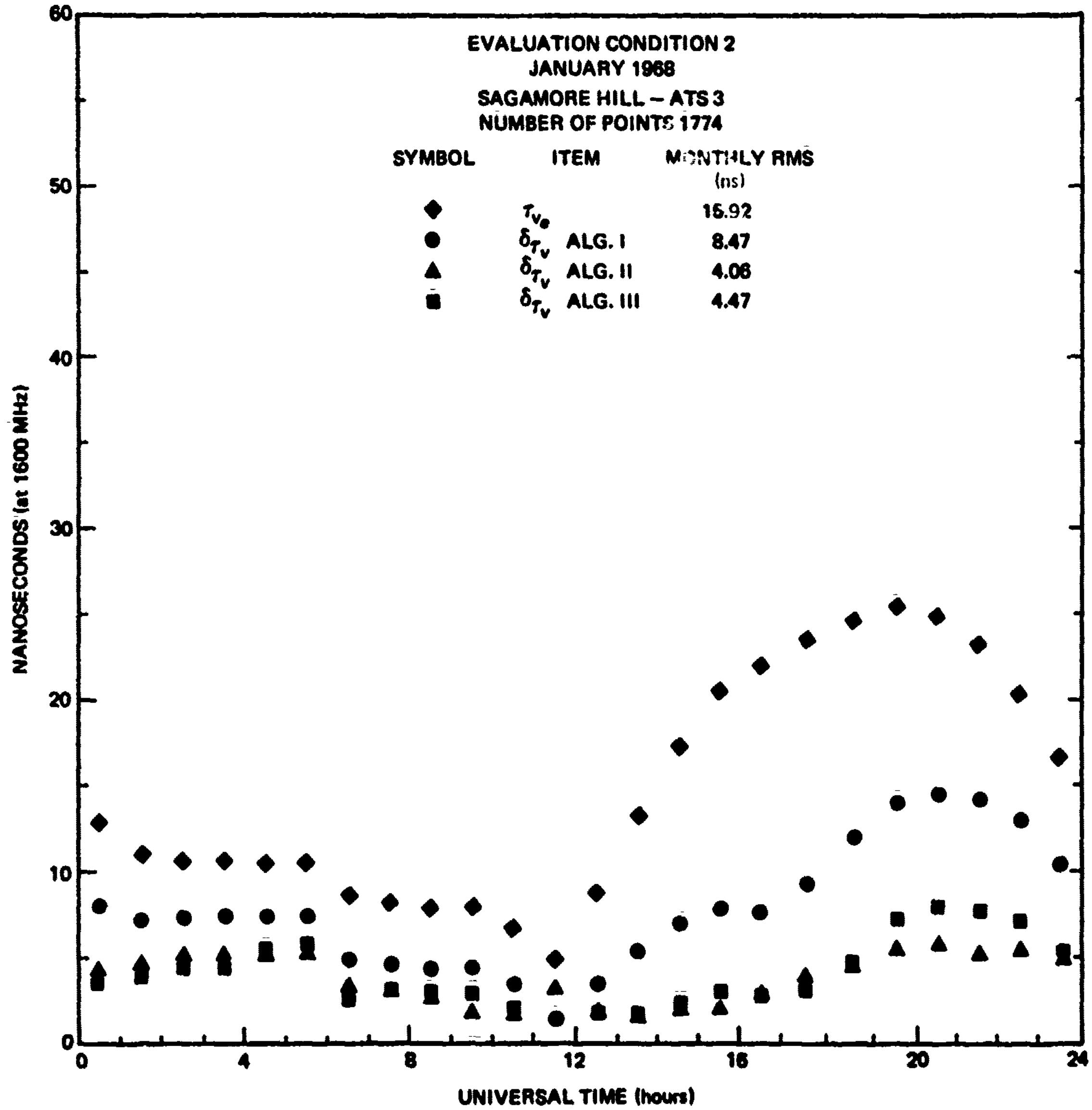

Fig. A.28 VERTICAL TIME DELAY AND RESIDUALS-HOURLY RMS OVER MONTH

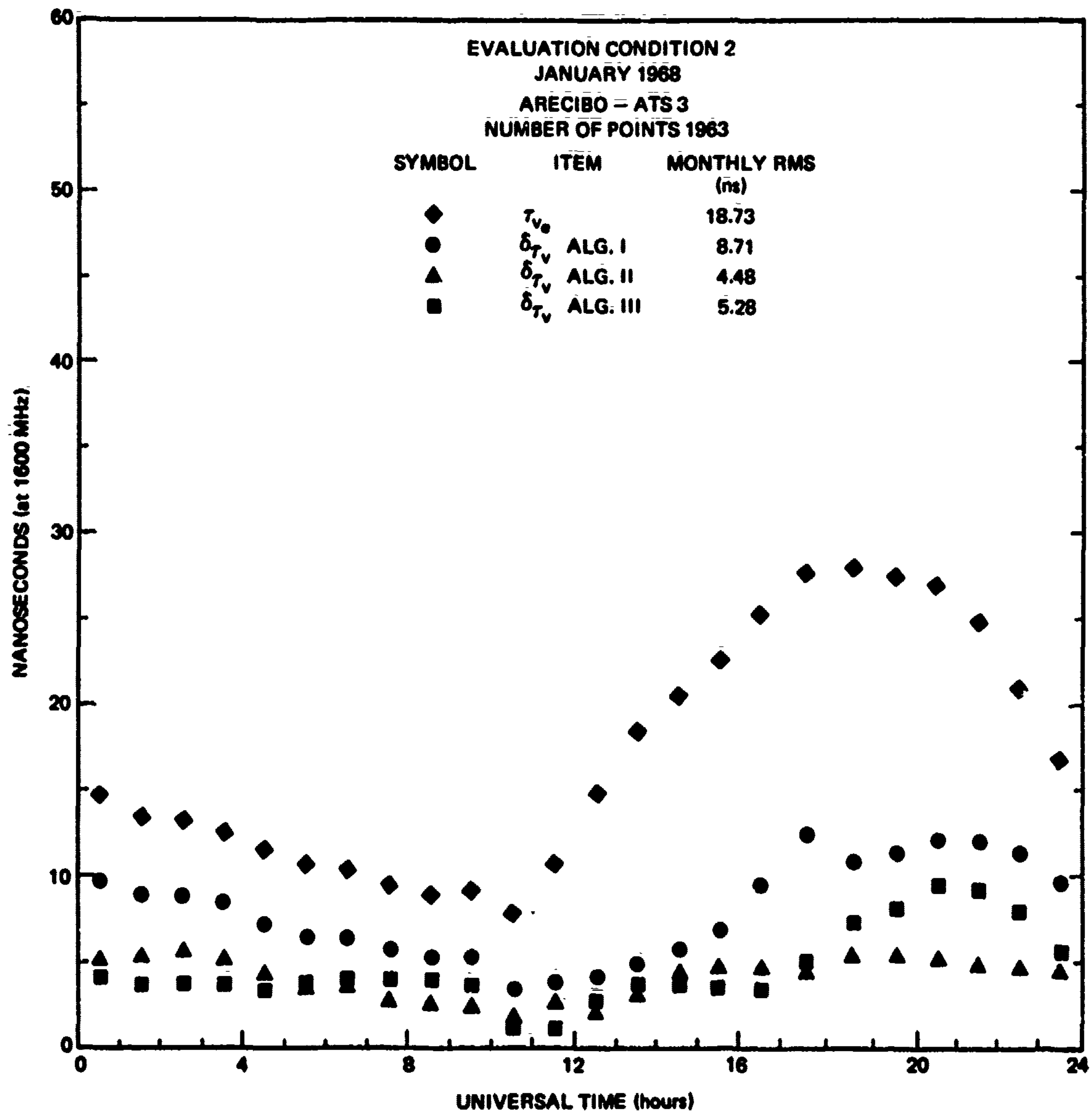

Fig. A.29 VERTICAL TIME DELAY AND RESIDUALS-HOURLY RMS OVER MONTH

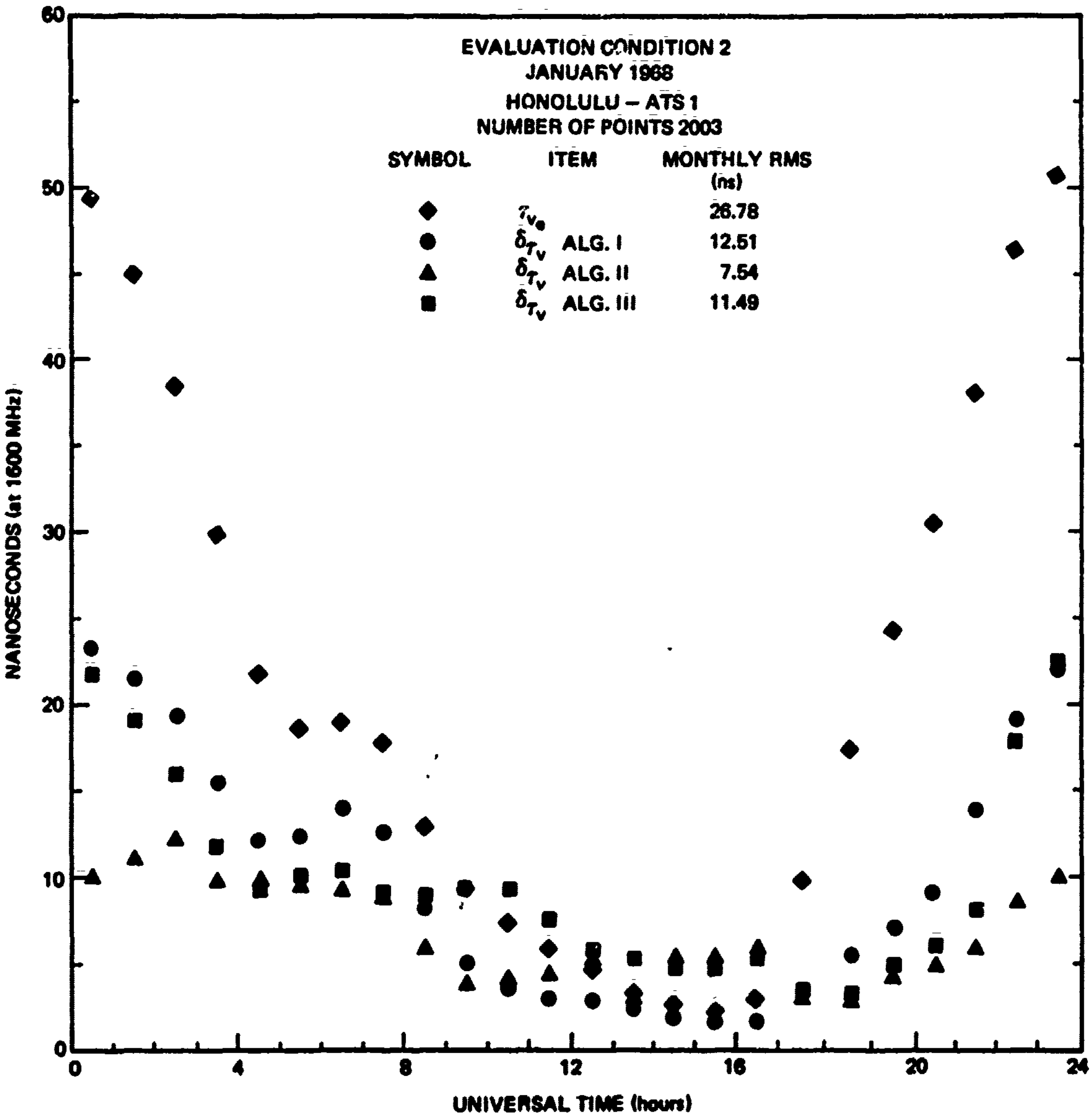

Fig. A.30 VERTICAL TIME DELAY AND RESIDUALS-HOURLY R..:S OVER MONTH

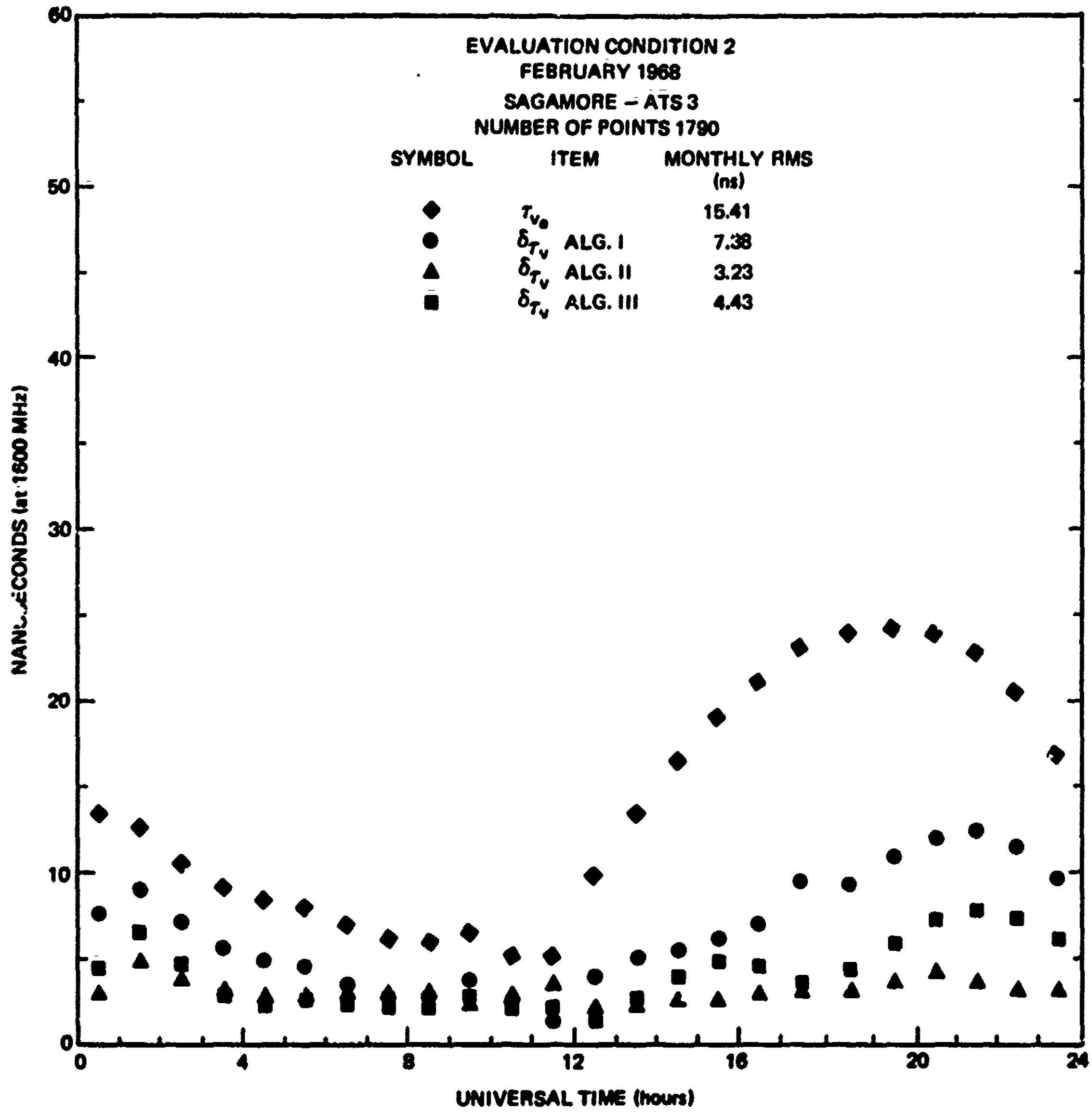

Fig. A.31 VERTICAL TIME DELAY AND RESIDUALS-HOURLY RMS OVER MONTH

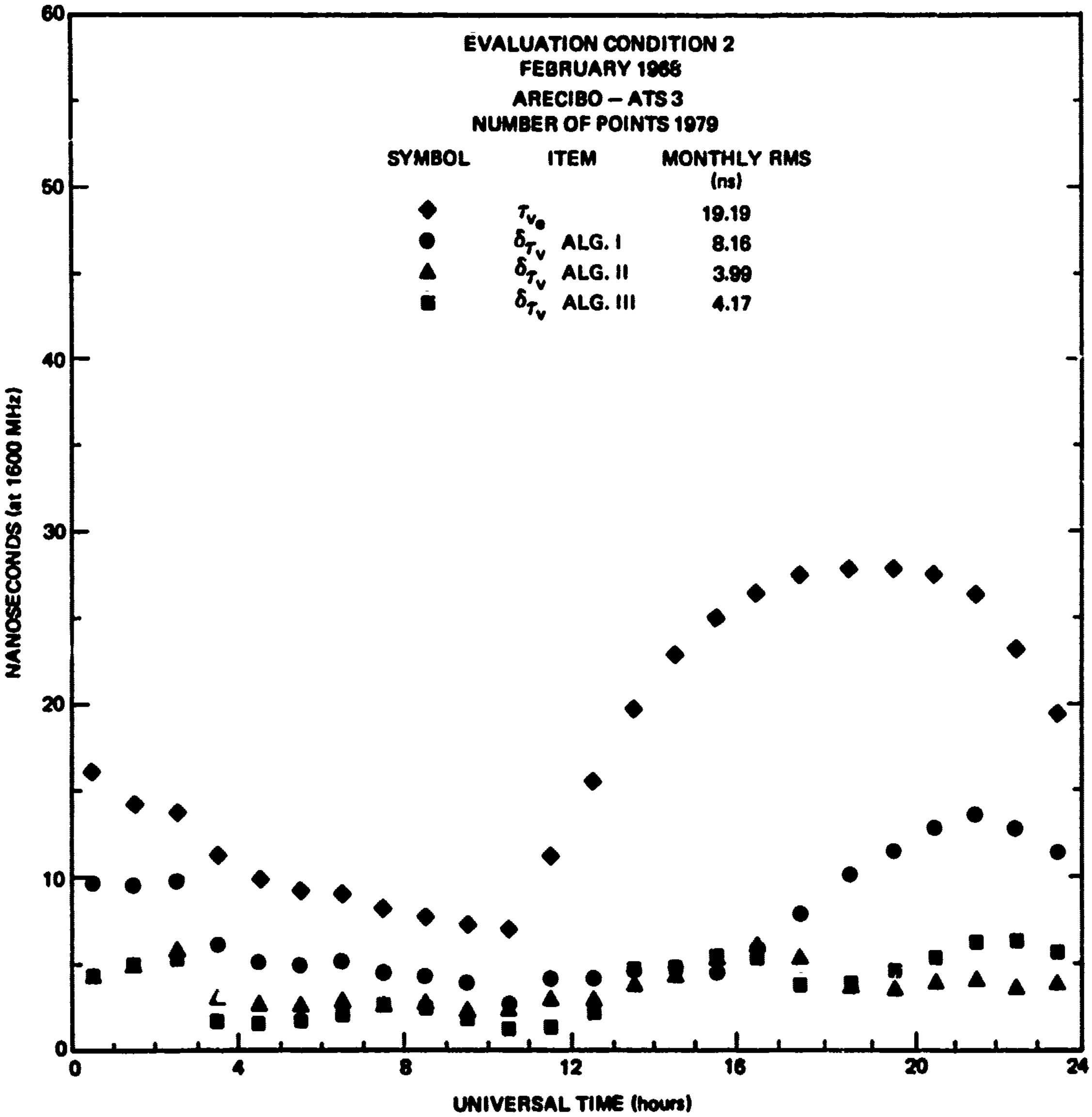

Fig. A.32 VERTICAL TIME DELAY AND RESIDUALS-HOURLY RMS OVER MONTH

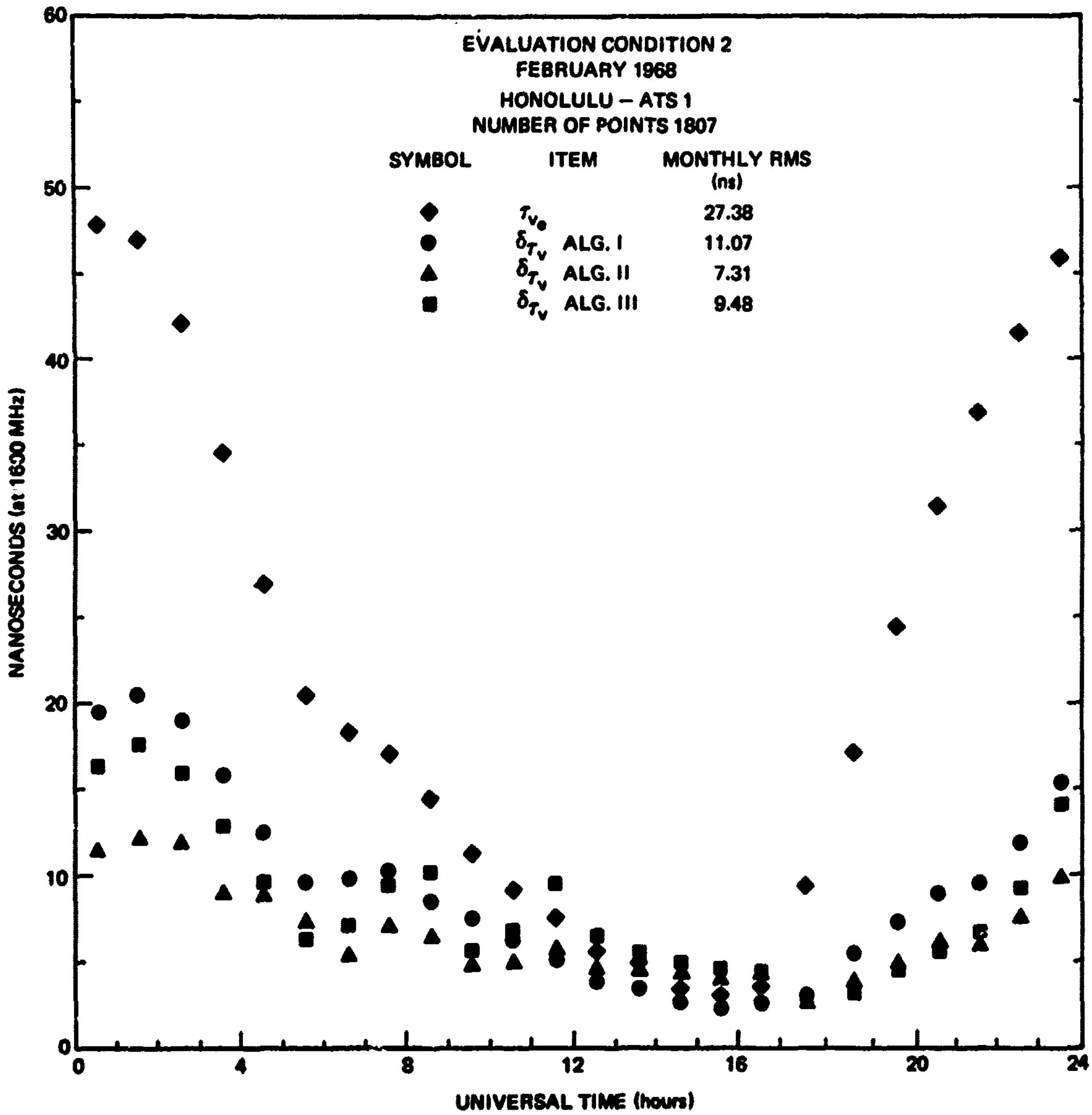

Fig. A.33 VERTICAL TIME DELAY AND RESIDUALS-HOURLY RMS OVER MONTH

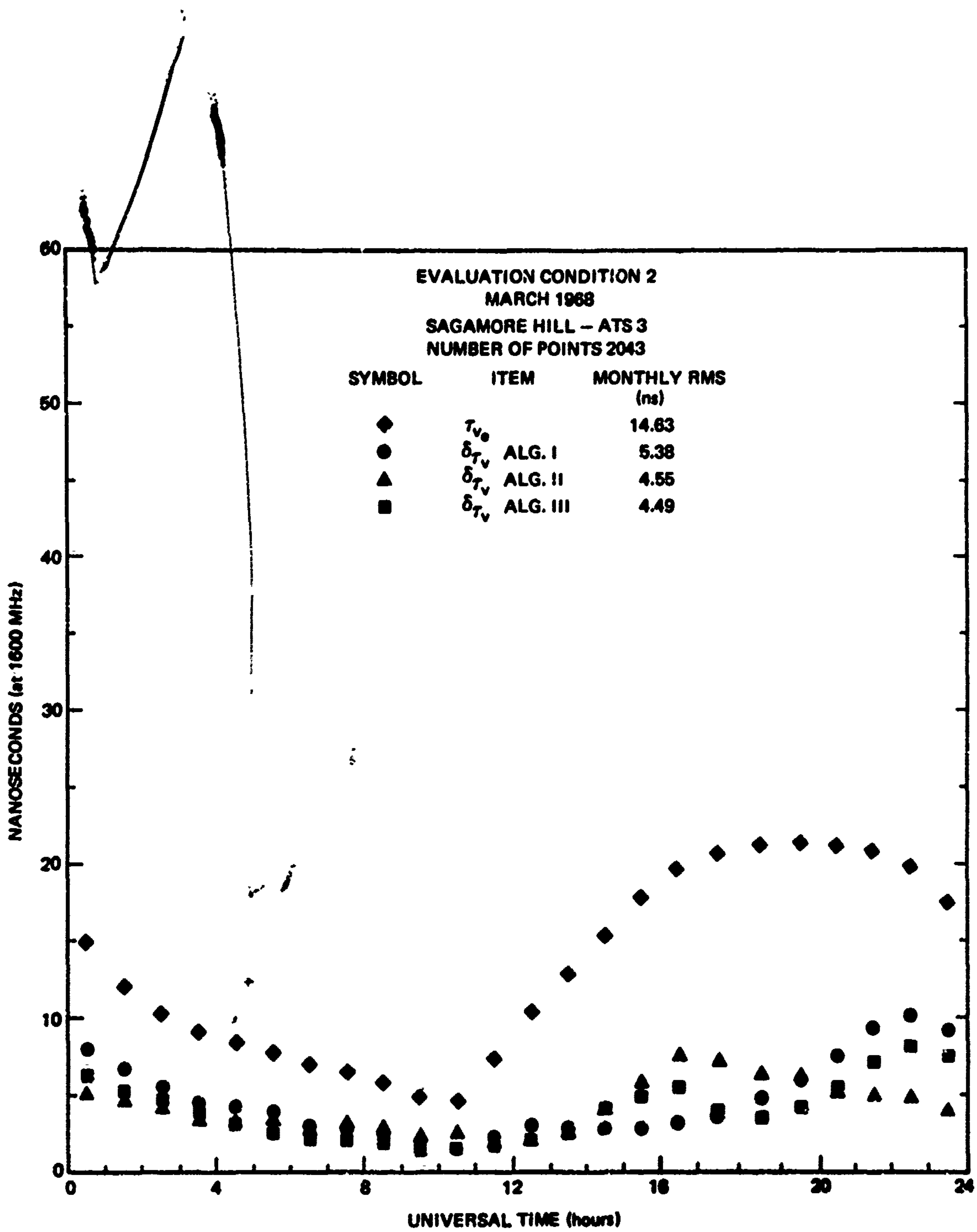

Fig. A.34 VERTICAL TIME DELAY AND RESIDUALS-HOURLY RMS OVER MONTH

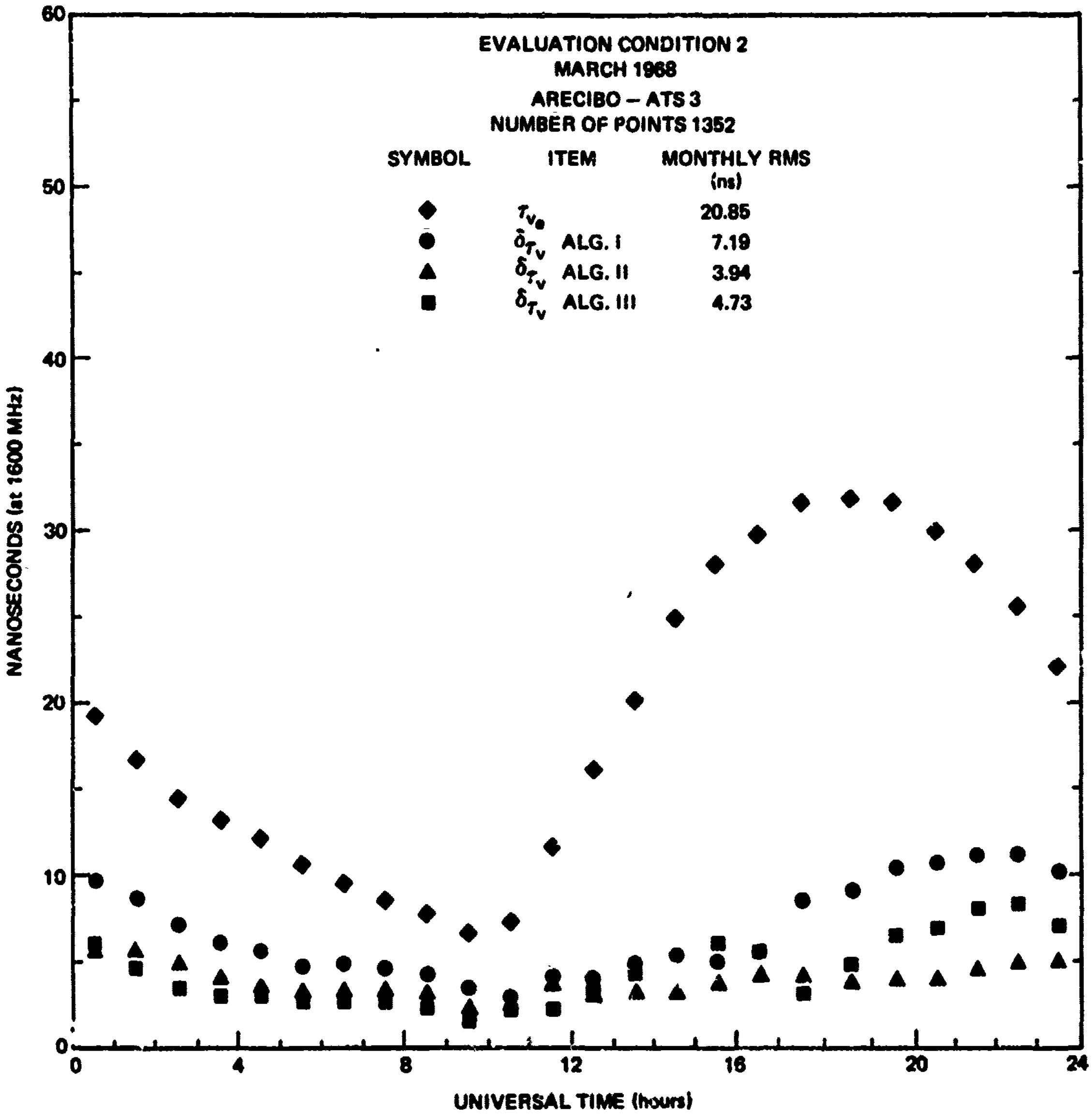

Fig. A.35 VERTICAL TIME DELAY AND RESIDUALS-HOURLY RMS OVER MONTH

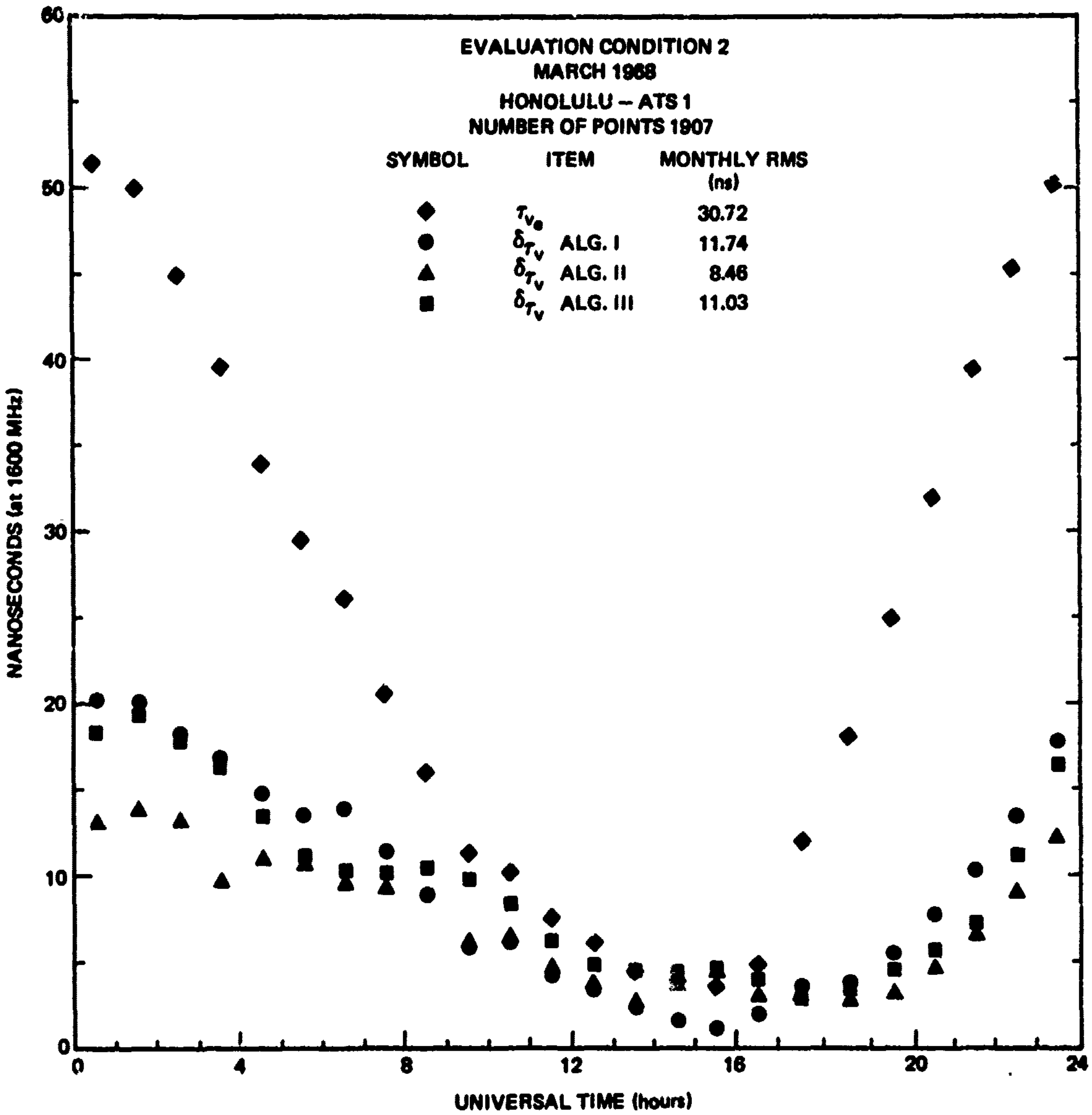

Fig. A.36 VERTICAL TIME DELAY AND RESIDUALS-HOURLY RMS OVER MONTH

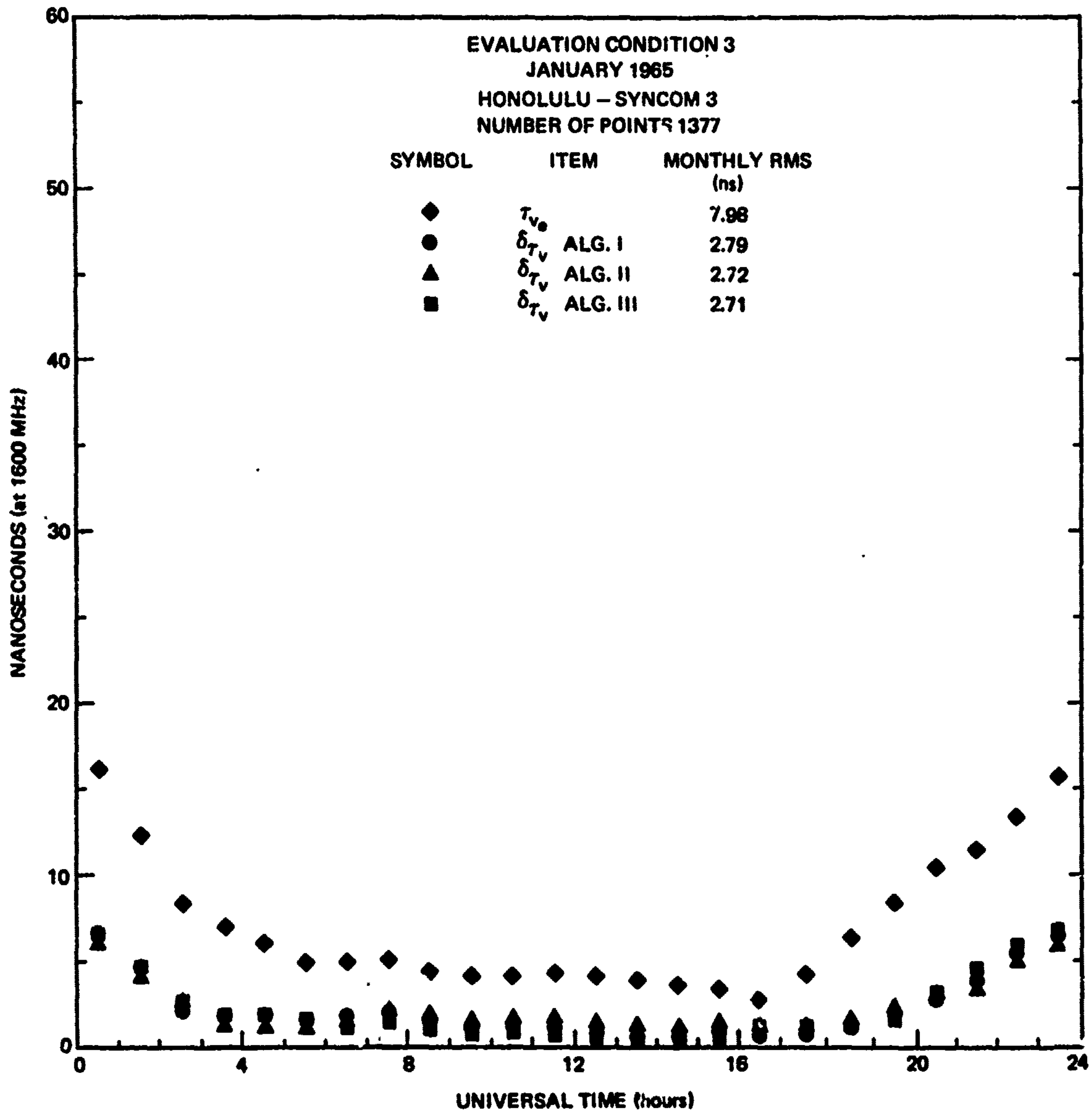

Fig. A.37 VERTICAL TIME DELAY AND RESIDUALS-HOURLY RMS OVER MONTH

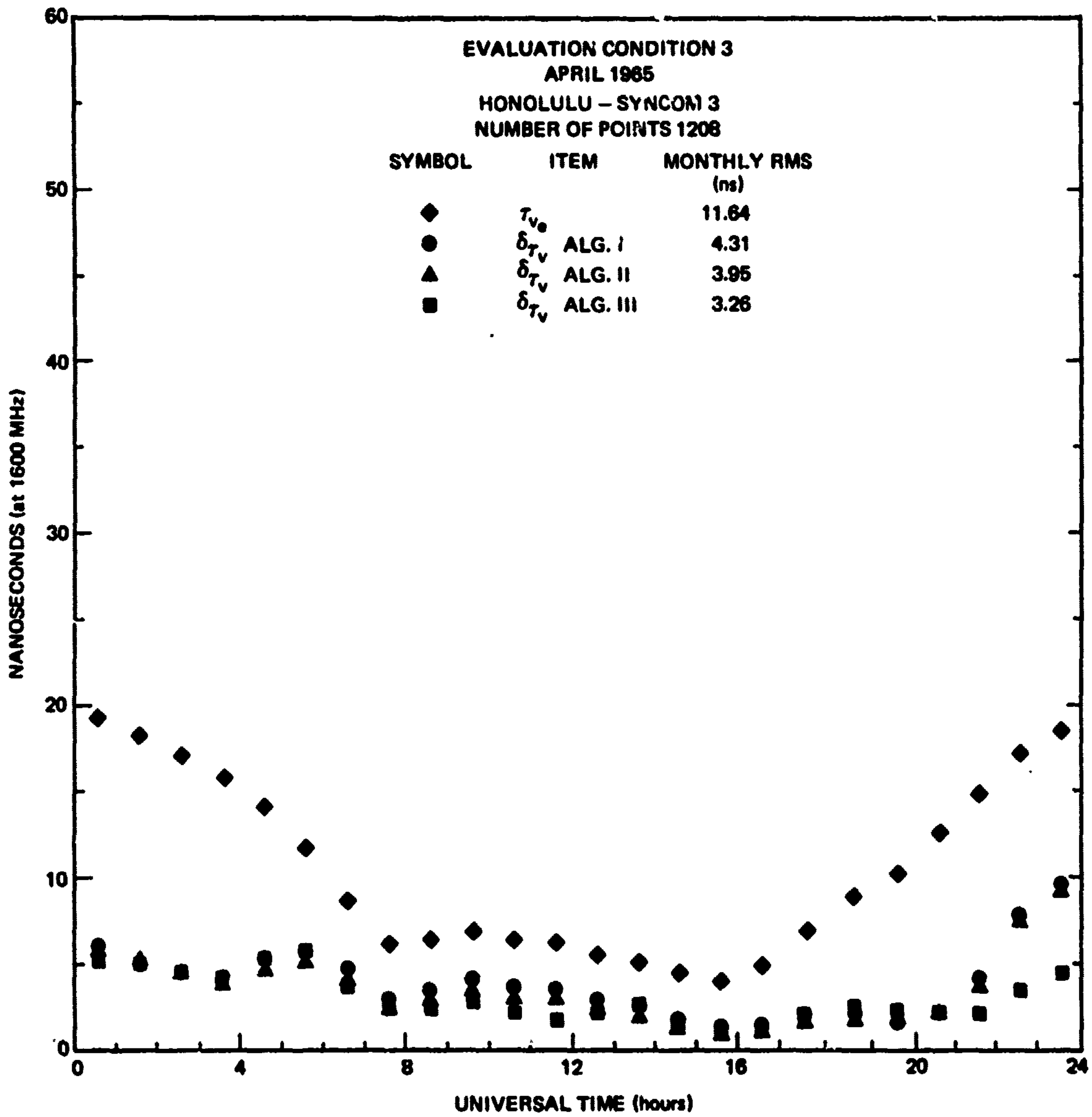

Fig. A.38 VERTICAL TIME DELAY AND RESIDUALS-HOURLY RMS OVER MONTH

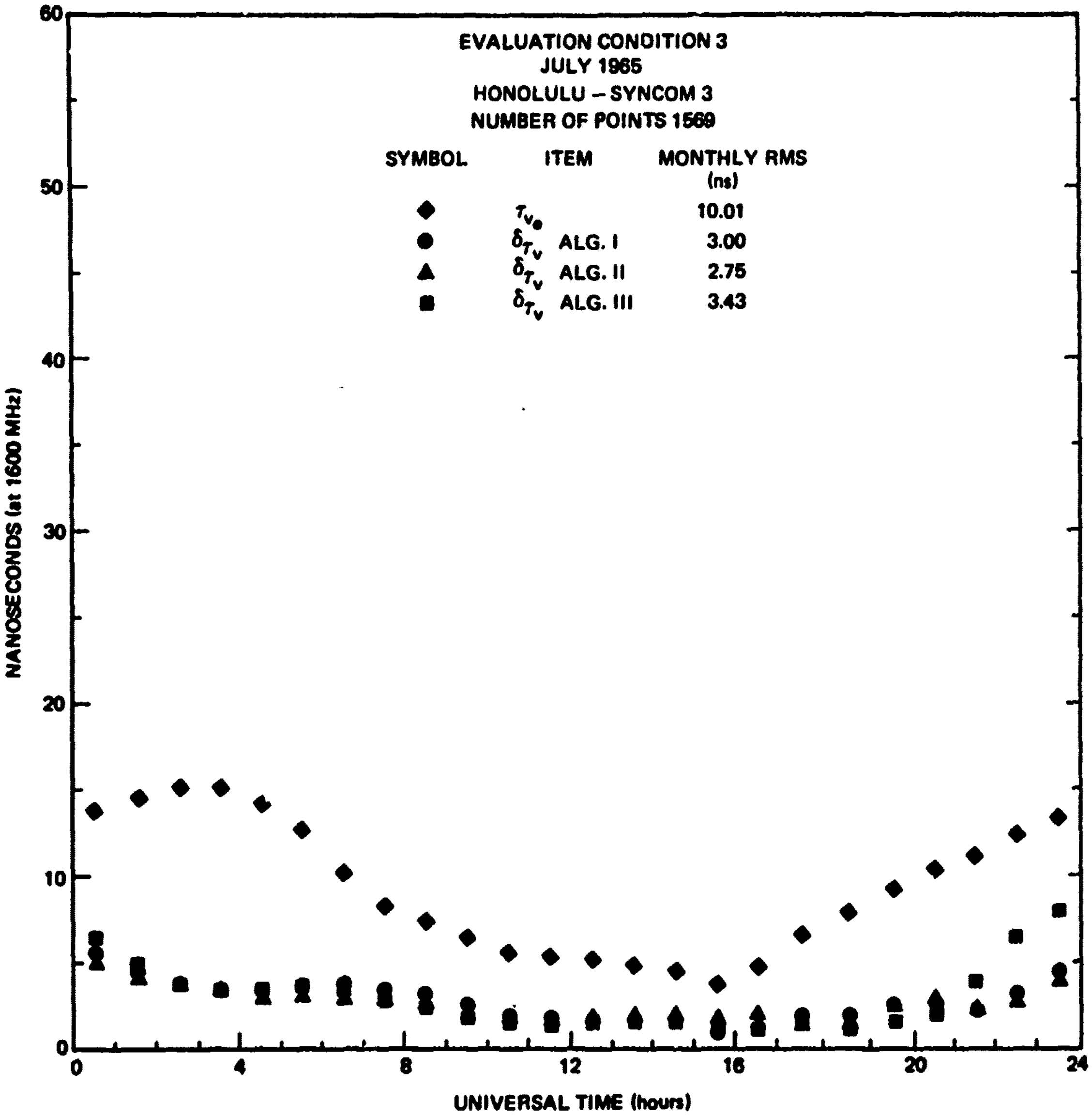

Fig. A.39 VERTICAL TIME DELAY AND RESIDUALS-HOURLY RMS OVER MONTH

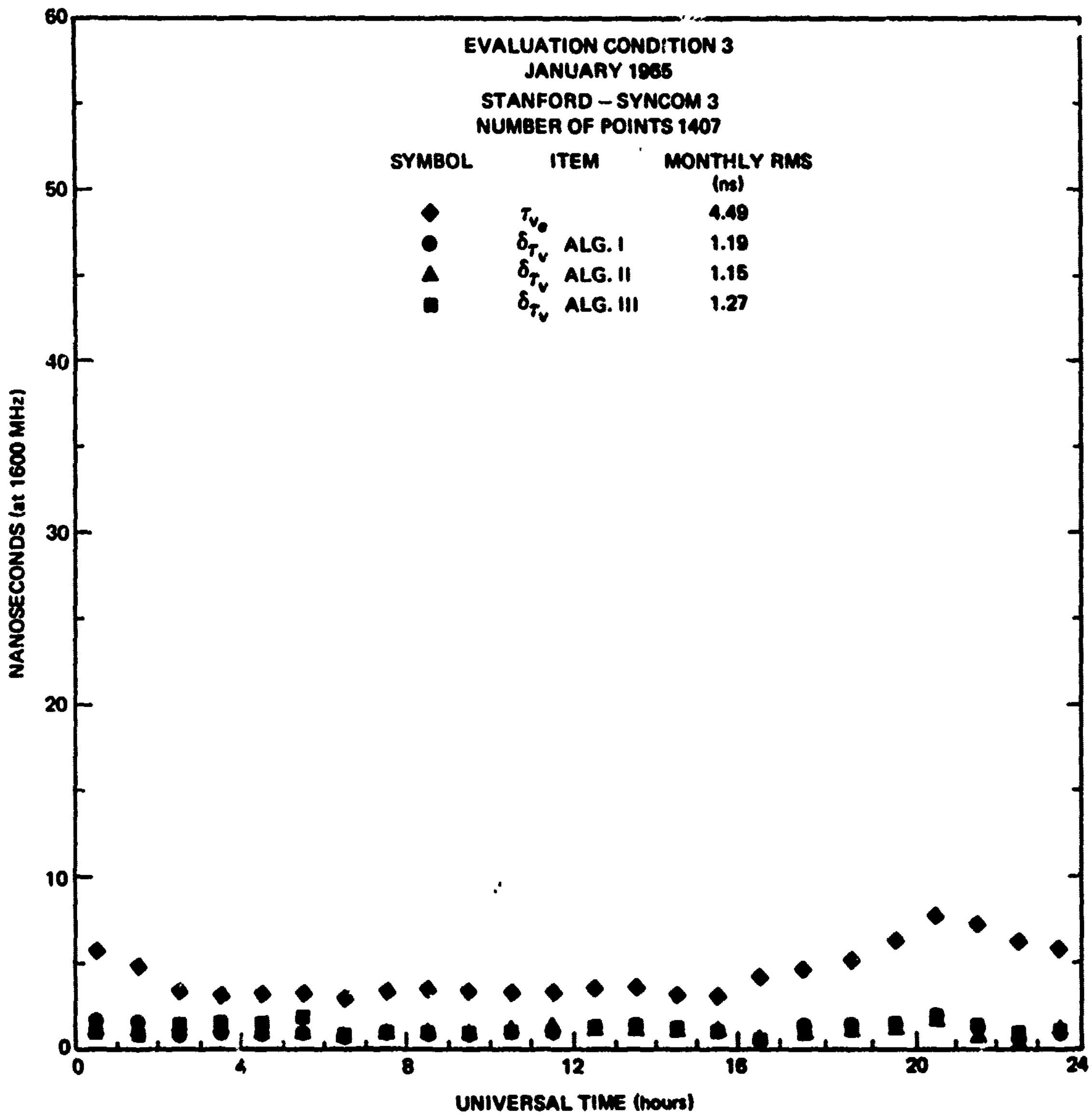

Fig. A.40 VERTICAL TIME DELAY AND RESIDUALS-HOURLY RMS OVER MONTH

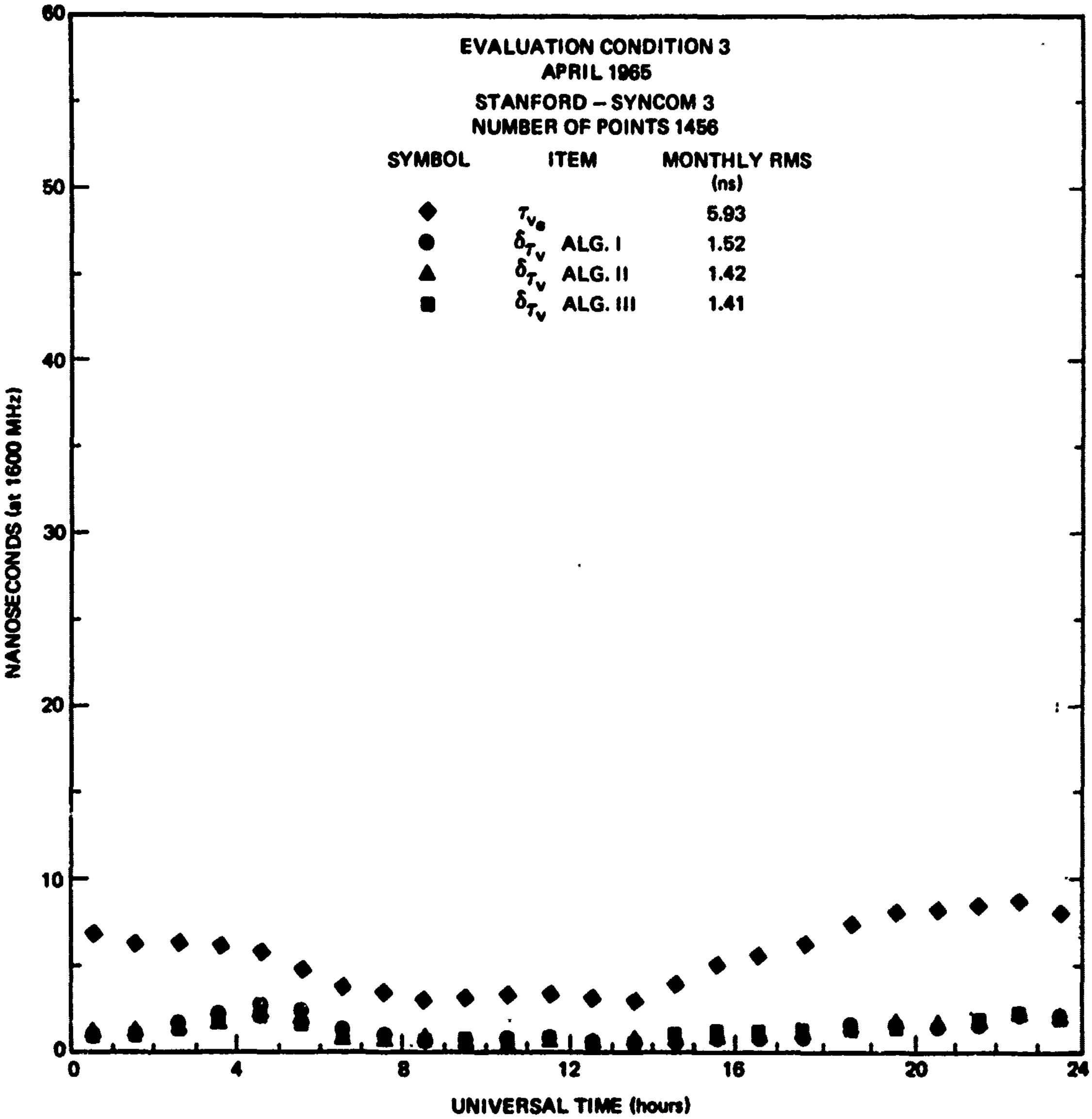

Fig. A.41 VERTICAL TIME DELAY AND RESIDUALS-HOURLY RMS OVER MONTH

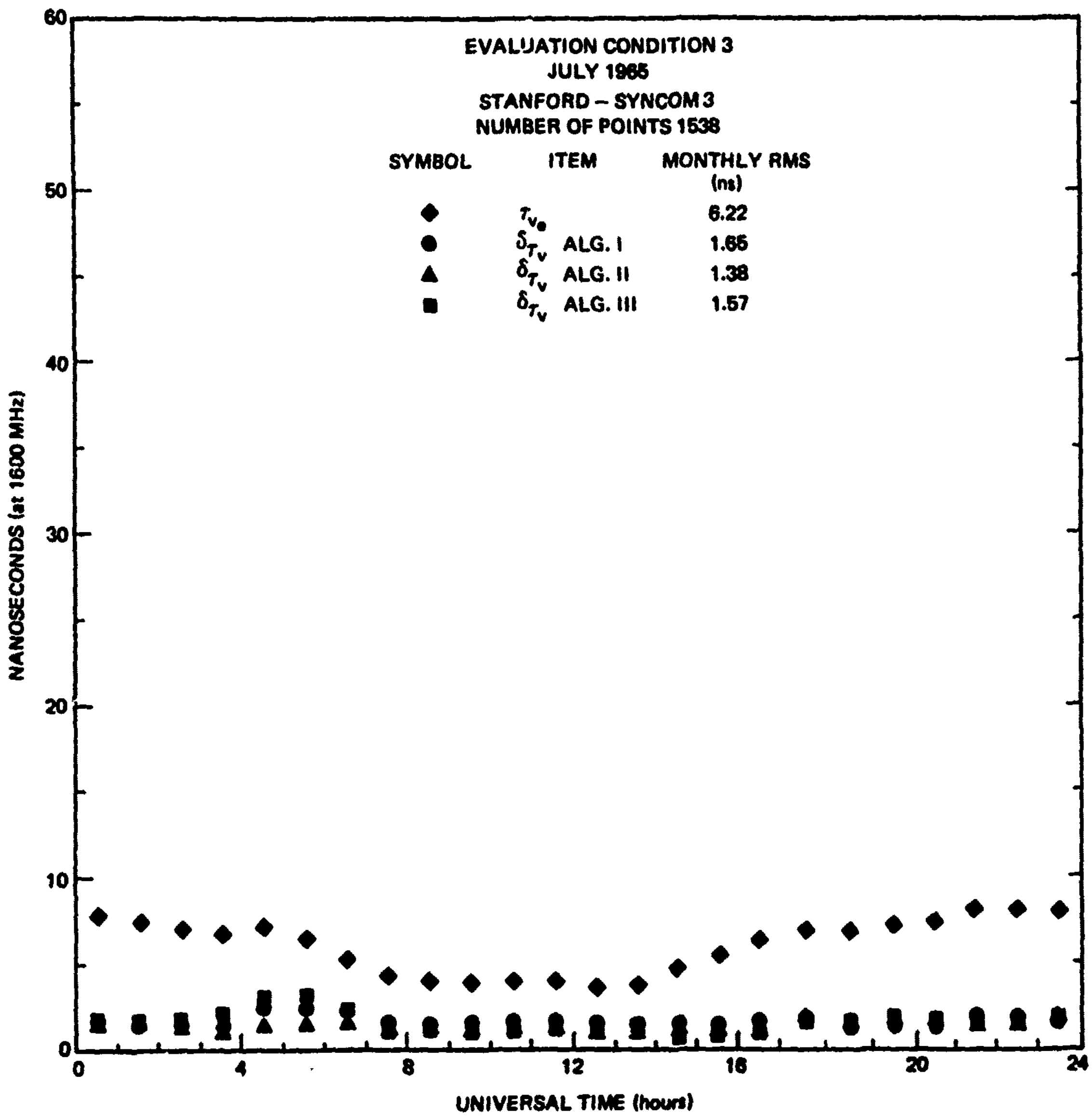

Fig. A.42 VERTICAL TIME DELAY AND RESIDUALS-HOURLY RMS OVER MONTH

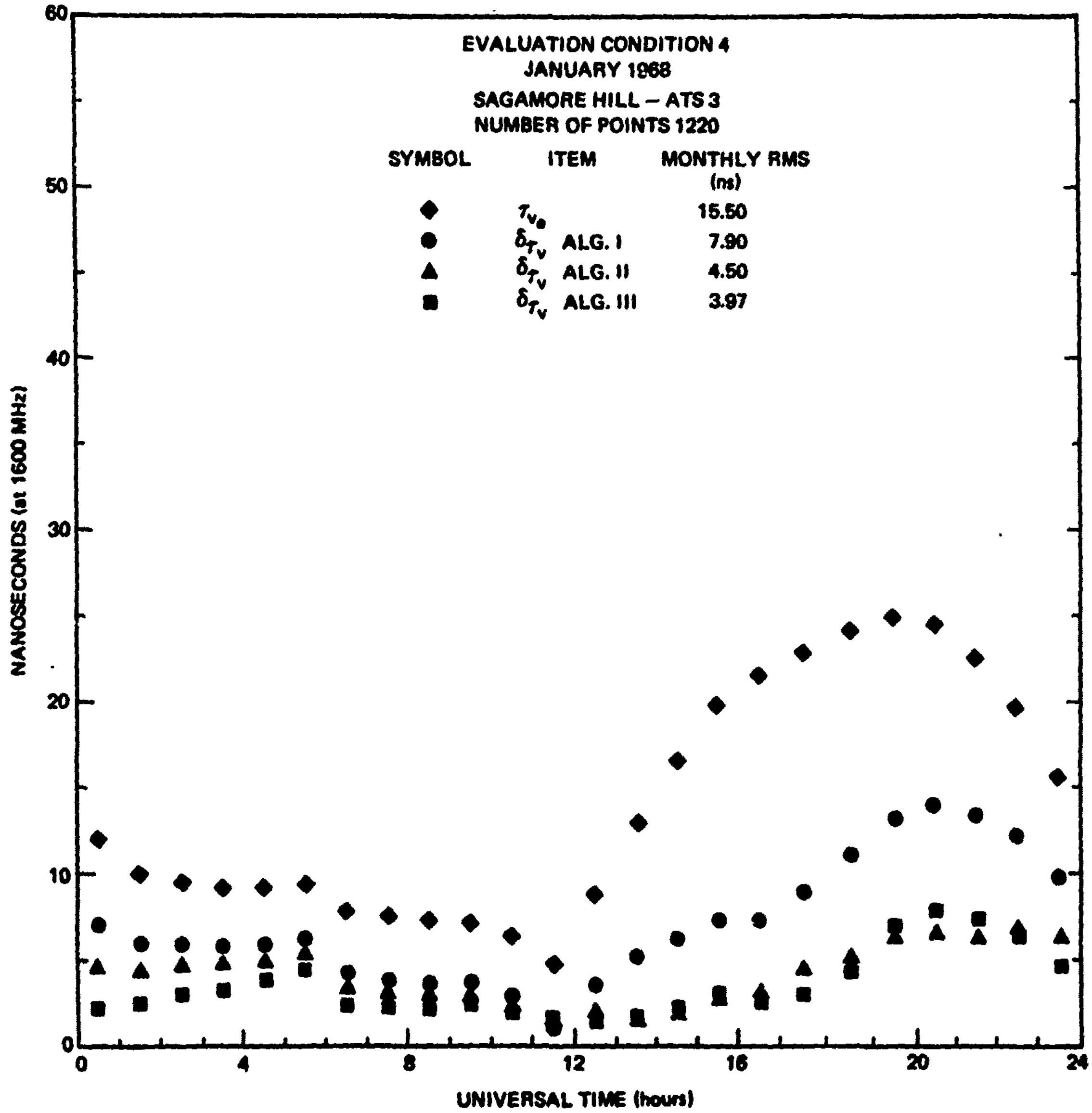

Fig. A.43 VERTICAL TIME DELAY AND RESIDUALS-HOURLY RMS OVER MONTH

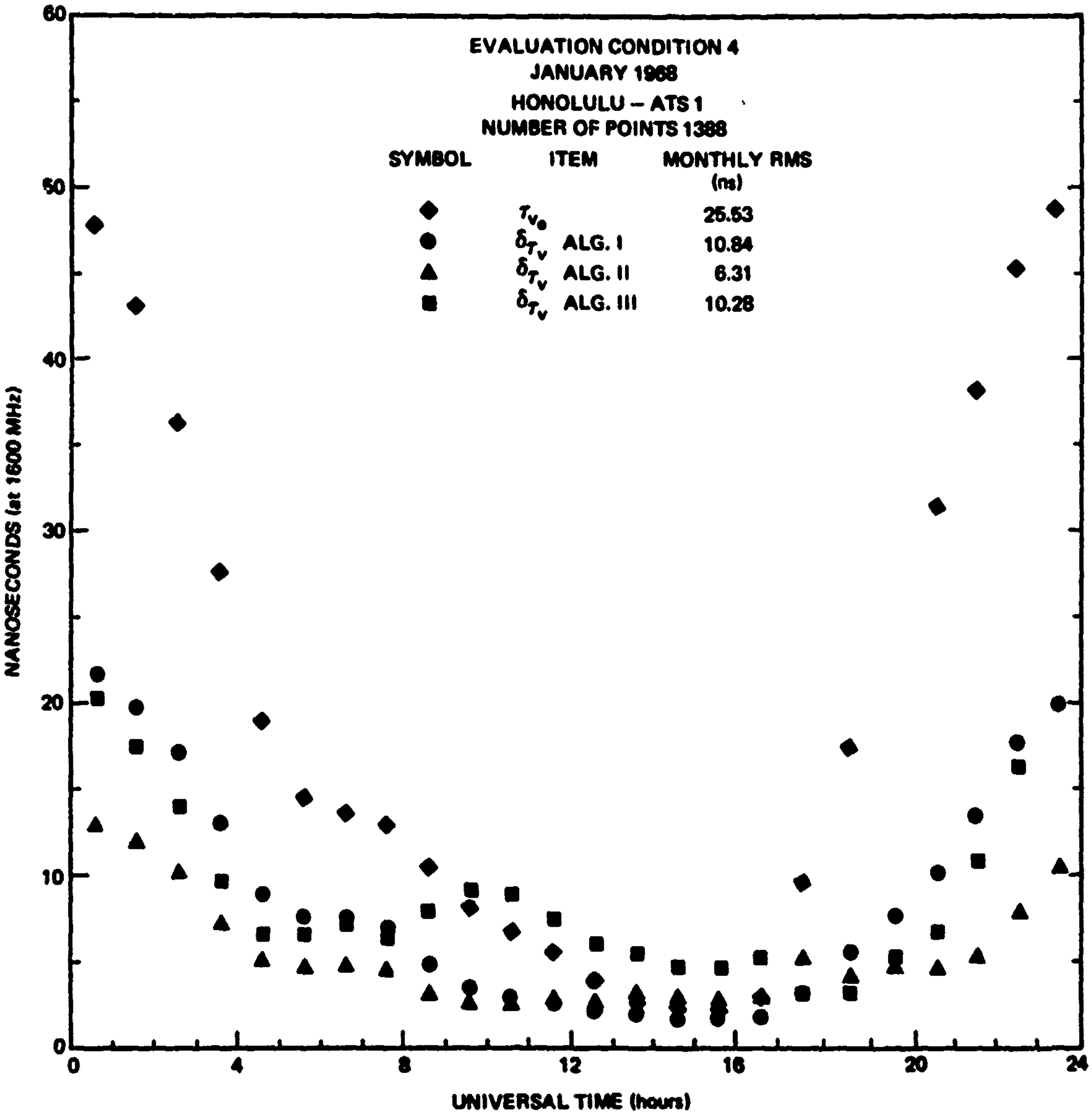

Fig. A.44 VERTICAL TIME DELAY AND RESIDUALS-HOURLY RMS OVER MONTH

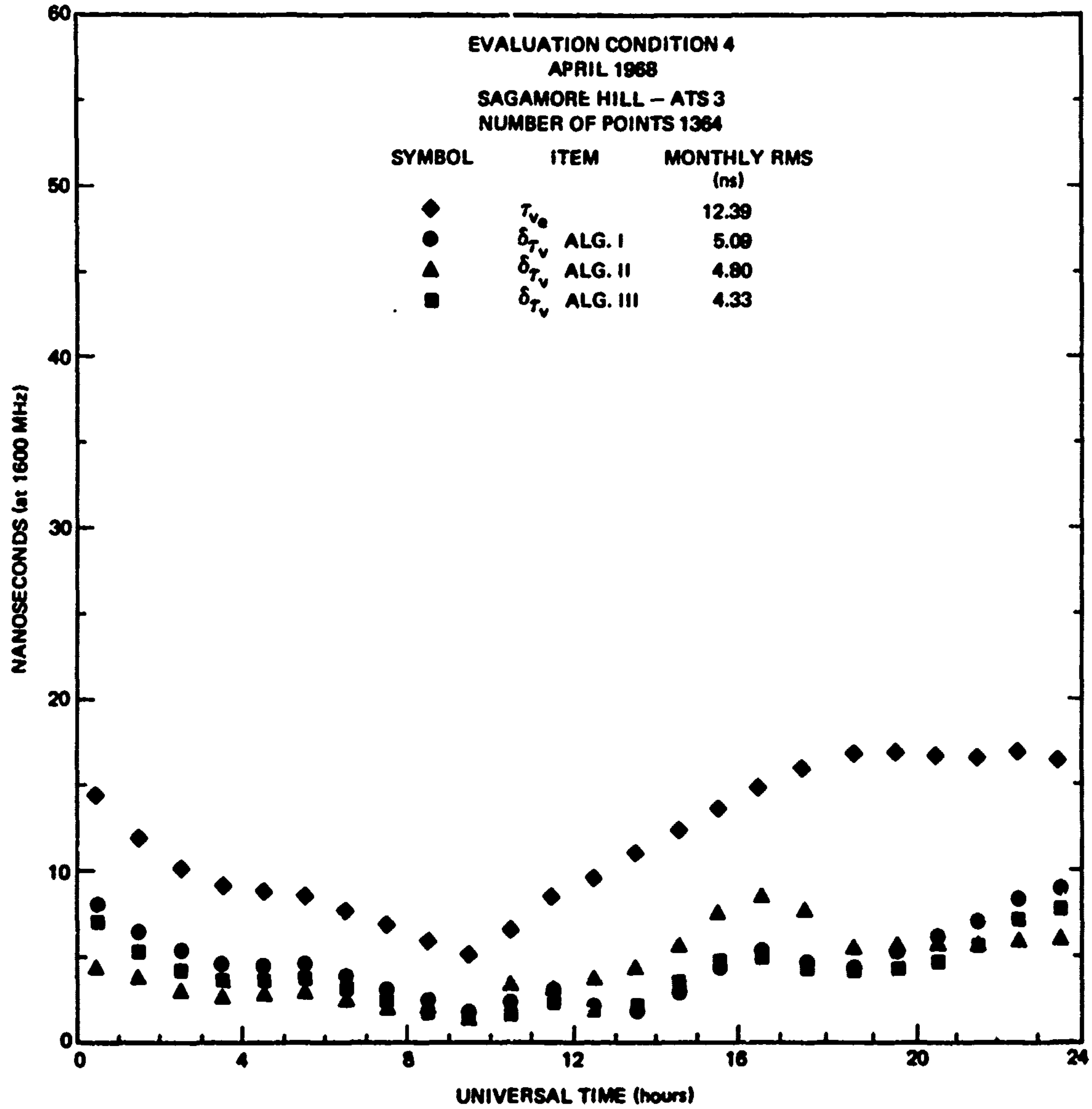

Fig. A.45 VERTICAL TIME DELAY AND RESIDUALS-HOURLY RMS OVER MONTH

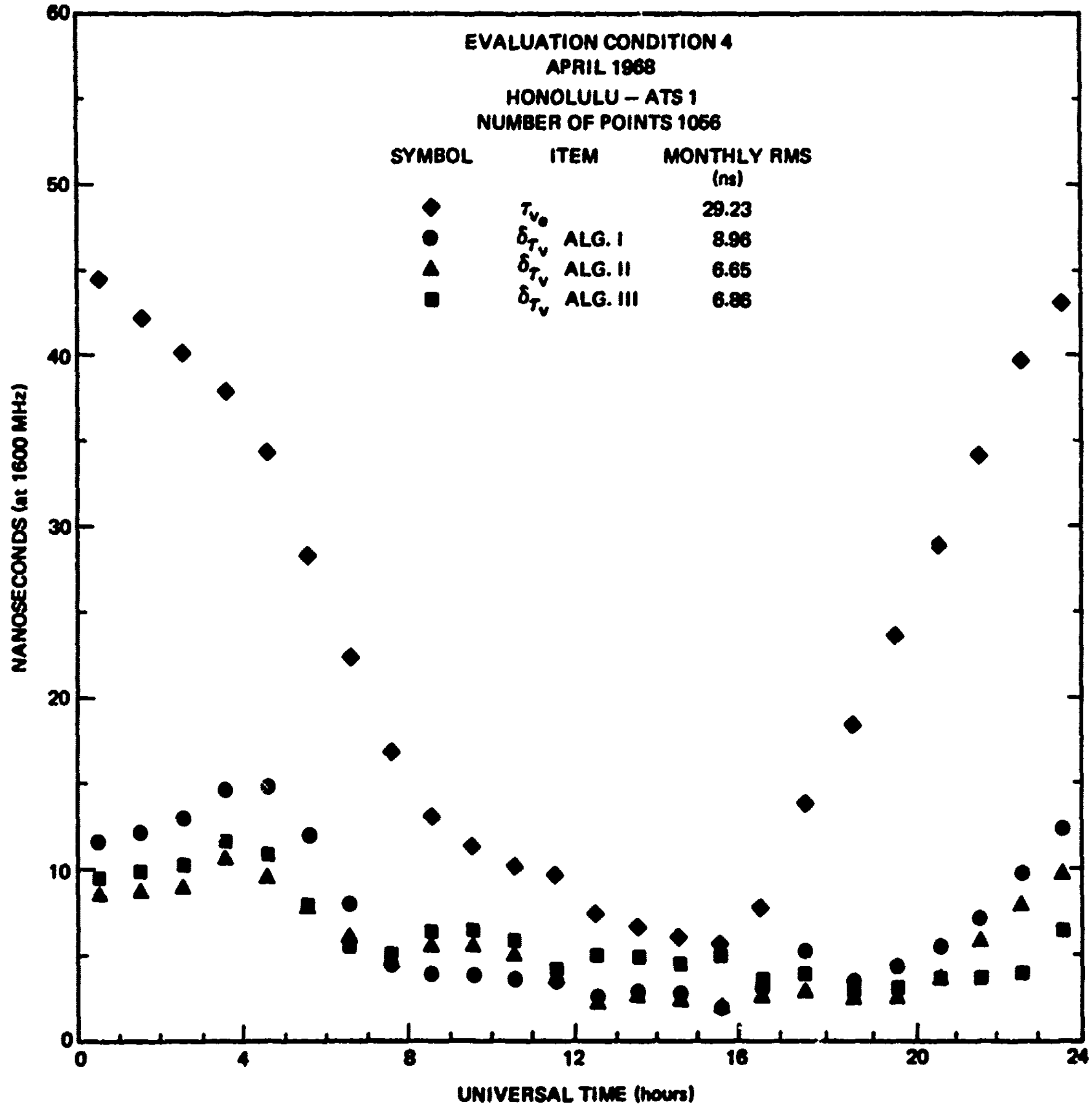

Fig. A.46 VERTICAL TIME DELAY AND RESIDUALS-HOURLY RMS OVER MONTH

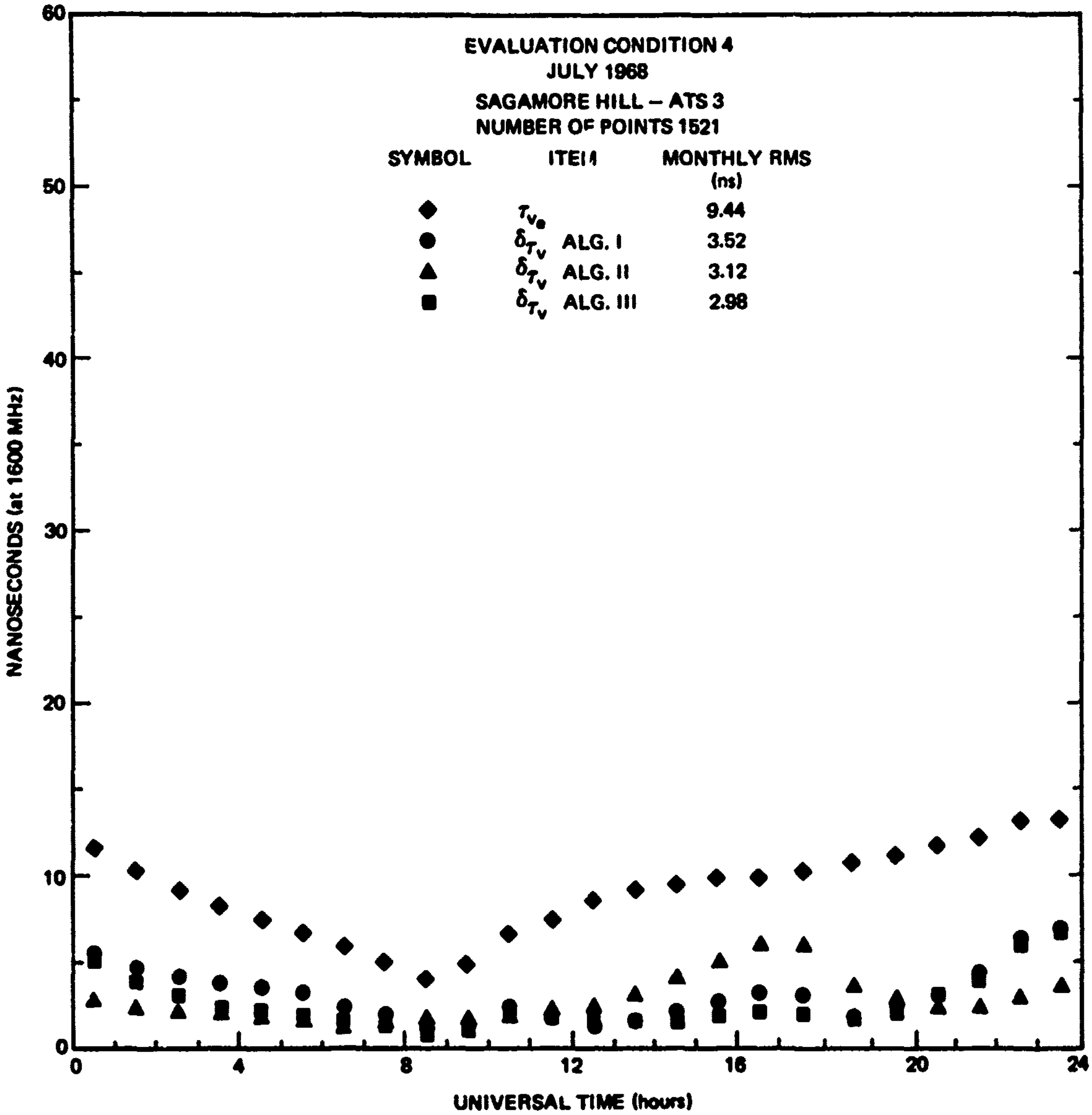

Fig. A.47 VERTICAL TIME DELAY AND RESIDUALS-HOURLY RMS OVER MONTH

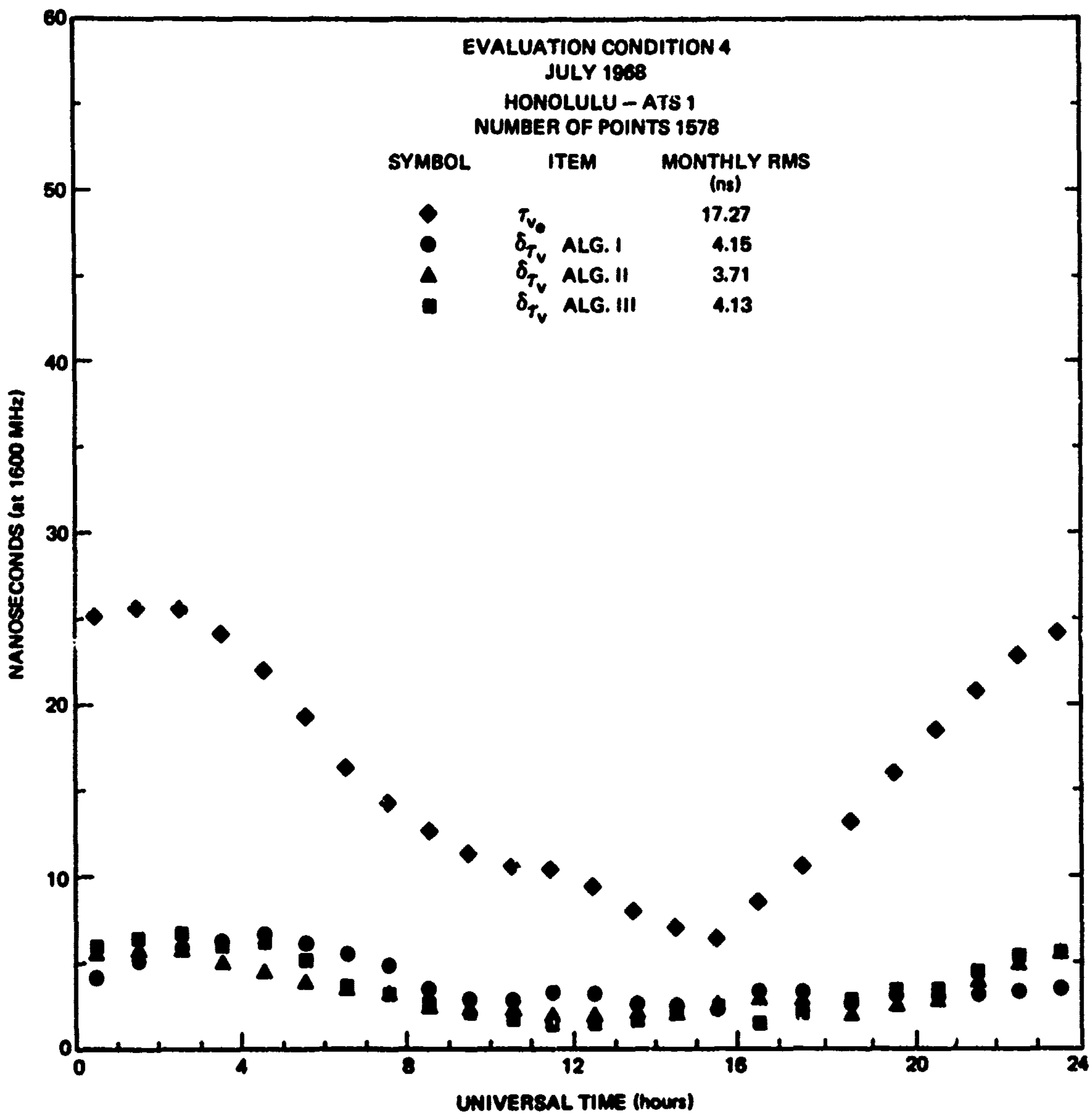

Fig. A.48 VERTICAL TIME DELAY AND RESIDUALS-HOURLY RMS OVER MONTH

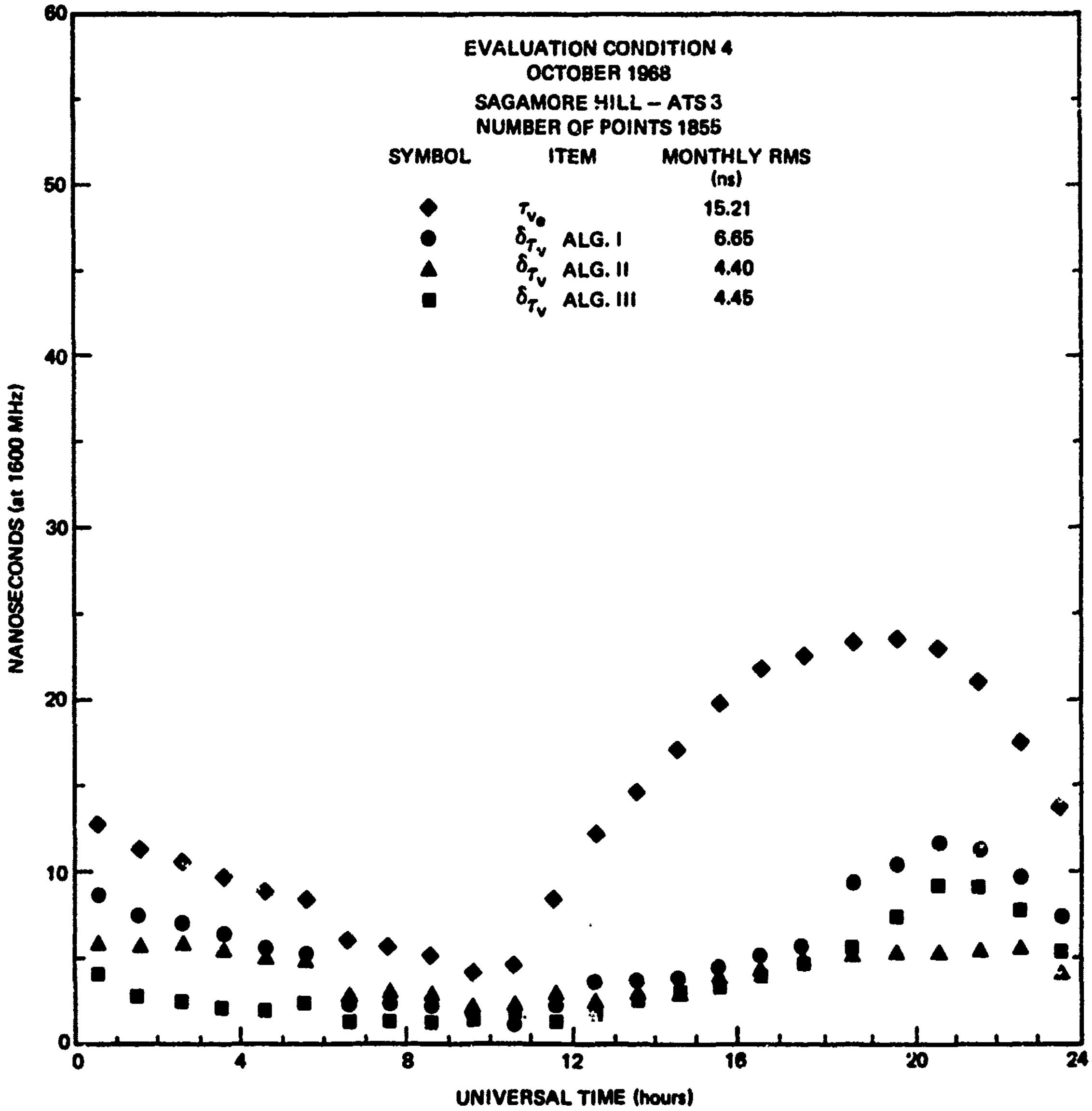

Fig. A.49 VERTICAL TIME DELAY AND RESIDUALS-HOURLY RMS OVER MONTH

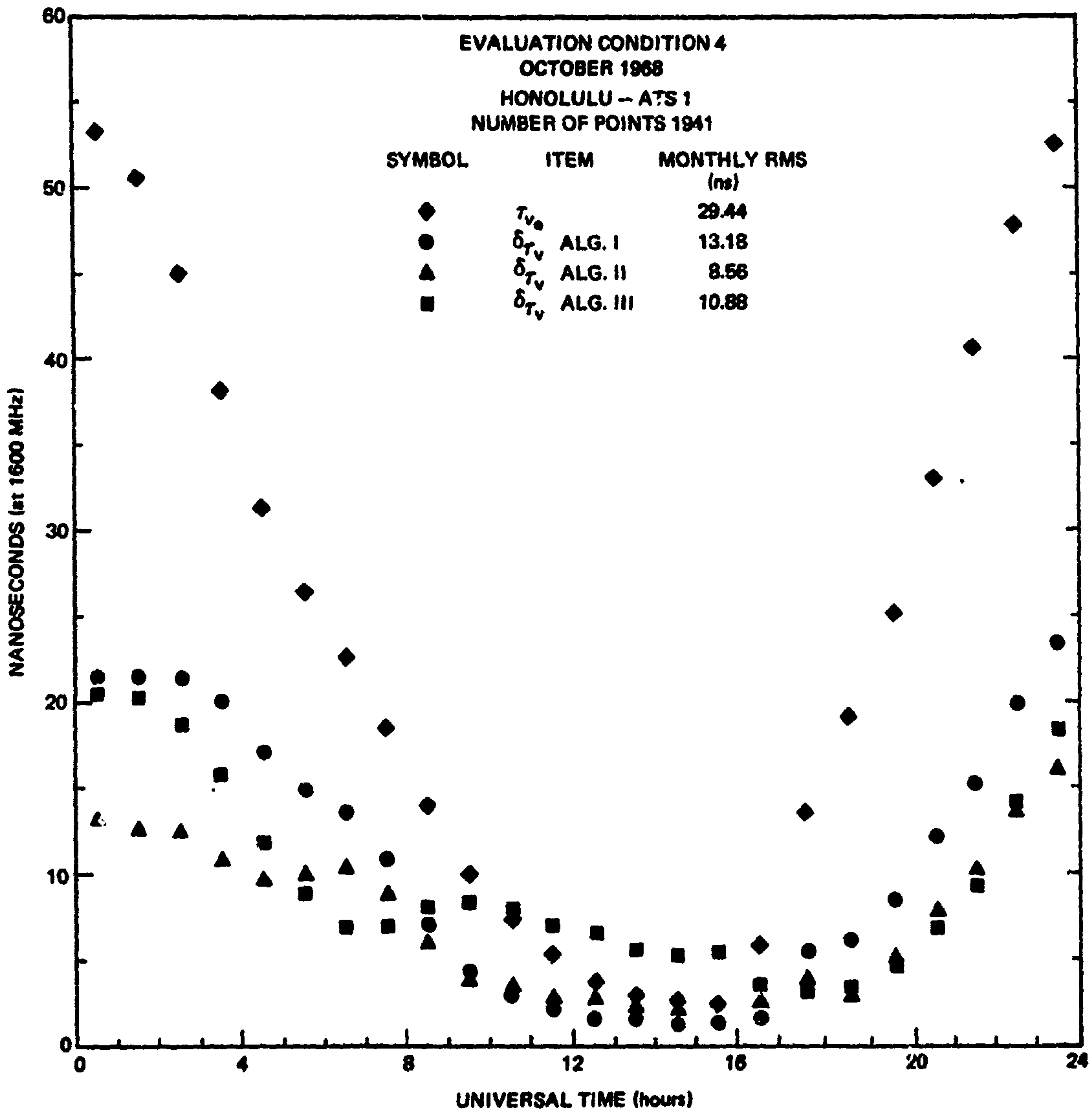

Fig. A.50 VERTICAL TIME DELAY AND RESIDUALS-HOURLY RMS OVER MONTH

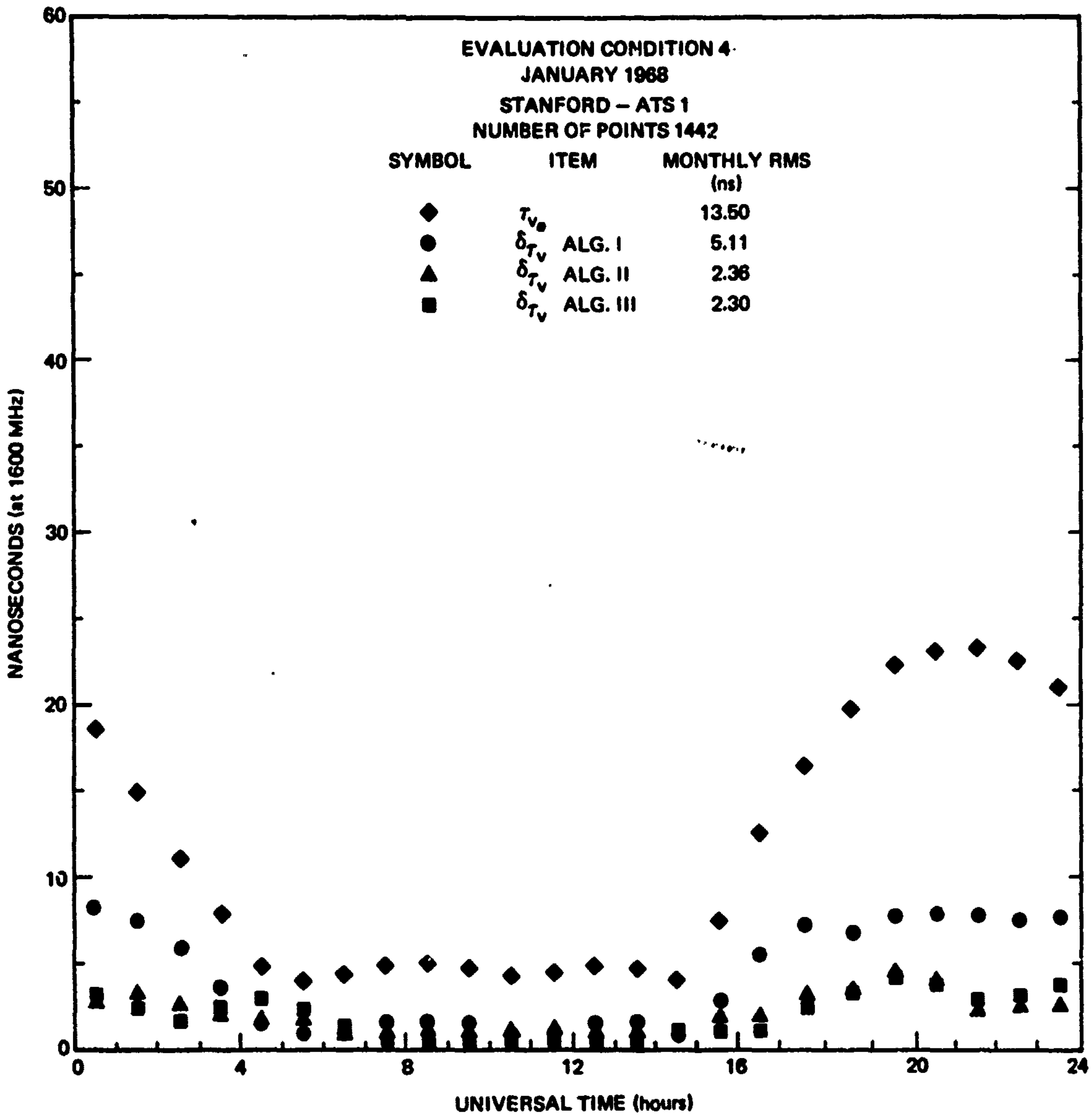

Fig. A.51 VERTICAL TIME DELAY AND RESIDUALS-HOURLY RMS OVER MONTH

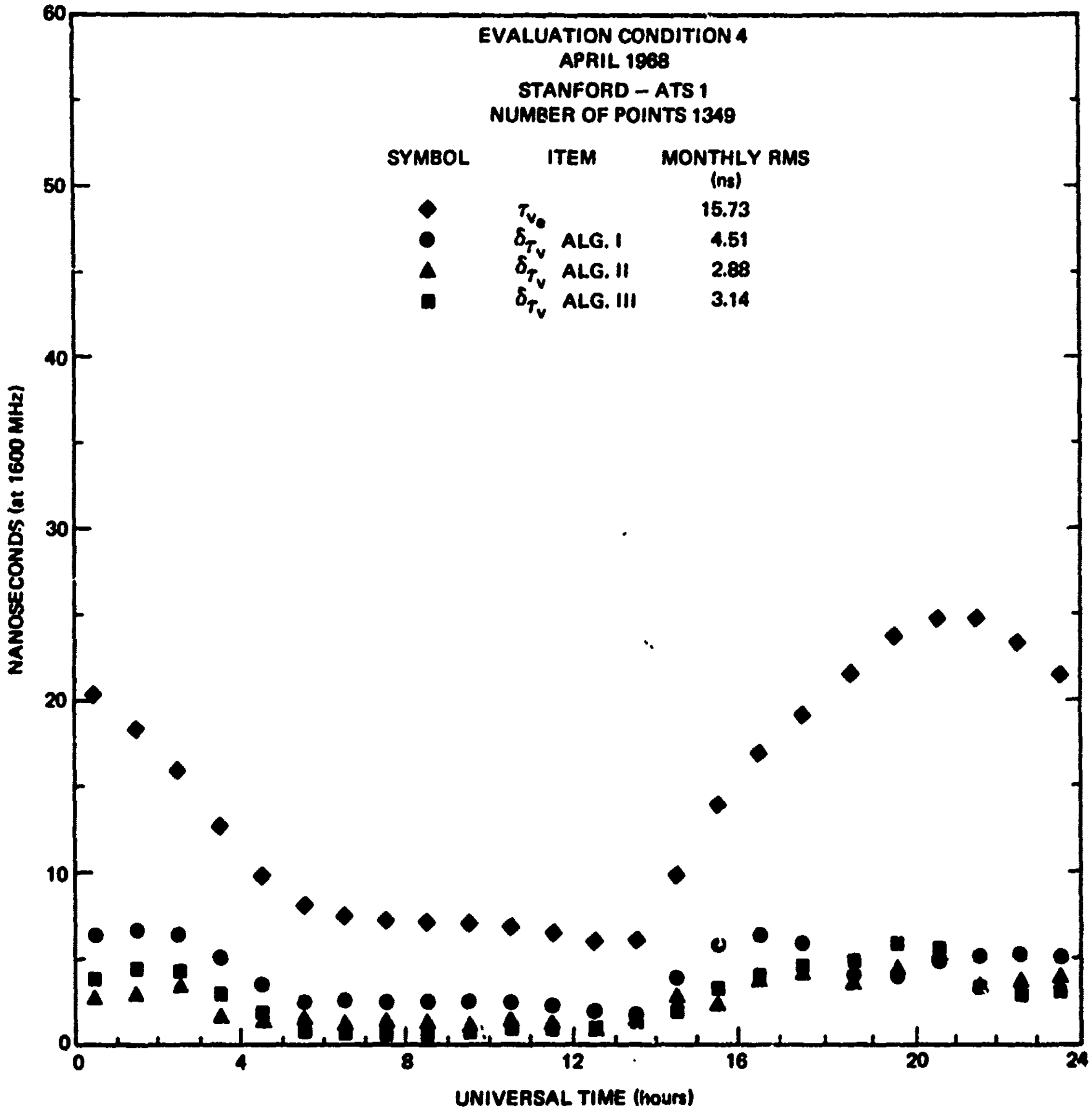

Fig. A.52 VERTICAL TIME DELAY AND RESIDUALS-HOURLY RMS OVER MONTH

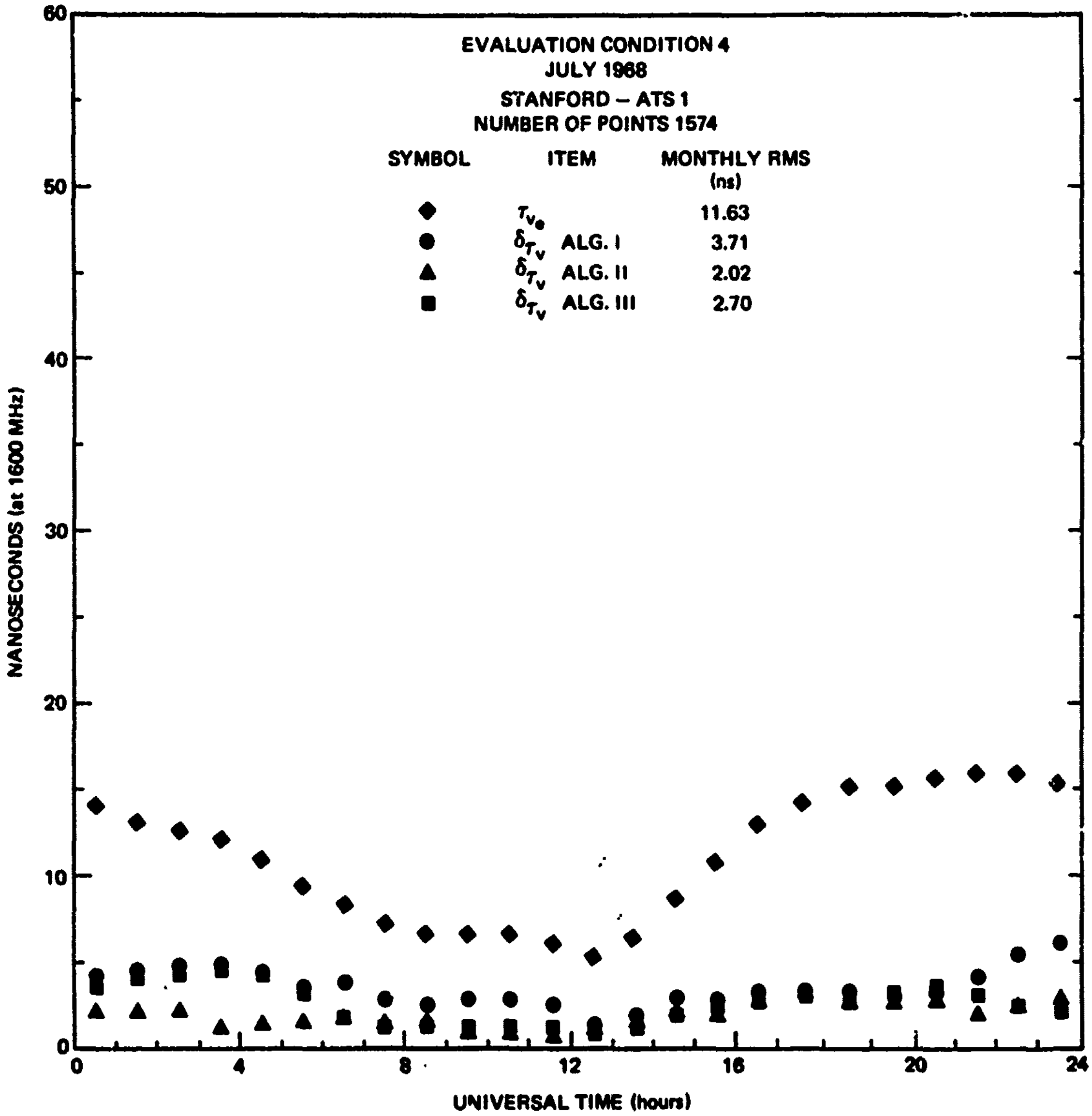

Fig. A.53 VERTICAL TIME DELAY AND RESIDUALS-HOURLY RMS OVER MONTH

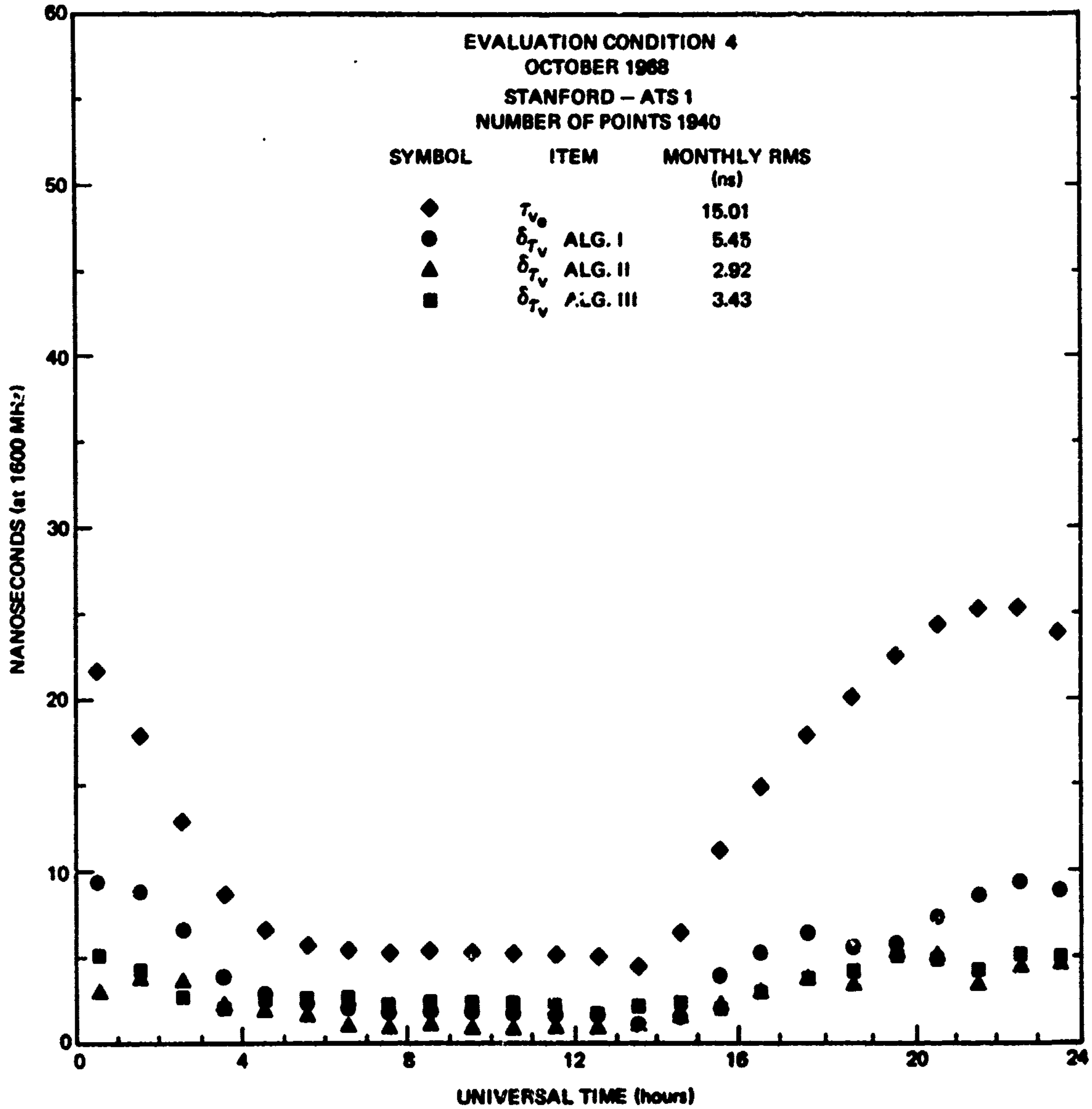

Fig. A.54 VERTICAL TIME DELAY AND RESIDUALS-HOURLY RMS OVER MONTH

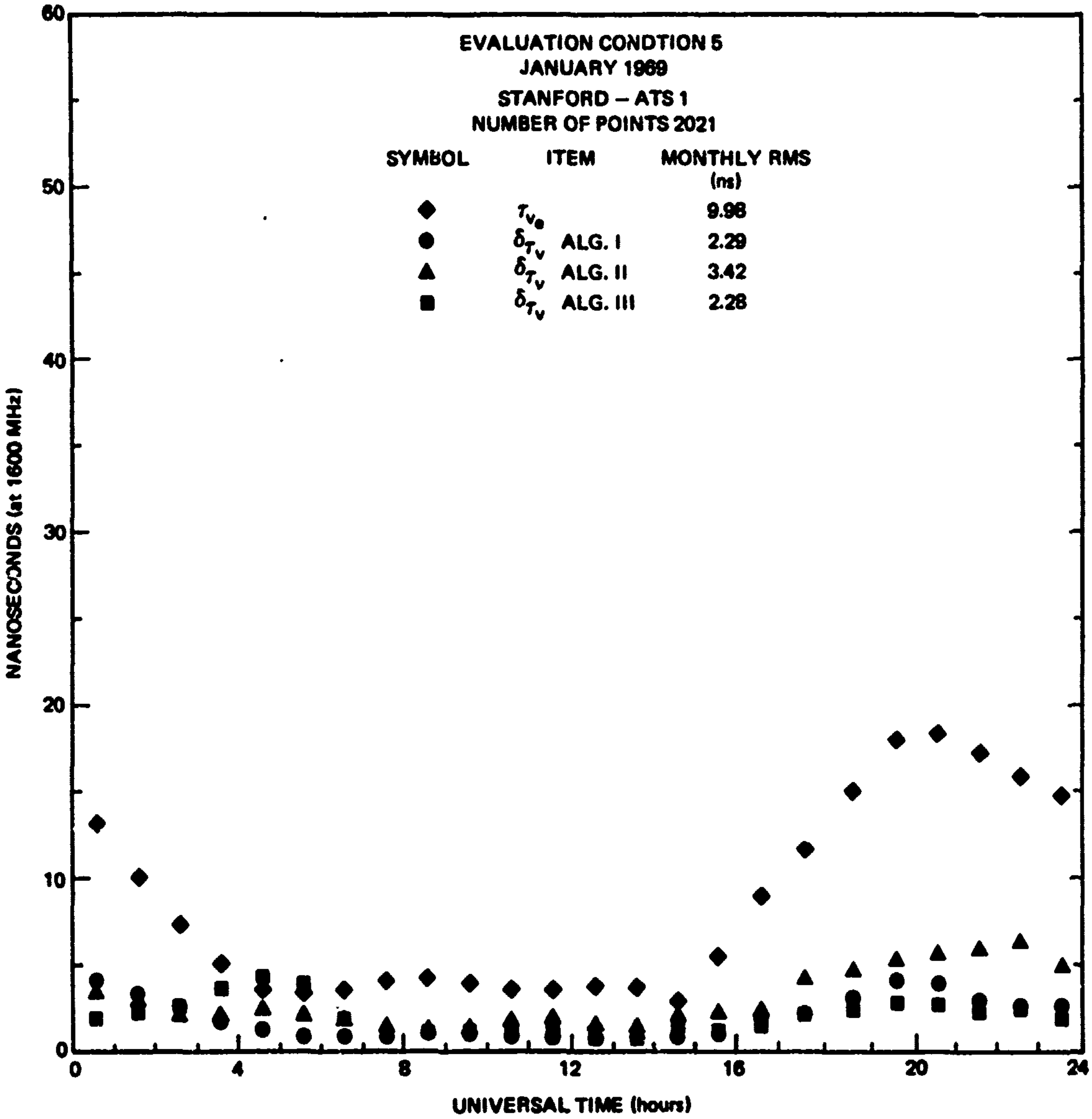

Fig. A.55 VERTICAL TIME DELAY AND RESIDUALS-HOURLY RMS OVER MONTH

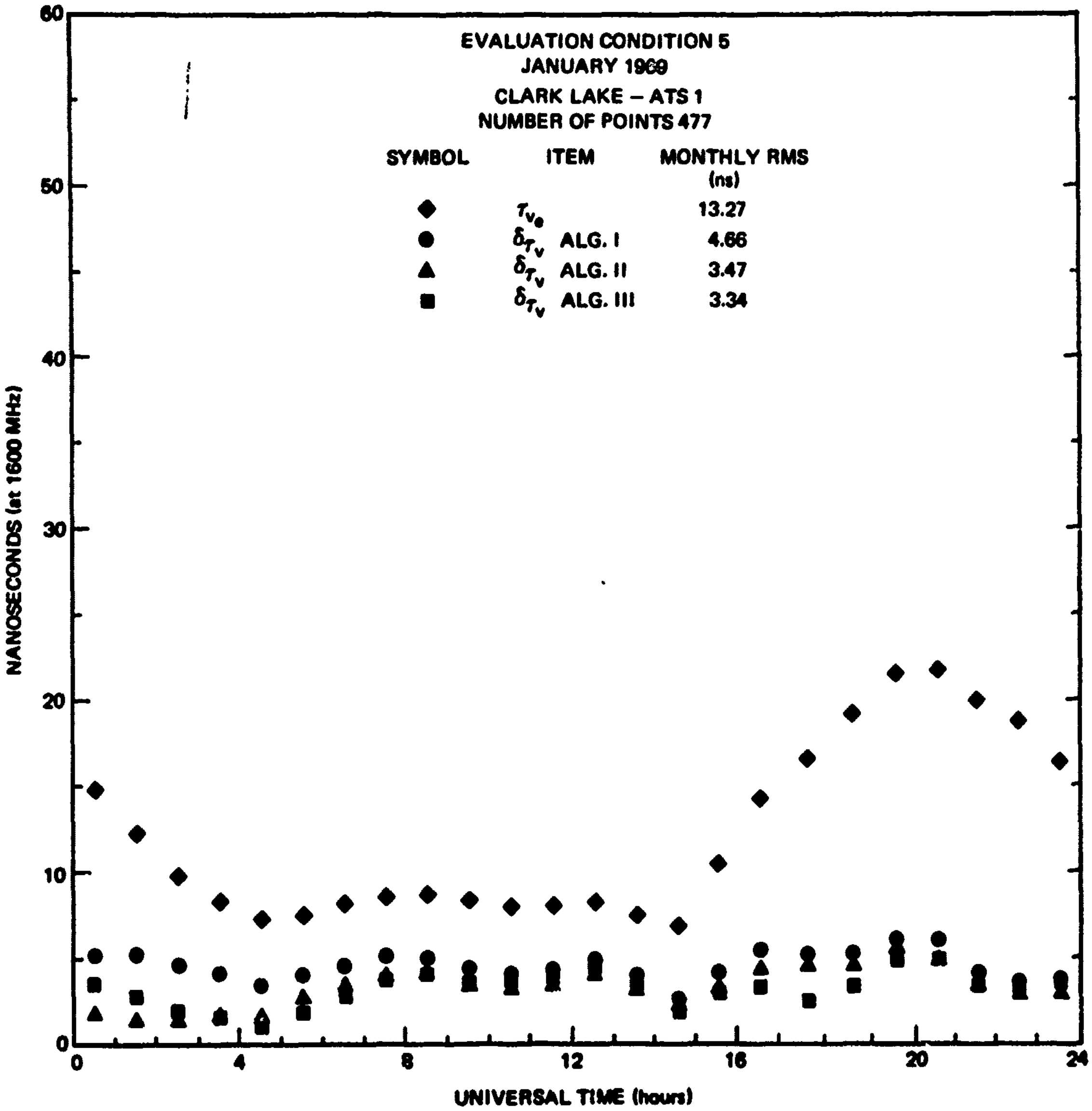

Fig. A.56 VERTICAL TIME DELAY AND RESIDUALS-HOURLY RMS OVER MONTH

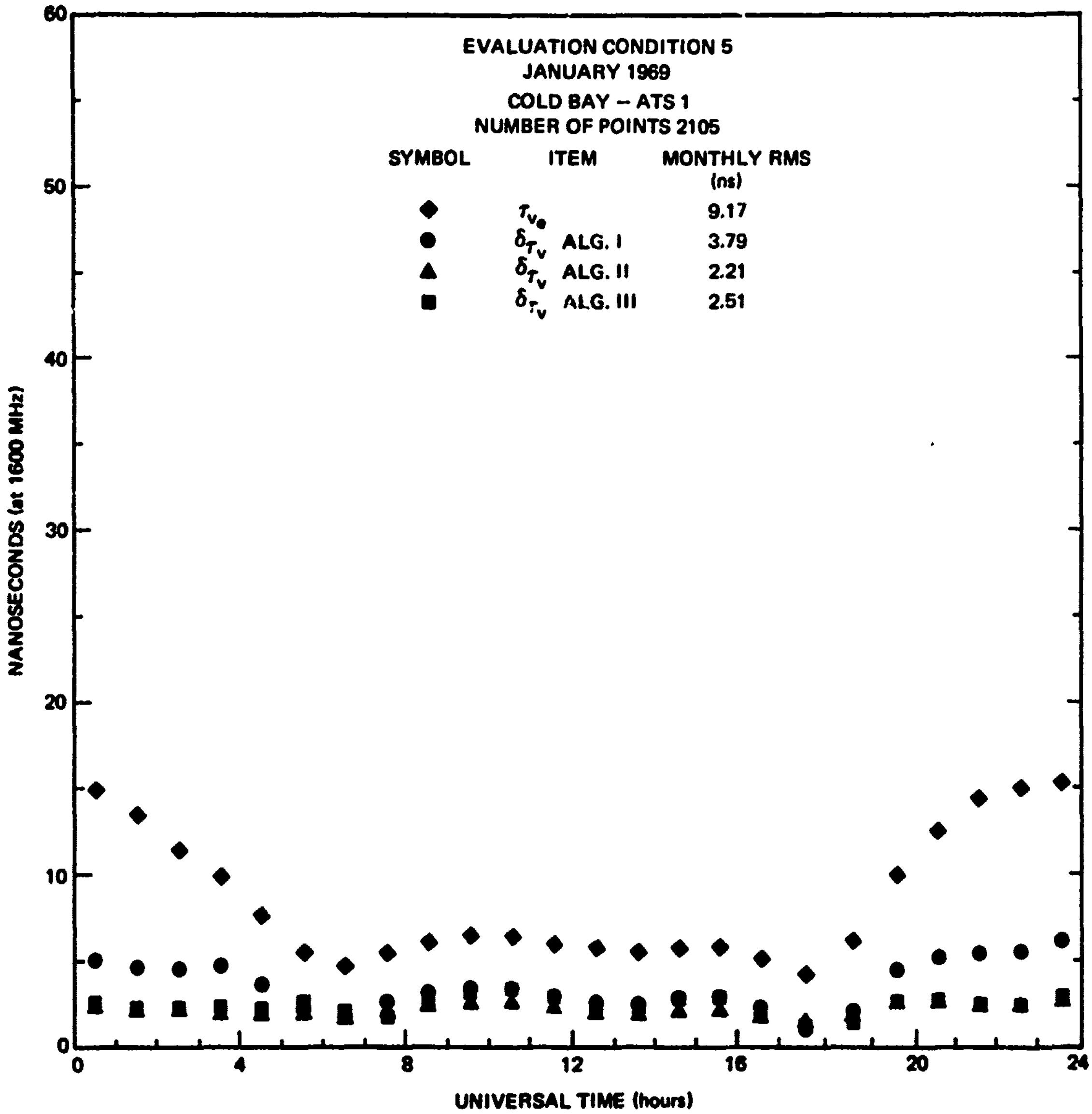

Fig. A.57 VERTICAL TIME DELAY AND RESIDUALS-HOURLY RMS OVER MONTH

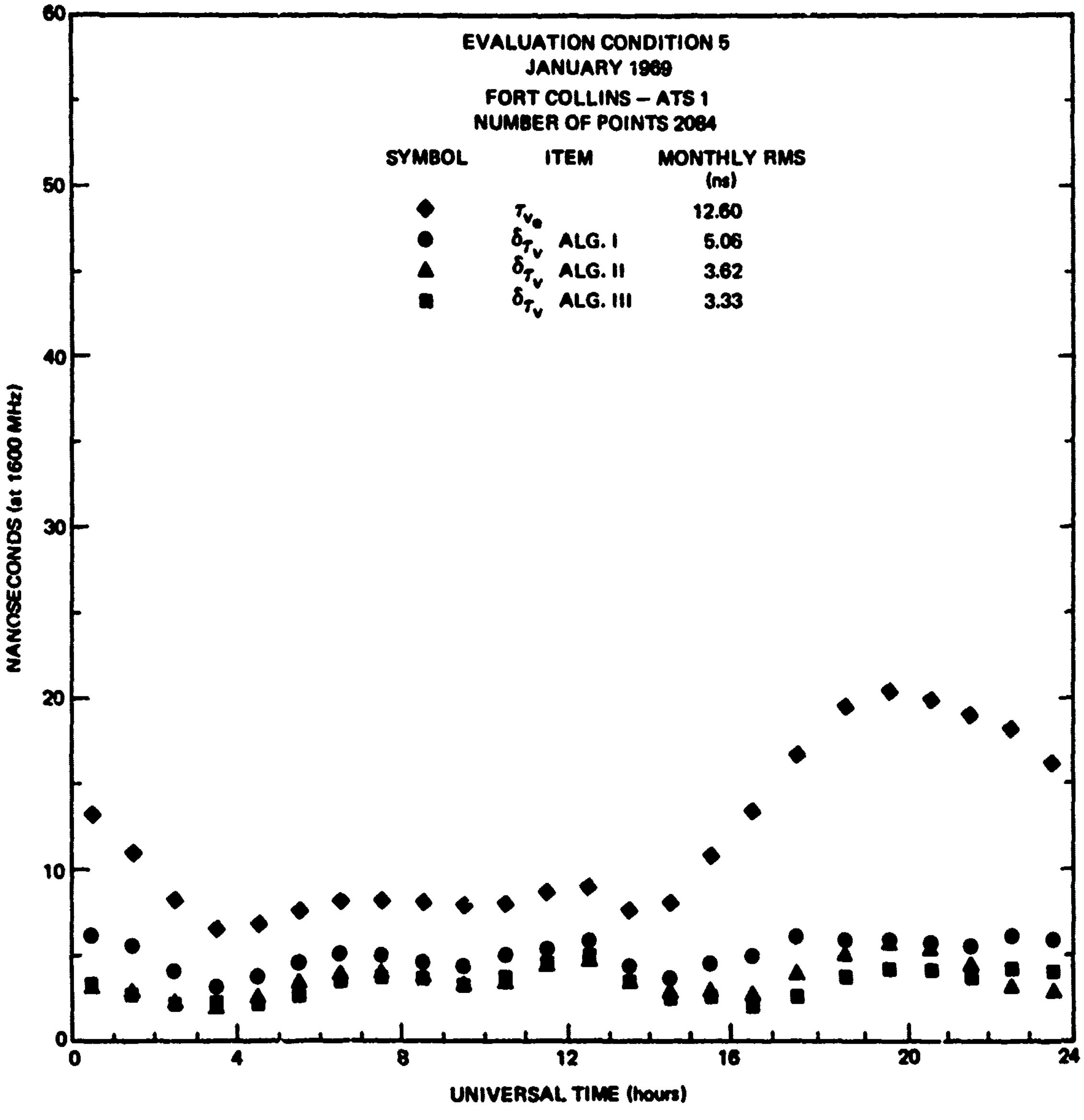

Fig. A.58 VERTICAL TIME DELAY AND RESIDUALS-HOURLY RMS OVER MONTH

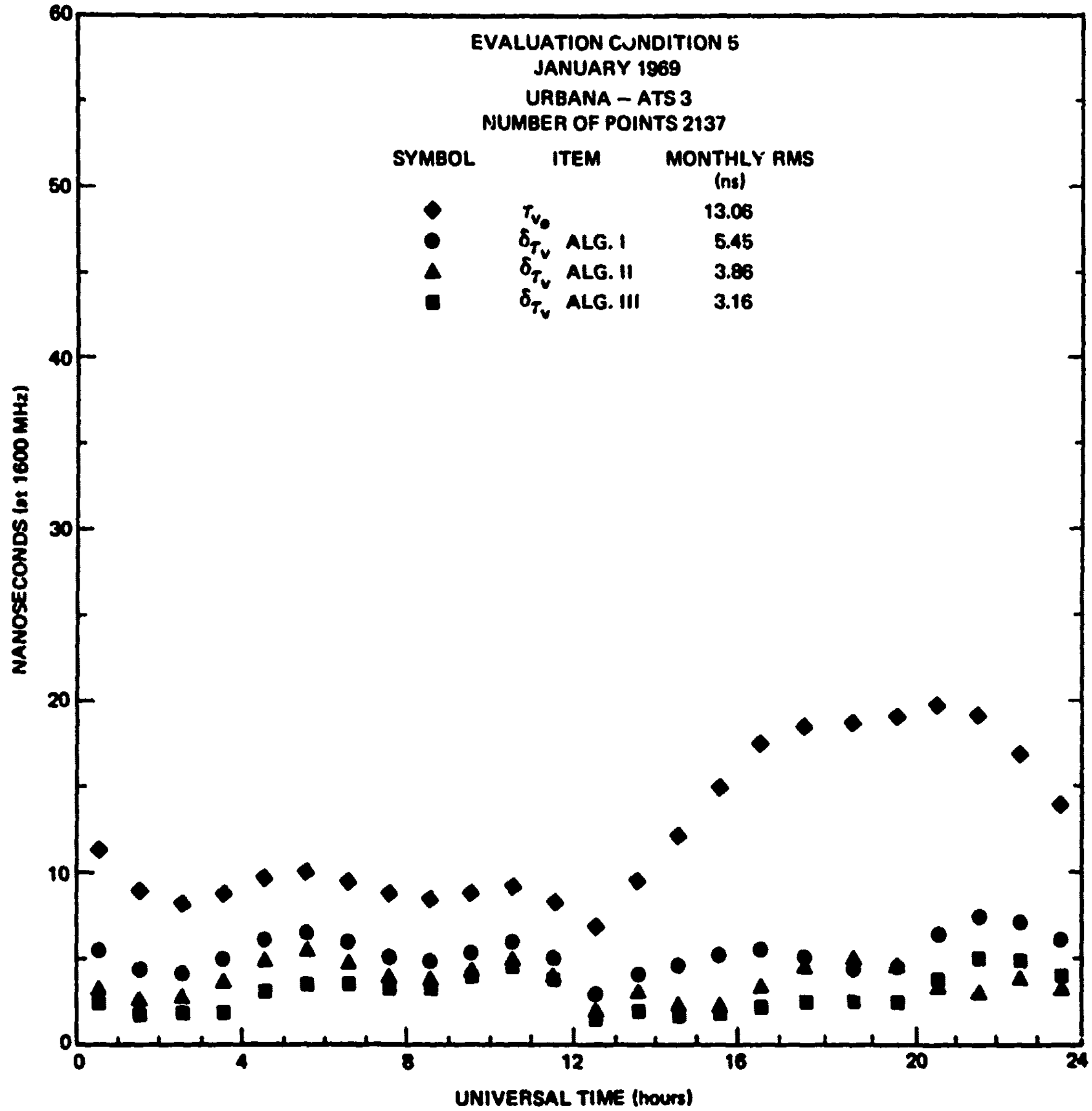

Fig. A.59 VERTICAL TIME DELAY AND RESIDUALS-HOURLY RMS OVER MONTH

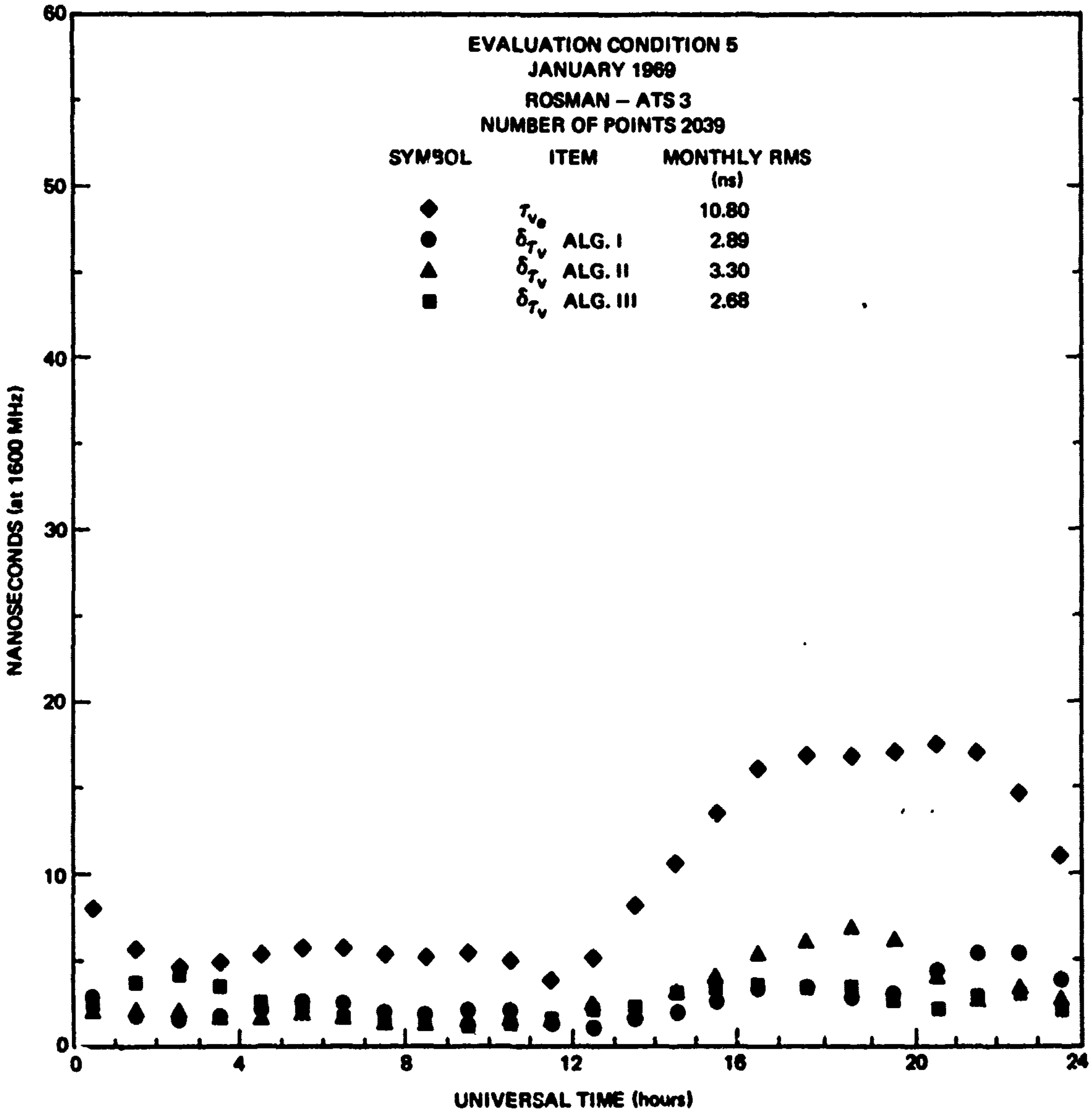

Fig. A.60 VERTICAL TIME DELAY AND RESIDUALS-HOURLY RMS OVER MONTH

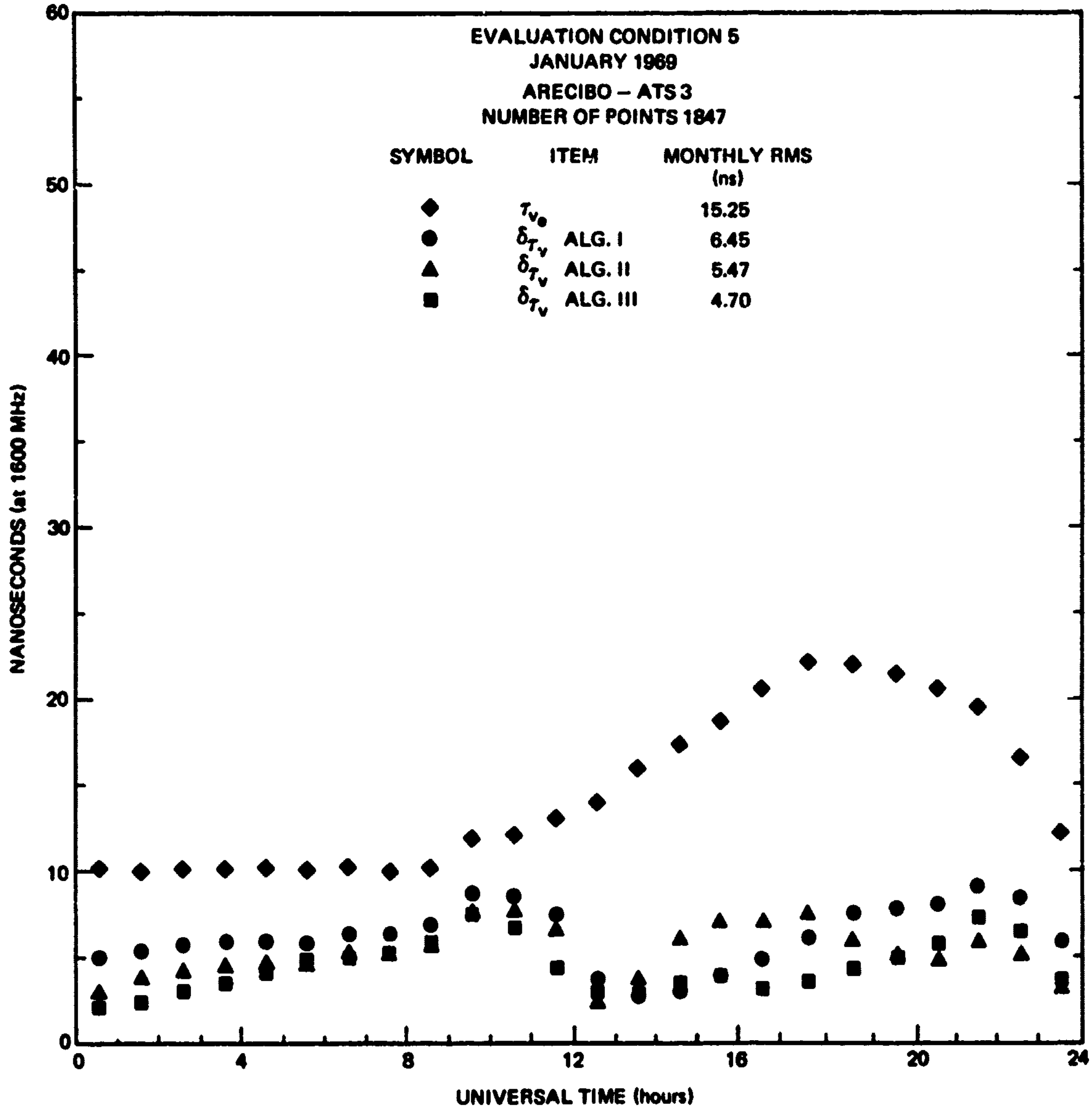

Fig. A.61 VERTICAL TIME DELAY AND RESIDUALS-HOURLY RMS OVER MONTH

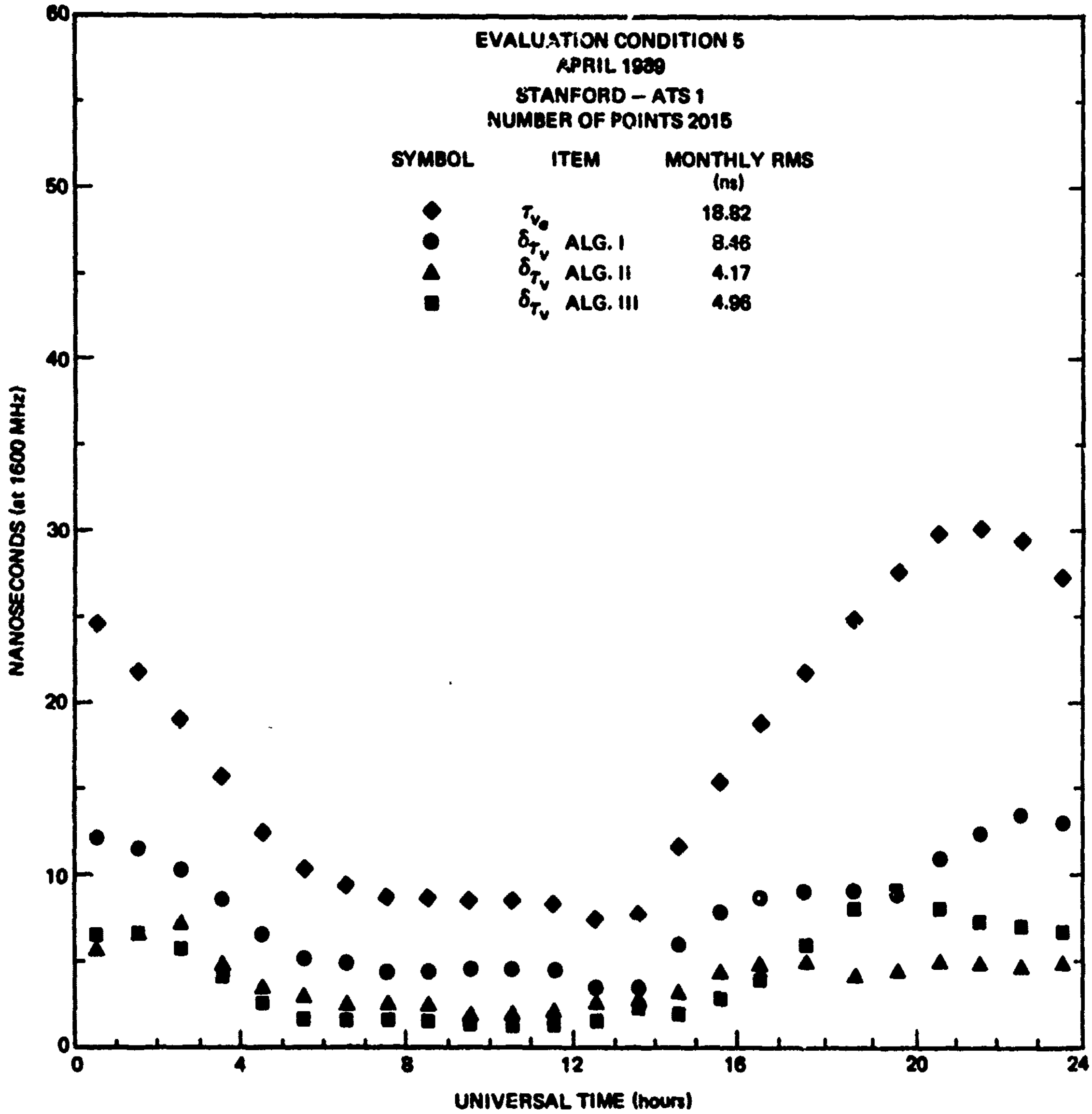

Fig. A.62 VERTICAL TIME DELAY AND RESIDUALS-HOURLY RMS OVER MONTH

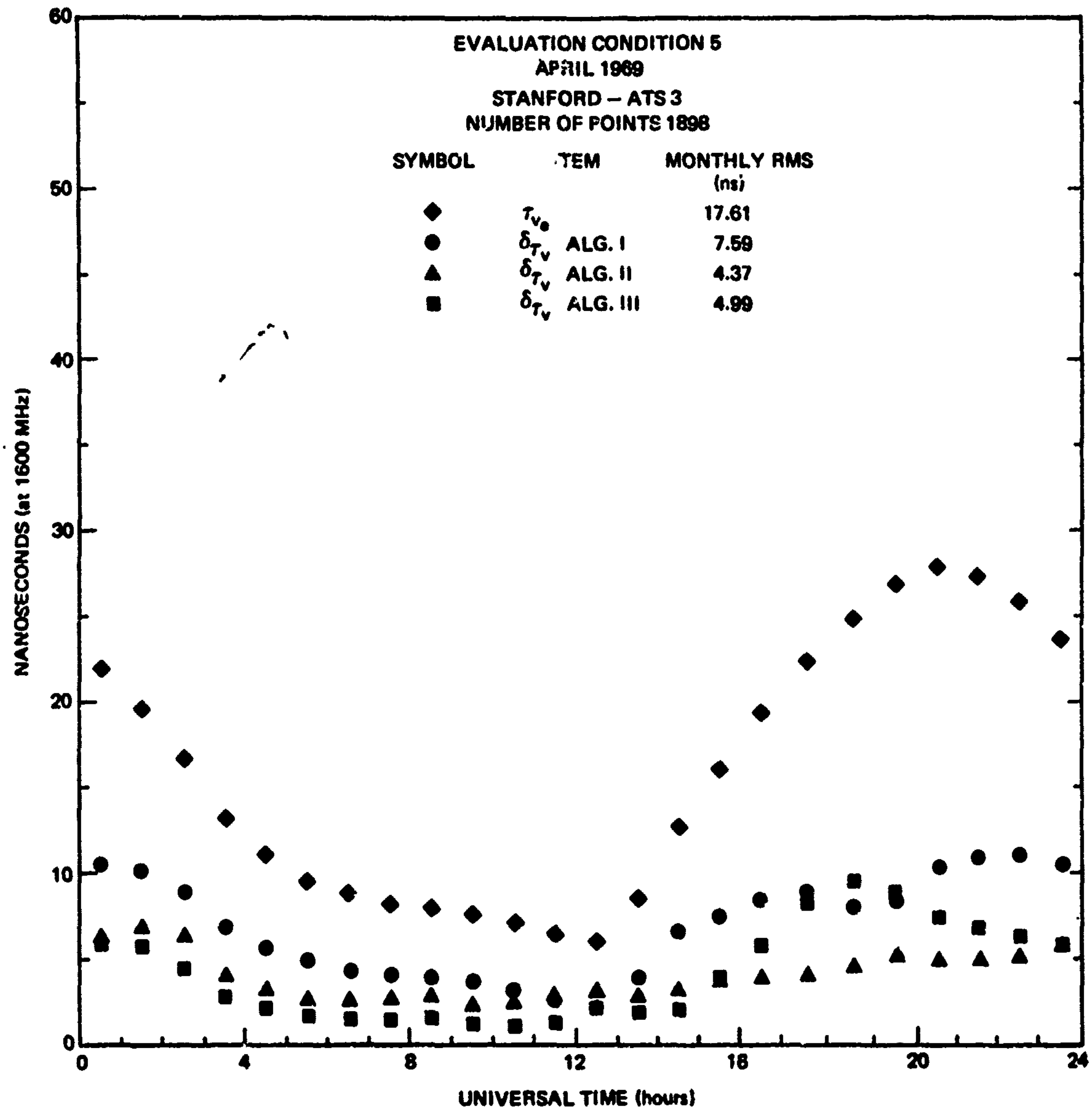

Fig. A.63 VERTICAL TIME DELAY AND RESIDUALS-HOURLY RMS OVER MONTH

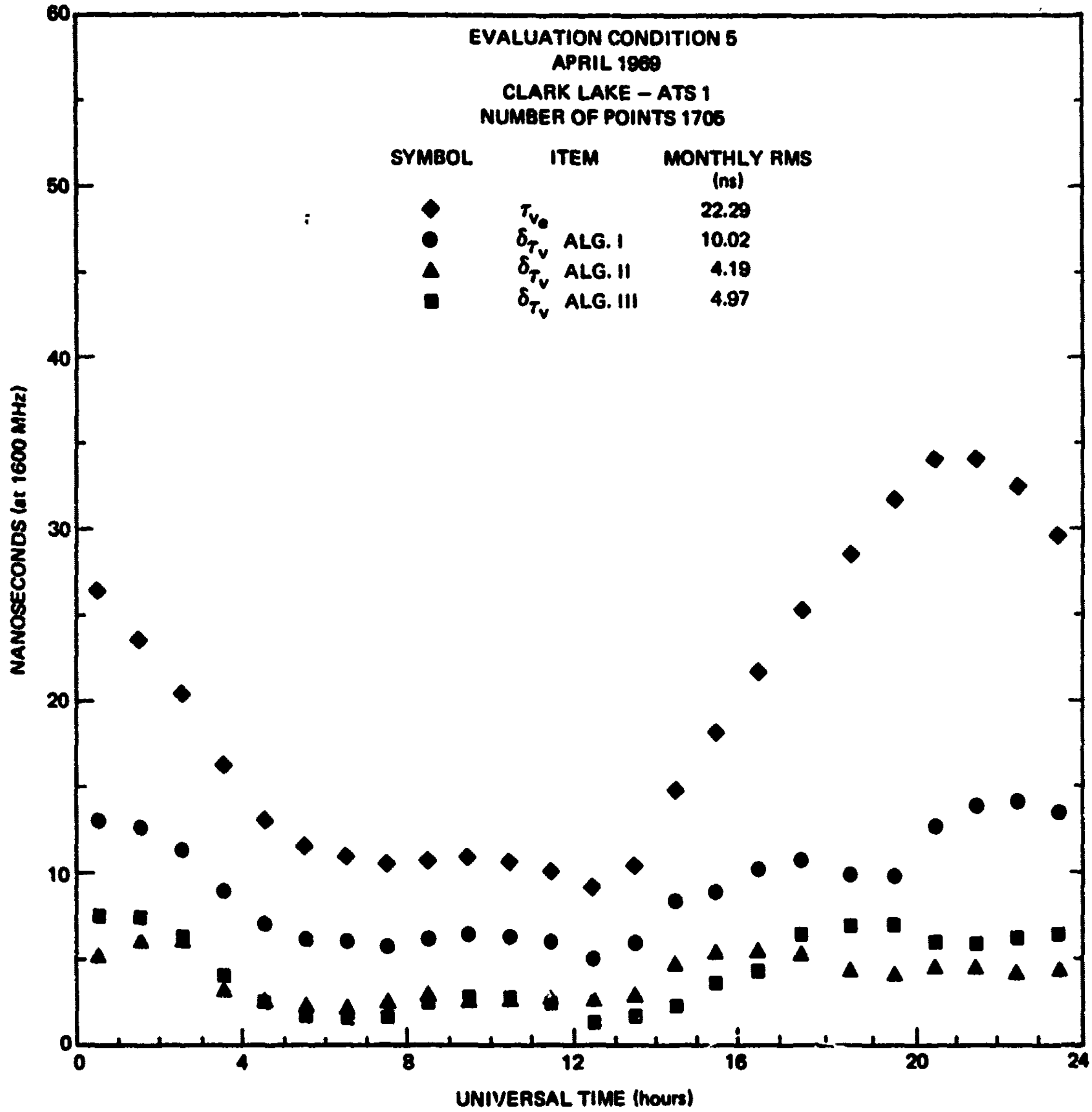

Fig. A.64 VERTICAL TIME DELAY AND RESIDUALS-HOURLY RMS OVER MONTH

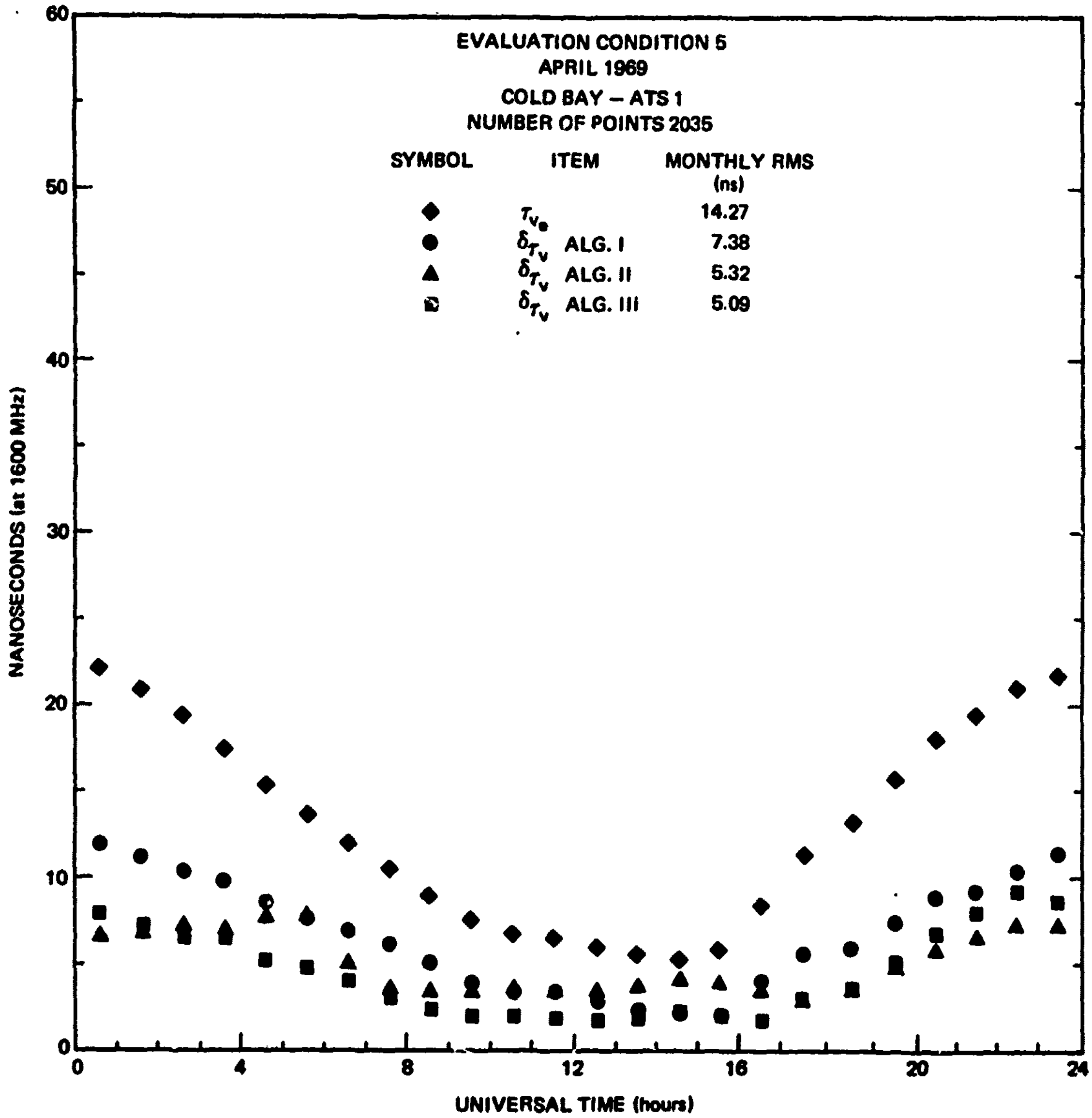

Fig. A.65 VERTICAL TIME DELAY AND RESIDUALS-HOURLY RMS OVER MONTH

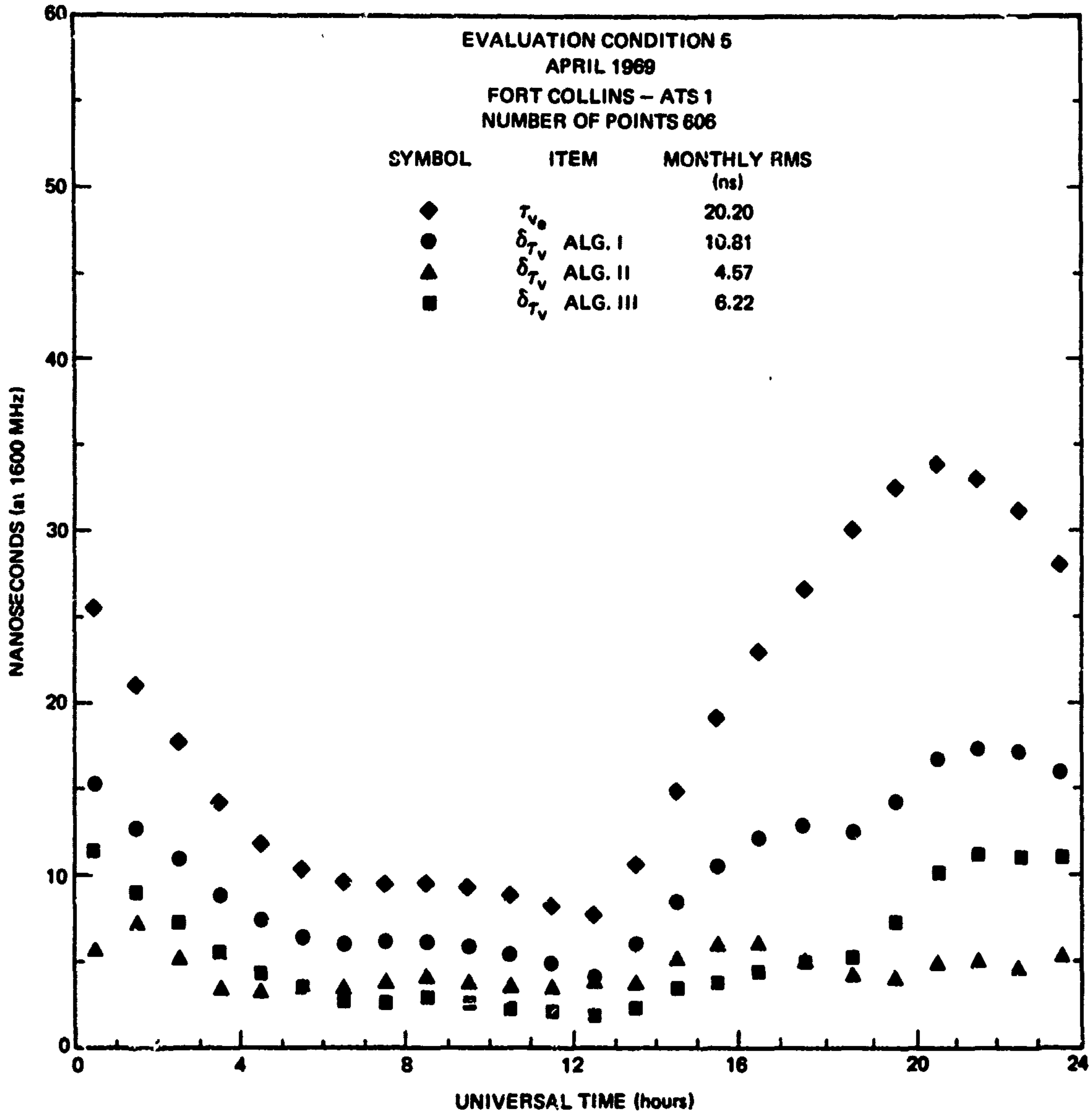

Fig. A.66 VERTICAL TIME DELAY AND RESIDUALS-HOURLY RMS OVER MONTH

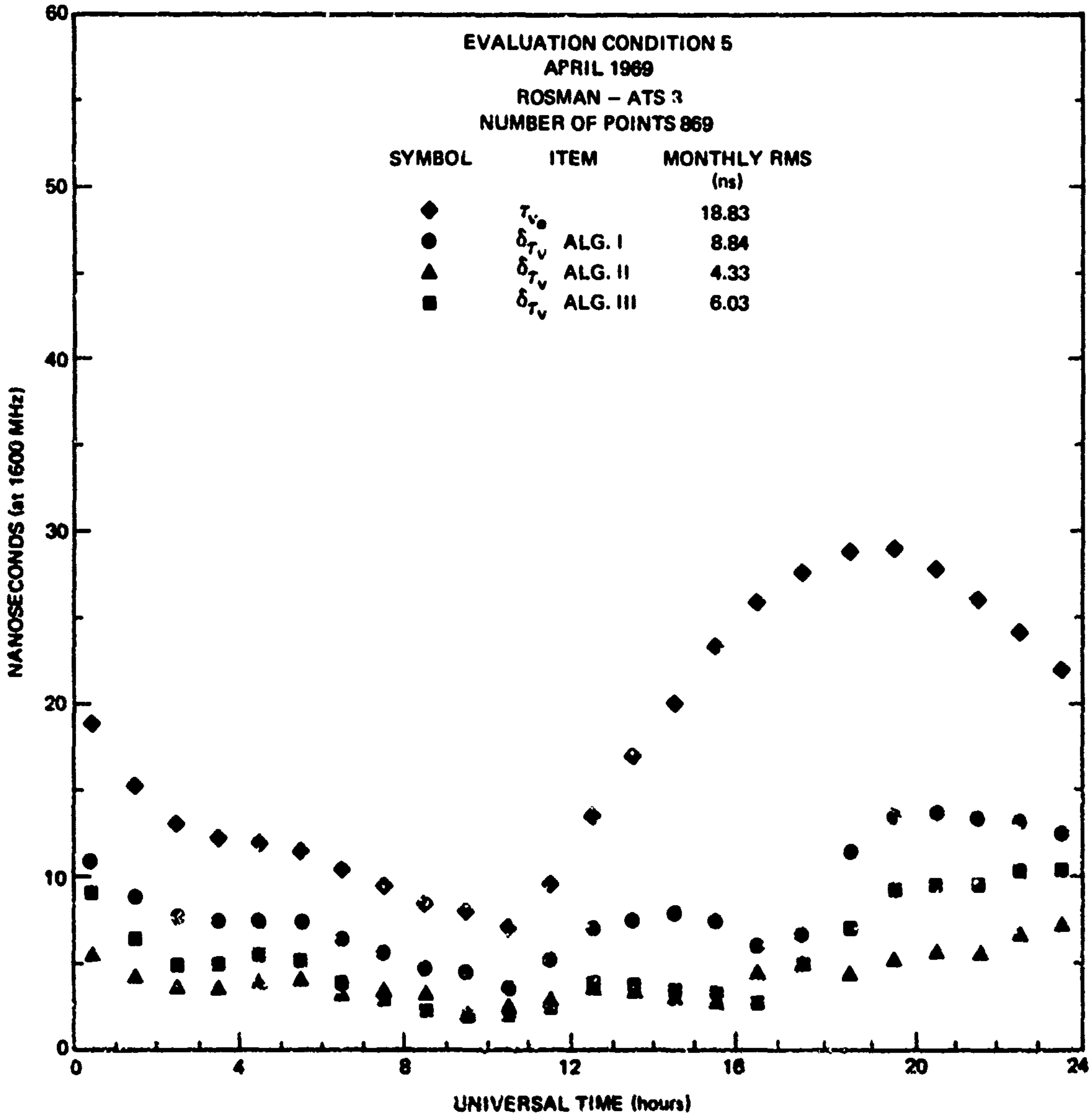

Fig. A.67 VERTICAL TIME DELAY AND RESIDUALS-HOURLY RMS OVER MONTH

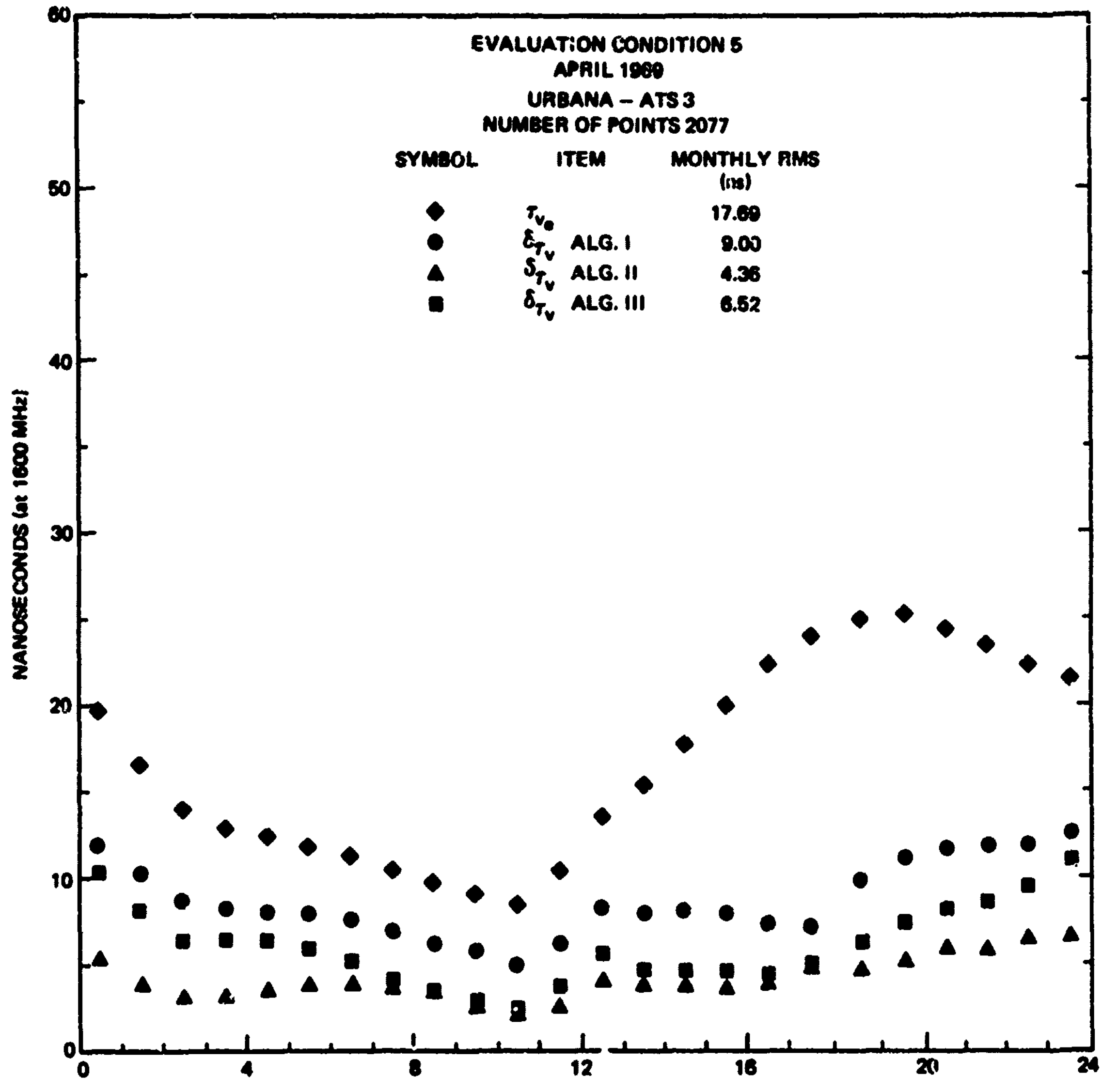

Fig. A.68 VERTICAL TIME DELAY AND RESIDUALS-HOURLY RMS OVER MONTH

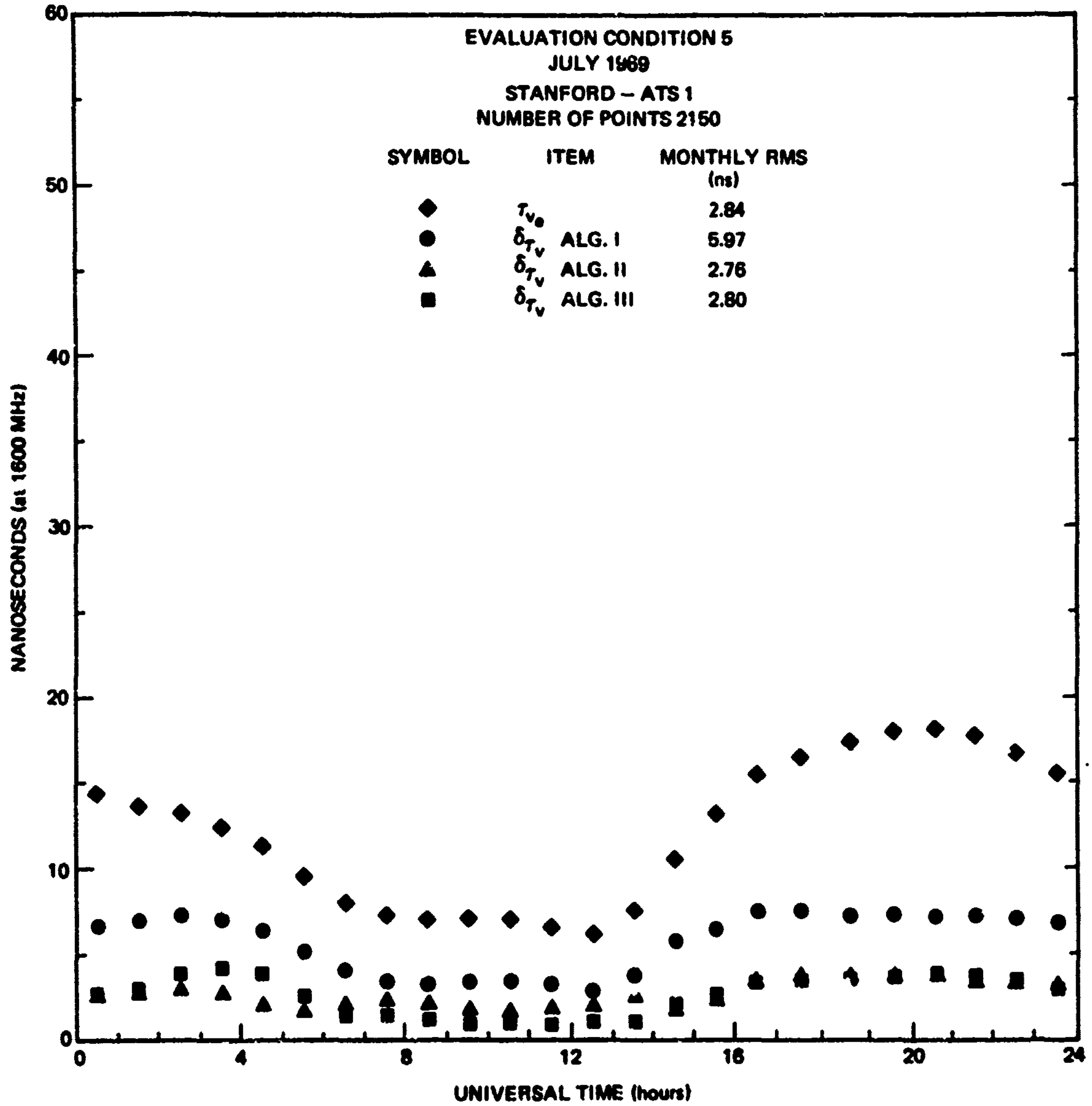

Fig. A.69 VERTICAL TIME DELAY AND RESIDUALS-HOURLY RMS OVER MONTH

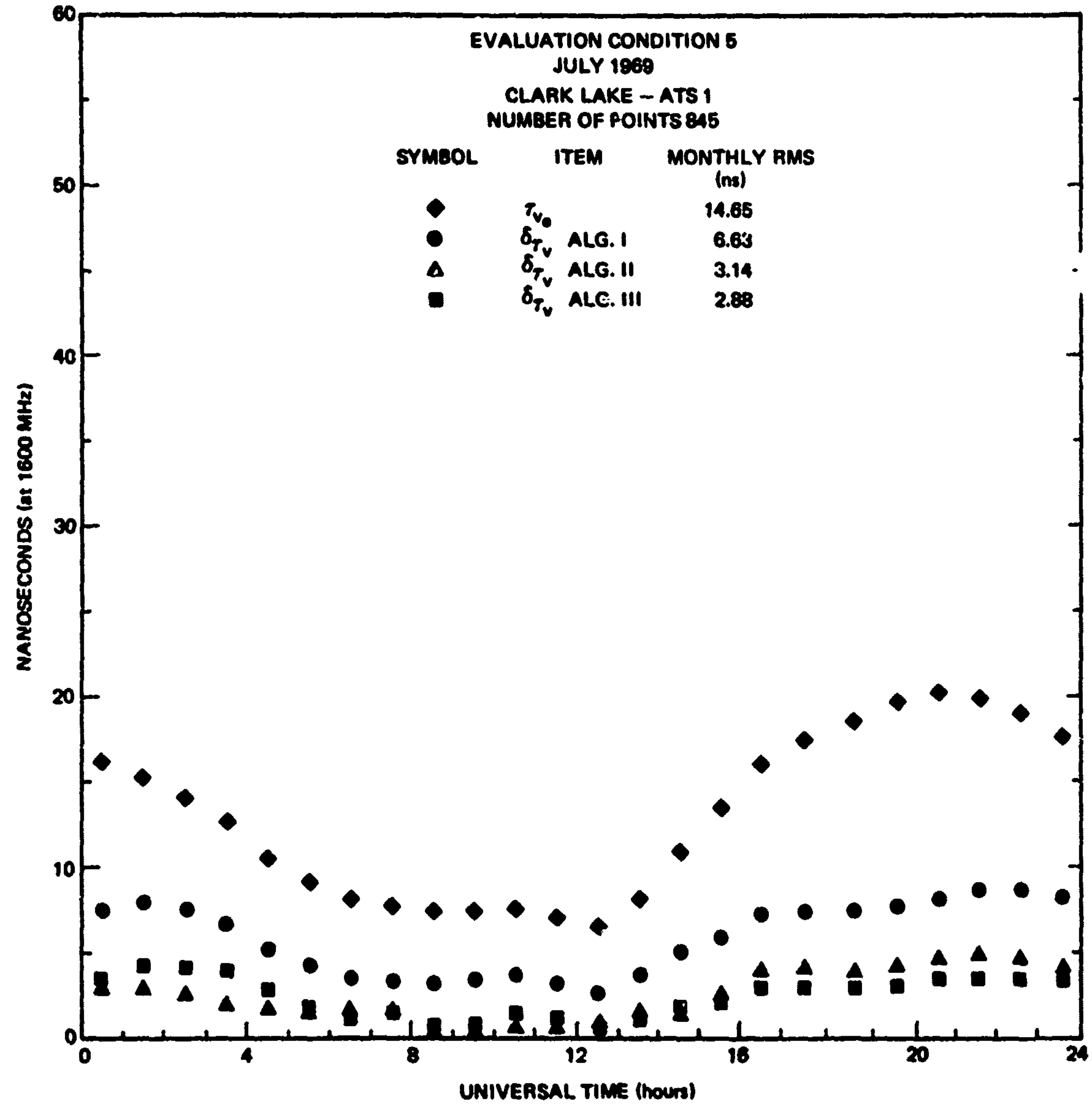

Fig. A.70 VERTICAL TIME DELAY AND RESIDUALS-HOURLY RMS OVER MONTH

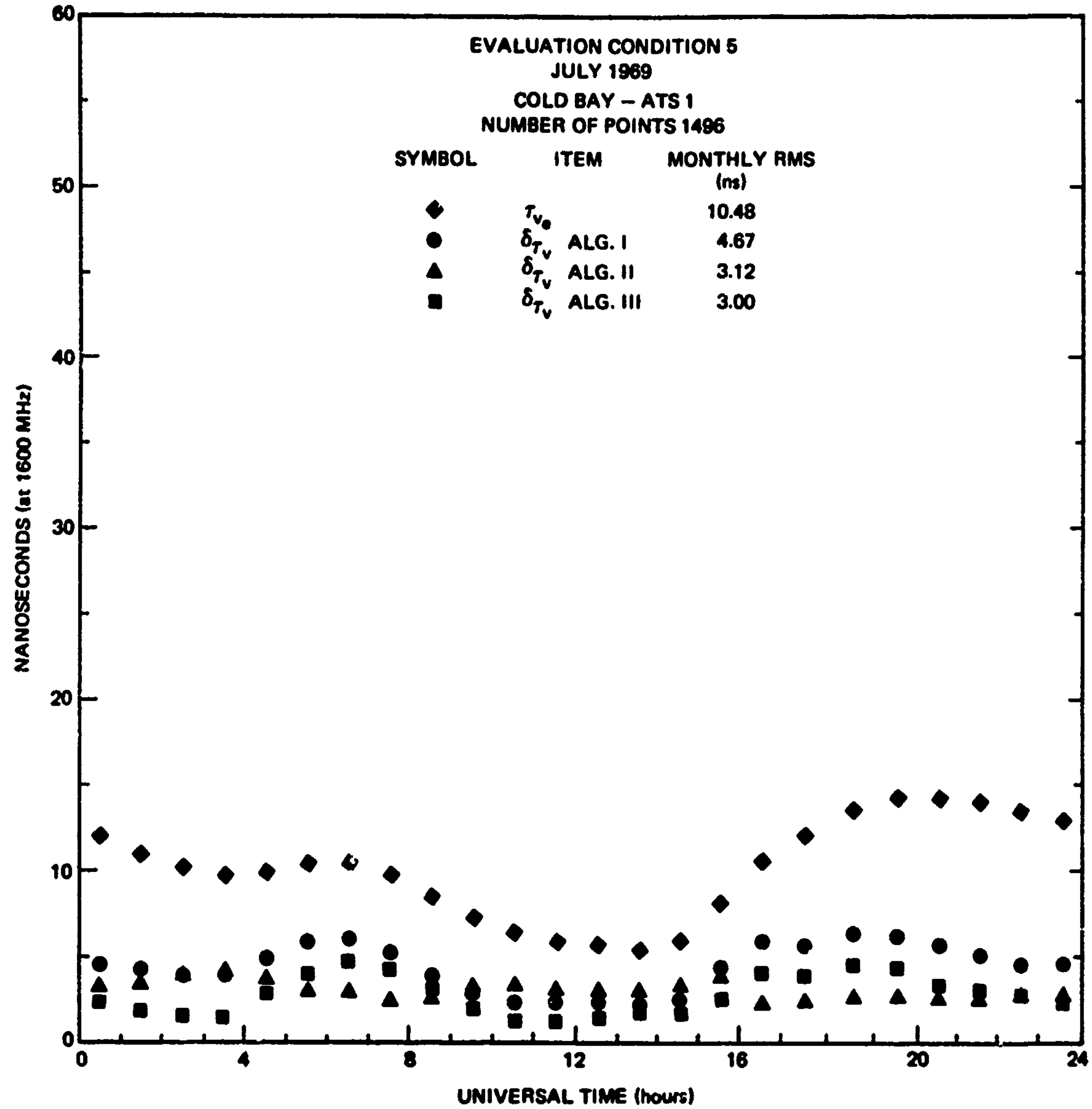

Fig. A.71 VERTICAL TIME DELAY AND RESIDUALS-HOURLY RMS OVER MONTH

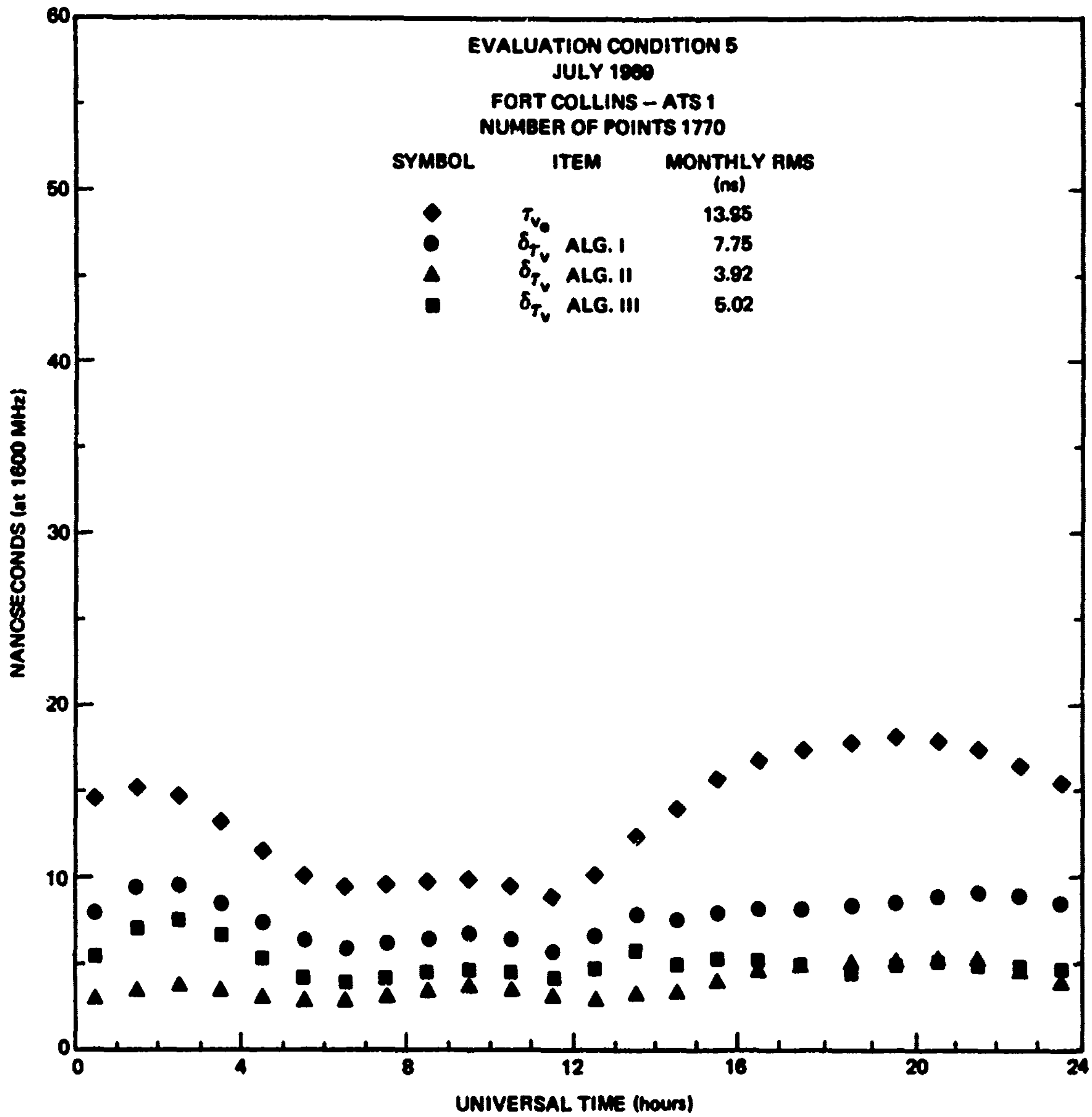

Fig. A.72 VERTICAL TIME DELAY AND RESIDUALS-HOURLY RMS OVER MONTH

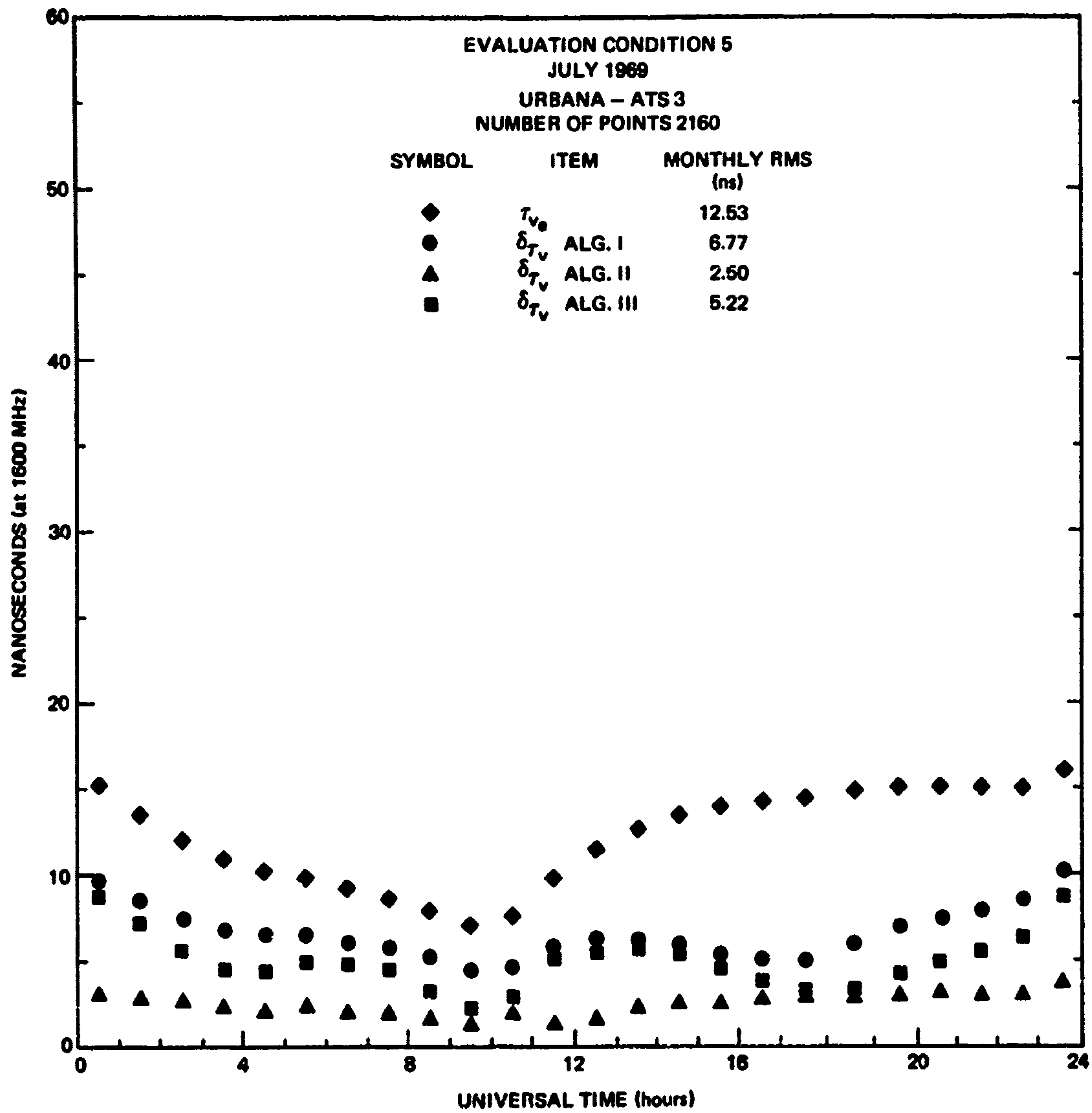

Fig. A.73 VERTICAL TIME DELAY AND RESIDUALS-HOURLY RMS OVER MONTH

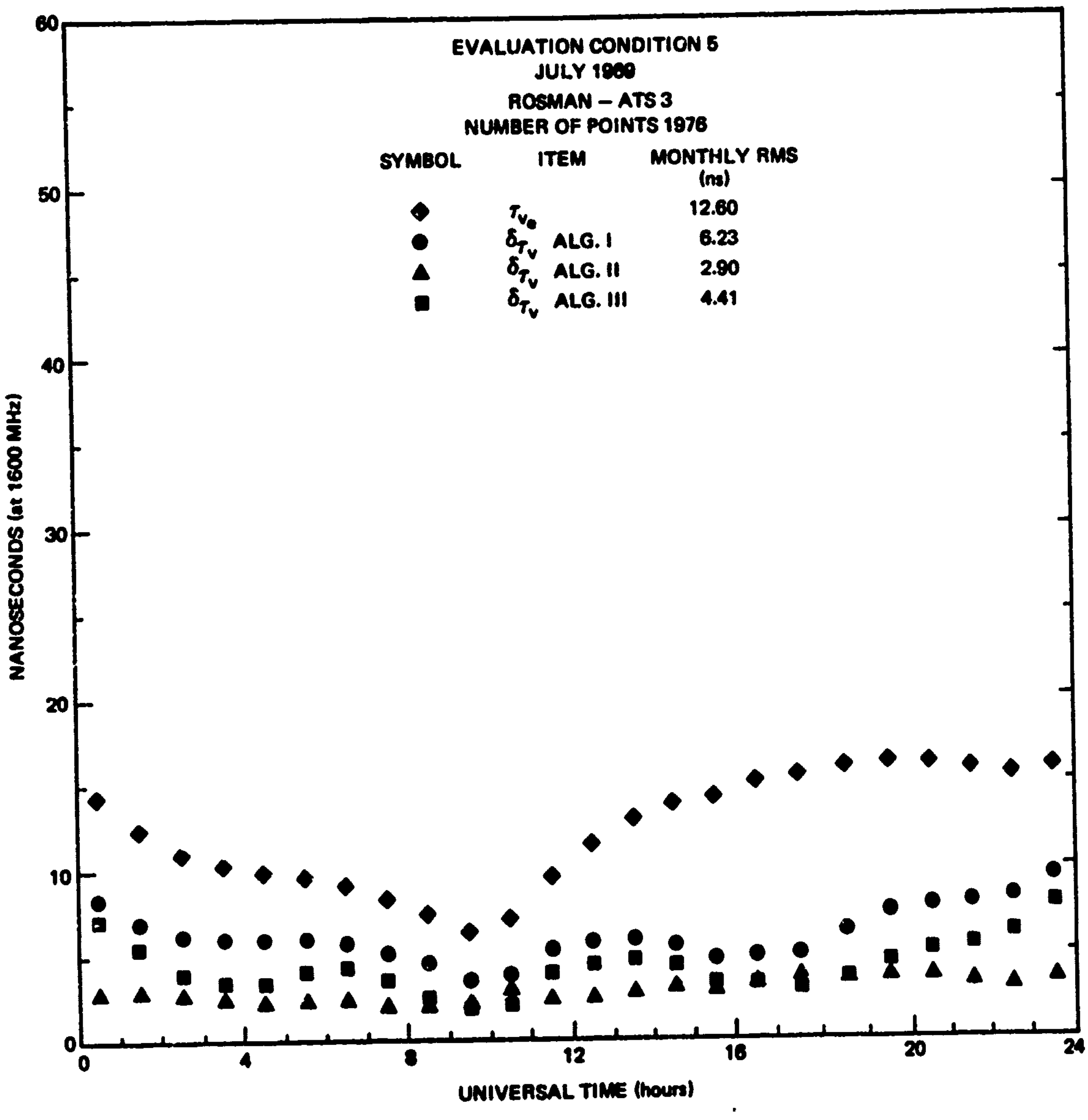

Fig. A.74 VERTICAL TIME DELAY AND RESIDUALS-HOURLY RMS OVER MONTH

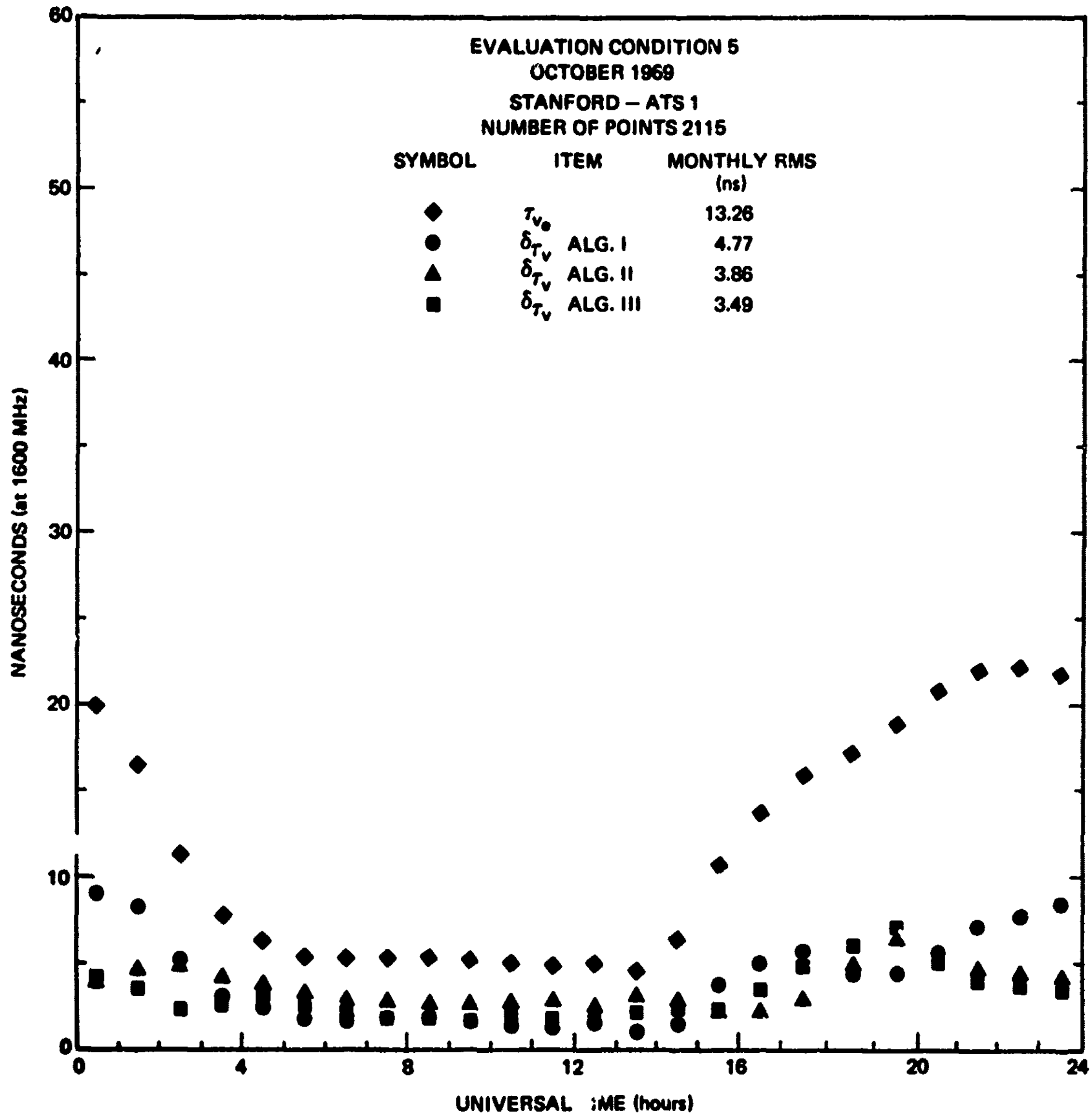

Fig. A.75 VERTICAL TIME DELAY AND RESIDUALS-HOURLY RMS OVER MONTH

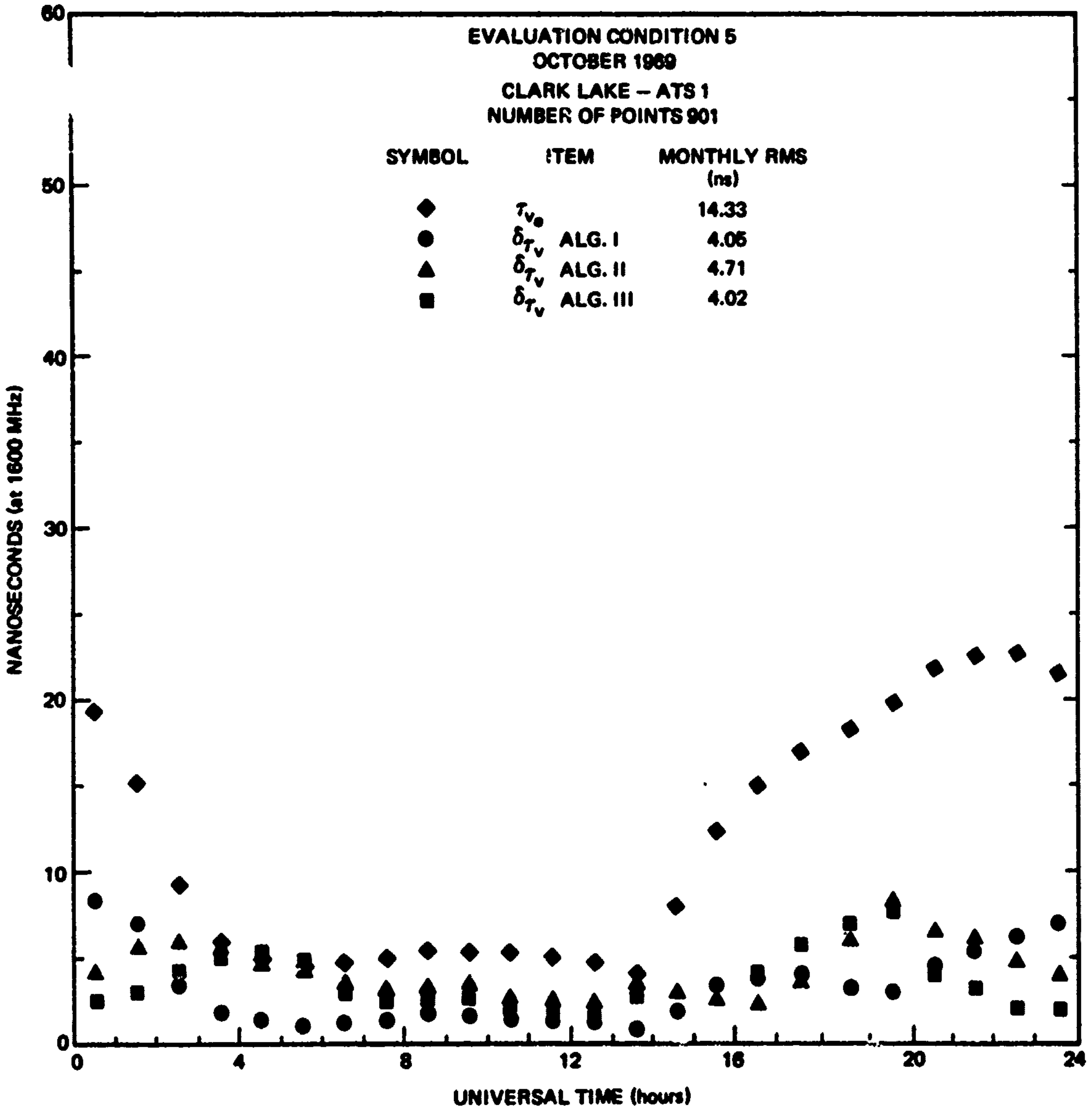

Fig. A.76 VERTICAL TIME DELAY AND RESIDUALS-HOURLY RMS OVER MONTH

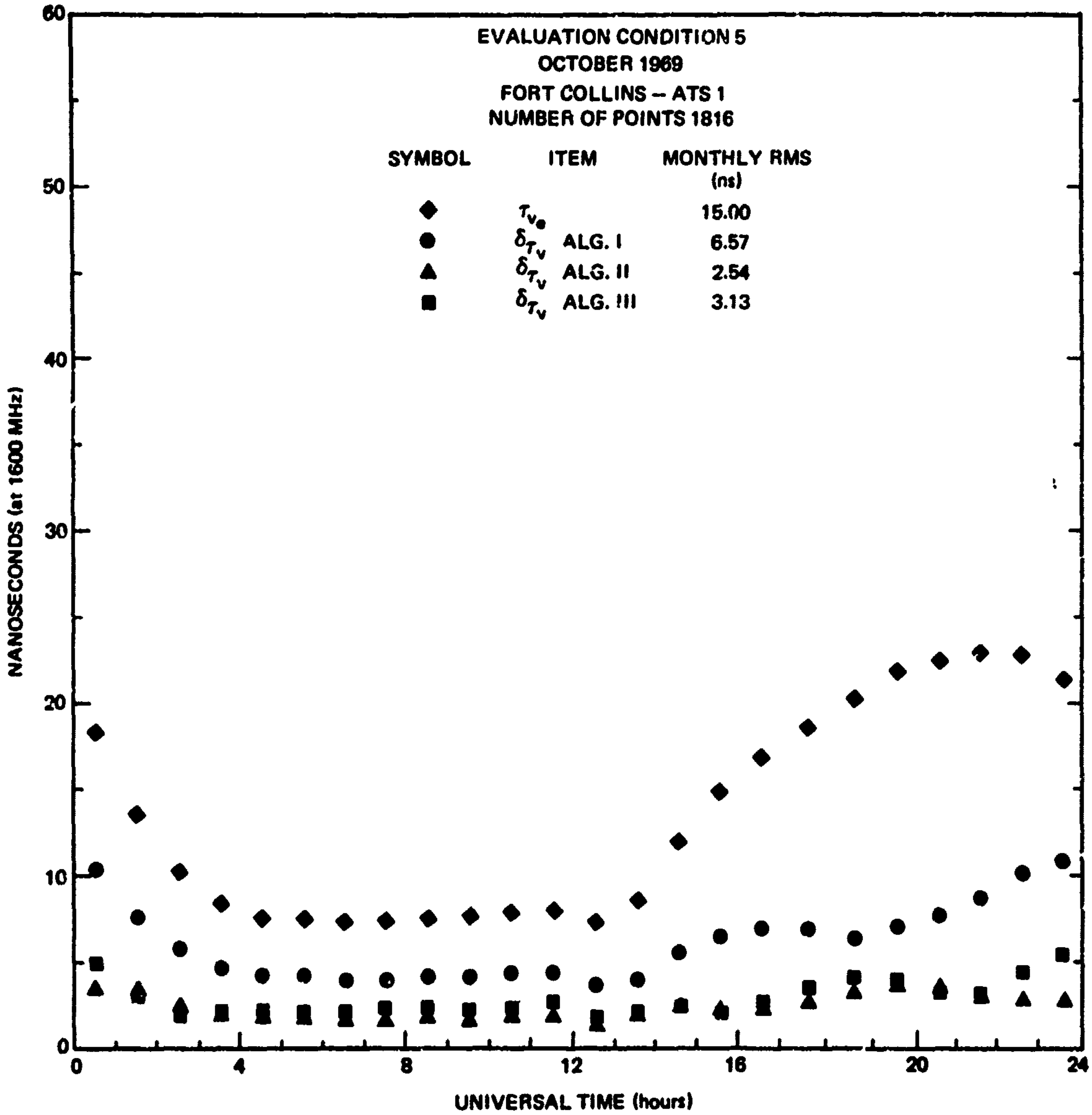

Fig. A.77 VERTICAL TIME DELAY AND RESIDUALS-HOURLY RMS OVER MONTH

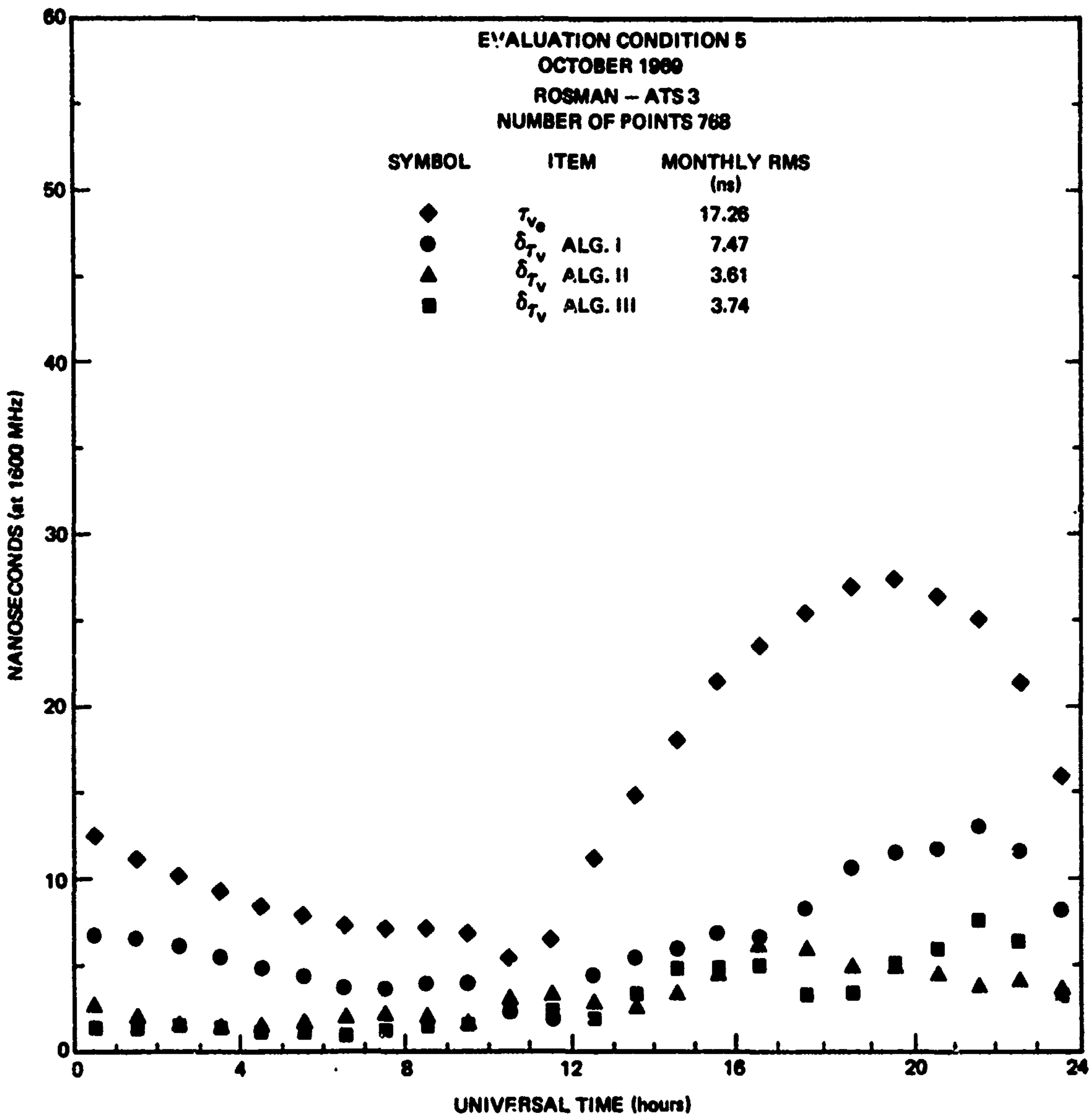

Fig. A.78 VERTICAL TIME DELAY AND RESIDUALS-HOURLY RMS OVER MONTH

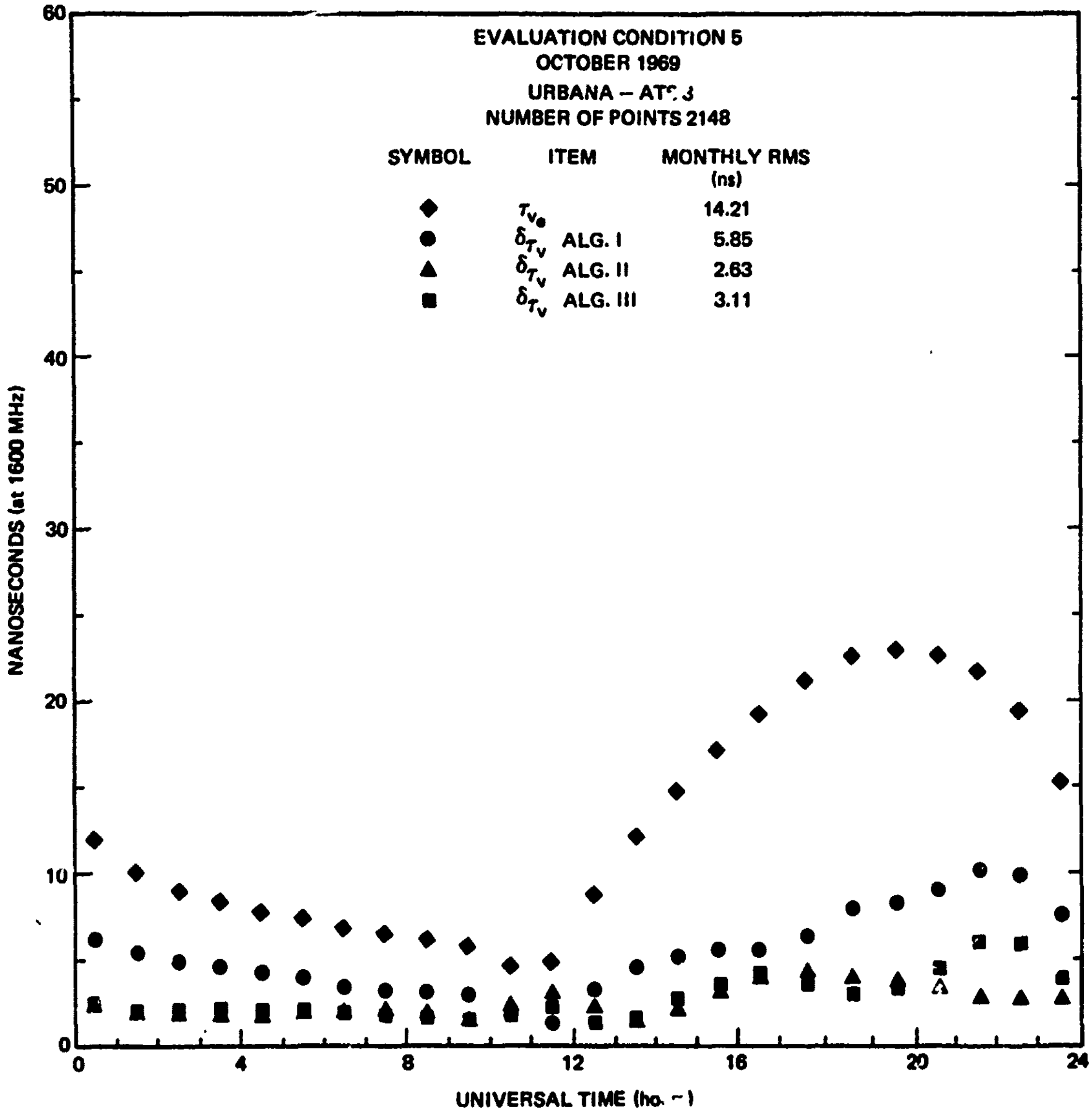

Fig. A.79 VERTICAL TIME DELAY AND RESIDUALS-HOURLY RMS OVER MONTH

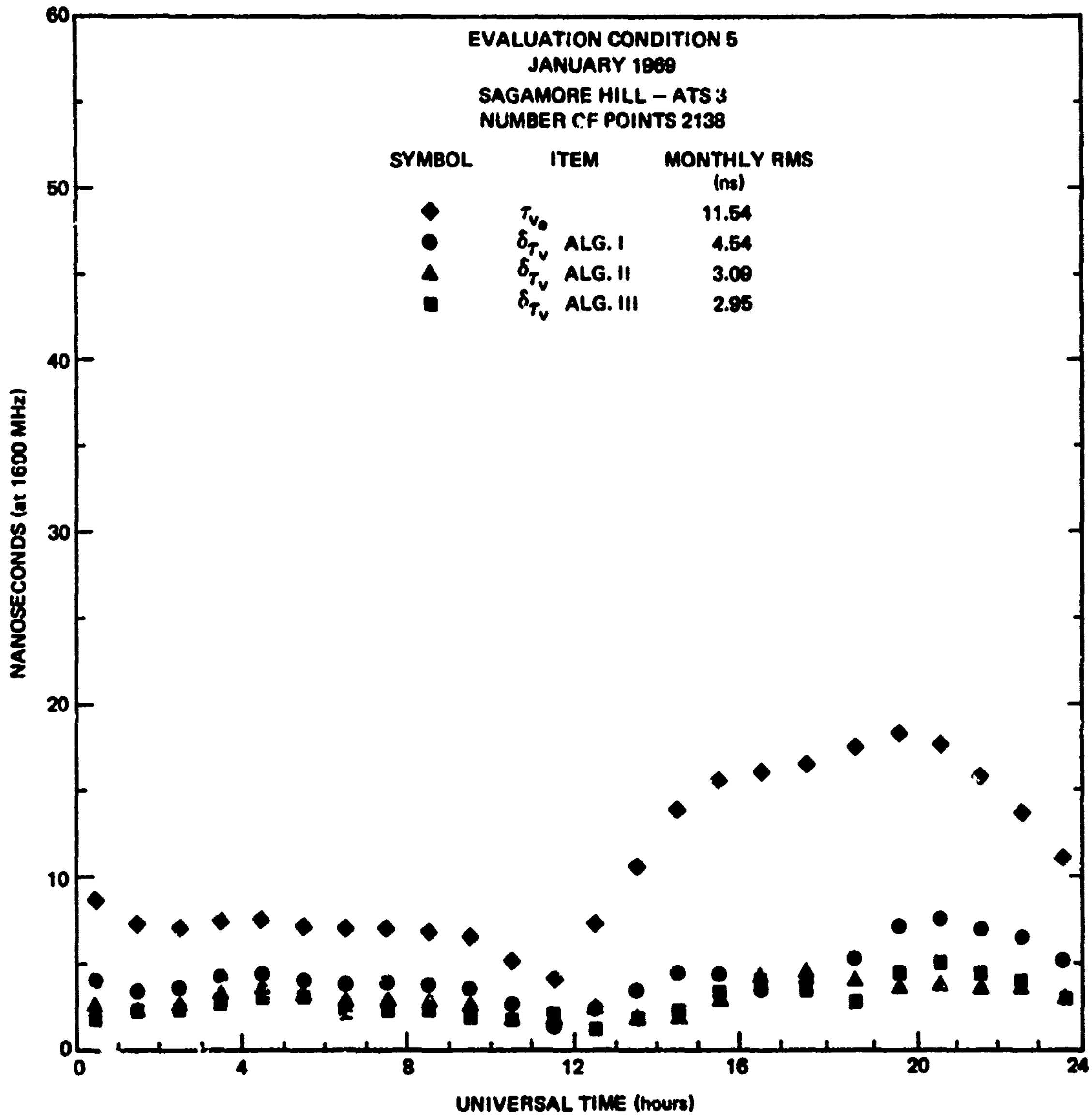

Fig. A.[illegible] VERTICAL TIME DELAY AND RESIDUALS-HOURLY RMS OVER MONTH

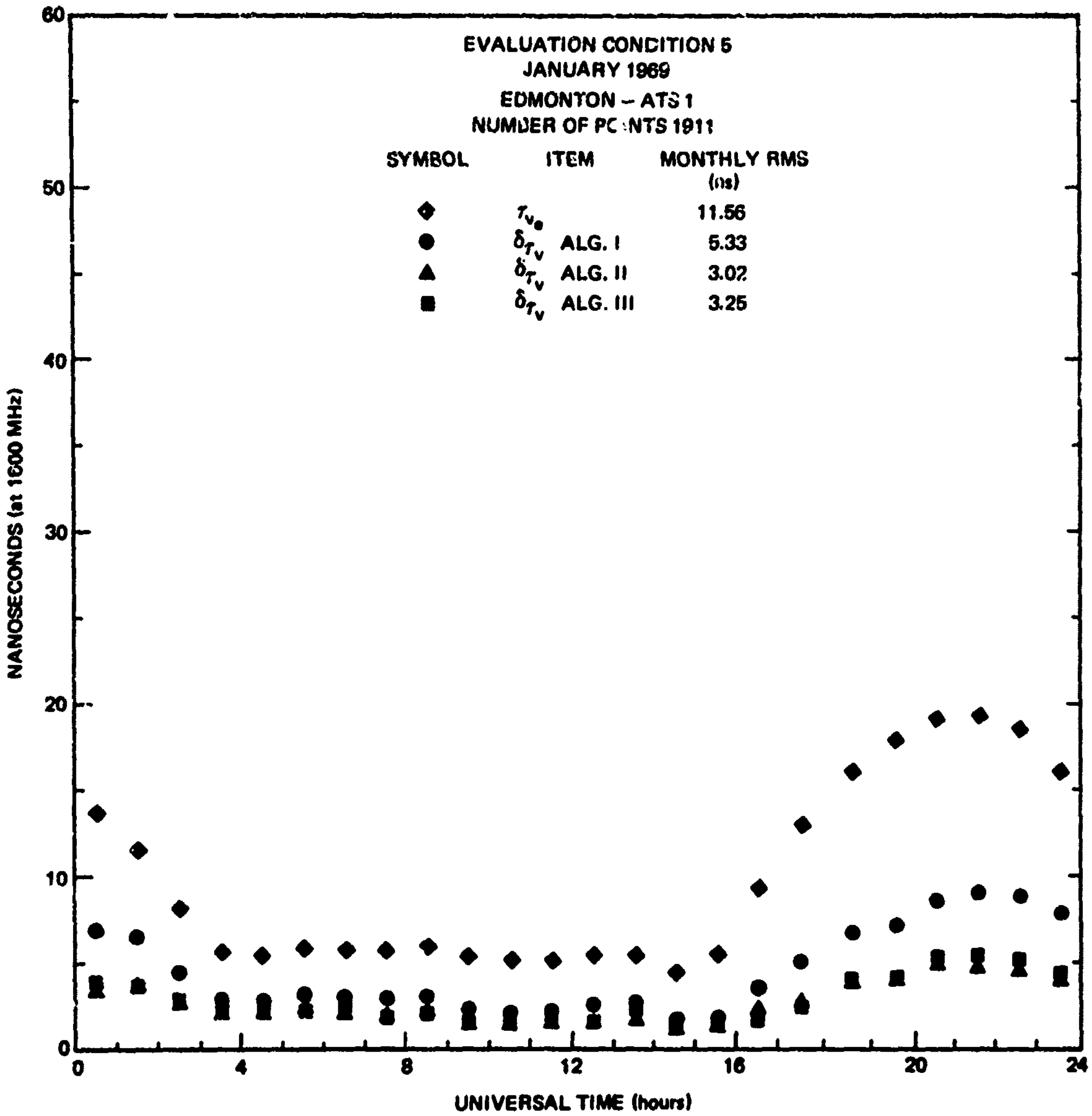

Fig. A.81 VERTICAL TIME DELAY AND RESIDUALS-HOURLY RMS OVER MONTH

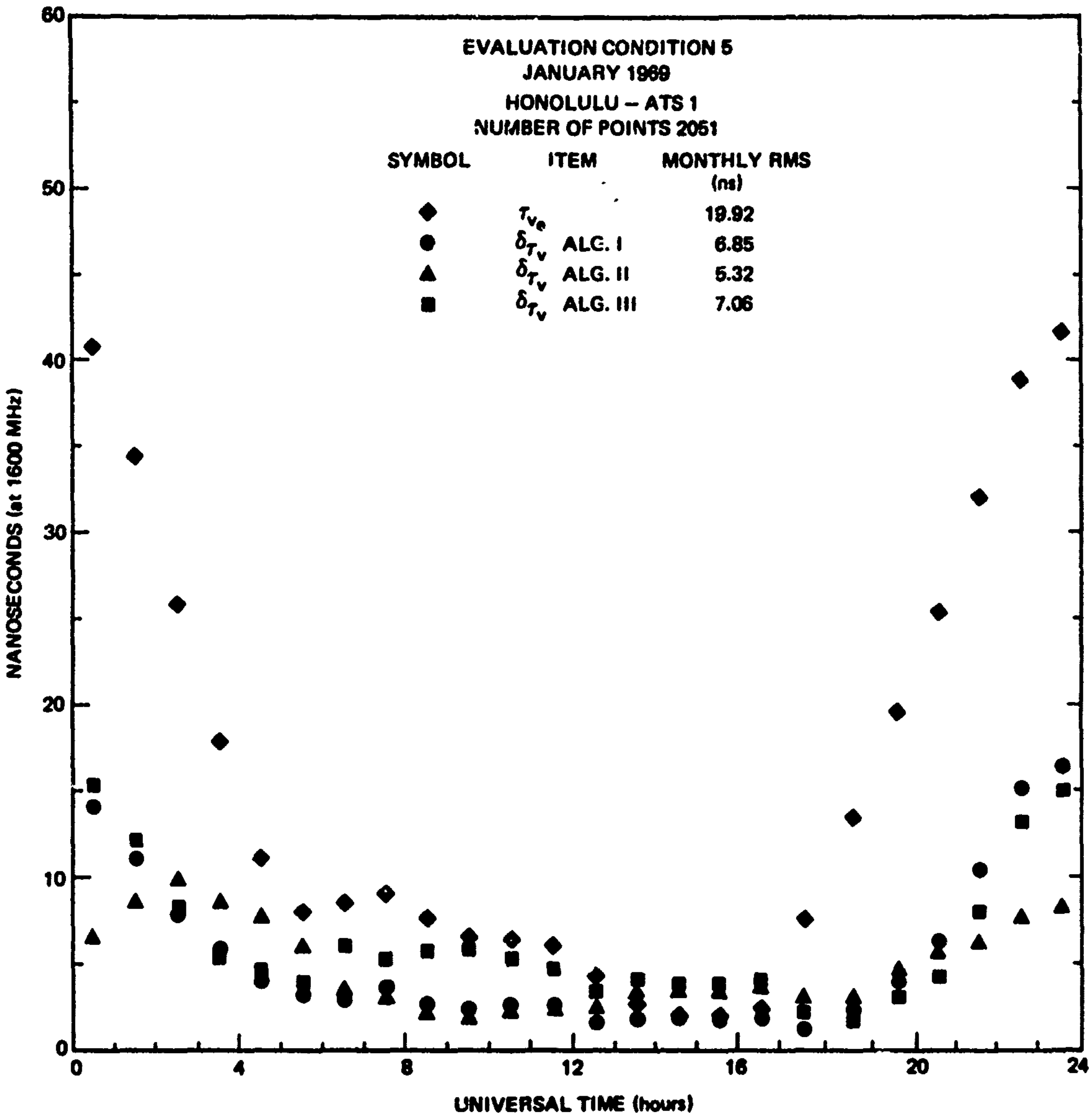

Fig. A.82 VERTICAL TIME DELAY AND RESIDUALS-HOURLY RMS OVER MONTH

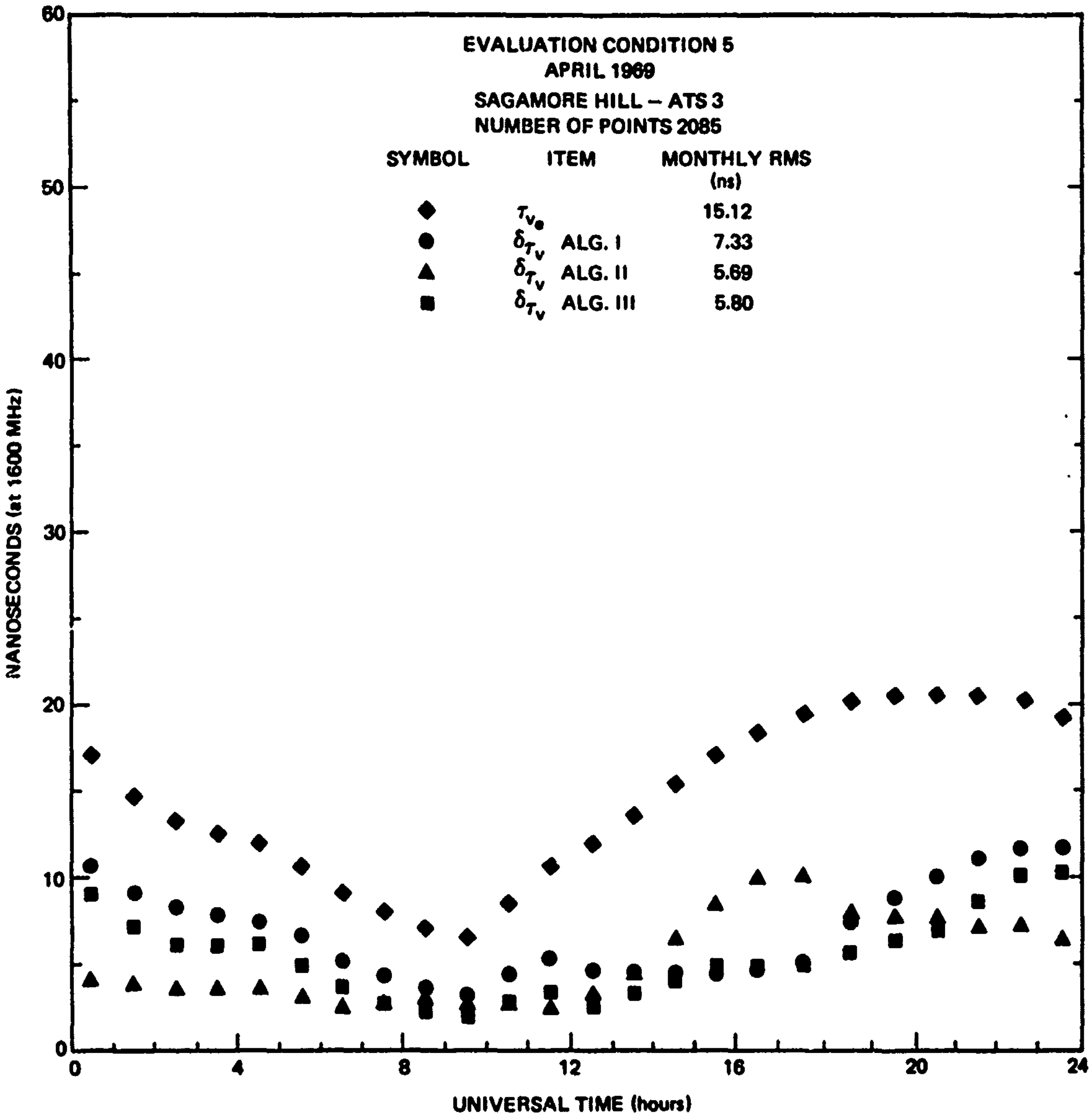

Fig. A.83 VERTICAL TIME DELAY AND RESIDUALS-HOURLY RMS OVER MONTH

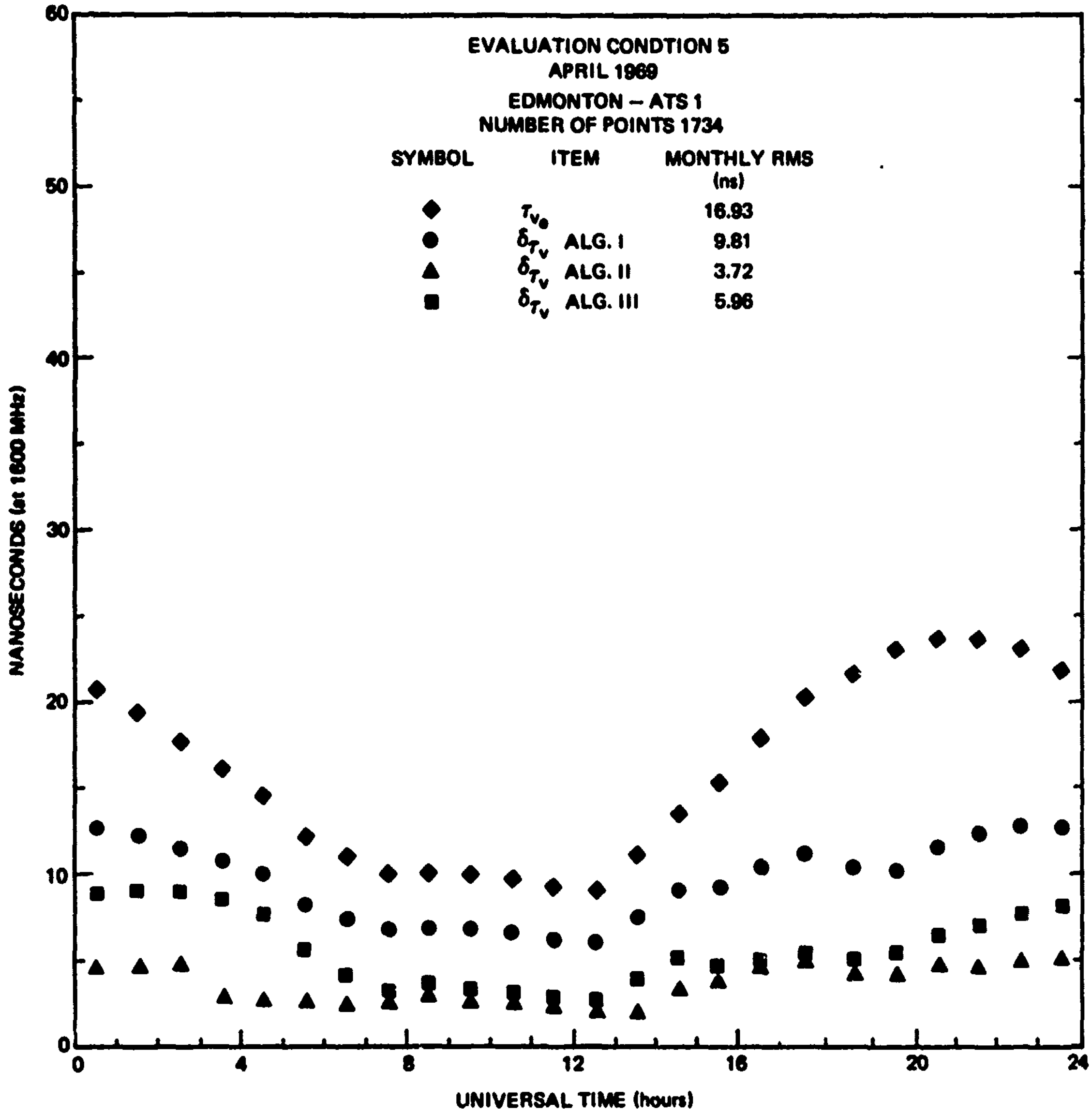

Fig. A.84 VERTICAL TIME DELAY AND RESIDUALS-HOURLY RMS OVER MONTH

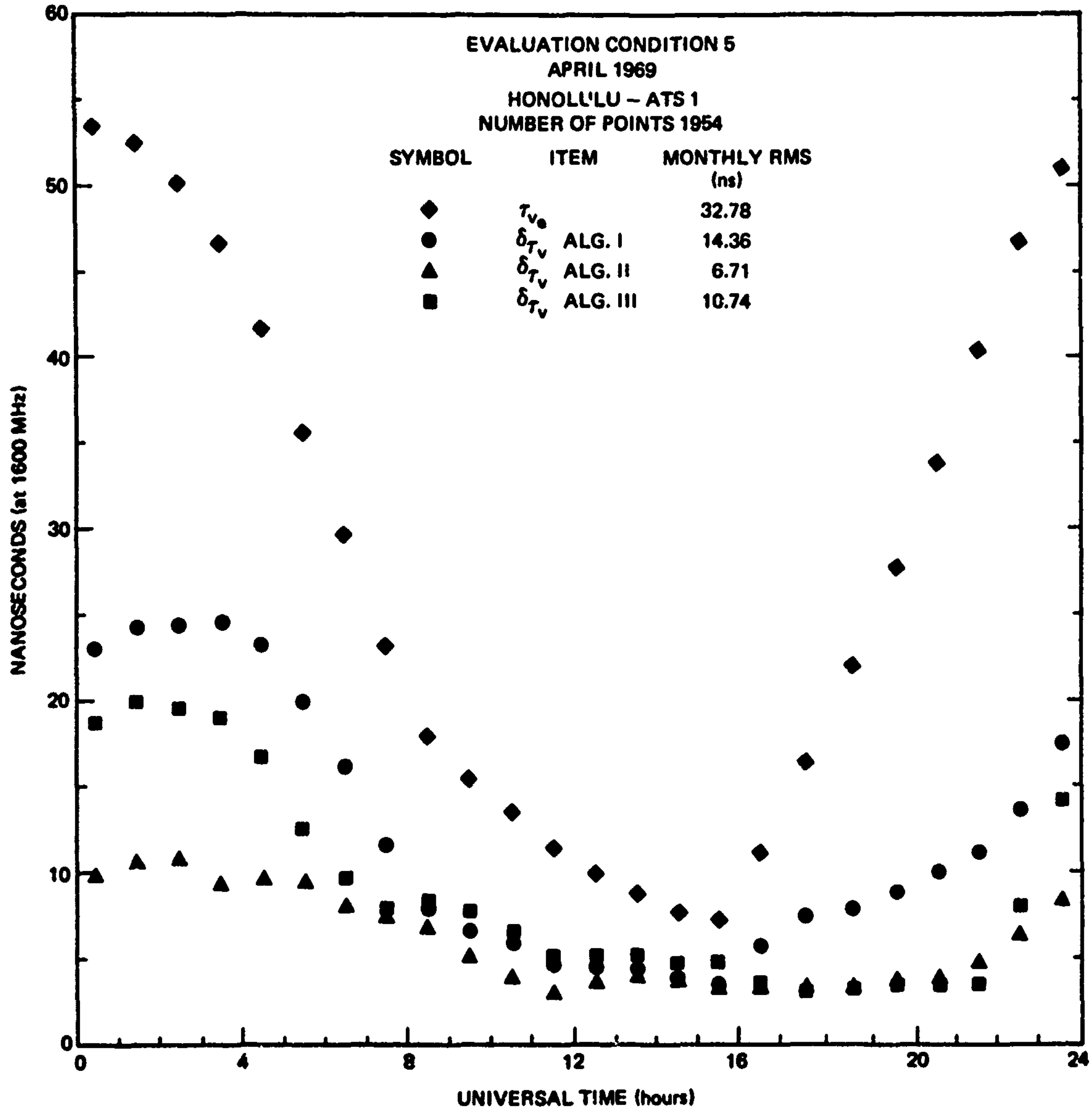

Fig. A.85 VERTICAL TIME DELAY AND RESIDUALS-HOURLY RMS OVER MONTH

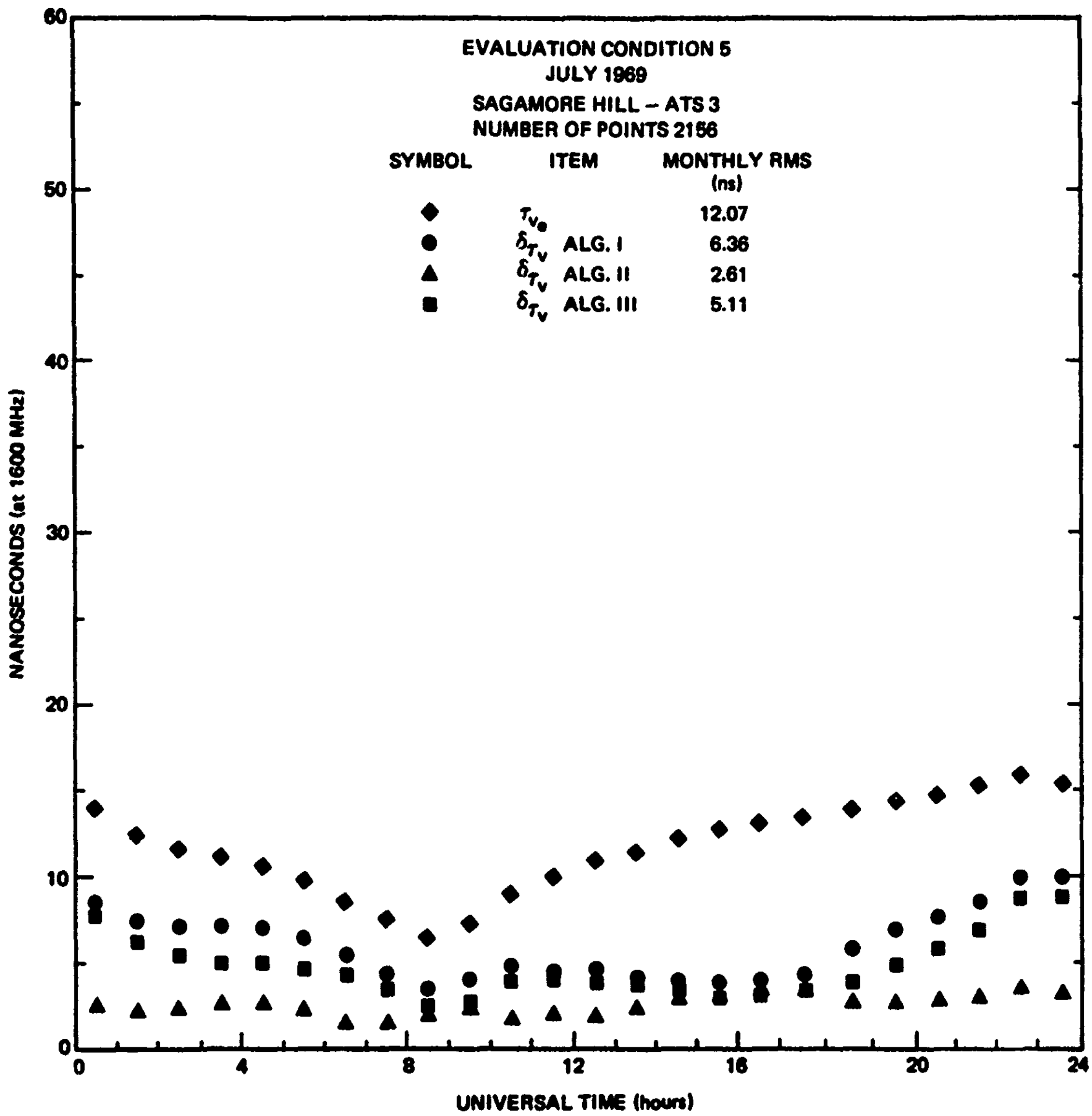

Fig. A.86 VERTICAL TIME DELAY AND RESIDUALS-HOURLY RMS OVER MONTH

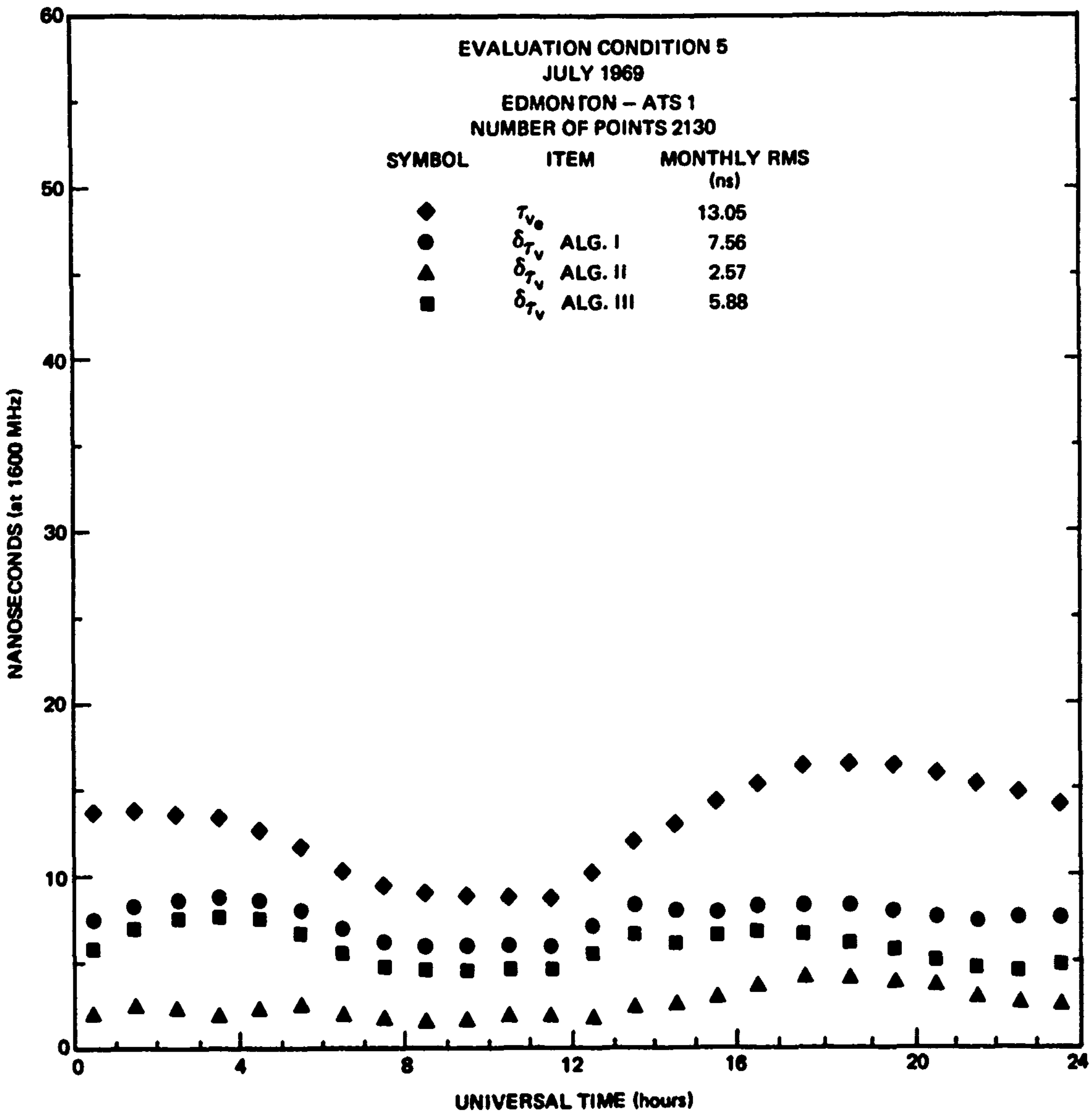

Fig. A.87 VERTICAL TIME DELAY AND RESIDUALS-HOURLY RMS OVER MONTH

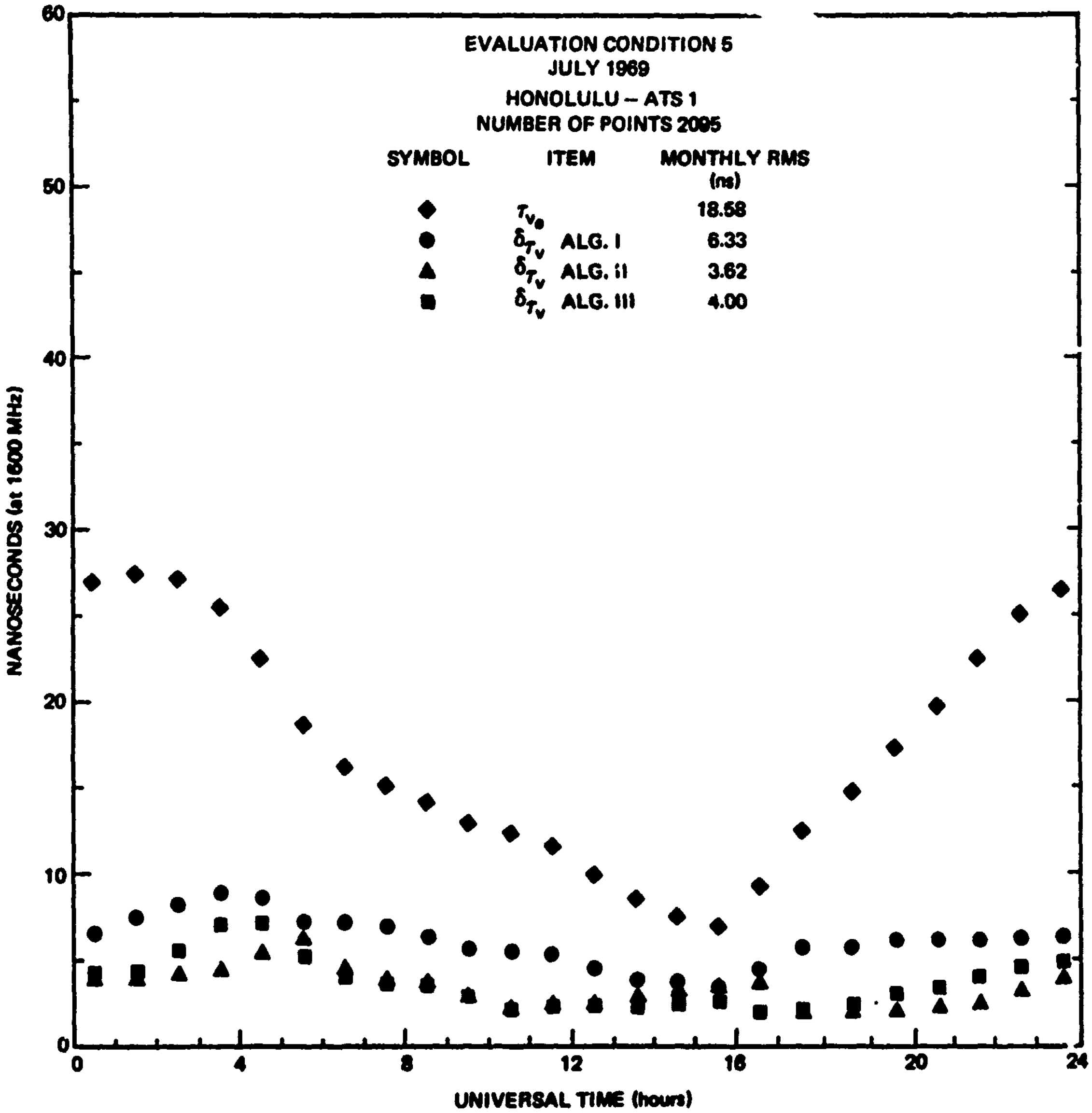

Fig. A.88 VERTICAL TIME DELAY AND RESIDUALS-HOURLY RMS OVER MONTH

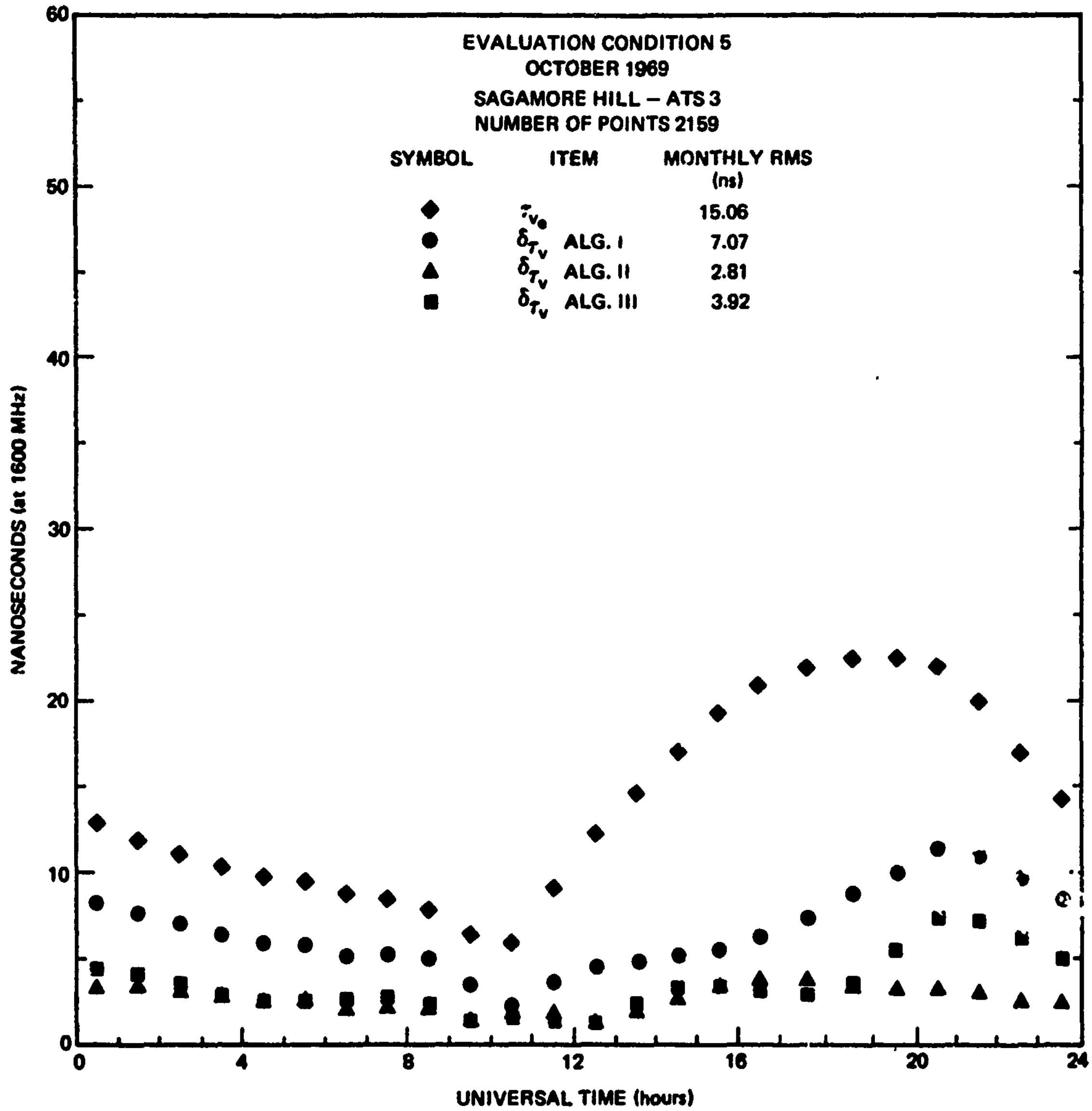

Fig. A.89 VERTICAL TIME DELAY AND RESIDUALS-HOURLY RMS OVER MONTH

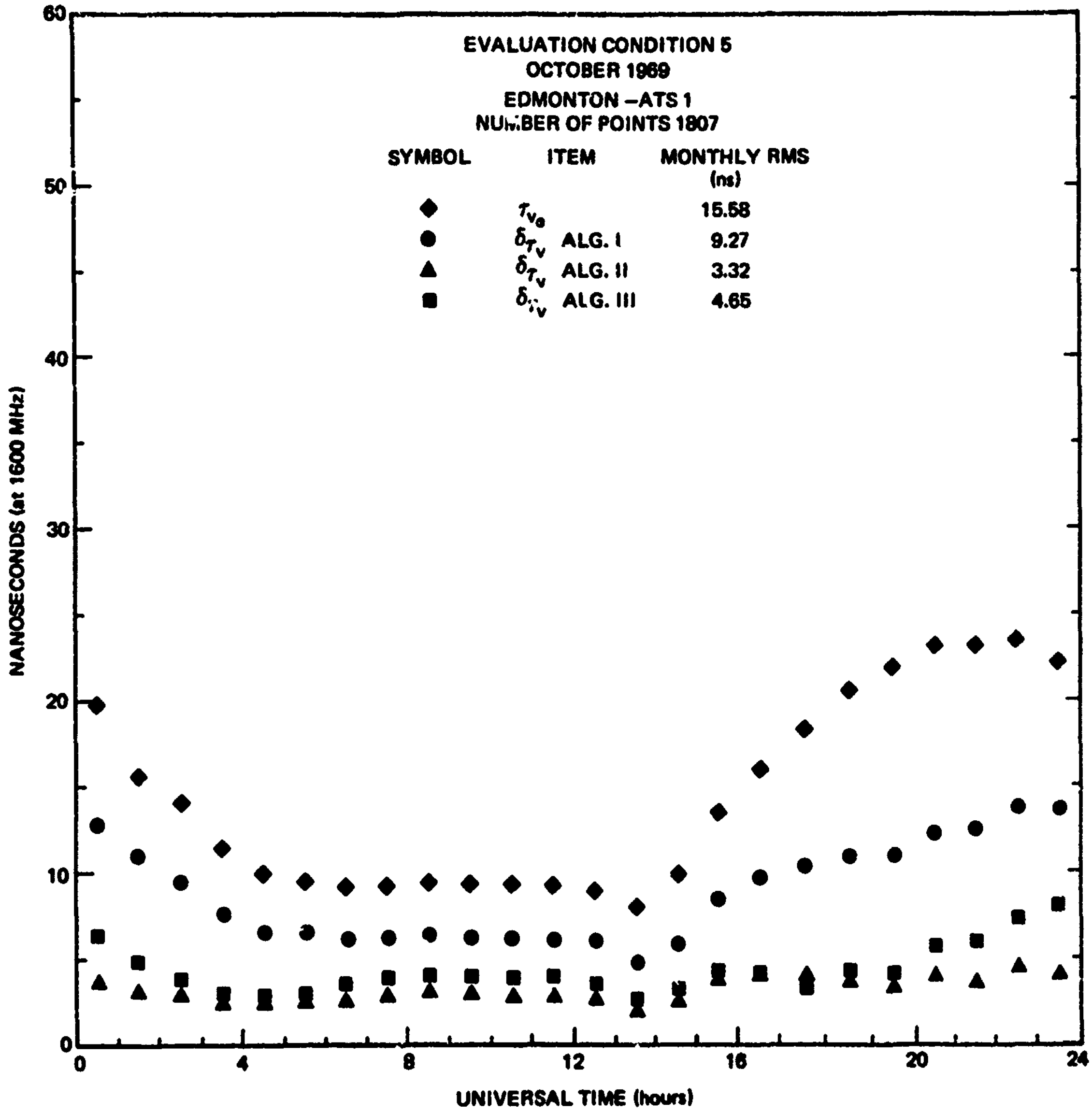

Fig. A.90 VERTICAL TIME DELAY AND RESIDUALS-HOURLY RMS OVER MONTH

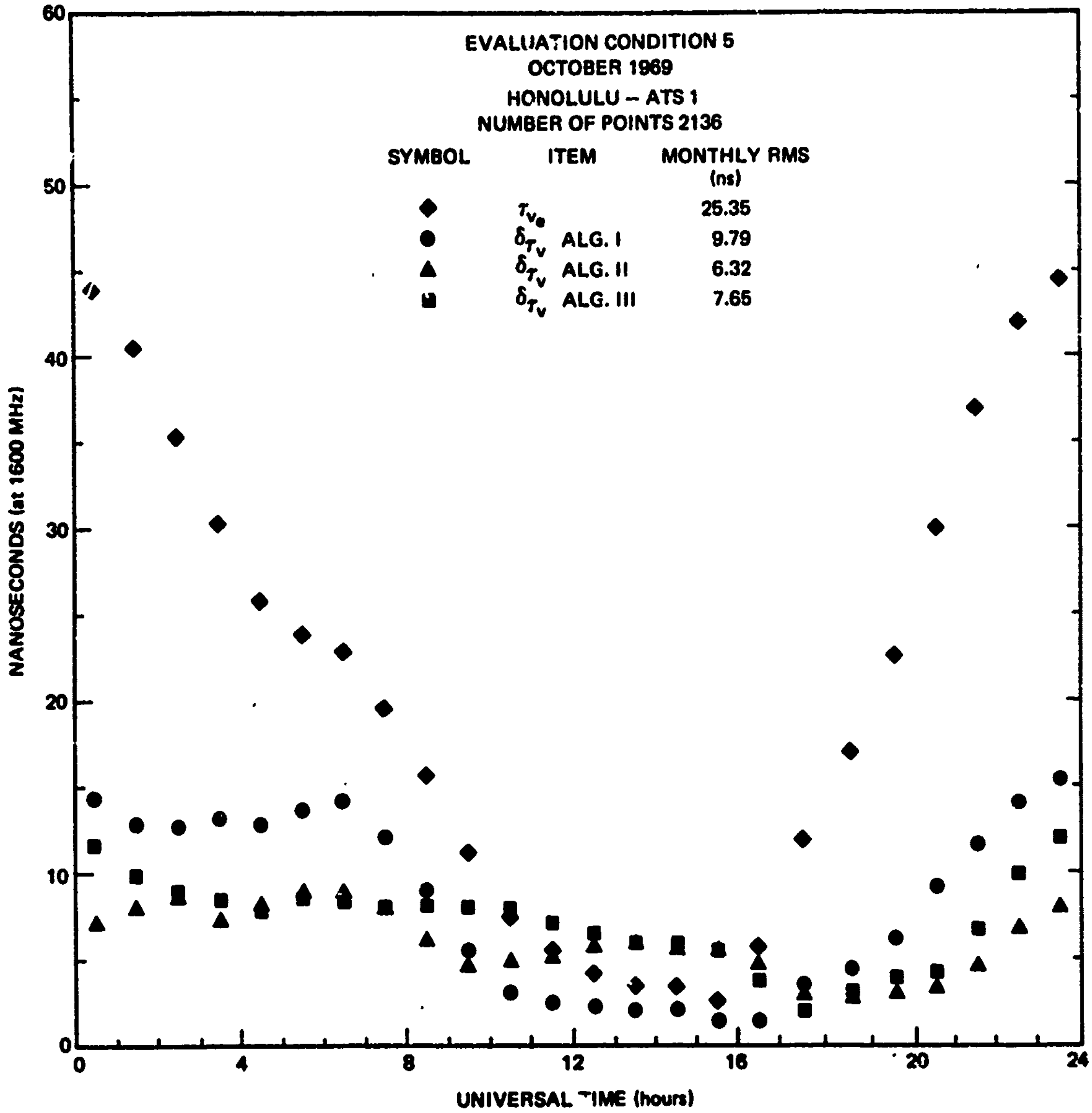

Fig. A.91 VERTICAL TIME DELAY AND RESIDUALS-HOURLY RMS OVER MONTH

APPENDIX B

TABLES OF NUMBER OF DATA IN EACH
UT HOUR INTERVAL

TABLE B.1

Number of Data Used in each UT Hour Interval

Evaluation Condition 1
Stanford - ATS1

Hour Interval	January 1968	Number of Data February 1968	March 1968
[0,1)	76	86	80
[1,2)	81	87	81
[2,3)	77	87	81
[3,4)	78	86	81
[4,5)	79	85	80
[5,6)	80	84	81
[6,7)	77	84	78
[7,8)	79	84	75
[8,9)	78	82	75
[9,10)	73	81	76
[10,11)	79	78	68
[11,12)	79	80	72
[12,13)	79	80	72
[13,14)	74	80	74
[14,15)	79	86	76
[15,16)	81	87	76
[16,17)	80	87	79
[17,18)	79	87	77
[18,19)	79	86	78
[19,20)	84	87	78
[20,21)	82	86	81
[21,22)	81	87	80
[22,23)	79	87	80
[23,24)	73	86	81

TABLE B.2

Number of Data Used in each UT Hour Interval

Evaluation Condition 1
Stanford - ATS3

Hour Interval	January 1968	Number of Data February 1968	March 1968
[0,1)	82	80	84
[1,2)	83	83	82
[2,3)	85	82	81
[3,4)	87	82	80
[4,5)	86	76	77
[5,6)	84	73	75
[6,7)	84	69	75
[7,8)	87	71	71
[8,9)	84	74	74
[9,10)	86	72	77
[10,11)	84	70	75
[11,12)	82	75	77
[12,13)	83	67	78
[13,14)	86	78	78
[14,15)	77	77	84
[15,16)	82	76	84
[16,17)	88	81	83
[17,18)	90	84	84
[18,19)	87	80	84
[19,20)	86	79	82
[20,21)	86	73	80
[21,22)	86	76	81
[22,23)	[illegible]	[illegible]	[illegible]
[23,24)	86	77	83

TABLE B.3

Number of Data Used in each UT Hour Interval

Evaluation Condition 1
Urbana - ATS3

Hour Interval	January 1968	Number of Data February 1968	March 1968
[0,1)	74	87	48
[1,2)	74	87	54
[2,3)	75	87	54
[3,4)	75	87	54
[4,5)	75	87	54
[5,6)	75	87	54
[6,7)	75	81	57
[7,8)	75	81	57
[8,9)	75	81	57
[9,10)	75	81	57
[10,11)	75	81	57
[11,12)	75	81	57
[12,13)	75	79	57
[13,14)	75	78	57
[14,15)	72	78	57
[15,16)	73	81	60
[16,17)	76	84	60
[17,18)	74	84	60
[18,19)	72	87	57
[19,20)	70	86	52
[20,21)	69	84	51
[21,22)	71	86	51
[22,23)	[illegible]	[illegible]	51
[23,24)	77	87	51

TABLE B.4

Number of Data Used in each UT Hour Interval

Evaluation Condition 1
Sagamore Hill-ATS3

Hour Interval	Number of Data January 1968	February 1968	March 1968
[0,1)	75	75	76
[1,2)	72	75	75
[2,3)	75	75	75
[3,4)	75	75	75
[4,5)	75	75	75
[5,6)	75	75	75
[6,7)	75	75	75
[7,8)	75	75	75
[8,9)	75	75	75
[9,10)	75	75	75
[10,11)	75	75	74
[11,12)	75	75	72
[12,13)	75	75	73
[13,14)	75	75	77
[14,15)	75	75	78
[15,16)	75	75	78
[16,17)	74	75	78
[17,18)	72	75	78
[18,19)	71	75	78
[19,20)	72	75	78
[20,21)	72	75	78
[21,22)	72	74	78
[22,23)	72	72	78
[23,24)	72	72	78

TABLE B.5

Number of Data Used in each UT Hour Interval

Evaluation Condition 1
Arecibo - ATS3

Hour Interval	January 1968	Number of Data February 1968	March 1968
[0,1)	84	[illegible]	54
[1,2)	83	82	54
[2,3)	79	82	54
[3,4)	77	83	53
[4,5)	74	84	54
[5,6)	75	80	54
[6,7)	75	80	52
[7,8)	76	77	54
[8,9)	78	81	54
[9,10)	78	77	53
[10,11)	80	75	54
[11,12)	81	78	52
[12,13)	83	76	49
[13,14)	81	80	51
[14,15)	87	81	51
[15,16)	84	87	51
[16,17)	87	87	51
[17,18)	85	87	48
[18,19)	89	86	47
[19,20)	85	87	48
[20,21)	83	86	48
[21,22)	85	87	51
[22,23)	87	87	50
[23,24)	87	87	51

TABLE B.6

Number of Data Used in each UT Hour Interval

Evaluation Condition 1
Honolulu - ATS1

Hour Interval	Number of Data January 1968	February 1968	March 1968
[0,1)	90	84	84
[1,2)	88	80	84
[2,3)	89	77	83
[3,4)	89	78	80
[4,5)	87	78	81
[5,6)	87	76	77
[6,7)	85	78	75
[7,8)	86	78	75
[8,9)	83	77	73
[9,10)	82	73	73
[10,11)	81	72	73
[11,12)	82	72	72
[12,13)	84	72	77
[13,14)	82	72	77
[14,15)	80	66	78
[15,16)	79	61	75
[16,17)	77	67	32
[17,18)	74	69	63
[18,19)	80	76	79
[19,20)	84	78	79
[20,21)	88	79	81
[21,22)	81	81	83
[22,23)	81	81	84
[23,24)	84	82	84

TABLE B.7

Number of Data Used in each UT Hour Interval

Evaluation Condition 2
Stanford - ATS1

Hour Interval	January 1968	Number of Data February 1968	March 1968
[0,1)	76	86	86
[1,2)	81	87	87
[2,3)	77	87	87
[3,4)	78	86	90
[4,5)	79	85	89
[5,6)	80	84	90
[6,7)	77	84	87
[7,8)	79	84	84
[8,9)	78	82	84
[9,10)	73	81	85
[10,11)	79	78	76
[11,12)	79	80	80
[12,13)	79	80	81
[13,14)	74	80	83
[14,15)	79	86	82
[15,16)	81	87	85
[16,17)	80	87	88
[17,18)	79	87	86
[18,19)	79	86	87
[19,20)	84	87	87
[20,21)	82	86	90
[21,22)	81	87	89
[22,23)	[illegible]	[illegible]	[illegible]
[23,24)	73	86	90

TABLE B.8

Number of Data Used in each UT Hour Interval

Evaluation Condition 2
Stanford - ATS3

Hour Interval	Number of Data January 1968	February 1968	March 1968
[0,1)	82	80	90
[1,2)	83	83	88
[2,3)	85	82	87
[3,4)	87	82	86
[4,5)	86	76	84
[5,6)	84	73	84
[6,7)	84	69	84
[7,8)	87	71	80
[8,9)	84	74	83
[9,10)	86	72	86
[10,11)	84	70	84
[11,12)	82	75	86
[12,13)	83	67	87
[13,14)	86	78	86
[14,15)	77	77	90
[15,16)	82	76	93
[16,17)	88	81	92
[17,18)	90	84	93
[18,19)	87	80	93
[19,20)	86	79	91
[20,21)	86	73	89
[21,22)	86	76	90
[22,23)	87	76	93
[23,24)	86	77	92

TABLE B.9

Number of Data Used in each UT Hour Interval

Evaluation Condition 2
Urbana - ATS3

Hour Interval	Number of Data January 1968	February 1968	March 1968
[0,1)	74	87	51
[1,2)	74	87	57
[2,3)	75	87	57
[3,4)	75	87	57
[4,5)	75	87	57
[5,6)	75	87	57
[6,7)	75	81	60
[7,8)	75	81	60
[8,9)	75	81	60
[9,10)	75	81	60
[10,11)	75	81	60
[11,12)	75	81	60
[12,13)	75	79	60
[13,14)	75	78	60
[14,15)	72	78	[illegible]
[15,16)	73	81	63
[16,17)	76	84	63
[17,18)	74	84	63
[18,19)	72	87	60
[19,20)	70	86	53
[20,21)	69	84	51
[21,22)	71	86	51
[22,23)	75	87	51
[23,24)	77	87	51

TABLE B.10

Number of Data Used in each UT Hour Interval

Evaluation Condition 2
Sagamore Hill - ATS3

Hour Interval	January 1968	Number of Data February 1968	March 1968
[0,1)	75	75	85
[1,2)	72	75	84
[2,3)	75	75	84
[3,4)	75	75	84
[4,5)	75	75	84
[5,6)	75	75	84
[6,7)	75	75	84
[7,8)	75	75	84
[8,9)	75	75	84
[9,10)	75	75	84
[10,11)	75	72	83
[11,12)	75	75	81
[12,13)	75	75	82
[13,14)	75	75	86
[14,15)	75	75	87
[15,16)	75	75	87
[16,17)	74	75	87
[17,18)	72	75	87
[18,19)	71	75	87
[19,20)	72	75	87
[20,21)	72	75	87
[21,22)	72	74	87
[22,23)	72	72	87
[23,24)	72	72	87

TABLE B.11

Number of Data Used in each UT Hour Interval

Evaluation Condition 2
Arecibo - ATS3

Hour Interval	Number of Data January 1968	February 1968	March 1968
[0,1)	84	82	57
[1,2)	83	82	57
[2,3)	79	82	57
[3,4)	77	83	56
[4,5)	74	84	57
[5,6)	75	80	57
[6,7)	75	80	55
[7,8)	76	77	57
[8,9)	78	81	57
[9,10)	78	77	56
[10,11)	80	75	60
[11,12)	81	78	58
[12,13)	83	76	55
[13,14)	81	80	57
[14,15)	87	81	57
[15,16)	84	87	57
[16,17)	87	87	57
[17,18)	85	87	54
[18,19)	89	86	53
[19,20)	85	87	54
[20,21)	83	86	54
[21,22)	85	87	57
[22,23)	87	87	[illegible]
[23,24)	87	87	57

TABLE B.12

Number of Data Used in each UT Hour Interval

Evaluation Condition 2
Honolulu - ATS1

Hour Interval	Number of Data January 1968	February 1968	March 1968
[0,1)	90	84	88
[1,2)	88	80	90
[2,3)	89	77	88
[3,4)	89	78	86
[4,5)	87	78	87
[5,6)	87	76	83
[6,7)	85	78	79
[7,8)	86	78	78
[8,9)	83	77	75
[9,10)	82	73	73
[10,11)	81	72	73
[11,12)	82	72	72
[12,13)	84	72	77
[13,14)	82	72	78
[14,15)	80	66	81
[15,16)	79	61	77
[16,17)	77	67	32
[17,18)	74	69	63
[18,19)	80	76	84
[19,20)	84	78	87
[20,21)	88	79	86
[21,22)	81	81	92
[22,23)	81	81	90
[23,24)	84	82	88

TABLE B.13

Number of Data Used in each UT Hour Interval

Evaluation Condition 3
Honolulu-Syncom3

Hour Interval	Number of Data January 1965	April 1965	July 1965
[0,1)	56	54	66
[1,2)	55	52	66
[2,3)	53	52	65
[3,4)	54	54	66
[4,5)	53	54	66
[5,6)	55	53	66
[6,7)	56	53	65
[7,8)	59	51	66
[8,9)	59	49	66
[9,10)	59	48	66
[10,11)	59	53	66
[11,12)	60	51	66
[12,13)	60	45	66
[13,14)	60	45	66
[14,15)	60	47	66
[15,16)	60	51	65
[16,17)	60	51	66
[17,18)	60	51	66
[18,19)	60	51	66
[19,20)	58	51	63
[20,21)	57	48	63
[21,22)	56	48	62
[22,23)	54	47	64
[23,24)	54	49	66

TABLE B.14

Number of Data Used in each UT Hour Interval

Evaluation Condition 3
Stanford-Syncom3

Hour Interval	Number of Data January 1965	April 1965	July 1965
[0,1)	55	63	65
[1,2)	60	63	65
[2,3)	60	63	66
[3,4)	60	63	64
[4,5)	60	63	66
[5,6)	59	63	66
[6,7)	60	63	66
[7,8)	60	63	63
[8,9)	60	63	63
[9,10)	60	63	63
[10,11)	60	63	63
[11,12)	60	63	64
[12,13)	60	54	61
[13,14)	60	49	58
[14,15)	60	53	64
[15,16)	60	54	66
[16,17)	59	57	65
[17,18)	57	62	66
[18,19)	54	63	65
[19,20)	59	63	63
[20,21)	57	63	62
[21,22)	57	62	63
[22,23)	57	60	65
[23,24)	53	60	66

TABLE B.15

Number of Data Used in each UT Hour Interval

Evaluation Condition 4
Sagamore Hill - ATS3

Hour Interval	Number of Data January 1968	April 1968	July 1968	October 1968
[0,1)	51	54	63	78
[1,2)	48	57	62	78
[2,3)	51	57	60	78
[3,4)	51	57	63	78
[4,5)	51	57	63	78
[5,6)	51	57	63	78
[6,7)	51	57	63	78
[7,8)	51	57	63	78
[8,9)	51	57	63	78
[9,10)	51	57	60	78
[10,11)	51	57	63	78
[11,12)	51	56	63	78
[12,13)	51	57	63	78
[13,14)	51	57	63	71
[14,15)	51	57	63	73
[15,16)	51	57	63	75
[16,17)	51	57	63	76
[17,18)	51	57	63	78
[18,19)	50	57	64	78
[19,20)	51	57	66	78
[20,21)	51	57	66	78
[21,22)	51	57	66	78
[22,23)	51	57	66	78
[23,24)	51	57	66	78

TABLE B.16

Number of Data Used in each UT Hour Interval

Evaluation Condition 4
Honolulu - ATS1

Hour Interval	Number of Data			
	January 1968	April 1968	July 1968	October 1968
[0,1)	63	56	66	80
[1,2)	61	57	66	81
[2,3)	62	57	66	81
[3,4)	62	57	66	81
[4,5)	60	56	66	81
[5,6)	60	42	66	81
[6,7)	59	38	66	81
[7,8)	59	34	66	81
[8,9)	59	27	66	81
[9,10)	57	28	66	81
[10,11)	57	33	63	81
[11,12)	57	39	65	81
[12,13)	57	34	65	81
[13,14)	57	39	66	81
[14,15)	55	39	66	81
[15,16)	54	29	65	81
[16,17)	53	16	66	80
[17,18)	52	41	66	81
[18,19)	56	53	66	81
[19,20)	60	54	66	81
[20,21)	63	56	66	81
[21,22)	54	57	66	80
[22,23)	54	57	66	81
[23,24)	57	57	66	81

TABLE B.17

Number of Data Used in each UT Hour Interval

Evaluation Condition 4
Stanford - ATS1

Hour Interval	Number of Data			
	January 1968	April 1968	July 1968	October 1968
[0,1)	53	57	66	80
[1,2)	60	56	66	80
[2,3)	60	56	65	81
[3,4)	60	57	66	81
[4,5)	63	57	66	81
[5,6)	62	56	66	79
[6,7)	61	57	66	81
[7,8)	59	57	66	81
[8,9)	60	57	65	81
[9,10)	57	56	65	81
[10,11)	63	56	65	81
[11,12)	62	57	64	81
[12,13)	61	55	66	81
[13,14)	56	56	65	81
[14,15)	61	56	66	81
[15,16)	63	57	66	81
[16,17)	61	56	66	81
[17,18)	59	54	66	81
[18,19)	62	56	66	81
[19,20)	63	57	65	81
[20,21)	62	56	64	81
[21,22)	60	57	66	81
[22,23)	60	56	66	81
[23,24)	54	54	66	81

TABLE B.18

Number of Data Used in each UT Hour Interval

Evaluation Condition 5
Stanford - ATS1

Hour Interval	Number of Data January 1969	April 1969	July 1969	October 1969
[0,1)	84	87	90	90
[1,2)	87	86	90	90
[2,3)	87	87	90	90
[3,4)	83	81	90	90
[4,5)	87	84	90	90
[5,6)	87	87	89	86
[6,7)	86	87	90	87
[7,8)	84	87	90	90
[8,9)	84	86	89	90
[9,10)	84	86	90	90
[10,11)	81	85	88	90
[11,12)	82	86	87	90
[12,13)	84	85	90	90
[13,14)	84	82	90	90
[14,15)	87	81	90	90
[15,16)	87	78	90	89
[16,17)	84	82	90	86
[17,18)	87	82	90	86
[18,19)	82	84	90	87
[19,20)	82	84	88	87
[20,21)	84	84	90	87
[21,22)	83	84	90	85
[22,23)	81	80	90	83
[23,24)	80	80	89	82

TABLE B.19

Number of Data Used in each UT Hour Interval

Evaluation Condition 5
Stanford - ATS3

Hour Interval	Number of Data April 1969
[0,1)	85
[1,2)	87
[2,3)	85
[3,4)	85
[4,5)	87
[5,6)	87
[6,7)	84
[7,8)	83
[8,9)	77
[9,10)	76
[10,11)	77
[11,12)	72
[12,13)	75
[13,14)	74
[14,15)	71
[15,16)	72
[16,17)	77
[17,18)	77
[18,19)	76
[19,20)	78
[20,21)	77
[21,22)	77
[22,23)	78
[23,24)	81

TABLE B.20

Number of Data Used in each UT Hour Interval

Evaluation Condition 5
Clark Lake - ATS1

Hour Interval	Number of Data			
	January 1969	April 1969	July 1969	October 1969
[0,1)	19	87	42	42
[1,2)	18	85	39	42
[2,3)	18	83	40	42
[3,4)	18	75	41	39
[4,5)	18	73	41	37
[5,6)	18	64	39	38
[6,7)	18	66	30	39
[7,8)	18	69	30	36
[8,9)	21	58	21	26
[9,10)	21	61	21	24
[10,11)	21	55	22	21
[11,12)	21	58	24	23
[12,13)	21	56	25	29
[13,14)	21	60	30	37
[14,15)	21	63	32	42
[15,16)	21	64	35	42
[16,17)	21	70	40	41
[17,18)	18	77	44	42
[18,19)	20	79	41	42
[19,20)	21	80	41	45
[20,21)	21	77	42	45
[21,22)	21	80	42	45
[22,23)	21	82	41	40
[23,24)	21	83	42	42

TABLE B.21

Number of Data Used in each UT Hour Interval

Evaluation Condition 5
Cold Bay - ATS1

Hour Interval	Number of Data January 1969	April 1969	July 1969
[0,1)	83	85	63
[1,2)	87	84	66
[2,3)	87	83	66
[3,4)	87	81	66
[4,5)	87	81	66
[5,6)	87	81	66
[6,7)	90	81	66
[7,8)	90	81	66
[8,9)	90	81	66
[9,10)	90	84	66
[10,11)	90	84	66
[11,12)	90	85	66
[12,13)	90	87	60
[13,14)	90	87	60
[14,15)	90	87	60
[15,16)	90	87	60
[16,17)	90	87	60
[17,18)	90	87	60
[18,19)	90	87	60
[19,20)	89	87	59
[20,21)	85	87	57
[21,22)	81	87	57
[22,23)	81	87	57
[23,24)	81	87	57

TABLE B.22

Number of Data Used in each UT Hour Interval

Evaluation Condition 5
Fort Collins - ATS1

Hour Interval	Number of Data			
	January 1969	April 1969	July 1969	October 1969
[0,1)	86	24	66	74
[1,2)	87	24	45	72
[2,3)	87	24	40	72
[3,4)	87	26	54	72
[4,5)	87	27	68	72
[5,6)	87	27	75	72
[6,7)	87	27	75	72
[7,8)	87	27	81	75
[8,9)	87	27	84	75
[9,10)	87	27	84	75
[10,11)	87	27	84	71
[11,12)	87	27	81	69
[12,13)	87	27	77	69
[13,14)	87	27	76	72
[14,15)	87	27	76	76
[15,16)	87	24	76	81
[16,17)	87	24	79	81
[17,18)	87	24	80	81
[18,19)	84	24	77	81
[19,20)	87	24	78	81
[20,21)	87	24	75	81
[21,22)	87	24	77	79
[22,23)	87	22	81	84
[23,24)	87	21	81	79

TABLE B.23

Number of Data Used in each UT Hour Interval

Evaluation Condition 5
Urbana - ATS3

Hour Interval	Number of Data January 1969	April 1969	July 1969	October 1969
[0,1)	90	87	90	90
[1,2)	90	87	90	90
[2,3)	90	87	90	90
[3,4)	90	87	90	90
[4,5)	90	87	90	90
[5,6)	90	87	90	90
[6,7)	90	87	90	90
[7,8)	90	87	90	90
[8,9)	90	87	90	90
[9,10)	90	87	90	90
[10,11)	90	87	90	90
[11,12)	90	87	90	90
[12,13)	90	87	90	90
[13,14)	90	87	90	90
[14,15)	90	87	90	90
[15,16)	89	87	90	87
[16,17)	86	85	90	87
[17,18)	84	84	90	87
[18,19)	86	84	90	87
[19,20)	86	84	90	90
[20,21)	87	87	90	90
[21,22)	89	87	90	90
[22,23)	90	87	90	90
[23,24)	90	87	90	90

TABLE B.24

Number of Data Used in each UT Hour Interval

Evaluation Condition 5
Rosman - ATS3

Hour Interval	Number of Data January 1969	April 1969	July 1969	October 1969
[0,1)	87	39	80	32
[1,2)	86	39	80	27
[2,3)	86	38	80	27
[3,4)	84	36	79	32
[4,5)	81	38	83	29
[5,6)	80	39	83	29
[6,7)	85	37	80	29
[7,8)	87	37	87	30
[8,9)	82	38	82	29
[9,10)	85	36	82	30
[10,11)	87	34	88	30
[11,12)	86	38	87	32
[12,13)	90	36	87	35
[13,14)	89	36	83	33
[14,15)	78	36	82	33
[15,16)	75	36	82	32
[16,17)	83	36	88	36
[17,18)	83	34	86	36
[18,19)	86	35	87	36
[19,20)	89	33	83	32
[20,21)	90	34	82	36
[21,22)	87	32	79	33
[22,23)	86	36	67	35
[23,24)	87	36	79	35

TABLE B.25

Number of Data Used in each UT Hour Interval

Evaluation Condition 5
Arecibo - ATS3

Hour Interval	January 1969	April 1969
[0,1)	82	3
[1,2)	81	3
[2,3)	82	3
[3,4)	74	3
[4,5)	70	3
[5,6)	69	3
[6,7)	72	3
[7,8)	81	3
[8,9)	71	3
[9,10)	73	3
[10,11)	71	3
[11,12)	78	3
[12,13)	76	3
[13,14)	79	3
[14,15)	82	3
[15,16)	79	2
[16,17)	79	0
[17,18)	73	0
[18,19)	71	0
[19,20)	75	0
[20,21)	79	0
[21,22)	77	0
[22,23)	86	0
[23,24)	87	0

TABLE B.26

Number of Data Used in each UT Hour Interval

Evaluation Condition 5
Sagamore Hill - ATS3

Hour Interval	Number of Data January 1969	April 1969	July 1969	October 1969
[0,1)	90	87	90	90
[1,2)	90	87	90	90
[2,3)	89	87	90	90
[3,4)	90	87	90	90
[4,5)	90	87	90	90
[5,6)	90	87	90	90
[6,7)	87	87	90	90
[7,8)	90	87	90	90
[8,9)	90	87	90	90
[9,10)	90	87	90	90
[10,11)	90	87	90	90
[11,12)	90	87	90	90
[12,13)	90	87	90	90
[13,14)	90	86	90	90
[14,15)	89	87	89	90
[15,16)	88	87	87	90
[16,17)	87	87	90	90
[17,18)	87	87	90	90
[18,19)	87	85	90	90
[19,20)	87	87	90	90
[20,21)	88	87	90	89
[21,22)	89	87	90	90
[22,23)	90	87	90	90
[23,24)	90	87	90	90

TABLE B.27

Number of Data Used in each UT Hour Interval

Evaluation Condition 5
Edmonton - ATS1

Hour Interval	Number of Data January 1969	April 1969	July 1969	October 1969
[0,1)	84	75	89	74
[1,2)	84	73	90	75
[2,3)	84	75	88	75
[3,4)	84	72	89	75
[4,5)	76	72	90	75
[5,6)	74	72	90	75
[6,7)	72	69	90	75
[7,8)	65	69	88	74
[8,9)	63	67	87	71
[9,10)	63	65	89	72
[10,11)	72	64	89	75
[11,12)	68	69	90	75
[12,13)	74	72	90	72
[13,14)	72	73	90	75
[14,15)	79	75	88	75
[15,16)	85	73	86	75
[16,17)	86	75	88	77
[17,18)	87	77	89	78
[18,19)	90	75	90	77
[19,20)	90	75	89	78
[20,21)	90	74	89	76
[21,22)	90	74	88	77
[22,23)	90	75	86	78
[23,24)	89	74	88	78

Number of Data Used in each UT Hour Interval

Evaluation Condition 5
Honolulu - ATS1

Hour Interval	Number of Data January 1969	April 1969	July 1969	October 1969
[0,1)	81	86	90	90
[1,2)	80	87	90	90
[2,3)	81	85	90	90
[3,4)	83	84	90	90
[4,5)	86	81	90	89
[5,6)	87	81	90	90
[6,7)	87	81	90	90
[7,8)	87	80	87	89
[8,9)	87	80	89	89
[9,10)	87	79	88	89
[10,11)	87	73	85	85
[11,12)	87	73	83	88
[12,13)	87	76	87	88
[13,14)	87	79	87	89
[14,15)	87	81	86	90
[15,16)	87	79	87	89
[16,17)	87	80	81	87
[17,18)	87	78	78	87
[18,19)	87	81	81	89
[19,20)	86	84	89	90
[20,21)	84	85	90	90
[21,22)	84	87	90	90
[22,23)	84	87	89	89
[23,24)	84	87	88	89

APPENDIX C

PLOTS OF VERTICAL TIME DELAY AND RESIDUALS - CUMULATIVE FREQUENCY DISTRIBUTION

Preceding page blank

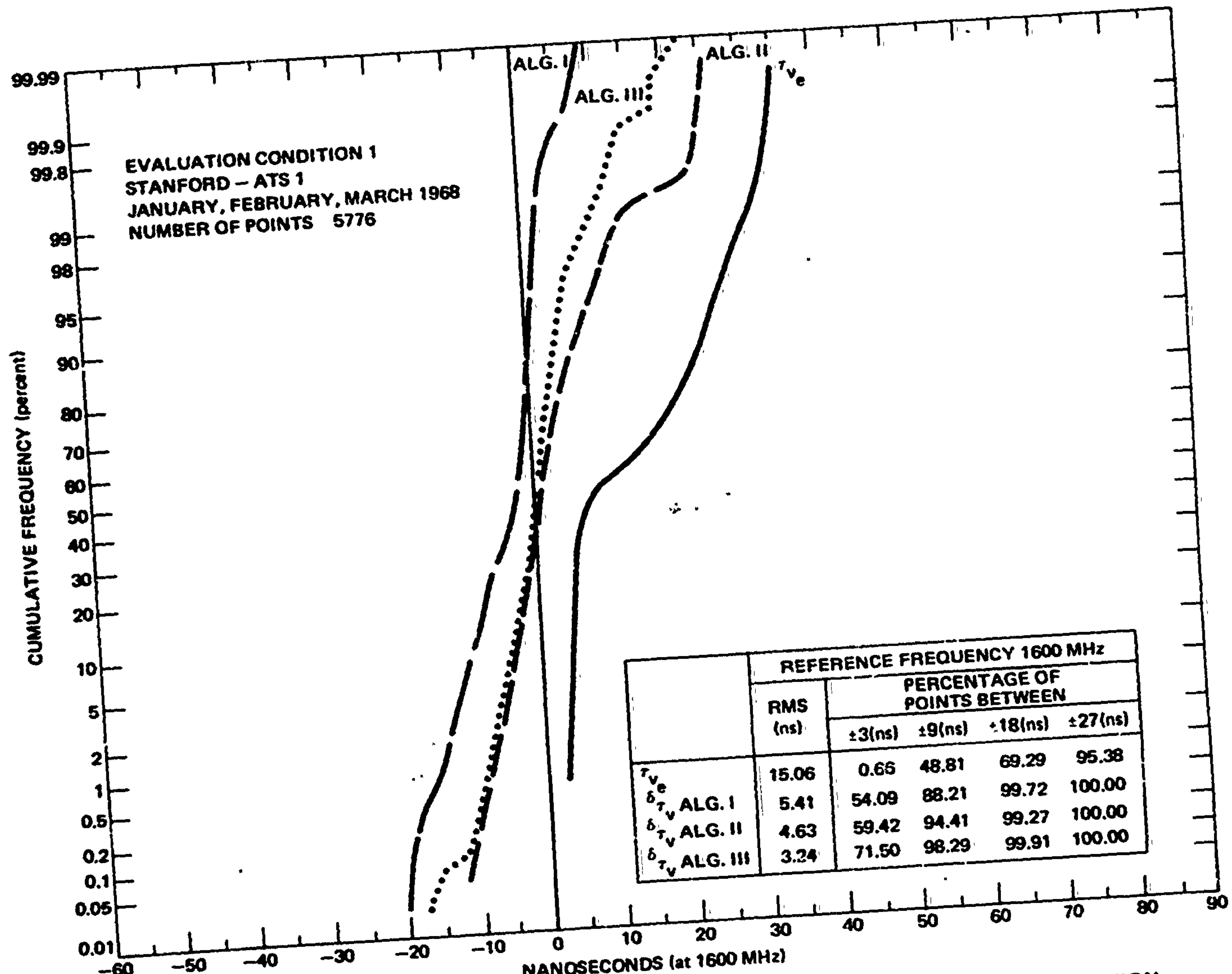

	RMS (ns)	REFERENCE FREQUENCY 1600 MHz PERCENTAGE OF POINTS BETWEEN ±3(ns)	±9(ns)	±18(ns)	±27(ns)
τ_{v_e}	15.06	0.66	48.81	69.29	95.38
δ_{τ_v} ALG. I	5.41	54.09	88.21	99.72	100.00
δ_{τ_v} ALG. II	4.63	59.42	94.41	99.27	100.00
δ_{τ_v} ALG. III	3.24	71.50	98.29	99.91	100.00

Fig. C.1 VERTICAL TIME DELAY AND RESIDUALS–CUMULATIVE FREQUENCY DISTRIBUTION

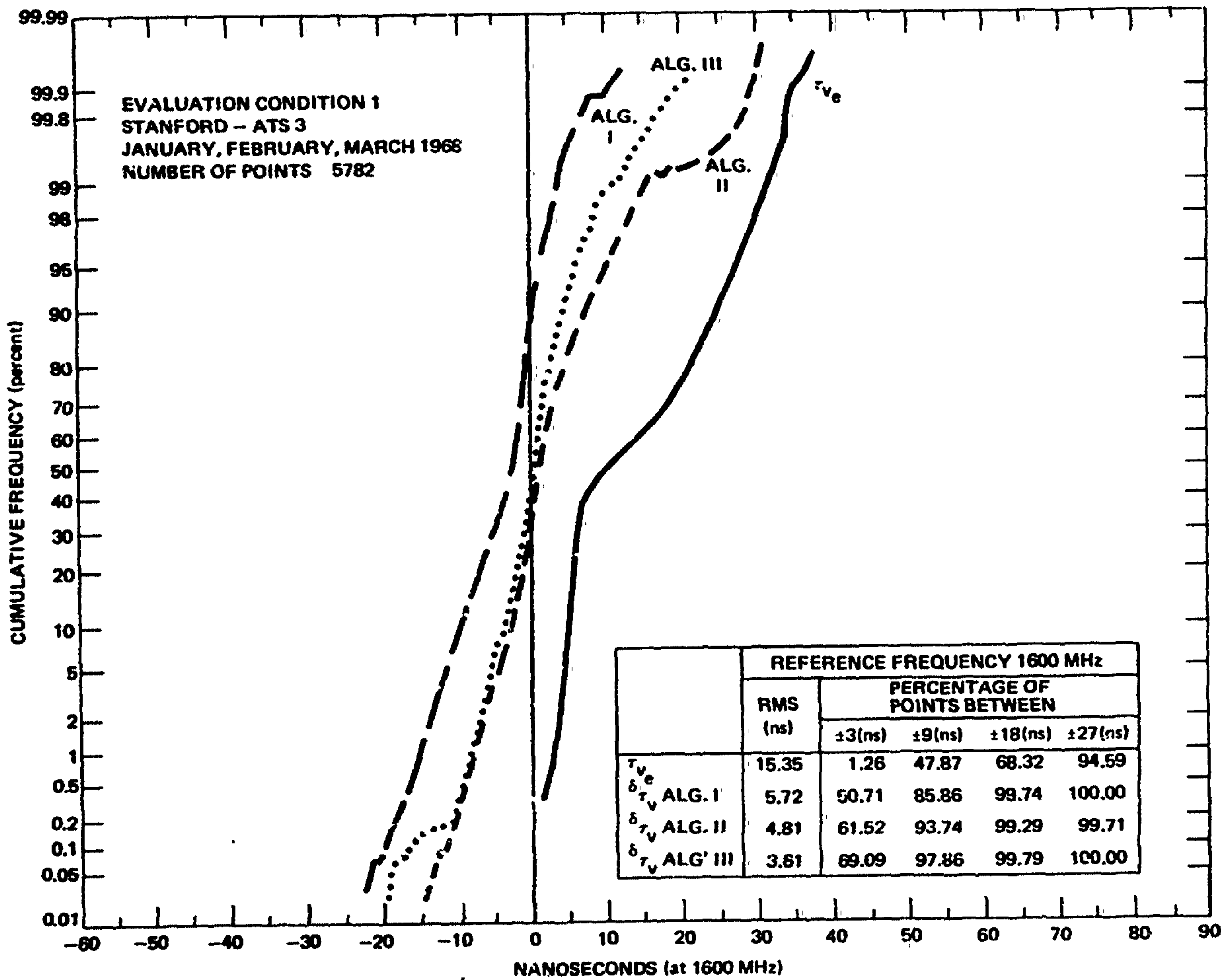

	REFERENCE FREQUENCY 1600 MHz				
	RMS (ns)	PERCENTAGE OF POINTS BETWEEN			
		±3(ns)	±9(ns)	±18(ns)	±27(ns)
τ_{v_e}	15.35	1.26	47.87	68.32	94.59
δ_{τ_v} ALG. I	5.72	50.71	85.86	99.74	100.00
δ_{τ_v} ALG. II	4.81	61.52	93.74	99.29	99.71
δ_{τ_v} ALG' III	3.61	89.09	97.86	99.79	100.00

Fig. C.2 VERTICAL TIME DELAY AND RESIDUALS–CUMULATIVE FREQUENCY DISTRIBUTION

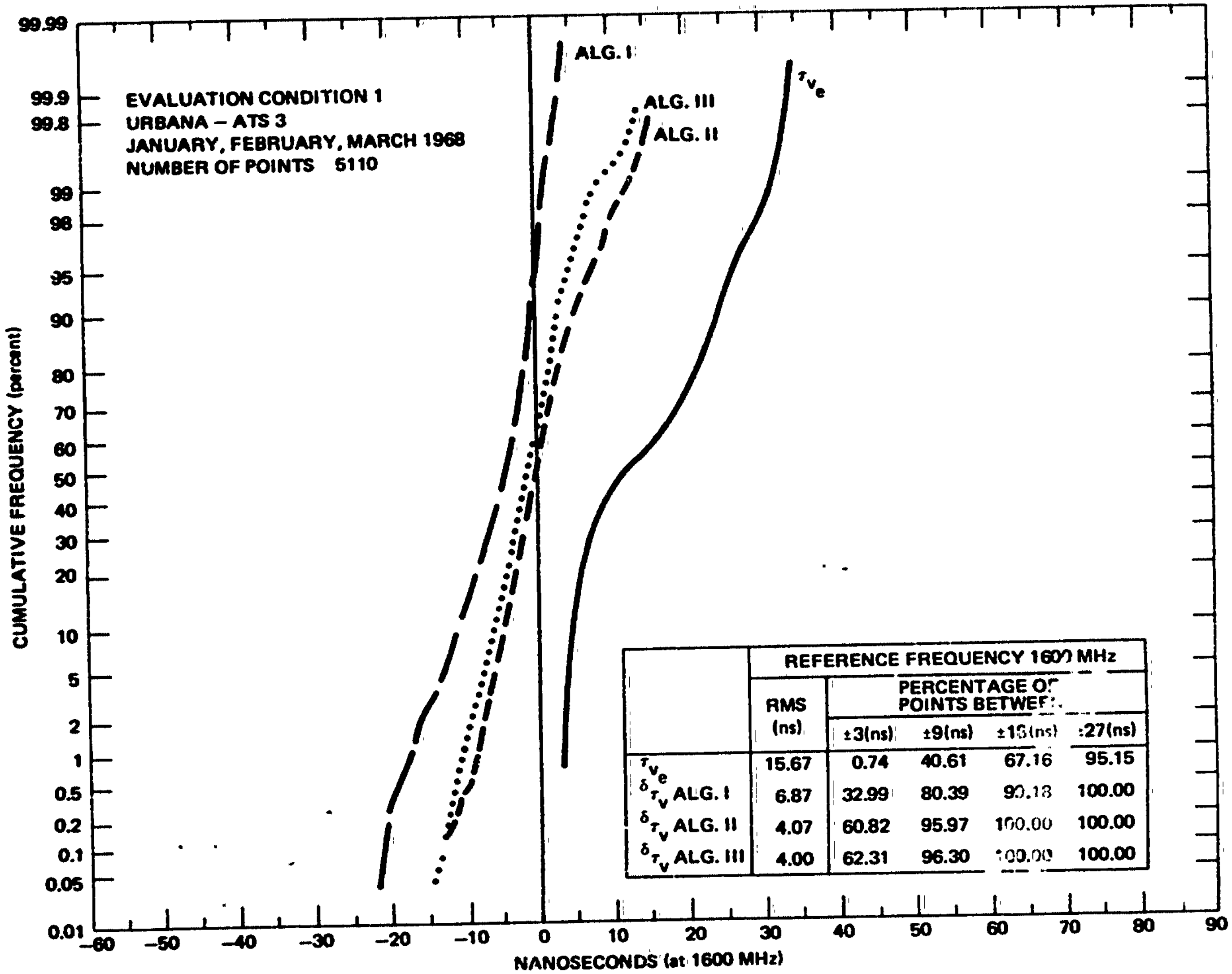

	REFERENCE FREQUENCY 1600 MHz				
	RMS (ns)	PERCENTAGE OF POINTS BETWEEN			
		±3(ns)	±9(ns)	±15(ns)	±27(ns)
τ_{v_e}	15.67	0.74	40.61	67.16	95.15
δ_{τ_v} ALG. I	6.87	32.99	80.39	90.18	100.00
δ_{τ_v} ALG. II	4.07	60.82	95.97	100.00	100.00
δ_{τ_v} ALG. III	4.00	62.31	96.30	100.00	100.00

Fig. C.3 VERTICAL TIME DELAY AND RESIDUALS–CUMULATIVE FREQUENCY DISTRIBUTION

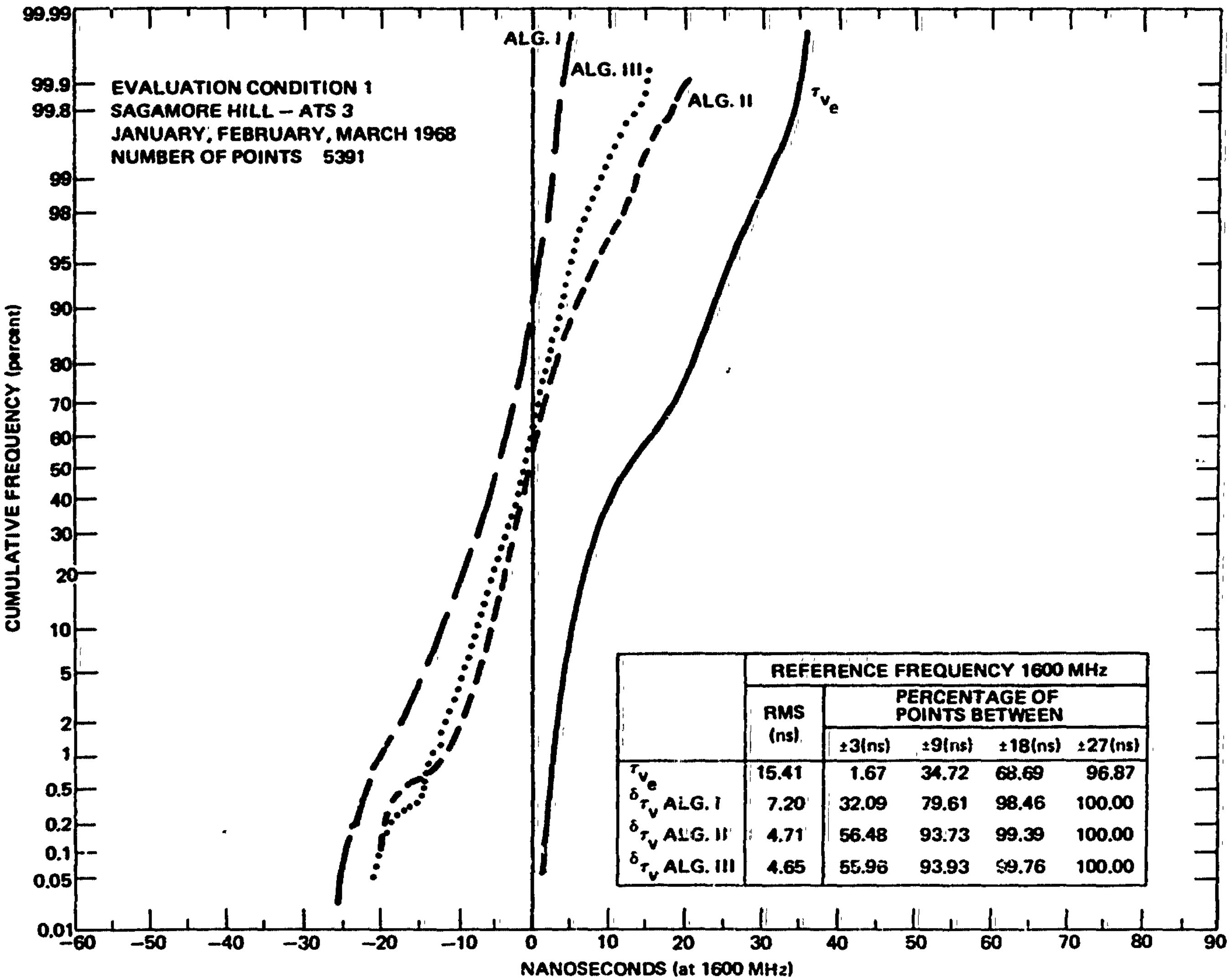

	REFERENCE FREQUENCY 1600 MHz				
	RMS (ns)	PERCENTAGE OF POINTS BETWEEN			
		±3(ns)	±9(ns)	±18(ns)	±27(ns)
τ_{v_e}	15.41	1.67	34.72	68.69	96.87
δ_{τ_v} ALG. I	7.20	32.09	79.61	98.46	100.00
δ_{τ_v} ALG. II	4.71	56.48	93.73	99.39	100.00
δ_{τ_v} ALG. III	4.65	55.96	93.93	99.76	100.00

Fig. C.4 VERTICAL TIME DELAY AND RESIDUALS–CUMULATIVE FREQUENCY DISTRIBUTION

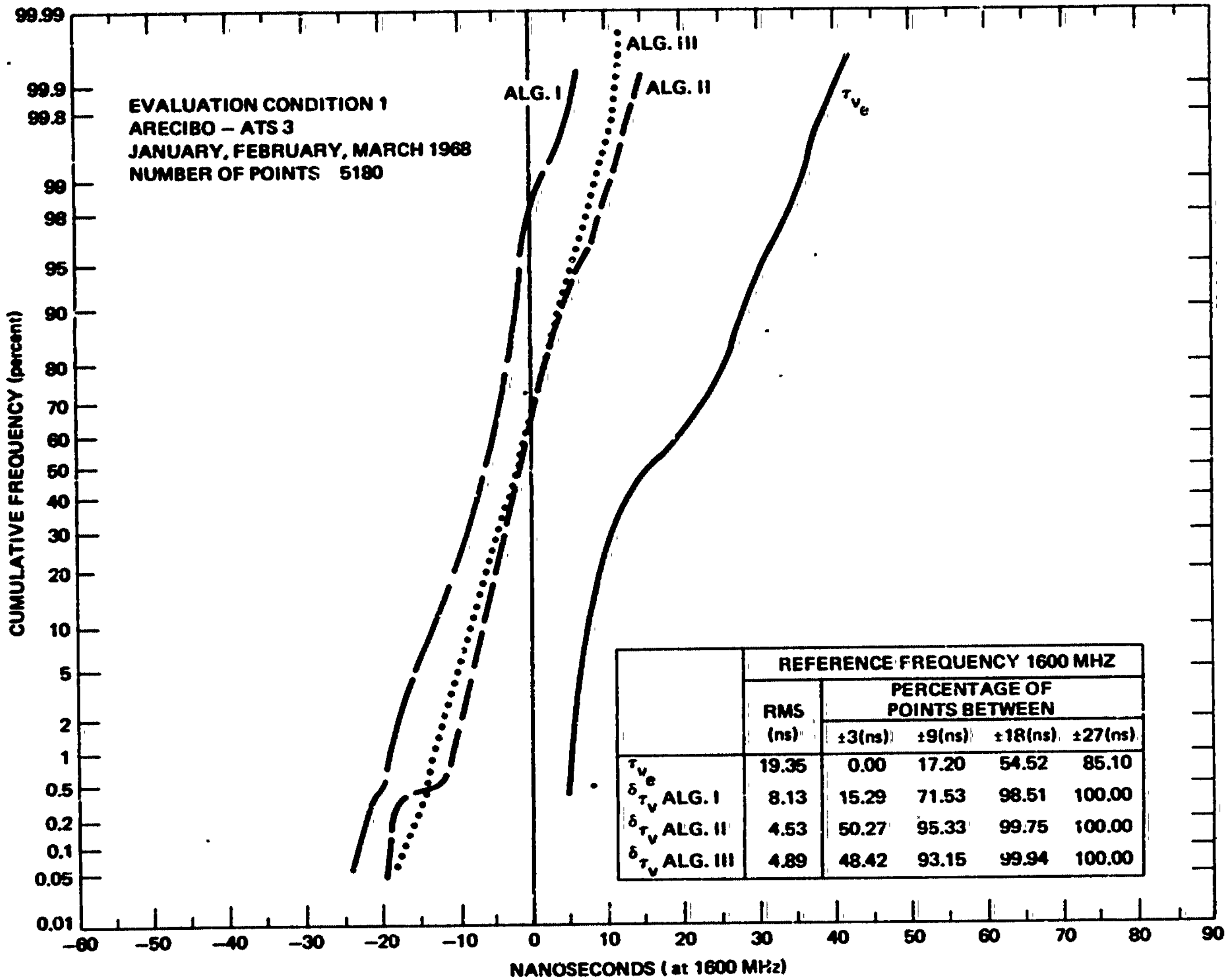

	REFERENCE FREQUENCY 1600 MHZ				
	RMS (ns)	PERCENTAGE OF POINTS BETWEEN			
		±3(ns)	±9(ns)	±18(ns)	±27(ns)
τ_{v_e}	19.35	0.00	17.20	54.52	85.10
δ_{τ_v} ALG. I	8.13	15.29	71.53	98.51	100.00
δ_{τ_v} ALG. II	4.53	50.27	95.33	99.75	100.00
δ_{τ_v} ALG. III	4.89	48.42	93.15	99.94	100.00

Fig. C.5 VERTICAL TIME DELAY AND RESIDUALS–CUMULATIVE FREQUENCY DISTRIBUTION

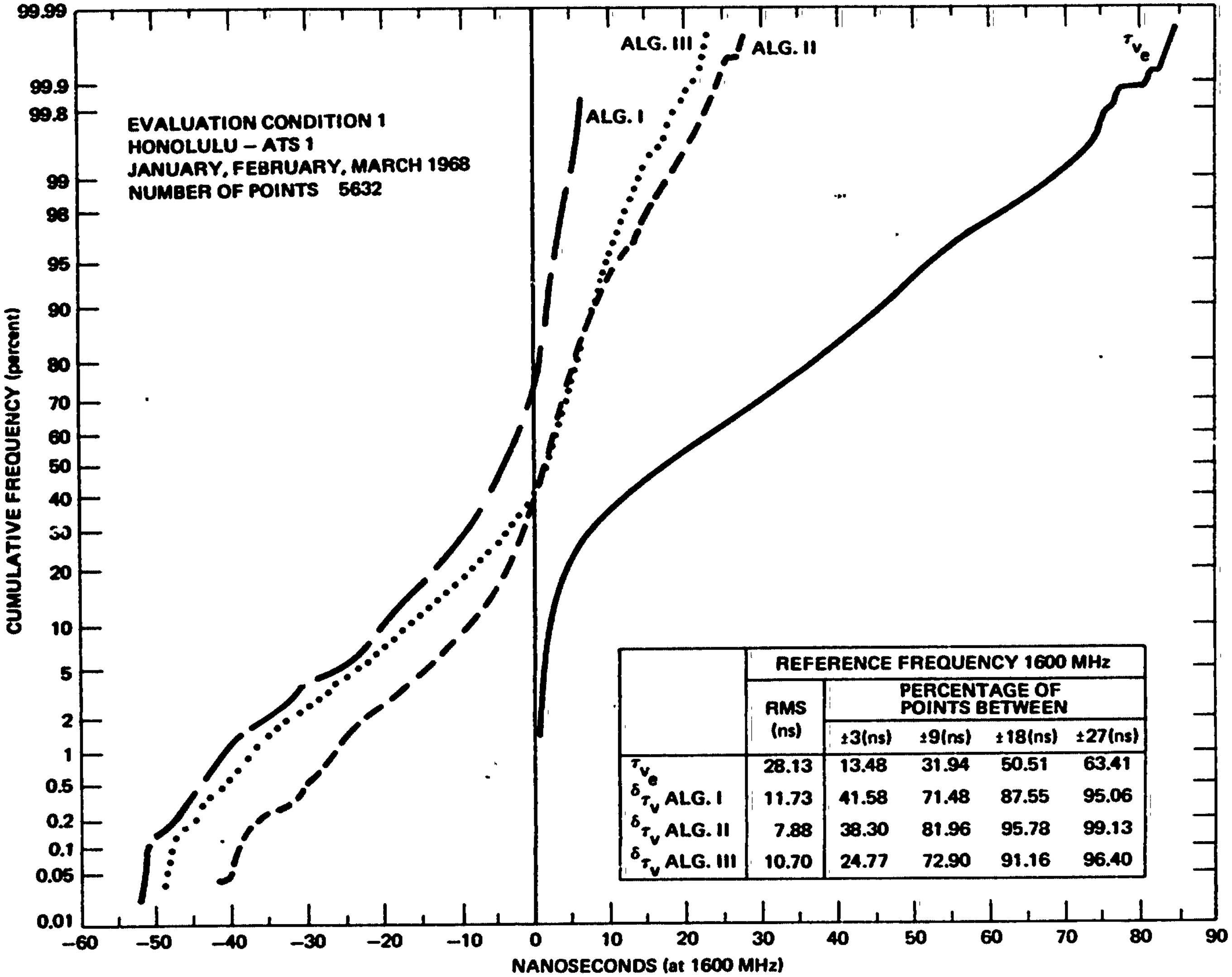

	REFERENCE FREQUENCY 1600 MHz				
	RMS (ns)	PERCENTAGE OF POINTS BETWEEN			
		±3(ns)	±9(ns)	±18(ns)	±27(ns)
τ_{v_e}	28.13	13.48	31.94	50.51	63.41
δ_{τ_v} ALG. I	11.73	41.58	71.48	87.55	95.06
δ_{τ_v} ALG. II	7.88	38.30	81.96	95.78	99.13
δ_{τ_v} ALG. III	10.70	24.77	72.90	91.16	96.40

Fig. C.6 VERTICAL TIME DELAY AND RESIDUALS–CUMULATIVE FREQUENCY DISTRIBUTION

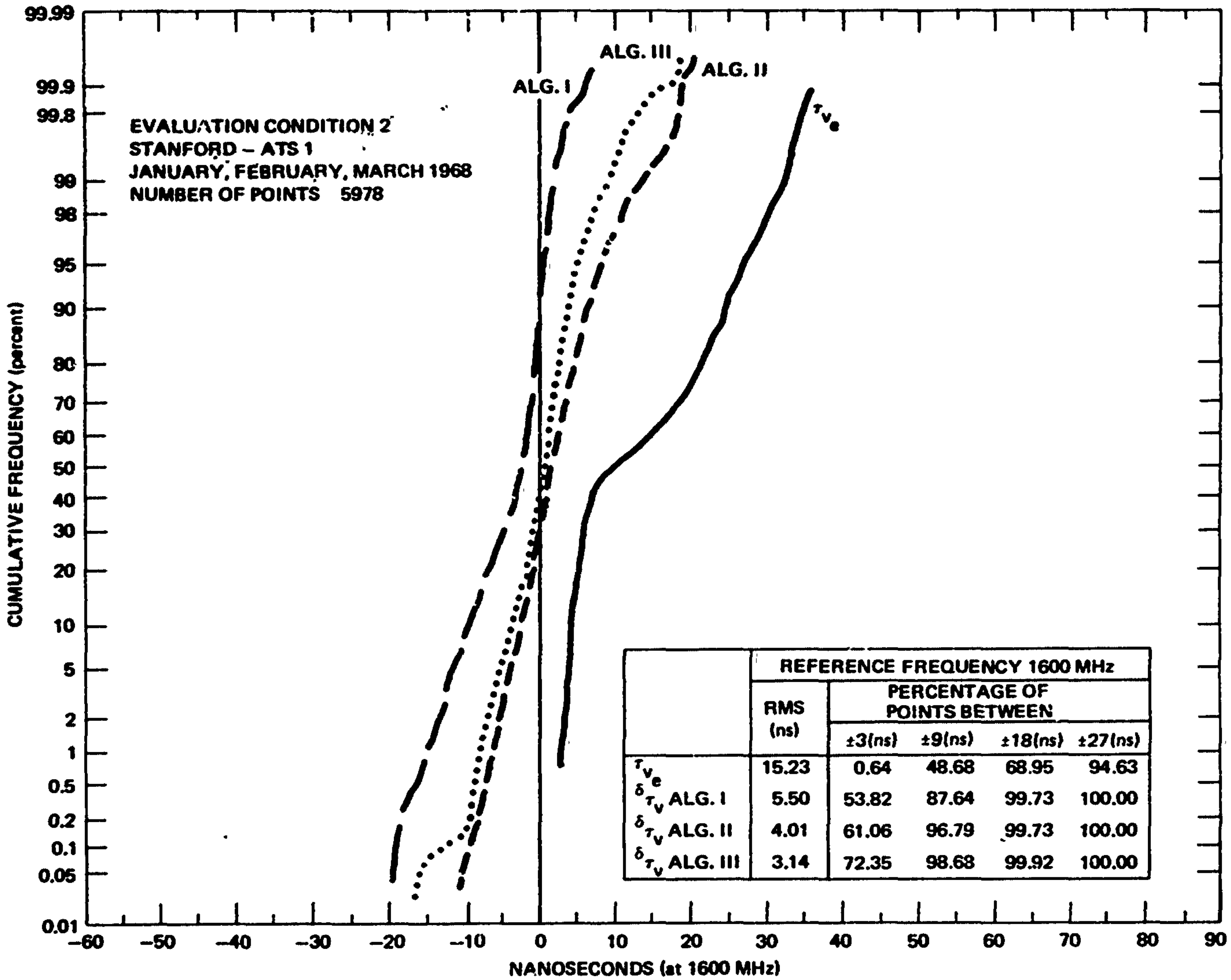

	REFERENCE FREQUENCY 1600 MHz				
	RMS (ns)	PERCENTAGE OF POINTS BETWEEN			
		±3(ns)	±9(ns)	±18(ns)	±27(ns)
τ_{v_e}	15.23	0.64	48.68	68.95	94.63
δ_{τ_v} ALG. I	5.50	53.82	87.64	99.73	100.00
δ_{τ_v} ALG. II	4.01	61.06	96.79	99.73	100.00
δ_{τ_v} ALG. III	3.14	72.35	98.68	99.92	100.00

Fig. C.7 VERTICAL TIME DELAY AND RESIDUALS–CUMULATIVE FREQUENCY DISTRIBUTION

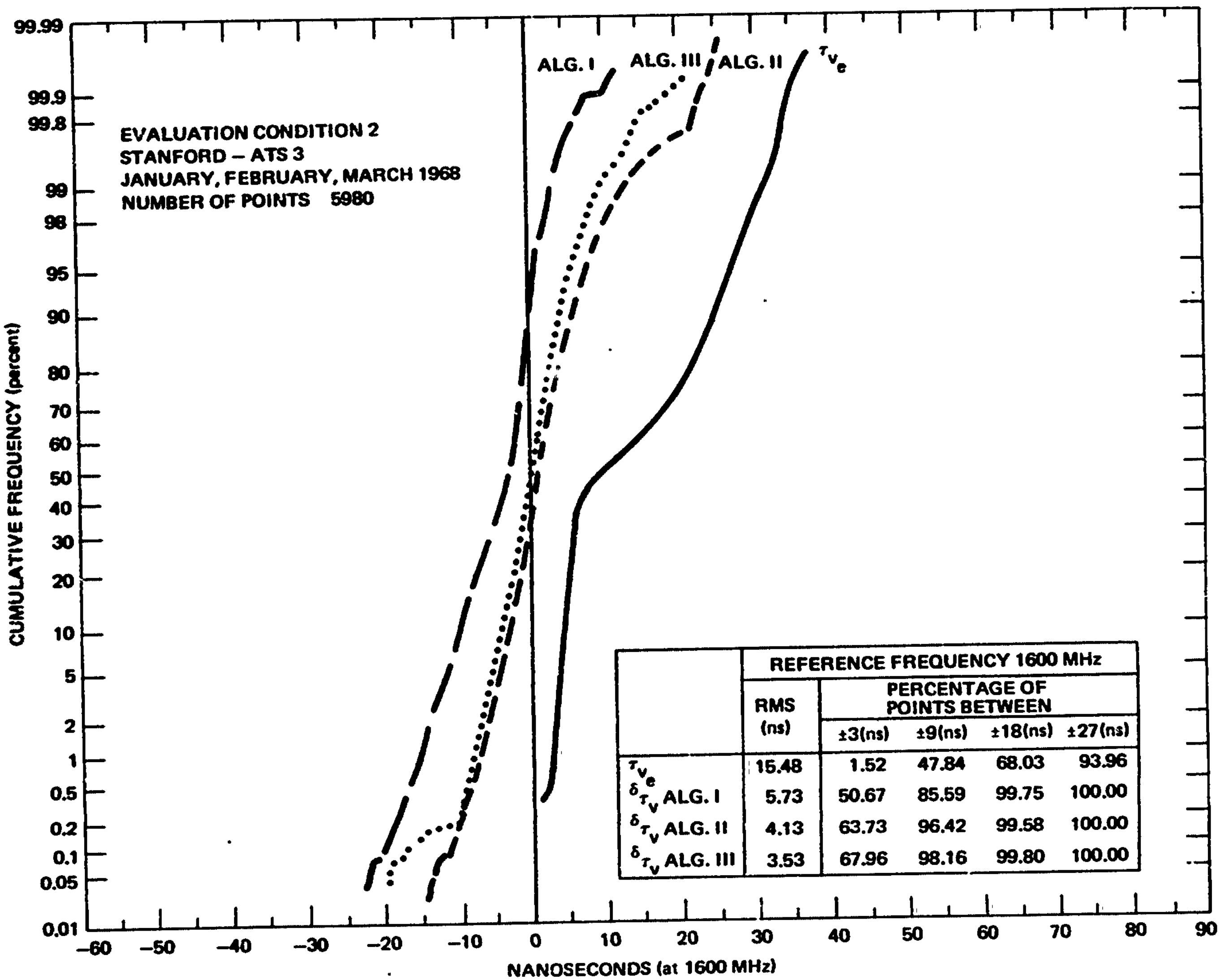

	REFERENCE FREQUENCY 1600 MHz				
	RMS (ns)	PERCENTAGE OF POINTS BETWEEN			
		±3(ns)	±9(ns)	±18(ns)	±27(ns)
τ_{v_e}	15.48	1.52	47.84	68.03	93.96
δ_{τ_v} ALG. I	5.73	50.67	85.59	99.75	100.00
δ_{τ_v} ALG. II	4.13	63.73	96.42	99.58	100.00
δ_{τ_v} ALG. III	3.53	67.96	98.16	99.80	100.00

Fig. C.8 VERTICAL TIME DELAY AND RESIDUALS–CUMULATIVE FREQUENCY DISTRIBUTION

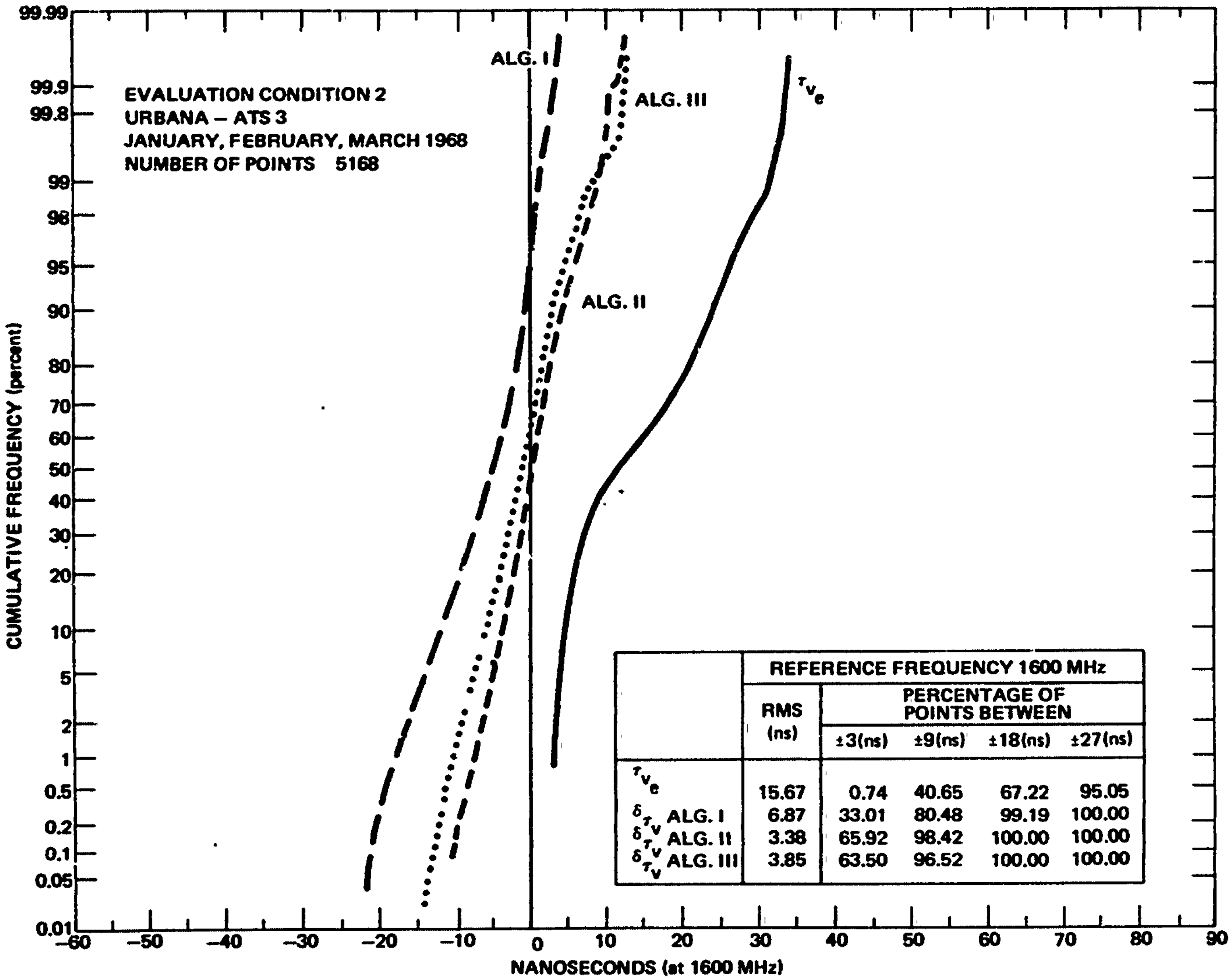

	REFERENCE FREQUENCY 1600 MHz				
	RMS (ns)	PERCENTAGE OF POINTS BETWEEN			
		±3(ns)	±9(ns)	±18(ns)	±27(ns)
τ_{v_e}	15.67	0.74	40.65	67.22	95.05
δ_{τ_v} ALG. I	6.87	33.01	80.48	99.19	100.00
δ_{τ_v} ALG. II	3.38	65.92	98.42	100.00	100.00
δ_{τ_v} ALG. III	3.85	63.50	96.52	100.00	100.00

Fig. C.9 VERTICAL TIME DELAY AND RESIDUALS—CUMULATIVE FREQUENCY DISTRIBUTION

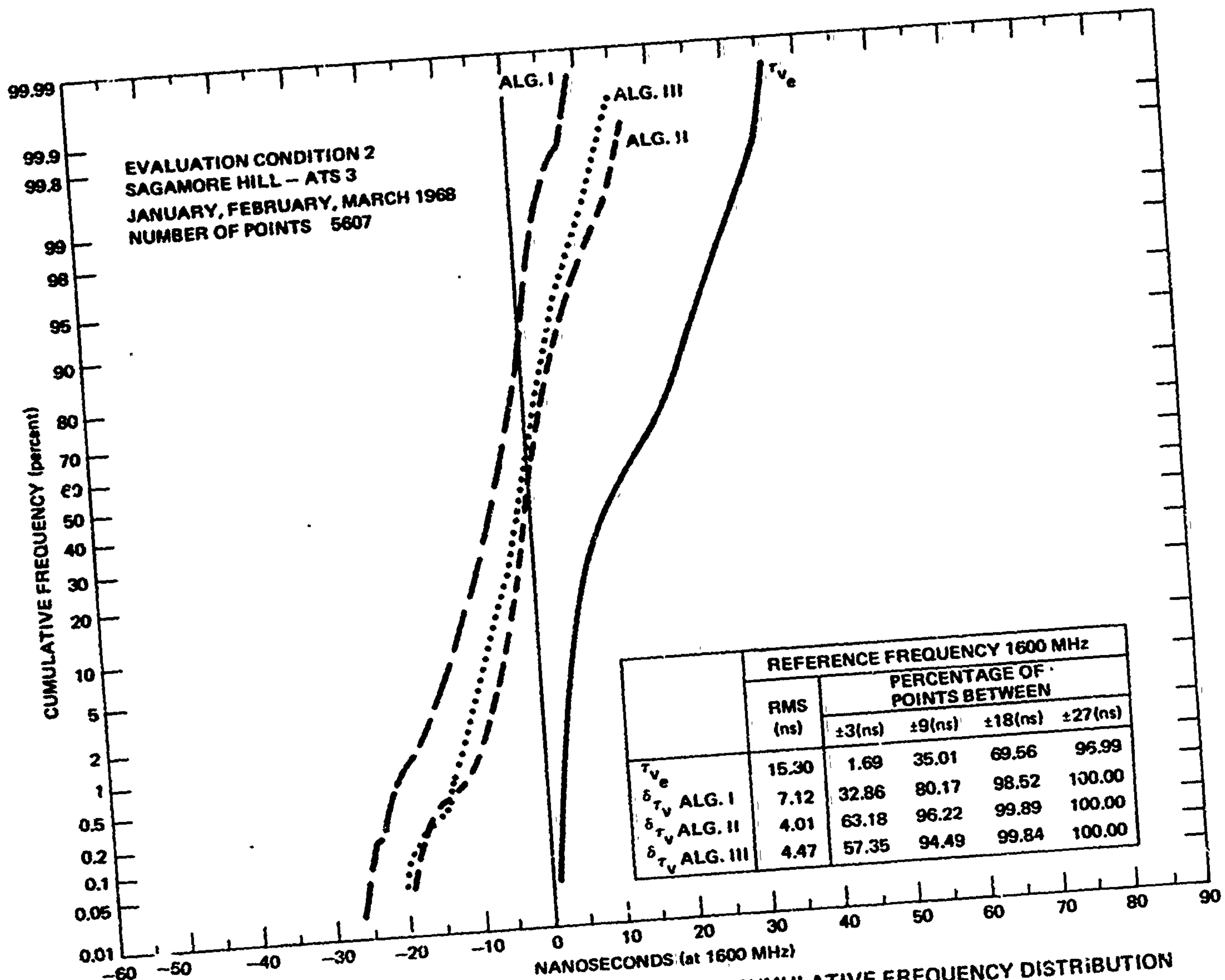

	REFERENCE FREQUENCY 1600 MHz				
	RMS (ns)	PERCENTAGE OF POINTS BETWEEN			
		±3(ns)	±9(ns)	±18(ns)	±27(ns)
τ_{v_e}	15.30	1.69	35.01	69.56	96.99
δ_{τ_v} ALG. I	7.12	32.86	80.17	98.52	100.00
δ_{τ_v} ALG. II	4.01	63.18	96.22	99.89	100.00
δ_{τ_v} ALG. III	4.47	57.35	94.49	99.84	100.00

Fig. C.10 VERTICAL TIME DELAY AND RESIDUALS–CUMULATIVE FREQUENCY DISTRIBUTION

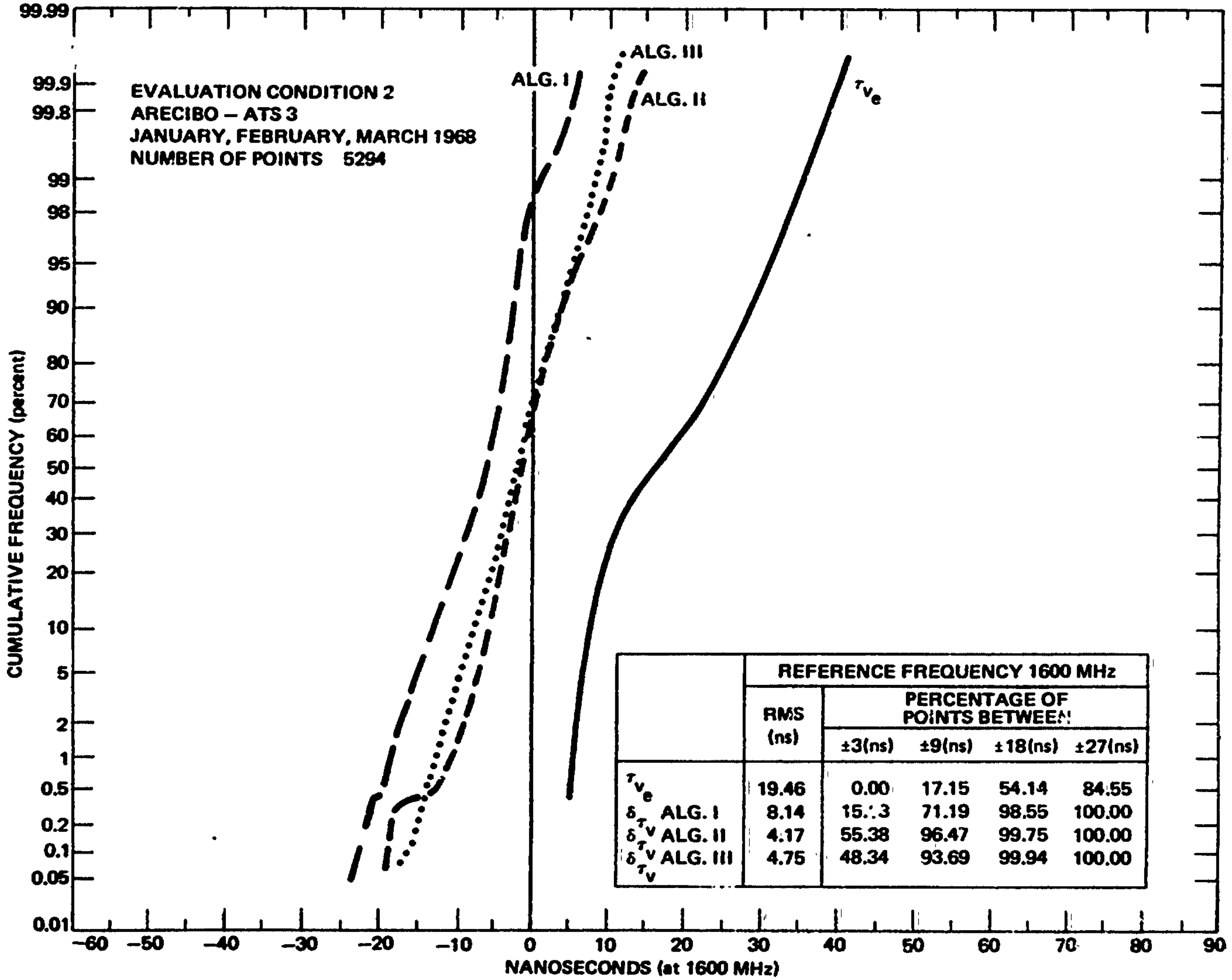

	REFERENCE FREQUENCY 1600 MHz				
	RMS (ns)	PERCENTAGE OF POINTS BETWEEN			
		±3(ns)	±9(ns)	±18(ns)	±27(ns)
τ_{v_e}	19.46	0.00	17.15	54.14	84.55
δ_{τ_v} ALG. I	8.14	15.[illegible]3	71.19	98.55	100.00
δ_{τ_v} ALG. II	4.17	55.38	96.47	99.75	100.00
δ_{τ_v} ALG. III	4.75	48.34	93.69	99.94	100.00

Fig. C.11 VERTICAL TIME DELAY AND RESIDUALS–CUMULATIVE FREQUENCY DISTRIBUTION

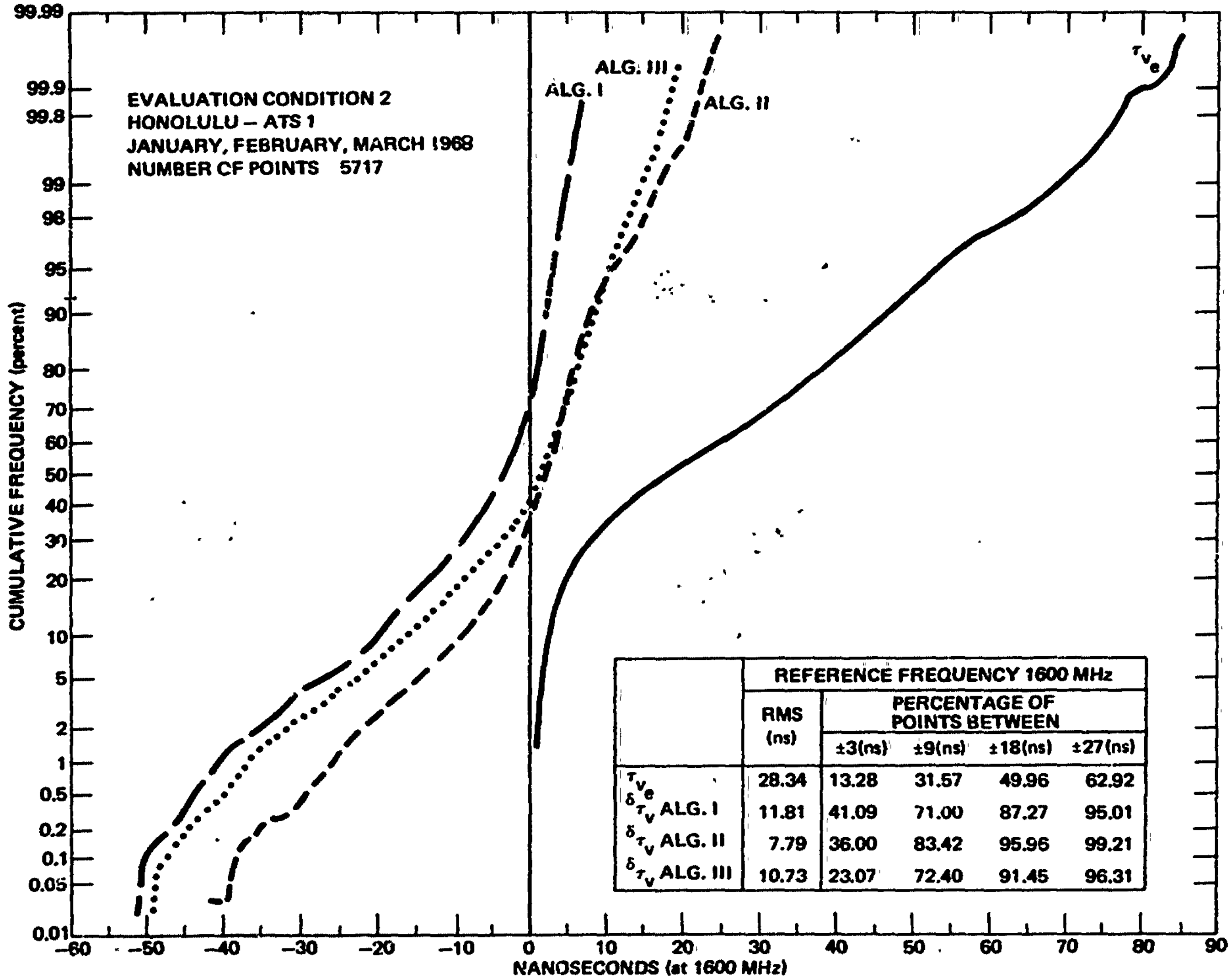

	REFERENCE FREQUENCY 1600 MHz				
	RMS (ns)	PERCENTAGE OF POINTS BETWEEN			
		±3(ns)	±9(ns)	±18(ns)	±27(ns)
τ_{v_e}	28.34	13.28	31.57	49.96	62.92
δ_{τ_v} ALG. I	11.81	41.09	71.00	87.27	95.01
δ_{τ_v} ALG. II	7.79	36.00	83.42	95.96	99.21
δ_{τ_v} ALG. III	10.73	23.07	72.40	91.45	96.31

Fig. C.12 VERTICAL TIME DELAY AND RESIDUALS–CUMULATIVE FREQUENCY DISTRIBUTION

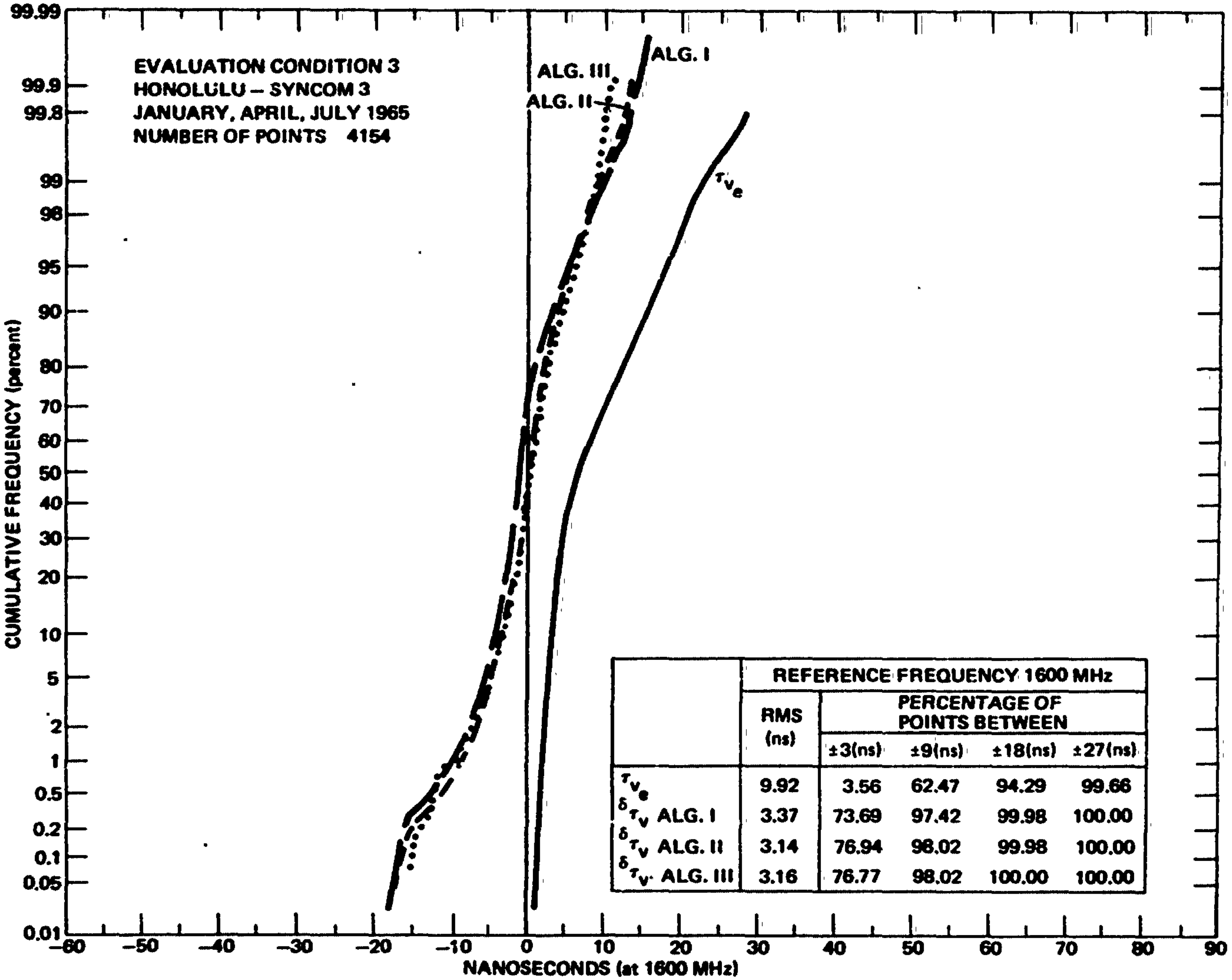

	REFERENCE FREQUENCY 1600 MHz				
	RMS (ns)	PERCENTAGE OF POINTS BETWEEN			
		±3(ns)	±9(ns)	±18(ns)	±27(ns)
τ_{v_e}	9.92	3.56	62.47	94.29	99.66
$\delta\tau_v$ ALG. I	3.37	73.69	97.42	99.98	100.00
$\delta\tau_v$ ALG. II	3.14	76.94	98.02	99.98	100.00
$\delta\tau_v$ ALG. III	3.16	76.77	98.02	100.00	100.00

Fig. C.13 VERTICAL TIME DELAY AND RESIDUALS–CUMULATIVE FREQUENCY DISTRIBUTION

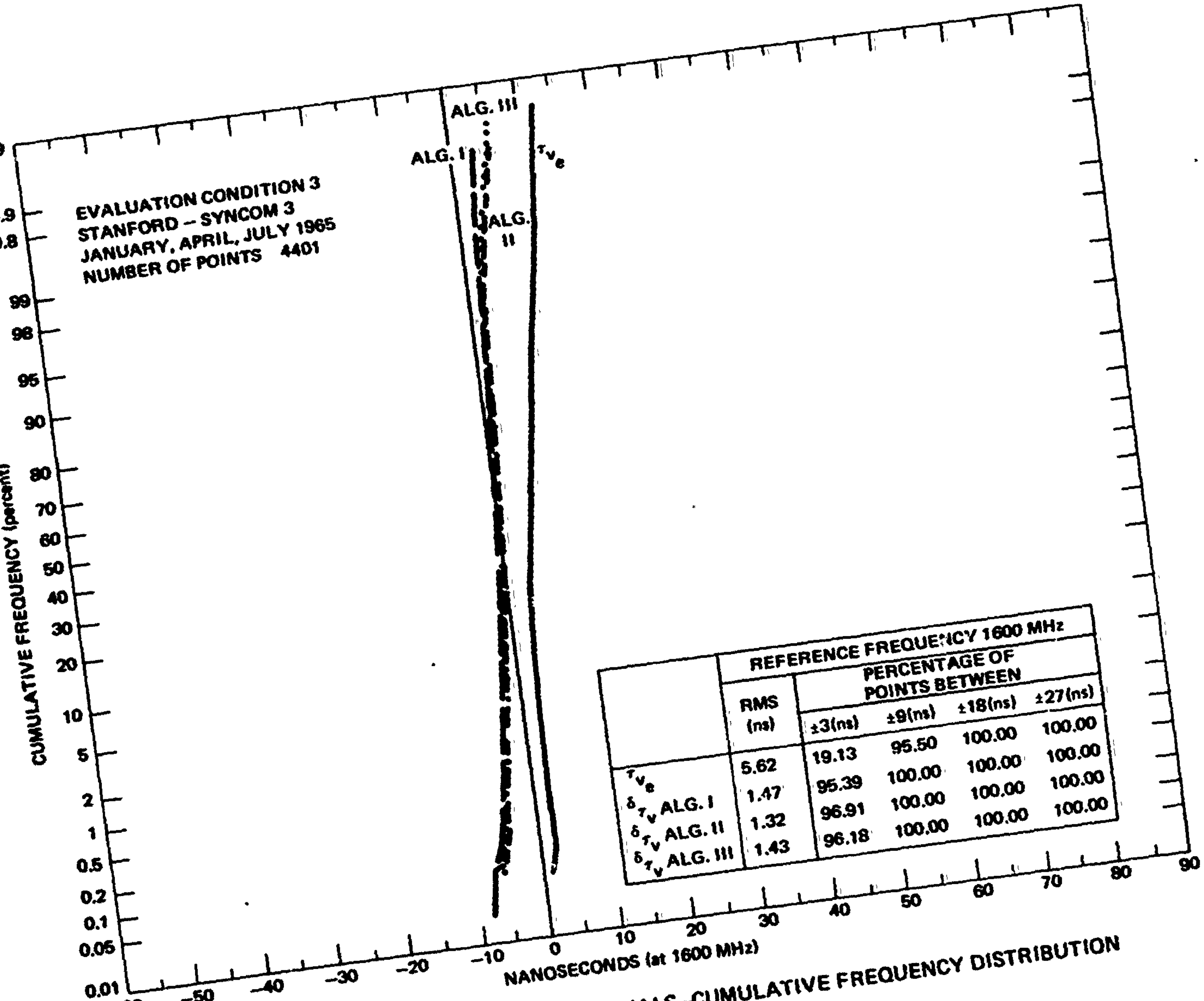

	RMS (ns)	REFERENCE FREQUENCY 1600 MHz PERCENTAGE OF POINTS BETWEEN ±3(ns)	±9(ns)	±18(ns)	±27(ns)
τ_{v_e}	5.62	19.13	95.50	100.00	100.00
δ_{τ_v} ALG. I	1.47	95.39	100.00	100.00	100.00
δ_{τ_v} ALG. II	1.32	96.91	100.00	100.00	100.00
δ_{τ_v} ALG. III	1.43	96.18	100.00	100.00	100.00

Fig. C.14 VERTICAL TIME DELAY AND RESIDUALS—CUMULATIVE FREQUENCY DISTRIBUTION

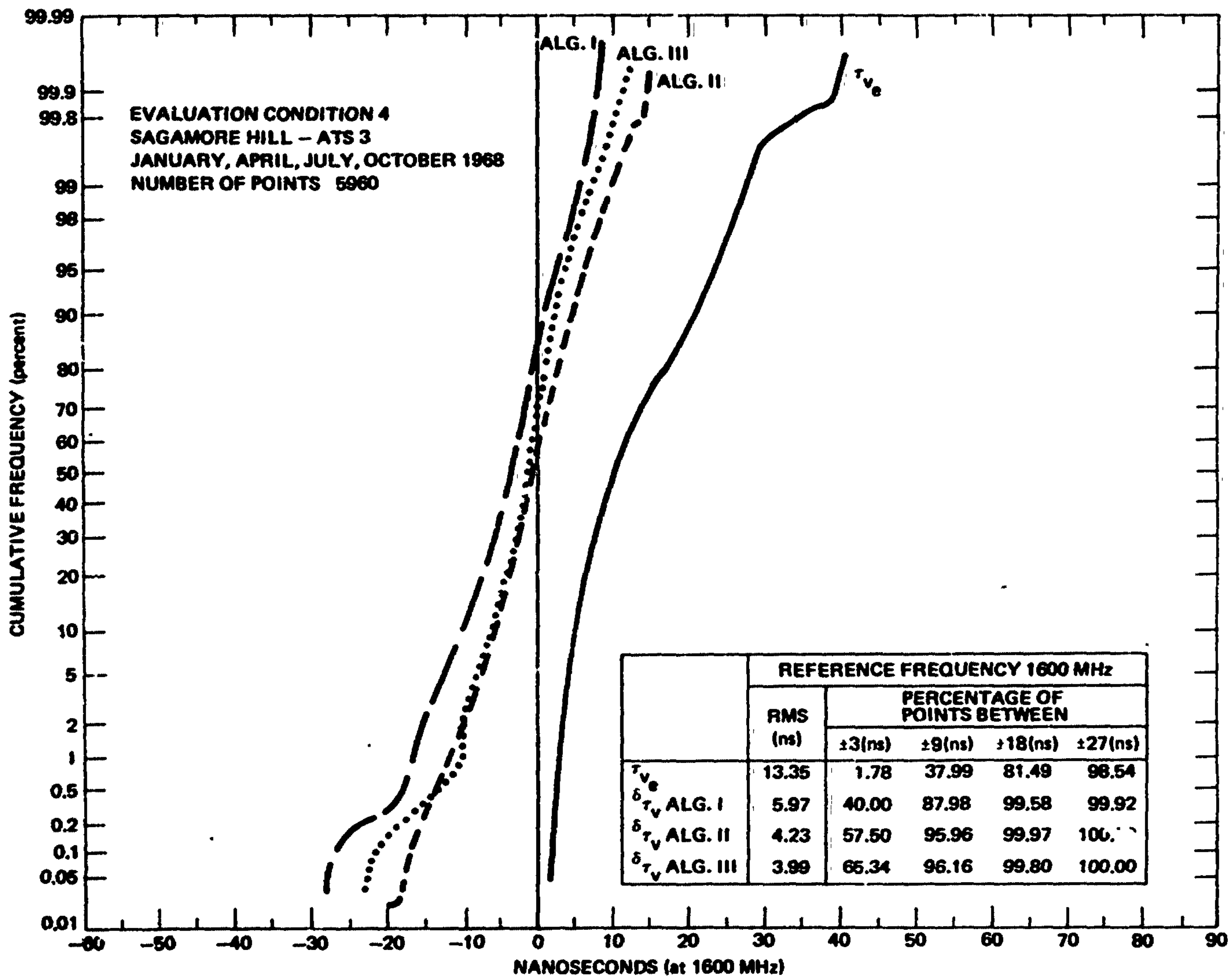

	REFERENCE FREQUENCY 1600 MHz				
	RMS (ns)	PERCENTAGE OF POINTS BETWEEN			
		±3(ns)	±9(ns)	±18(ns)	±27(ns)
τ_{v_e}	13.35	1.78	37.99	81.49	98.54
δ_{τ_v} ALG. I	5.97	40.00	87.98	99.58	99.92
δ_{τ_v} ALG. II	4.23	57.50	95.96	99.97	100.[illegible]
δ_{τ_v} ALG. III	3.99	65.34	96.16	99.80	100.00

Fig. C.15 VERTICAL TIME DELAY AND RESIDUALS–CUMULATIVE FREQUENCY DISTRIBUTION

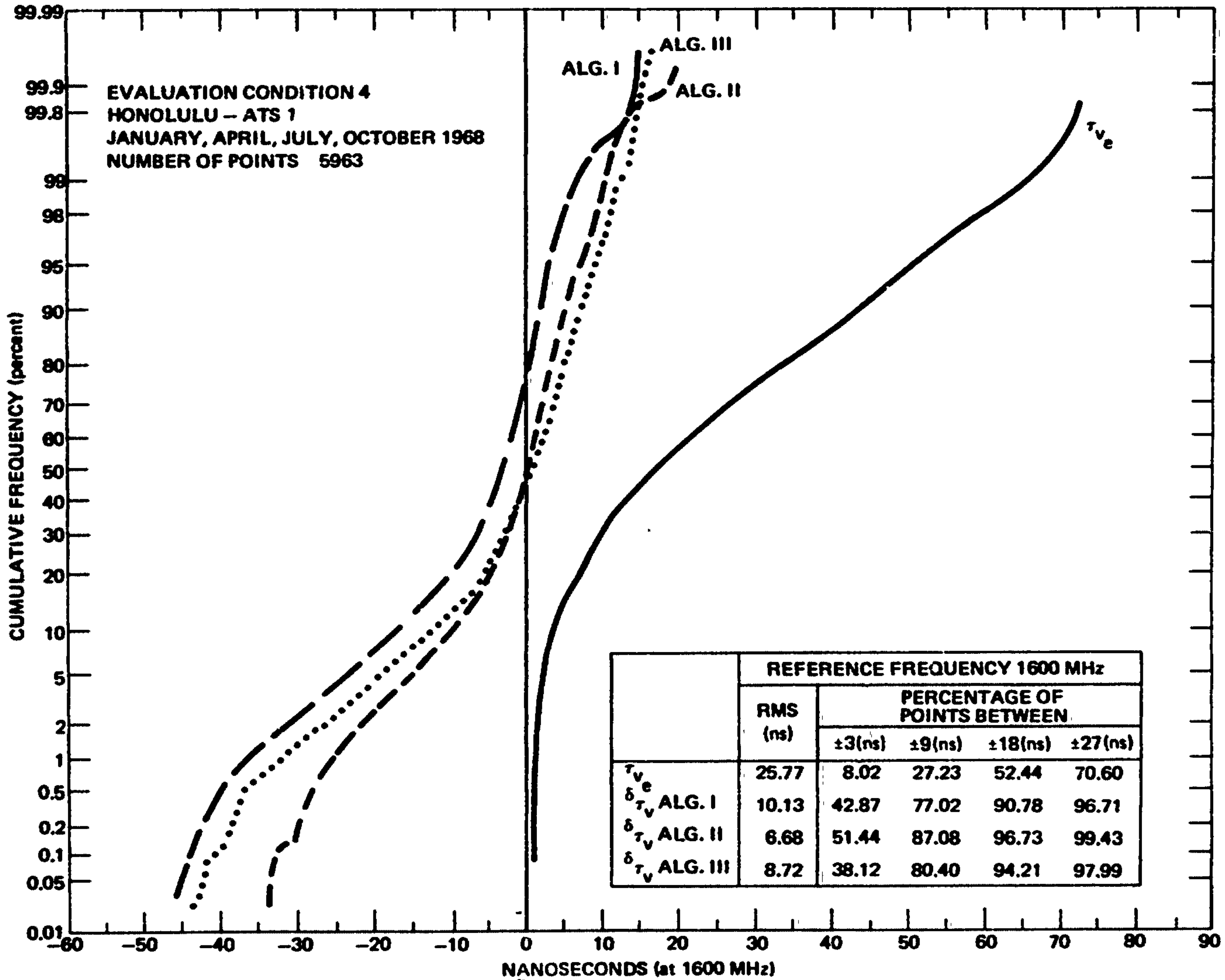

	REFERENCE FREQUENCY 1600 MHz				
	RMS (ns)	PERCENTAGE OF POINTS BETWEEN			
		±3(ns)	±9(ns)	±18(ns)	±27(ns)
τ_{v_e}	25.77	8.02	27.23	52.44	70.60
δ_{τ_v} ALG. I	10.13	42.87	77.02	90.78	96.71
δ_{τ_v} ALG. II	6.68	51.44	87.08	96.73	99.43
δ_{τ_v} ALG. III	8.72	38.12	80.40	94.21	97.99

Fig. C.16 VERTICAL TIME DELAY AND RESIDUALS–CUMULATIVE FREQUENCY DISTRIBUTION

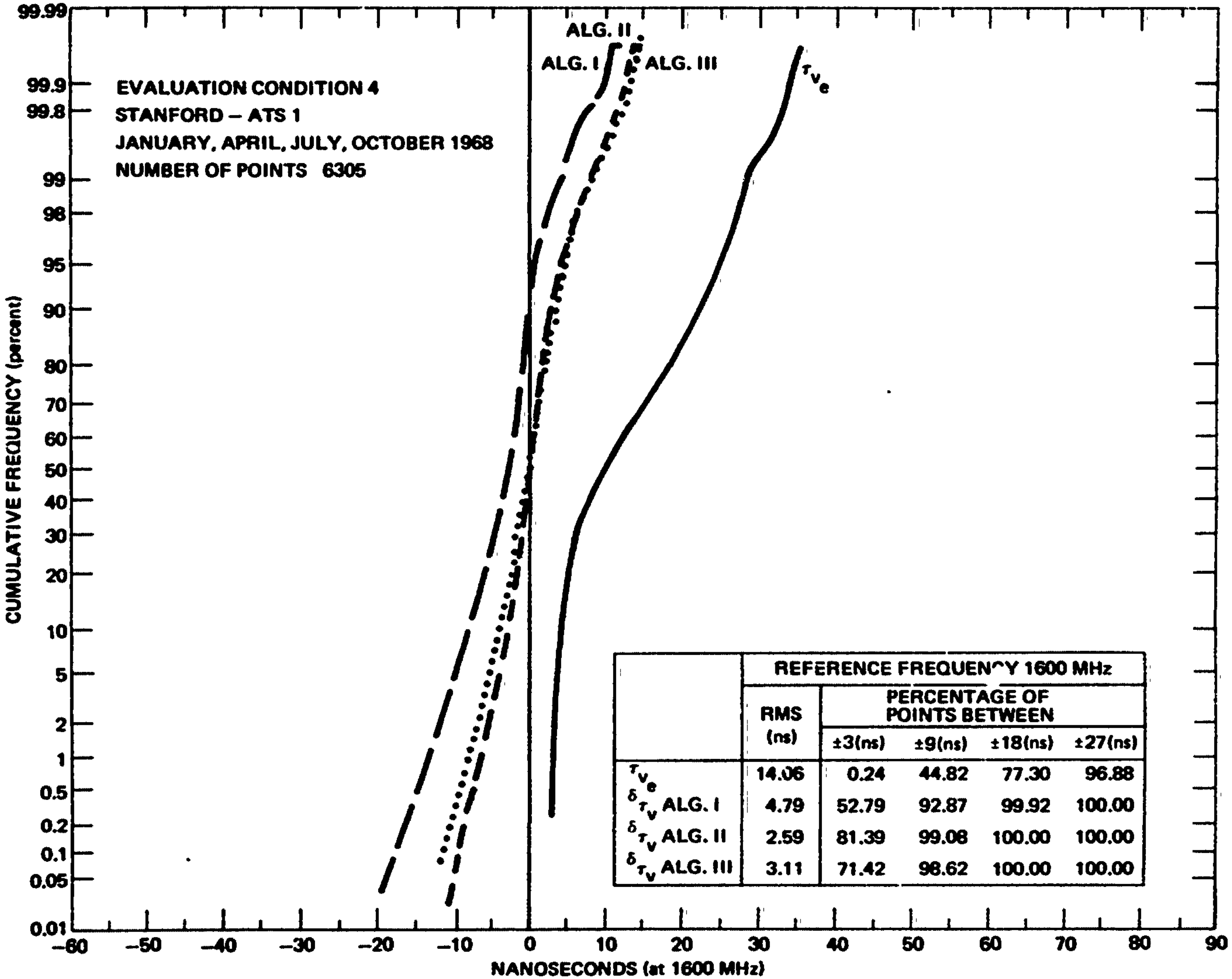

	REFERENCE FREQUEN^Y 1600 MHz				
	RMS (ns)	PERCENTAGE OF POINTS BETWEEN			
		±3(ns)	±9(ns)	±18(ns)	±27(ns)
τ_{v_e}	14.06	0.24	44.82	77.30	96.88
δ_{τ_v} ALG. I	4.79	52.79	92.87	99.92	100.00
δ_{τ_v} ALG. II	2.59	81.39	99.08	100.00	100.00
δ_{τ_v} ALG. III	3.11	71.42	98.62	100.00	100.00

Fig. C.17 VERTICAL TIME DELAY AND RESIDUALS–CUMULATIVE FREQUENCY DISTRIBUTION

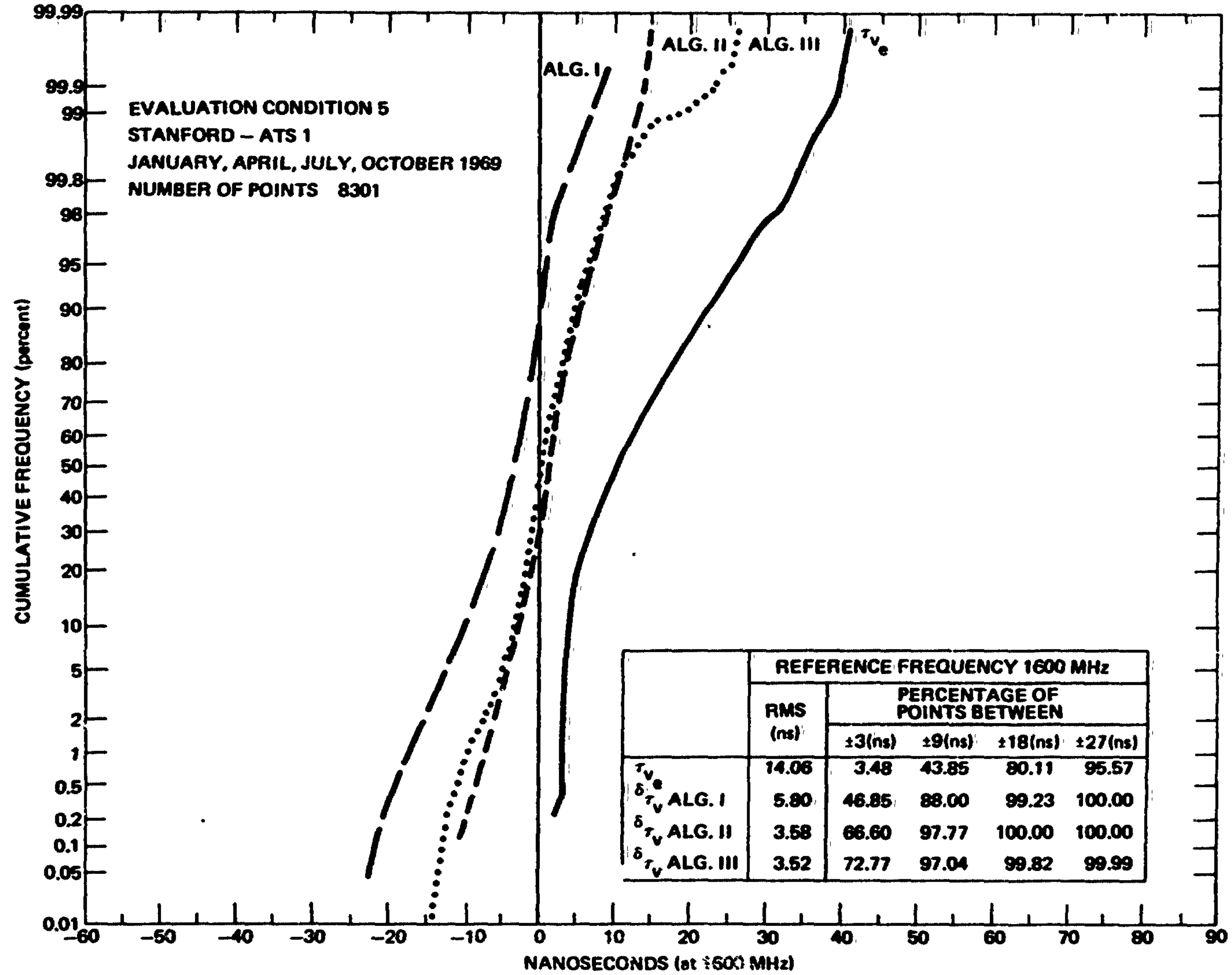

	REFERENCE FREQUENCY 1600 MHz				
	RMS (ns)	PERCENTAGE OF POINTS BETWEEN			
		±3(ns)	±9(ns)	±18(ns)	±27(ns)
τ_{v_e}	14.06	3.48	43.85	80.11	95.57
δ_{τ_v} ALG. I	5.80	46.85	88.00	99.23	100.00
δ_{τ_v} ALG. II	3.58	66.60	97.77	100.00	100.00
δ_{τ_v} ALG. III	3.52	72.77	97.04	99.82	99.99

Fig. C.18 VERTICAL TIME DELAY AND RESIDUALS–CUMULATIVE FREQUENCY DISTRIBUTION

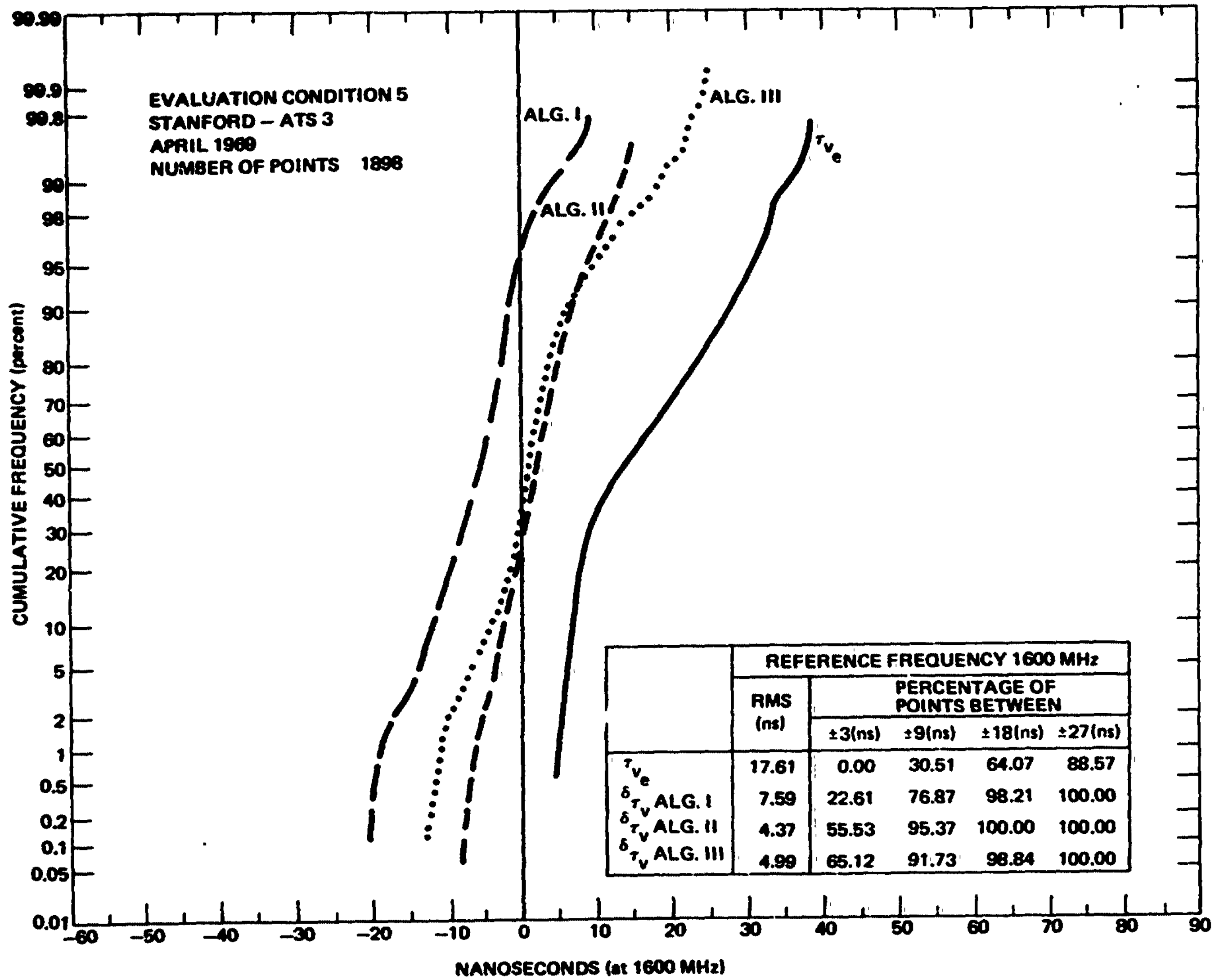

	REFERENCE FREQUENCY 1600 MHz				
	RMS (ns)	PERCENTAGE OF POINTS BETWEEN			
		±3(ns)	±9(ns)	±18(ns)	±27(ns)
τ_{v_e}	17.61	0.00	30.51	64.07	88.57
δ_{τ_v} ALG. I	7.59	22.61	76.87	98.21	100.00
δ_{τ_v} ALG. II	4.37	55.53	95.37	100.00	100.00
δ_{τ_v} ALG. III	4.99	65.12	91.73	98.84	100.00

Fig. C.19 VERTICAL TIME DELAY AND RESIDUALS–CUMULATIVE FREQUENCY DISTRIBUTION

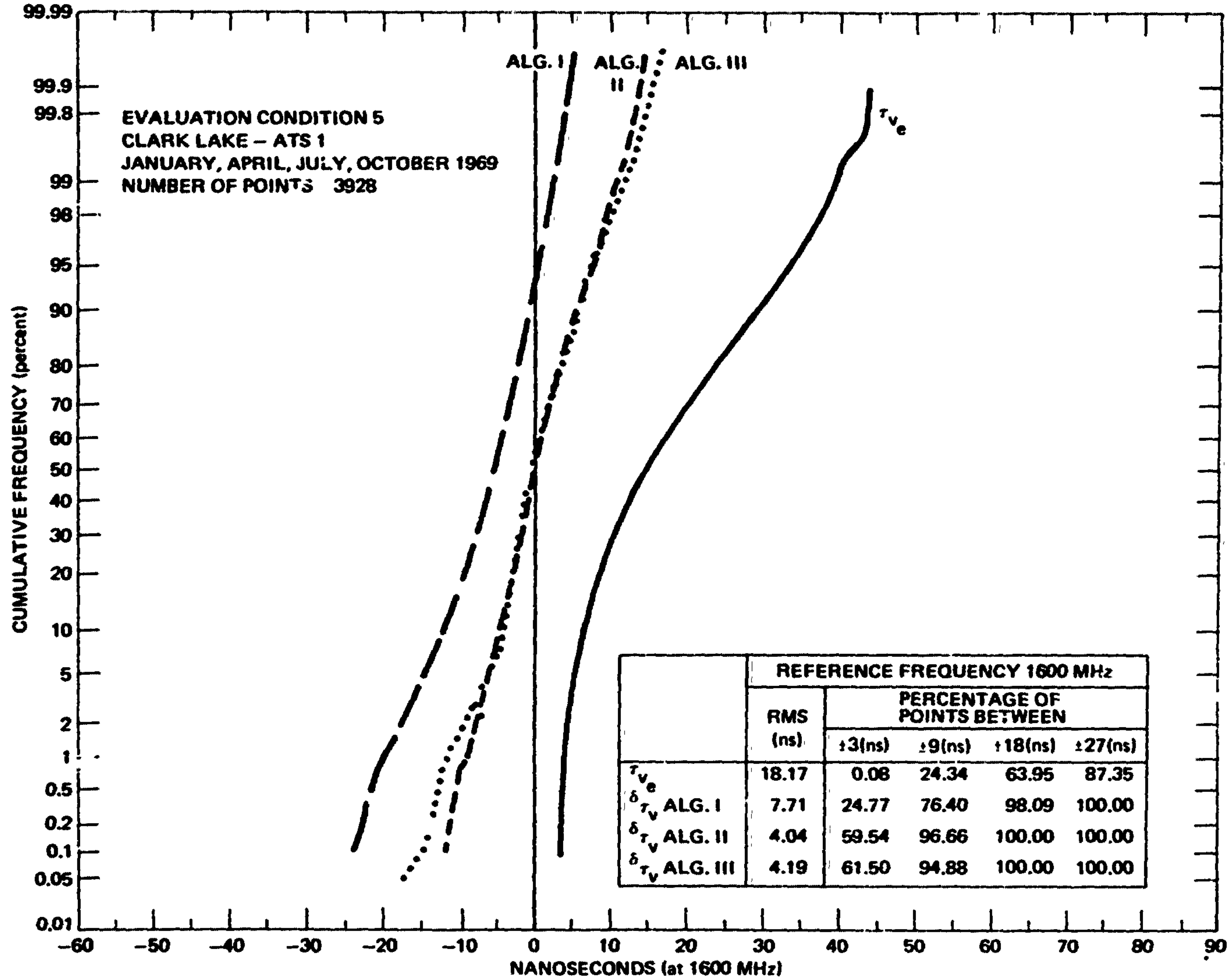

	RMS (ns)	±3(ns)	±9(ns)	±18(ns)	±27(ns)
	REFERENCE FREQUENCY 1600 MHz				
		PERCENTAGE OF POINTS BETWEEN			
τ_{v_e}	18.17	0.08	24.34	63.95	87.35
δ_{τ_v} ALG. I	7.71	24.77	76.40	98.09	100.00
δ_{τ_v} ALG. II	4.04	59.54	96.66	100.00	100.00
δ_{τ_v} ALG. III	4.19	61.50	94.88	100.00	100.00

Fig. C.20 VERTICAL TIME DELAY AND RESIDUALS–CUMULATIVE FREQUENCY DISTRIBUTION

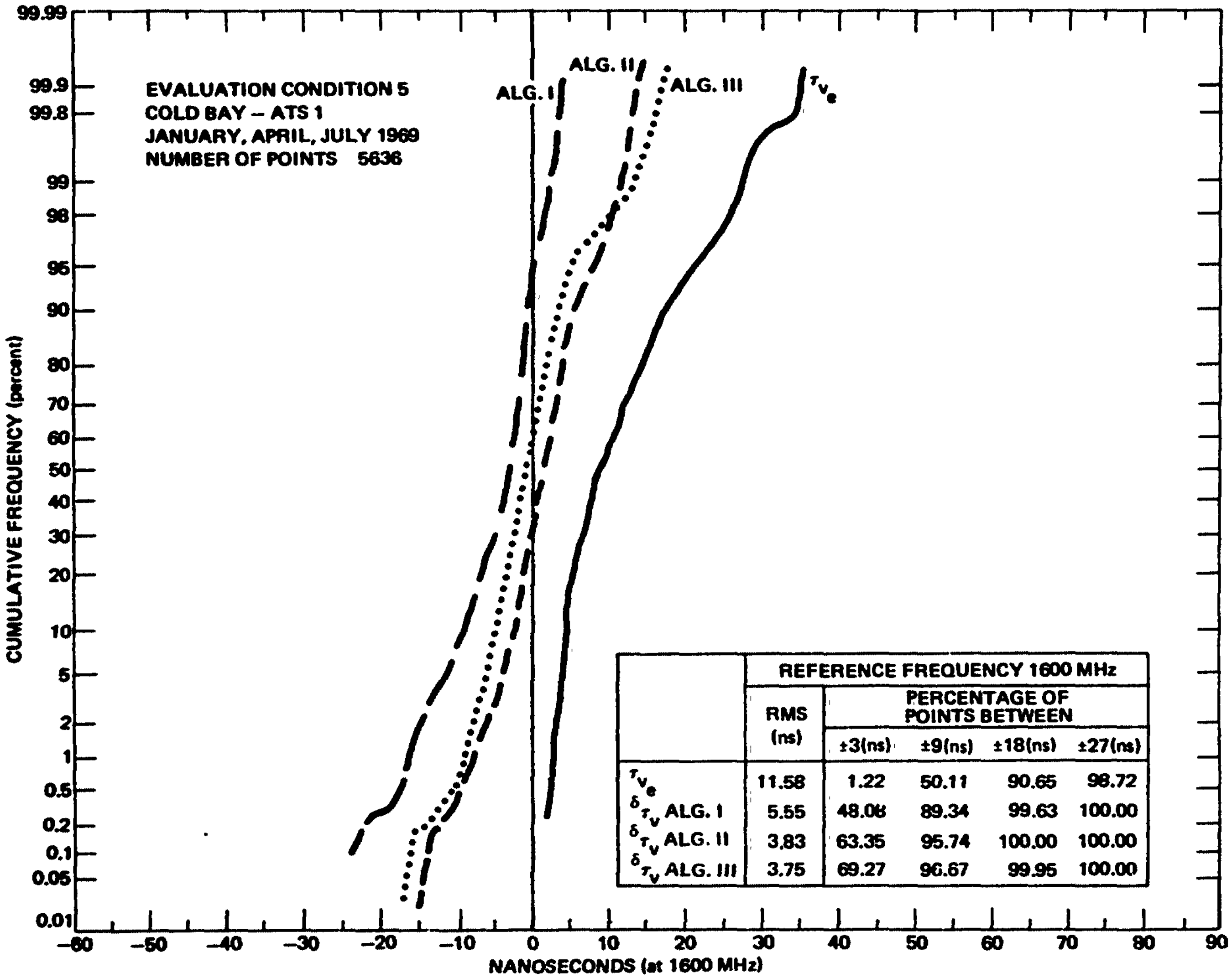

	REFERENCE FREQUENCY 1600 MHz				
	RMS (ns)	PERCENTAGE OF POINTS BETWEEN			
		±3(ns)	±9(ns)	±18(ns)	±27(ns)
τ_{v_e}	11.58	1.22	50.11	90.65	98.72
δ_{τ_v} ALG. I	5.55	48.08	89.34	99.63	100.00
δ_{τ_v} ALG. II	3.83	63.35	95.74	100.00	100.00
δ_{τ_v} ALG. III	3.75	69.27	96.67	99.95	100.00

Fig. C.21 VERTICAL TIME DELAY AND RESIDUALS–CUMULATIVE FREQUENCY DISTRIBUTION

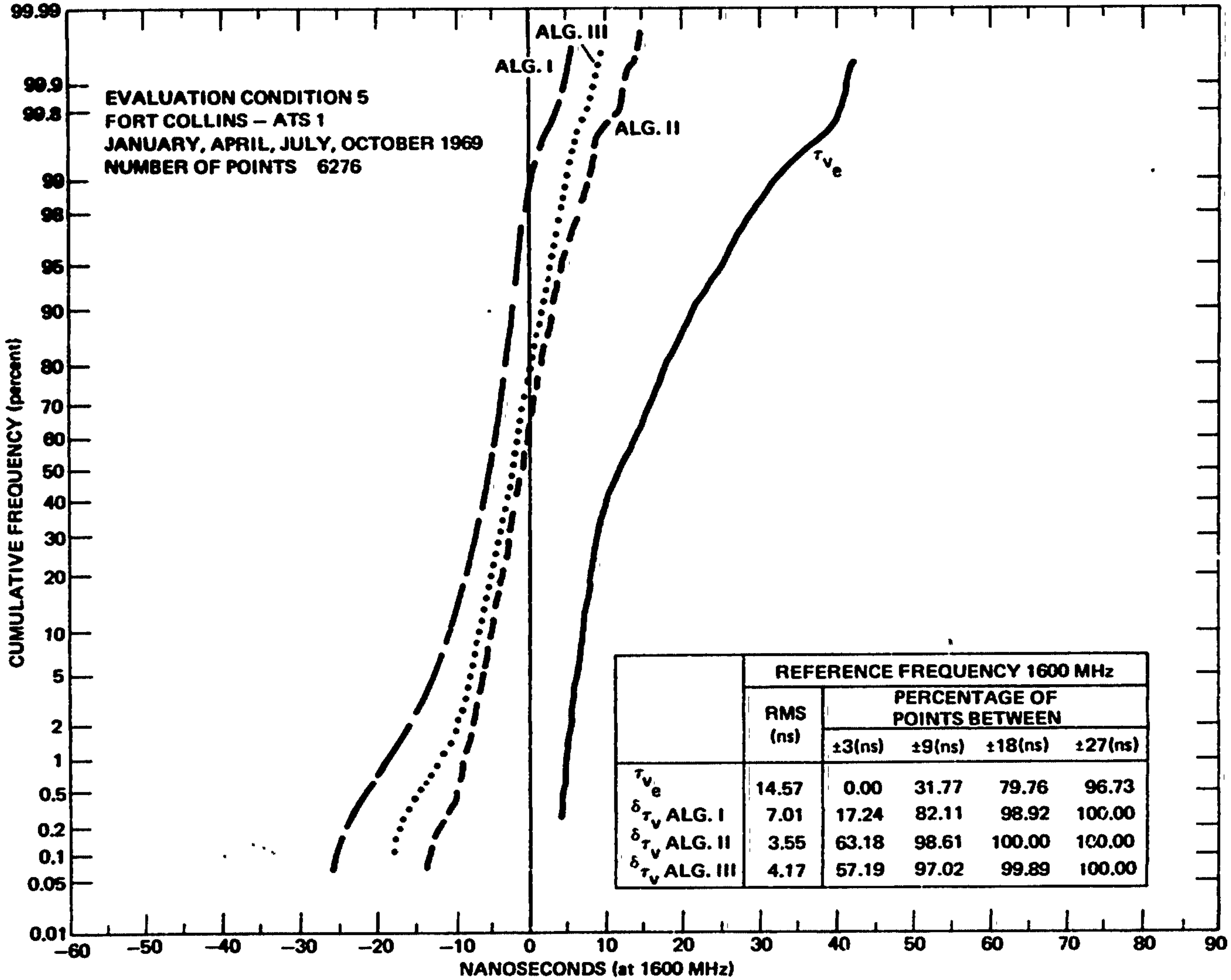

	REFERENCE FREQUENCY 1600 MHz				
	RMS (ns)	PERCENTAGE OF POINTS BETWEEN			
		±3(ns)	±9(ns)	±18(ns)	±27(ns)
τ_{v_e}	14.57	0.00	31.77	79.76	96.73
δ_{τ_v} ALG. I	7.01	17.24	82.11	98.92	100.00
δ_{τ_v} ALG. II	3.55	63.18	98.61	100.00	100.00
δ_{τ_v} ALG. III	4.17	57.19	97.02	99.89	100.00

Fig. C.22 VERTICAL TIME DELAY AND RESIDUALS–CUMULATIVE FREQUENCY DISTRIBUTION

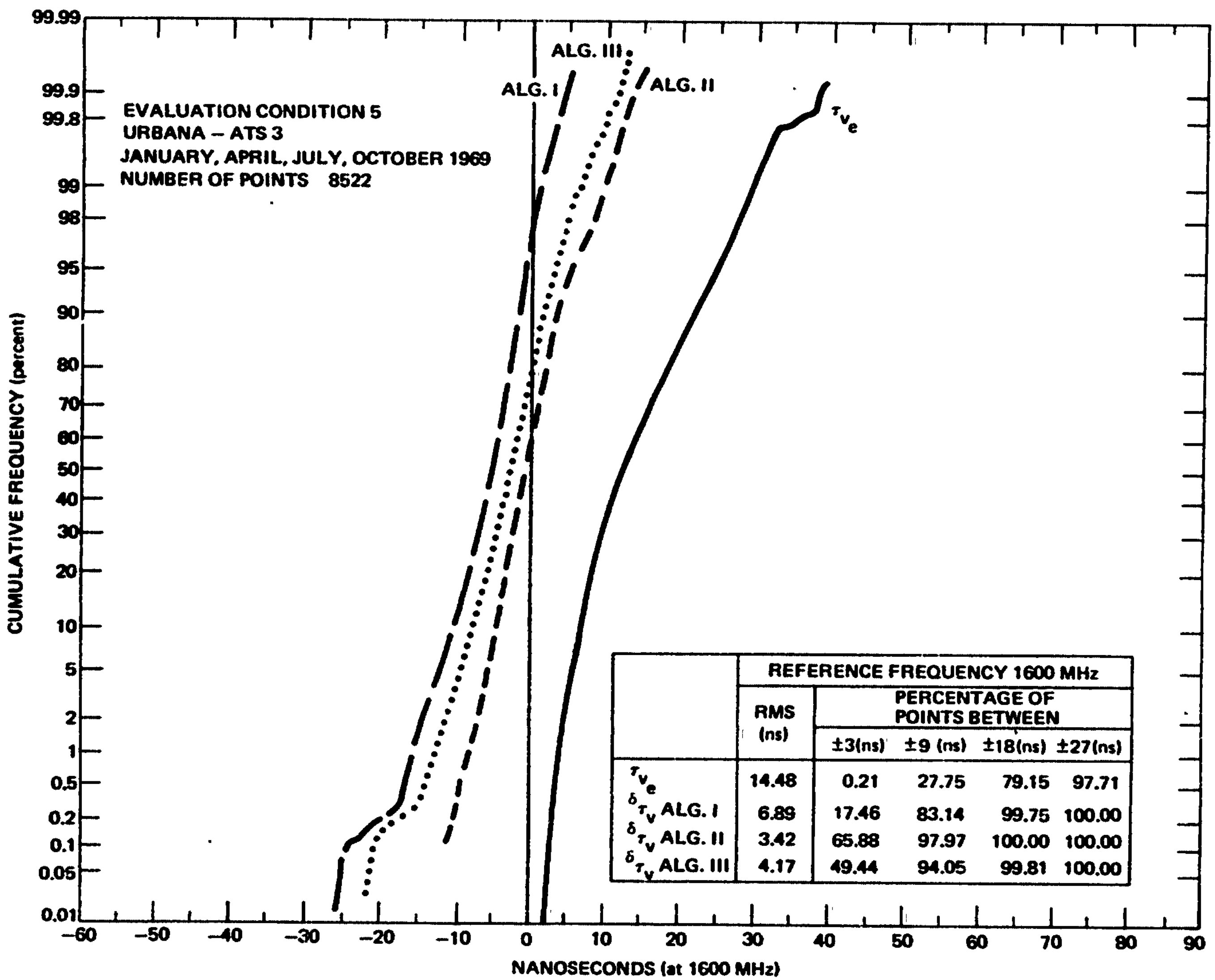

	REFERENCE FREQUENCY 1600 MHz				
	RMS (ns)	PERCENTAGE OF POINTS BETWEEN			
		±3(ns)	±9 (ns)	±18(ns)	±27(ns)
τ_{v_e}	14.48	0.21	27.75	79.15	97.71
δ_{τ_v} ALG. I	6.89	17.46	83.14	99.75	100.00
δ_{τ_v} ALG. II	3.42	65.88	97.97	100.00	100.00
δ_{τ_v} ALG. III	4.17	49.44	94.05	99.81	100.00

Fig. C.23 VERTICAL TIME DELAY AND RESIDUALS–CUMULATIVE FREQUENCY DISTRIBUTION

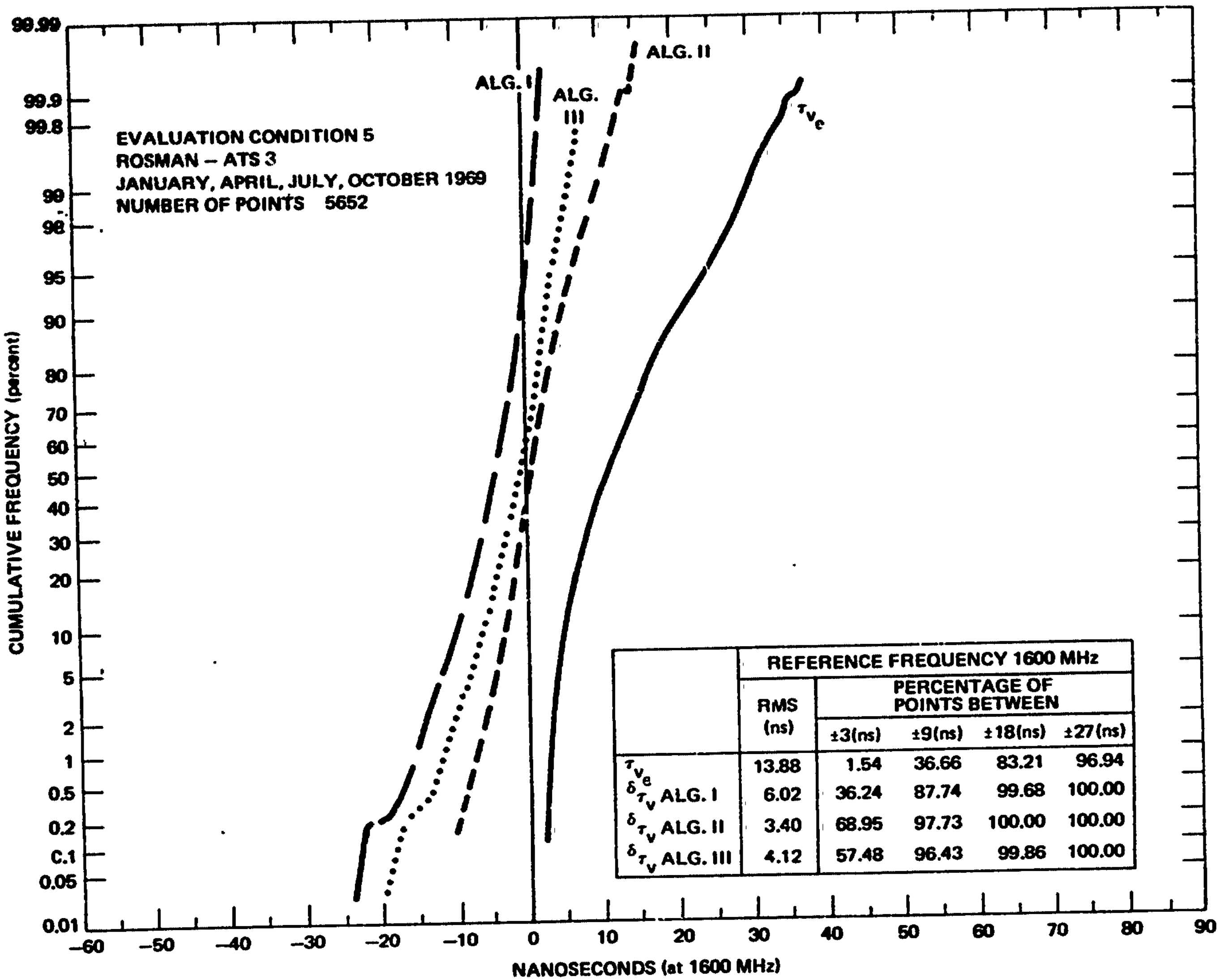

	REFERENCE FREQUENCY 1600 MHz				
	RMS (ns)	PERCENTAGE OF POINTS BETWEEN			
		±3(ns)	±9(ns)	±18(ns)	±27(ns)
τ_{v_e}	13.88	1.54	36.66	83.21	96.94
δ_{τ_v} ALG. I	6.02	36.24	87.74	99.68	100.00
δ_{τ_v} ALG. II	3.40	68.95	97.73	100.00	100.00
δ_{τ_v} ALG. III	4.12	57.48	96.43	99.86	100.00

Fig. C.24 VERTICAL TIME DELAY AND RESIDUALS–CUMULATIVE FREQUENCY DISTRIBUTION

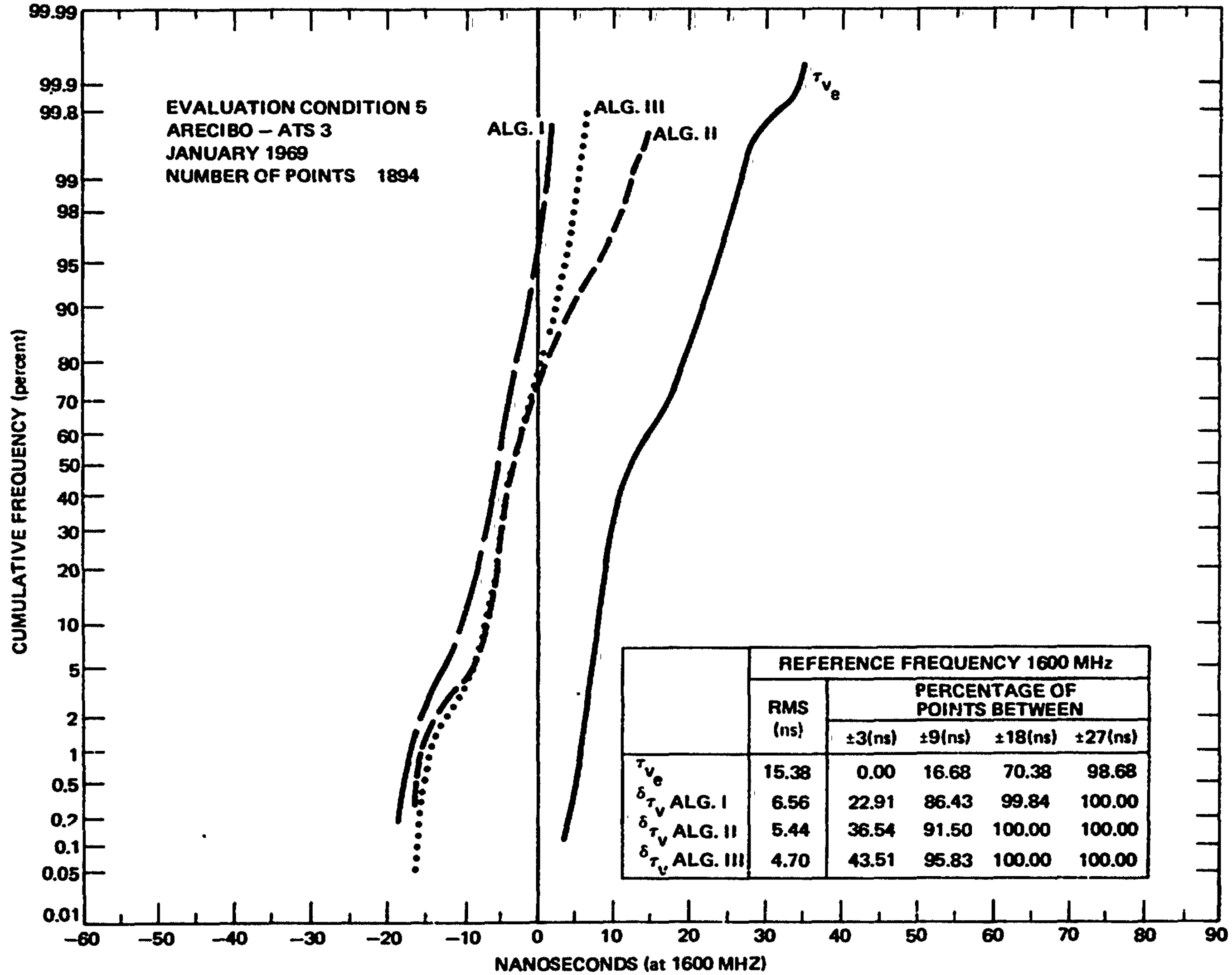

	RMS (ns)	PERCENTAGE OF POINTS BETWEEN (REFERENCE FREQUENCY 1600 MHz)			
		±3(ns)	±9(ns)	±18(ns)	±27(ns)
τ_{v_e}	15.38	0.00	16.68	70.38	98.68
δ_{τ_v} ALG. I	6.56	22.91	86.43	99.84	100.00
δ_{τ_v} ALG. II	5.44	36.54	91.50	100.00	100.00
δ_{τ_v} ALG. III	4.70	43.51	95.83	100.00	100.00

Fig. C.25 VERTICAL TIME DELAY AND RESIDUALS–CUMULATIVE FREQUENCY DISTRIBUTION

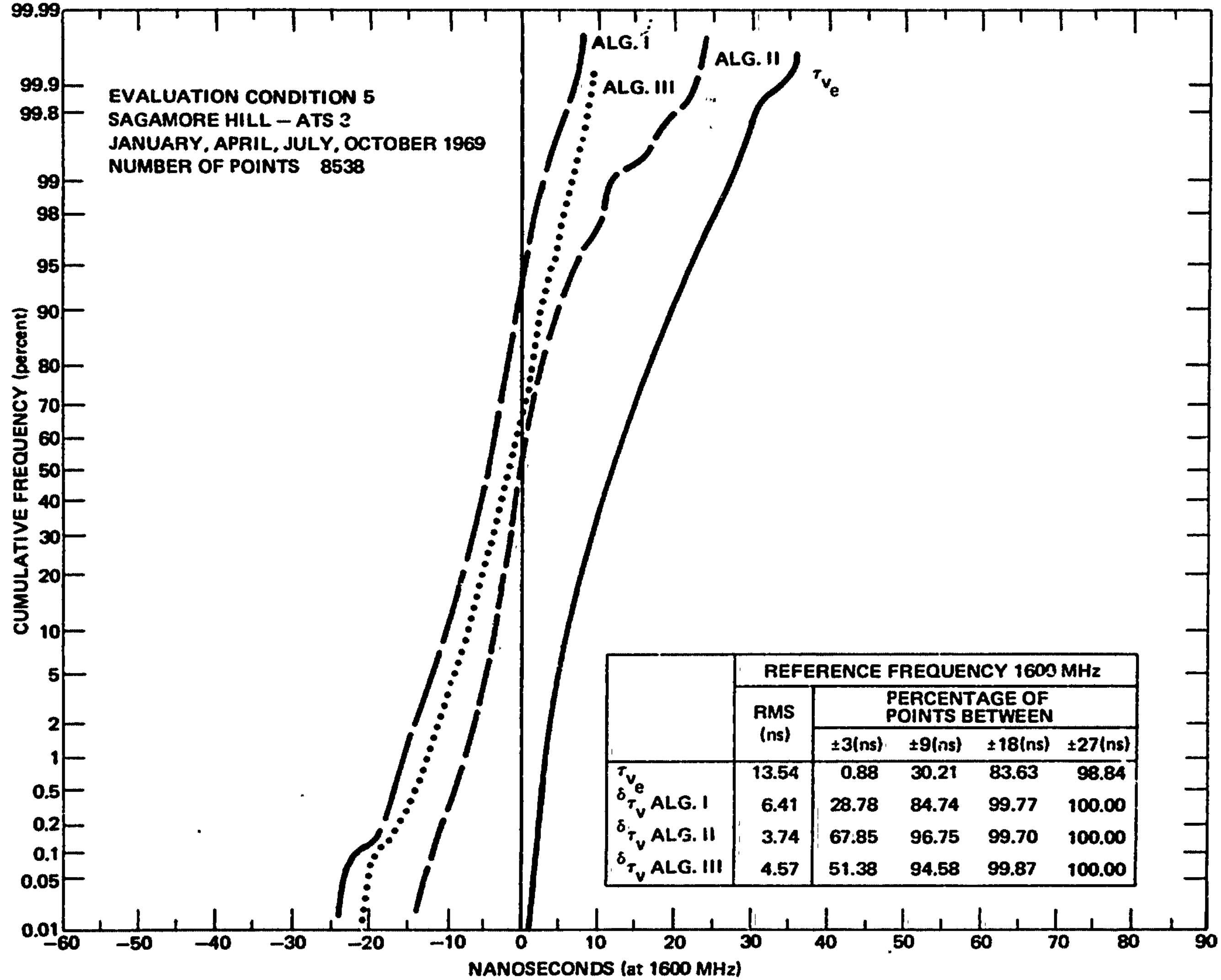

	RMS (ns)	PERCENTAGE OF POINTS BETWEEN ±3(ns)	±9(ns)	±18(ns)	±27(ns)
REFERENCE FREQUENCY 1600 MHz					
τ_{v_e}	13.54	0.88	30.21	83.63	98.84
$\delta\tau_v$ ALG. I	6.41	28.78	84.74	99.77	100.00
$\delta\tau_v$ ALG. II	3.74	67.85	96.75	99.70	100.00
$\delta\tau_v$ ALG. III	4.57	51.38	94.58	99.87	100.00

Fig. C.26 VERTICAL TIME DELAY AND RESIDUALS–CUMULATIVE FREQUENCY DISTRIBUTION

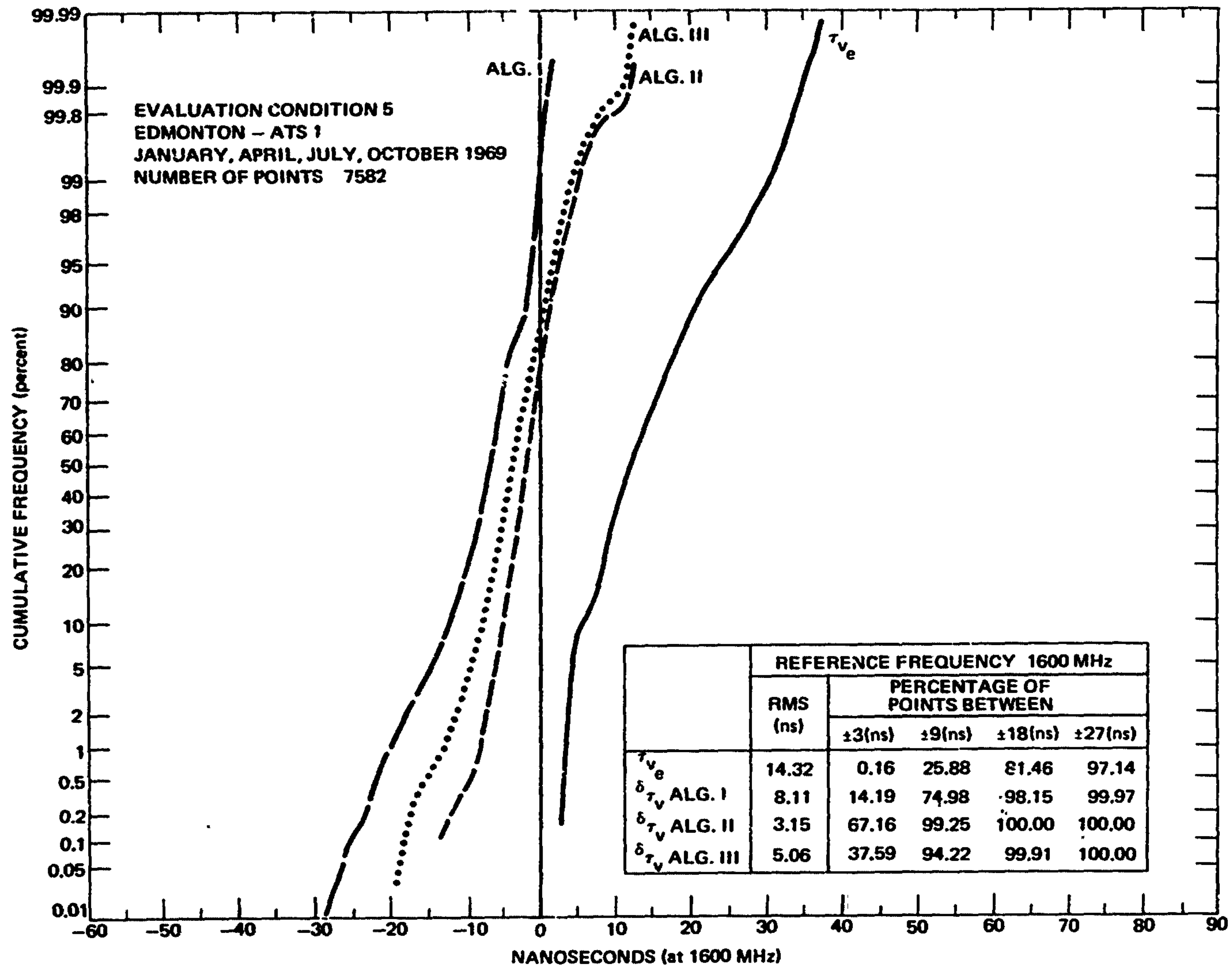

	RMS (ns)	PERCENTAGE OF POINTS BETWEEN ±3(ns)	±9(ns)	±18(ns)	±27(ns)
REFERENCE FREQUENCY 1600 MHz					
τ_{v_e}	14.32	0.16	25.88	81.46	97.14
δ_{τ_v} ALG. I	8.11	14.19	74.98	98.15	99.97
δ_{τ_v} ALG. II	3.15	67.16	99.25	100.00	100.00
δ_{τ_v} ALG. III	5.06	37.59	94.22	99.91	100.00

Fig. C.27 VERTICAL TIME DELAY AND RESIDUALS–CUMULATIVE FREQUENCY DISTRIBUTION

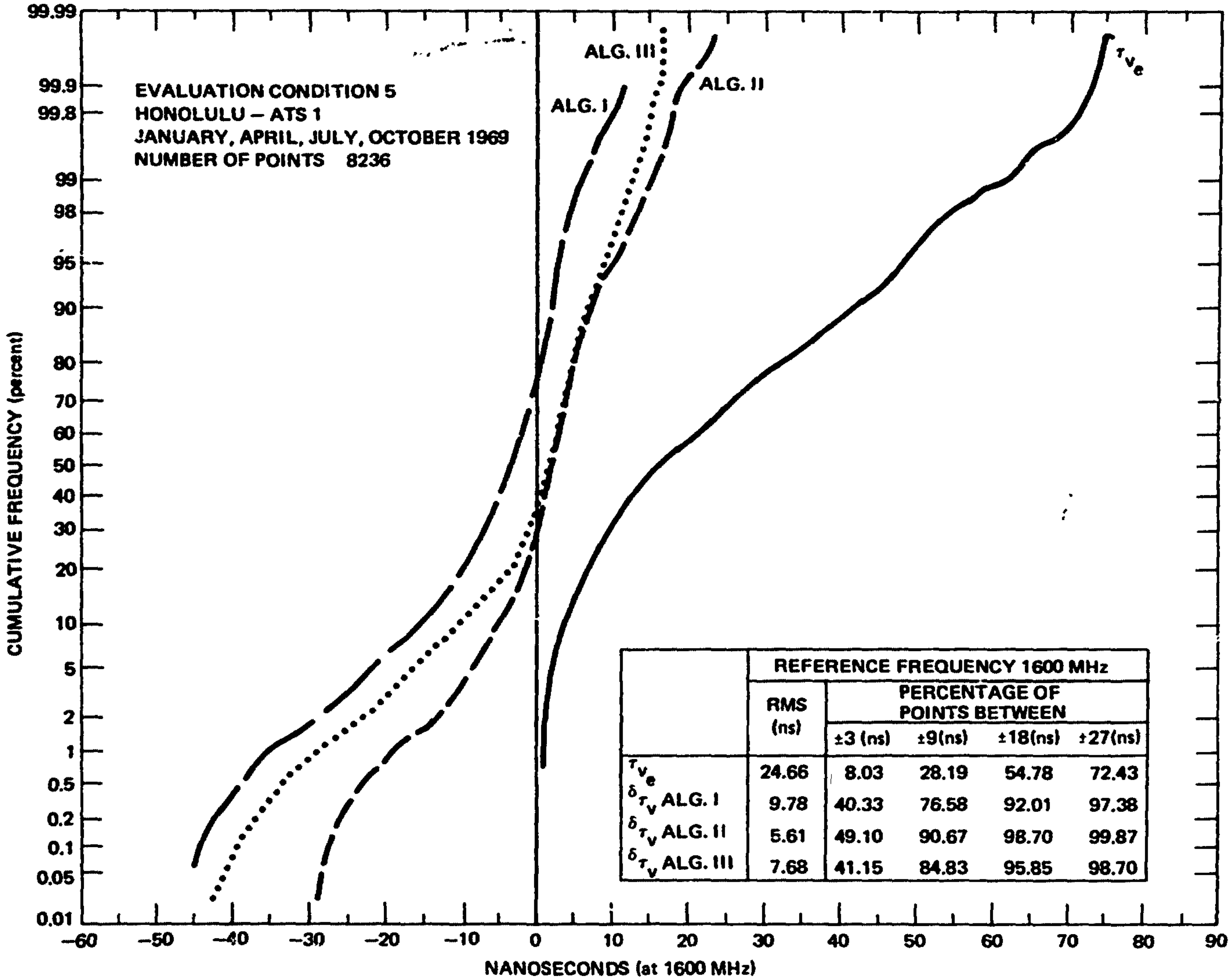

	REFERENCE FREQUENCY 1600 MHz				
	RMS (ns)	PERCENTAGE OF POINTS BETWEEN			
		±3 (ns)	±9(ns)	±18(ns)	±27(ns)
τ_{v_e}	24.66	8.03	28.19	54.78	72.43
$\delta\tau_v$ ALG. I	9.78	40.33	76.58	92.01	97.38
$\delta\tau_v$ ALG. II	5.61	49.10	90.67	98.70	99.87
$\delta\tau_v$ ALG. III	7.68	41.15	84.83	95.85	98.70

Fig. C.28 VERTICAL TIME DELAY AND RESIDUALS–CUMULATIVE FREQUENCY DISTRIBUTION

APPENDIX D

TABLES OF CORRELATION COEFFICIENTS OF VERTICAL TIME DELAY — HOURLY VALUES OBTAINED OVER A MONTH

TABLE D.1

Correlation Coefficients of Vertical Time Delay Residuals

Evaluation Condition 1

January 1968

Correlation Pair: Stanford ATS1 - Stanford ATS3

UT Hour Interval	$\delta\tau_v$ Alg. I	$\delta\tau_v$ Alg. II	$\delta\tau_v$ Alg. III	Number of Residual Pairs
[0, 1)	0.88529	0.98449	0.92406	71
[1, 2)	0.95480	0.98271	0.95806	74
[2, 3)	0.96240	0.98417	0.95277	74
[3, 4)	0.95407	0.98192	0.96210	75
[4, 5)	0.89589	0.97265	0.96460	75
[5, 6)	0.87765	0.97985	0.98054	75
[6, 7)	0.86595	0.97945	0.95146	75
[7, 8)	0.80537	0.97218	0.97618	76
[8, 9)	0.80144	0.96738	0.98144	74
[9,10)	0.76886	0.93321	0.86092	72
[10,11)	0.78534	0.95397	0.87352	75
[11,12)	0.72677	0.92667	0.84524	73
[12,13)	0.72629	0.93257	0.81735	75
[13,14)	0.77943	0.95763	0.89214	70
[14,15)	0.69843	0.89836	0.94677	68
[15,16)	0.93526	0.71108	0.94870	73
[16,17)	0.82363	0.91706	0.93856	78
[17,18)	0.87617	0.88189	0.94329	79
[18,19)	0.93872	0.90328	0.93867	78
[19,20)	0.95681	0.95852	0.96204	81
[20,21)	0.93210	0.95542	0.92947	79
[21,22)	0.90339	0.94098	0.92312	77
[22,23)	0.97370	0.95569	0.90037	76
[23,24)	0.79833	0.95701	0.90859	70

Nominal Value in Degrees for Month

	Stanford ATS1	Stanford ATS3
Elevation	37.5	38.0
Azimuth	221.5	139.5
Eff. Latitude	34.6	34.6
Eff. Longitude	234.8	240.7

TABLE D.2

Correlation Coefficients of Vertical Time Delay Residuals

Evaluation Condition 1

January 1968

Correlation Pair: Stanford ATS3 - Urbana ATS3

UT Hour Interval	$\delta\tau_v$ Alg. I	$\delta\tau_v$ Alg. II	$\delta\tau_v$ Alg. III	Number of Residual Pairs
[0, 1)	0.55786	0.86797	0.71087	67
[1, 2)	0.65277	0.83296	0.88188	67
[2, 3)	0.86183	0.88260	0.93690	70
[3, 4)	0.76562	0.85510	0.90914	72
[4, 5)	0.71567	0.83159	0.88165	72
[5, 6)	0.77158	0.84777	0.82262	69
[6, 7)	0.64089	0.87519	0.68178	70
[7, 8)	0.64631	0.90355	0.68050	72
[8, 9)	0.54572	0.86289	0.57142	69
[9,10)	0.35266	0.66151	0.33737	70
[10,11)	0.10366	0.61164	0.27891	70
[11,12)	0.06496	0.60554	0.29182	67
[12,13)	0.40377	0.84770	0.61265	71
[13,14)	-0.03113	0.33983	0.52458	71
[14,15)	0.34020	0.17991	0.41851	62
[15,16)	0.14085	0.17923	0.19539	65
[16,17)	0.51958	0.67566	0.44974	74
[17,18)	0.70404	0.70394	0.77694	74
[18,19)	0.79030	0.80406	0.77092	69
[19,20)	0.70982	0.81915	0.68069	66
[20,21)	0.70357	0.85755	0.57941	65
[21,22)	0.52066	0.87521	0.45197	67
[22,23)	0.53987	0.89979	0.40737	72
[23,24)	0.53429	0.86105	0.46574	73

Nominal Value in Degrees for Month

	Stanford ATS3	Urbana ATS3
Elevation	38.0	43.2
Azimuth	139.5	190.2
Eff. Latitude	34.6	37.0
Eff. Longitude	240.7	271.1

TABLE D.3

Correlation Coefficients of Vertical Time Delay Residuals

Evaluation Condition 1

January 1968

Correlation Pair: Urbana ATS3 - Sagamore Hill ATS3

UT Hour Interval	$\delta\tau_v$ Alg. I	$\delta\tau_v$ Alg. II	$\delta\tau_v$ Alg. III	Number of Residual Pairs
[0, 1)	0.74112	0.89590	0.73224	71
[1, 2)	0.85433	0.91970	0.90762	68
[2, 3)	0.90341	0.93597	0.93846	72
[3, 4)	0.89478	0.93069	0.92910	72
[4, 5)	0.93672	0.95397	0.95230	72
[5, 6)	0.89572	0.92717	0.93255	72
[6, 7)	0.87370	0.91917	0.86619	72
[7, 8)	0.84925	0.89935	0.81938	72
[8, 9)	0.80731	0.88079	0.75036	72
[9,10)	0.82023	0.75601	0.70517	72
[10,11)	0.61087	0.64939	0.43932	72
[11,12)	0.55762	0.74448	0.53729	72
[12,13)	0.24660	0.49711	0.56745	72
[13,14)	0.64433	0.61122	0.64512	72
[14,15)	0.70254	0.59184	0.60915	69
[15,16)	0.85907	0.54366	0.80950	69
[16,17)	0.77290	0.72017	0.65185	69
[17,18)	0.82833	0.90542	0.91546	65
[18,19)	0.95107	0.93390	0.96026	62
[19,20)	0.94842	0.94357	0.95074	61
[20,21)	0.89211	0.93161	0.85594	60
[21,22)	0.94354	0.96518	0.92004	52
[22,23)	0.82776	0.90359	0.76913	66
[23,24)	0.81430	0.88323	0.74110	68

Nominal Value in Degrees for Month

	Urbana ATS3	Sagamore Hill ATS3
Elevation	43.2	25.1
Azimuth	190.2	213.3
Eff. Latitude	37.0	39.2
Eff. Longitude	271.1	286.3

TABLE D.4

Correlation Coefficients of Vertical Time Delay Residuals

Evaluation Condition 1

February 1968

Correlation Pair: Stanford ATS3 - Stanford ATS1

UT Hour Interval	$\delta\tau_v$ Alg. I	$\delta\tau_v$ Alg. II	$\delta\tau_v$ Alg. III	Number of Residual Pairs
[0, 1)	0.96[illegible]58	0.97313	0.95545	79
[1, 2)	0.96836	0.97008	0.96969	83
[2, 3)	0.96857	0.96582	0.97241	82
[3, 4)	0.92948	0.94240	0.93999	81
[4, 5)	0.87526	0.91880	0.92449	73
[5, 6)	0.90816	0.90899	0.92774	70
[6, 7)	0.85046	0.93139	0.90563	65
[7, 8)	0.72016	0.93108	0.84691	69
[8, 9)	0.72973	0.94888	0.85136	70
[9,10)	0.73302	0.94358	0.86162	63
[10,11)	0.49536	0.92223	0.76909	64
[11,12)	0.40497	0.91648	0.76000	69
[12,13)	0.34736	0.90466	0.63961	62
[13,14)	0.33182	0.91083	0.63075	71
[14,15)	0.33900	0.73517	0.63841	75
[15,16)	0.77647	0.88552	0.84054	76
[16,17)	0.73250	0.87305	0.88532	81
[17,18)	0.87449	0.90904	0.91703	84
[18,19)	0.90037	0.86164	0.89251	79
[19,20)	0.91822	0.88279	0.91065	79
[20,21)	0.[illegible]	0.85913	0.84272	73
[21,22)	0.86477	0.88776	0.91484	76
[22,23)	0.8[illegible]	0.92430	0.9[illegible]263	76
[23,24)	[illegible]	0.92574	0.94522	76

Nominal Value in Degrees for Month

	Stanford ATS3	Stanford ATS1
Elevation	32.6	37.6
Azimuth	129.7	221.3
Eff. Latitude	34.5	34.6
Eff. Longitude	241.9	234.8

TABLE D.5

Correlation Coefficients of Vertical Time Delay Residuals

Evaluation Condition 1

February 1968

Correlation Pair: Stanford ATS3 - Urbana ATS3

UT Hour Interval	$\delta\tau_v$ Alg. I	$\delta\tau_v$ Alg. II	$\delta\tau_v$ Alg. III	Number of Residual Pairs
[0, 1)	0.87531	0.85148	0.82030	80
[1, 2)	0.89421	0.72649	0.78133	83
[2, 3)	0.88523	0.79827	0.78597	82
[3, 4)	0.87914	0.80050	0.71296	82
[4, 5)	0.85756	0.85092	0.72660	76
[5, 6)	0.81725	0.79147	0.71872	69
[6, 7)	0.76339	0.77482	0.73812	63
[7, 8)	0.67951	0.78631	0.66769	64
[8, 9)	0.59814	0.82519	0.65830	69
[9,10)	0.34512	0.68677	0.46111	66
[10,11)	0.12796	0.74640	0.43806	62
[11,12)	0.35764	0.91821	0.43757	66
[12,13)	0.29498	0.39518	0.52261	61
[13,14)	0.25711	0.17982	0.58242	67
[14,15)	0.44933	0.49872	0.54812	67
[15,16)	0.67994	0.73252	0.7111[illegible]	70
[16,17)	0.76463	0.78519	0.78[illegible]	79
[17,18)	0.61597	0.83573	0.77695	81
[18,19)	0.49061	0.82714	0.87595	80
[19,20)	0.45661	0.71547	0.81901	78
[20,21)	0.50630	0.69899	0.75418	71
[21,22)	0.73899	0.77070	0.71925	75
[22,23)	0.89211	0.87957	0.80065	76
[23,24)	0.86544	0.87511	0.79331	77

Nominal Value in Degrees for Month

	Stanford ATS3	Urbana ATS3
Elevation	32.6	43.6
Azimuth	129.7	176.5
Eff. Latitude	34.5	37.0
Eff. Longitude	241.9	272.0

TABLE D.6

Correlation Coefficients of Vertical Time Delay Residuals

Evaluation Condition 1

February 1968

Correlation Pair: Urbana ATS3 - Sagamore Hill ATS3

UT Hour Interval	$\delta\tau_v$ Alg. I	$\delta\tau_v$ Alg. II	$\delta\tau_v$ Alg. III	Number of Residual Pairs
[0, 1)	0.81611	0.71212	0.73514	75
[1, 2)	0.79111	0.75552	0.74649	75
[2, 3)	0.75950	0.72725	0.70083	75
[3, 4)	0.78246	0.79169	0.74923	75
[4, 5)	0.64257	0.71771	0.59947	75
[5, 6)	0.51649	0.63639	0.50296	75
[6, 7)	0.42571	0.62081	0.46148	69
[7, 8)	0.35629	0.63620	0.35863	69
[8, 9)	0.42693	0.74061	0.42983	69
[9,10)	0.55726	0.76049	0.60057	69
[10,11)	0.45547	0.78503	0.55174	66
[11,12)	0.51033	0.65329	0.57669	69
[12,13)	0.64103	0.75238	0.53926	67
[13,14)	0.73153	0.83229	0.55411	66
[14,15)	0.82596	0.82870	0.70165	66
[15,16)	0.79942	0.74112	0.73354	69
[16,17)	0.79446	0.69295	0.75561	72
[17,18)	0.80223	0.66380	0.78254	72
[18,19)	0.84693	0.69476	0.81510	75
[19,20)	0.88876	0.82118	0.86431	74
[20,21)	0.89527	0.87126	0.86538	72
[21,22)	0.88276	0.89008	0.83243	73
[22,23)	0.91393	0.87766	0.84839	72
[23,24)	0.89764	0.75374	0.84693	72

Nominal Value in Degrees for Month

	Urbana ATS3	Sagamore Hill ATS3
Elevation	43.6	38.4
Azimuth	176.5	201.8
Eff. Latitude	37.0	39.5
Eff. Longitude	272.0	287.4

TABLE D .7

Correlation Coefficients of Vertical Time Delay Residuals

Evaluation Condition 1

March 1968

Correlation Pair: Stanford ATS3 - Stanford ATS1

UT Hour Interval	$\delta\tau_v$ Alg. I	$\delta\tau_v$ Alg. II	$\delta\tau_v$ Alg. III	Number of Residual Pairs
[0, 1)	0.93808	0.98627	0.93199	80
[1, 2)	0.93861	0.98888	0.93192	79
[2, 3)	0.91785	0.98509	0.91525	78
[3, 4)	0.85795	0.96036	0.84358	77
[4, 5)	0.68041	0.93813	0.76336	73
[5, 6)	0.36975	0.93716	0.76447	72
[6, 7)	0.43615	0.93522	0.68318	69
[7, 8)	0.46895	0.94899	0.63481	65
[8, 9)	0.45484	0.95616	0.61644	66
[9,10)	0.38603	0.92551	0.58380	69
[10,11)	0.34561	0.92039	0.63247	61
[11,12)	0.28696	0.91891	0.60589	66
[12,13)	0.08208	0.88009	0.56105	66
[13,14)	0.14592	0.83217	0.62639	68
[14,15)	0.57837	0.42733	0.64183	76
[15,16)	0.72459	0.75371	0.71479	76
[16,17)	0.85578	0.86170	0.81981	78
[17,18)	0.89608	0.92416	0.89245	77
[18,19)	0.90069	0.93516	0.90127	76
[19,20)	0.87990	0.93627	0.89077	76
[20,21)	0.83275	0.90928	0.80494	77
[21,22)	0.91285	0.96289	0.91644	77
[22,23)	0.91656	0.96615	0.93184	80
[23,24)	0.90767	0.96756	0.93575	80

Nominal Value in Degrees for Month

	Stanford ATS3	Stanford ATS1
Elevation	31.3	37 7
Azimuth	127.8	221.2
Eff. Latitude	34.5	34.6
Eff. Longitude	242.2	234.8

TABLE D.8

Correlation Coefficients of Vertical Time Delay Residuals

Evaluation Condition 1

March 1968

Correlation Pair: Stanford ATS3 - Urbana ATS3

UT Hour Interval	$\delta\tau_v$ Alg. I	$\delta\tau_v$ Alg. II	$\delta\tau_v$ Alg. III	Number of Residual Pairs
[0, 1)	0.34541	0.89340	0.27344	48
[1, 2)	0.32413	0.81515	0.12522	53
[2, 3)	0.39000	0.73588	0.20349	54
[3, 4)	0.42578	0.77391	0.19053	54
[4, 5)	0.31085	0.82792	0.25890	50
[5, 6)	0.08059	0.84487	0.19811	49
[6, 7)	-0.07281	0.80044	0.11574	50
[7, 8)	-0.14806	0.83545	0.05310	46
[8, 9)	0.15078	0.88125	0.39304	52
[9,10)	0.22214	0.82848	0.60475	52
[10,11)	0.20092	0.85184	0.58462	50
[11,12)	-0.03879	0.59614	0.28925	52
[12,13)	-0.25293	-0.32500	0.03869	50
[13,14)	-0.19550	-0.13853	0.07129	51
[14,15)	0.23805	0.44943	0.16088	57
[15,16)	0.48169	0.62388	0.34929	60
[16,17)	0.54530	0.66374	0.40794	59
[17,18)	0.58787	0.71657	0.49628	60
[18,19)	0.60571	0.73901	0.39951	57
[19,20)	0.52549	0.76166	0.27781	50
[20,21)	0.60523	0.80216	0.32667	46
[21,22)	0.64394	0.85535	0.51842	48
[22,23)	0.64642	0.86292	0.54554	51
[23,24)	0.58190	0.87013	0.45529	50

Nominal Value in Degrees for Month

	Stanford ATS3	Urbana ATS3
Elevation	31.3	43.0
Azimuth	127.8	173.6
Eff. Latitude	34.5	37.0
Eff. Longitude	242.2	272.2

TABLE D.9

Correlation Coefficients of Vertical Time Delay Residuals

Evaluation Condition 1

March 1968

Correlation Pair: Urbana ATS3 - Sagamore Hill ATS3

UT Hour Interval	$\delta\tau_v$ Alg. I	$\delta\tau_v$ Alg. II	$\delta\tau_v$ Alg. III	Number of Residual Pairs
[0, 1)	0.78087	0.90723	0.83617	45
[1, 2)	0.78188	0.91531	0.85003	49
[2, 3)	0.65501	0.90782	0.70144	48
[3, 4)	0.56087	0.90128	0.54048	48
[4, 5)	0.52638	0.90165	0.50693	49
[5, 6)	0.51493	0.91094	0.52354	48
[6, 7)	0.38719	0.89076	0.40848	51
[7, 8)	0.39809	0.90595	0.39303	51
[8, 9)	0.38568	0.89671	0.37032	51
[9,10)	0.41275	0.85532	0.49713	51
[10,11)	0.54557	0.76788	0.62877	50
[11,12)	0.58506	0.45435	0.62760	48
[12,13)	0.47667	0.51753	0.05928	48
[13,14)	0.52780	0.24408	0.17061	50
[14,15)	0.51219	0.44047	0.51446	51
[15,16)	0.61349	0.54918	0.41867	54
[16,17)	0.62763	0.64603	0.42388	54
[17,18)	0.71454	0.77492	0.55330	54
[18,19)	0.74900	0.90289	0.55553	51
[19,20)	0.78557	0.94425	0.50890	46
[20,21)	0.75804	0.96156	0.44606	45
[21,22)	0.78299	0.97399	0.65645	45
[22,23)	0.80288	0.97033	0.67196	45
[23,24)	0.86388	0.95863	0.73588	45

Nominal Value in Degrees for Month

	Urbana ATS3	Sagamore Hill ATS3
Elevation	43.5	39.0
Azimuth	173.6	199.[illegible]
Eff. Latitude	37.0	39.3
Eff. Longitude	272.2	287.7

TABLE D.10

Correlation Coefficients of Vertical Time Delay Residuals

Evaluation Condition 2

January 1968

Correlation Pair: Stanford ATS3 - Stanford ATS1

UT Hour Interval	$\delta\tau_v$ Alg. I	$\delta\tau_v$ Alg. II	$\delta\tau_v$ Alg. III	Number of Residual Pairs
[0, 1)	0.88529	0.97550	0.90903	71
[1, 2)	0.95480	0.97442	0.94575	74
[2, 3)	0.96240	0.97558	0.93431	74
[3, 4)	0.95407	0.97317	0.94698	75
[4, 5)	0.89689	0.96613	0.95310	76
[5, 6)	0.87756	0.97536	0.97533	75
[6, 7)	0.86595	0.97118	0.94020	75
[7, 8)	0.80587	0.95775	0.87077	76
[8, 9)	0.80144	0.95463	0.86405	74
[9,10)	0.76886	0.93954	0.84809	72
[10,11)	0.78554	0.95918	0.86845	75
[11,12)	0.72877	0.93353	0.84109	73
[12,13)	0.72629	0.93454	0.79605	75
[13,14)	0.77943	0.96081	0.88382	70
[14,15)	0.69843	0.90599	0.82712	68
[15,16)	0.93626	0.64535	0.93644	73
[16,17)	0.82368	0.88096	0.92311	78
[17,18)	0.87617	0.86081	0.93663	79
[18,19)	0.93872	0.89224	0.93532	78
[19,20)	0.95691	0.95438	0.96043	81
[20,21)	0.93210	0.94930	0.92244	79
[21,22)	0.90339	0.92361	0.90316	77
[22,23)	0.87370	0.93965	0.87341	76
[23,24)	0.79838	0.93595	0.88411	70

Nominal Value in Degrees for Month

	Stanford ATS3	Stanford ATS1
Elevation	38.0	37.5
Azimuth	139.5	221.5
Eff. Latitude	34.6	34.6
Eff. Longitude	240.7	234.8

TABLE D.11

Correlation Coefficients of Vertical Time Delay Residuals

Evaluation Condition 2

February 1968

Correlation Pair: Stanford ATS3 - Stanford ATS1

UT Hour Interval	$\delta\tau_v$ Alg. I	$\delta\tau_v$ Alg. II	$\delta\tau_v$ Alg. III	Number of Residual Pairs
[0, 1)	0.96068	0.96361	0.94674	79
[1, 2)	0.96836	0.96001	0.95297	83
[2, 3)	0.96857	0.95519	0.96673	82
[3, 4)	0.92948	0.92533	0.92588	81
[4, 5)	0.87525	0.89082	0.90875	73
[5, 6)	0.90816	0.87648	0.92023	70
[6, 7)	0.85046	0.88929	0.69746	65
[7, 8)	0.72016	0.89096	0.8[illegible]358	69
[8, 9)	0.70978	0.92339	0.94725	70
[9,10)	0.73302	0.92184	0.95870	63
[10,11)	0.48536	0.89056	0.75153	64
[11,12)	0.40497	0.87998	0.74958	69
[12,13)	0.34786	0.87659	0.62266	62
[13,14)	0.33182	0.88621	0.61348	71
[14,15)	0.32990	0.67588	0.62267	75
[15,16)	0.77647	0.87595	0.63615	76
[16,17)	0.78250	0.85251	0.88078	81
[17,18)	0.87449	0.90132	0.91402	84
[18,19)	0.90087	0.84588	0.87262	79
[19,20)	0.91822	0.86913	0.89306	79
[20,21)	0.85950	0.85014	0.82645	73
[21,22)	0.85477	0.87297	0.89679	75
[22,23)	0.89367	0.90736	0.92648	76
[23,24)	0.90456	0.90736	0.9361[illegible]	76

Nominal Value in Degrees for Month

	Stanford ATS3	Stanford ATS1
Elevation	32.6	37.6
Azimuth	129.7	221.3
Eff. Latitude	34.5	34.6
Eff. Longitude	241.9	234.8

TABLE D.12

Correlation Coefficients of Vertical Time Delay Residuals

Evaluation Condition 2

March 1968

Correlation Pair: Stanford ATS3 - Stanford ATS1

UT Hour Interval	$\delta\tau_v$ Alg. I	$\delta\tau_v$ Alg. II	$\delta\tau_v$ Alg. III	Number of Residual Pairs
[0, 1)	0.95124	0.97658	0.94088	86
[1, 2)	0.94834	0.97794	0.93341	85
[2, 3)	0.92799	0.97351	0.91255	84
[3, 4)	0.87438	0.93670	0.84349	83
[4, 5)	0.69815	0.89519	0.73363	80
[5, 6)	0.38115	0.90269	0.76402	81
[6, 7)	0.44390	0.90635	0.72083	78
[7, 8)	0.47674	0.92500	0.68822	74
[8, 9)	0.48438	0.93449	0.68437	75
[9,10)	0.41334	0.89568	0.64845	78
[10,11)	0.37989	0.87633	0.67244	69
[11,12)	0.31999	0.87603	0.64514	74
[12,13)	0.13518	0.85345	0.59170	75
[13,14)	0.18711	0.78764	0.64396	76
[14,15)	0.59781	0.38356	0.64918	79
[15,16)	0.72325	0.79459	0.70998	85
[16,17)	0.85630	0.87005	0.81647	87
[17,18)	0.89971	0.91594	0.89641	86
[18,19)	0.91414	0.92453	0.91130	87
[19,20)	0.90261	0.91816	0.89405	85
[20,21)	0.86206	0.87443	0.82990	86
[21,22)	0.92654	0.94623	0.92478	86
[22,23)	0.92945	0.95089	0.93499	89
[23,24)	0.92605	0.95161	0.94257	89

Nominal Value in Degrees for Month

	Stanford ATS3	Stanford ATS1
Elevation	31.3	37.7
Azimuth	127.8	221.2
Eff. Latitude	34.5	34.6
Eff. Longitude	242.2	234.8

TABLE D.13

Correlation Coefficients of Vertical Time Delay Residuals

Evaluation Condition 5

January 1969

Correlation Pair: Stanford ATS1 - Clark Lake ATS1

UT Hour Interval	$\delta\tau_v$ Alg. I	$\delta\tau_v$ Alg. II	$\delta\tau_v$ Alg. III	Number of Residual Pairs
[0, 1)	0.95487	[illegible]	0.95383	14
[1, 2)	0.95721	0.82820	0.94168	15
[2, 3)	0.81897	0.51454	0.65292	15
[3, 4)	0.96544	0.91123	0.94047	15
[4, 5)	0.96208	0.71675	0.87132	15
[5, 6)	0.83233	0.79735	0.50697	15
[6, 7)	0.66185	0.57943	0.43250	15
[7, 8)	0.82399	0.60789	0.60146	12
[8, 9)	0.55161	0.57726	0.40511	18
[9,10)	0.66821	0.43017	0.50087	18
[10,11)	0.69098	0.51395	0.58258	18
[11,12)	0.69354	0.67553	0.59559	18
[12,13)	0.84145	0.91247	0.80513	18
[13,14)	0.93350	0.89441	0.85053	18
[14,15)	0.60107	0.72230	0.55218	18
[15,16)	0.80921	0.82739	0.67258	18
[16,17)	0.89755	0.63902	0.62549	16
[17,18)	0.93030	0.91110	0.81032	15
[18,19)	0.95069	0.95353	0.91373	14
[19,20)	0.96640	0.97562	0.95166	17
[20,21)	0.92216	0.87569	0.73085	18
[21,22)	0.81573	0.91754	0.64315	18
[22,23)	0.91236	0.93173	0.88471	16
[23,24)	0.96513	0.95817	0.95192	14

Nominal Value in Degrees for Month

	Stanford ATS1	Clark Lake ATS1
Elevation	37.7	37.3
Azimuth	221.1	230.3
Eff. Latitude	34.6	30.9
Eff. Longitude	234.8	240.1

TABLE D.14

Correlation Coefficients of Vertical Time Delay Residuals

Evaluation Condition 5

January 1969

Correlation Pair: Stanford ATS1 - Fort Collins ATS1

UT Hour Interval	$\delta\tau_v$ Alg. I	$\delta\tau_v$ Alg. II	$\delta\tau_v$ Alg. III	Number of Residual Pairs
[0, 1)	0.45385	0.81245	0.71356	80
[1, 2)	0.64558	0.76800	0.78479	84
[2, 3)	0.58731	0.52816	0.71265	84
[3, 4)	0.54785	0.44513	0.69444	80
[4, 5)	0.64775	0.57516	0.70243	84
[5, 6)	0.55332	0.50535	0.60146	84
[6, 7)	0.59405	0.52725	0.64643	83
[7, 8)	0.53080	0.56131	0.60731	81
[8, 9)	0.20929	0.28091	0.32809	81
[9,10)	0.20074	0.13759	0.36739	81
[10,11)	0.17136	0.15264	0.39334	78
[11,12)	0.27575	0.29773	0.49409	79
[12,13)	0.26709	0.33416	0.46464	81
[13,14)	0.29338	0.42861	0.52103	81
[14,15)	-0.07934	0.09112	0.30257	84
[15,16)	0.32901	0.37118	0.55199	84
[16,17)	0.21681	0.55015	0.51529	81
[17,18)	0.42402	0.74145	0.57468	84
[18,19)	0.85141	0.93891	0.84563	76
[19,20)	0.75195	0.93536	0.81326	79
[20,21)	0.67397	0.90107	0.73993	81
[21,22)	0.74781	0.94712	0.73545	80
[22,23)	0.81513	0.77069	0.79759	78
[23,24)	0.80572	0.57085	0.77432	77

Nominal Value in Degrees for Month

	Stanford ATS1	Fort Collins ATS1
Elevation	37.7	25.0
Azimuth	221.1	236.8
Eff. Latitude	34.6	37.0
Eff. Longitude	234.8	248.5

TABLE D. 15

Correlation Coefficients of Vertical Time Delay Residuals

Evaluation Condition 5

January 1969

Correlation Pair: Rosman ATS3 - Urbana ATS3

UT Hour Interval	$\delta\tau_v$ Alg. I	$\delta\tau_v$ Alg. II	$\delta\tau_v$ Alg. III	Number of Residual Pairs
[0, 1)	0.88849	0.91204	0.90733	87
[1, 2)	0.86178	0.88787	0.91360	86
[2, 3)	0.85770	0.87098	0.91716	86
[3, 4)	0.84107	0.83793	0.87710	84
[4, 5)	0.85292	0.85990	0.86443	81
[5, 6)	0.77327	0.77747	0.74593	80
[6, 7)	0.77093	0.71246	0.68585	85
[7, 8)	0.70367	0.66961	0.62349	87
[8, 9)	0.69997	0.69397	0.65564	82
[9,10)	0.56653	0.57361	0.52388	85
[10,11)	0.56254	0.65197	0.55012	87
[11,12)	0.65617	0.72789	0.65395	86
[12,13)	0.53651	0.27765	0.51046	90
[13,14)	0.72156	0.71297	0.64535	89
[14,15)	0.80759	0.56045	0.65505	78
[15,16)	0.83777	0.84865	0.73024	75
[16,17)	0.88290	0.94459	0.85247	82
[17,18)	0.86229	0.95842	0.84184	80
[18,19)	0.93415	0.98307	0.93455	84
[19,20)	0.93154	0.97977	0.92705	85
[20,21)	0.93729	0.96051	0.91385	87
[21,22)	0.93222	0.93457	0.90219	86
[22,23)	0.94582	0.96859	0.93032	86
[23,24)	0.93982	0.95427	0.91144	87

Nominal Value in Degrees for Month

	Rosman ATS3	Urbana ATS3
Elevation	46.7	39.6
Azimuth	156.9	151.8
Eff. Latitude	32.6	37.0
Eff. Longitude	278.4	273.8

TABLE D.16

Correlation Coefficients of Vertical Time Delay Residuals

Evaluation Condition 5

January 1969

Correlation Pair: Arecibo ATS3 - Cold Bay ATS1

UT Hour Interval	$\delta\tau_v$ Alg. I	$\delta\tau_v$ Alg. II	$\delta\tau_v$ Alg. III	Number of Residual Pairs
[0, 1)	0.45110	0.31124	0.30969	75
[1, 2)	0.27405	0.01066	0.30857	[illegible]
[2, 3)	0.49717	0.22758	0.58733	[illegible]
[3, 4)	0.33164	0.22624	0.26046	72
[4, 5)	0.01135	0.01445	-0.01244	70
[5, 6)	0.01189	0.20774	0.05704	68
[6, 7)	-0.33431	-0.02233	-0.18494	72
[7, 8)	-0.50112	-0.21175	-0.39288	81
[8, 9)	-0.45907	-0.34402	-0.43142	71
[9,10)	-0.31575	-0.37285	-0.27297	73
[10,11)	-0.33737	-0.44060	-0.23413	71
[11,12)	-0.28321	-0.35775	-0.13825	78
[12,13)	-0.14427	-0.00141	-0.22528	76
[13,14)	-0.03034	0.30286	-0.12922	79
[14,15)	0.05383	0.33173	-0.01469	82
[15,16)	0.14994	0.31241	0.04231	79
[16,17)	0.18345	0.28349	0.02242	79
[17,18)	0.32086	0.33001	0.19044	73
[18,19)	0.23633	-0.29457	0.13712	71
[19,20)	0.25142	-0.24574	0.17454	74
[20,21)	0.00496	0.18133	0.12705	74
[21,22)	-0.10123	0.21490	0.14447	70
[22,23)	-0.19508	0.12457	0.17117	77
[23,24)	0.12106	0.35150	0.38700	78

Nominal Value in Degrees for Month

	Arecibo ATS3	Cold Bay ATS1
Elevation	68.1	26.0
Azimuth	187.7	164.7
Eff. Latitude	17.3	49.8
Eff. Longitude	293.1	199.5

TABLE D.18

Correlation Coefficients of Vertical Time Delay Residuals

Evaluation Condition 5

April 1969

Correlation Pair: Stanford ATS1 - Fort Collins ATS1

UT Hour Interval	$\delta\tau_v$ Alg. I	$\delta\tau_v$ Alg. II	$\delta\tau_v$ Alg. III	Number of Residual Pairs
(0, 1)	0.89298	0.90993	0.88389	24
(1, 2)	0.86817	0.94460	0.87474	23
(2, 3)	0.80884	0.83570	0.93235	24
(3, 4)	0.90499	0.75884	0.88612	25
(4, 5)	0.91346	0.84660	0.92745	27
(5, 6)	0.81762	0.83549	0.85046	27
(6, 7)	0.67195	0.82032	0.69120	27
(7, 8)	0.70652	0.87799	0.72269	27
(8, 9)	0.66674	0.89649	0.69985	26
(9,10)	0.51246	0.88524	0.55634	26
(10,11)	0.58589	0.92239	0.63157	26
(11,12)	0.70345	0.93451	0.75566	27
(12,13)	0.51374	0.94198	0.57786	26
(13,14)	0.05592	-0.26118	0.15395	25
(14,15)	-0.03259	0.53086	-0.07925	27
(15,16)	0.74870	0.63486	0.54571	24
(16,17)	0.81179	0.61260	0.70128	24
(17,18)	0.85643	0.60730	0.82553	23
(18,19)	0.87087	0.77391	0.84089	24
(19,20)	0.90217	0.72881	0.87996	24
(20,21)	0.90299	0.76915	0.85544	24
(21,22)	0.94345	0.85114	0.94396	24
(22,23)	0.95588	0.85864	0.95159	22
(23,24)	0.95635	0.89494	0.95232	21

Nominal Value in Degrees for Month

	Stanford ATS1	Fort Collins ATS1
Elevation	37.9	25.2
Azimuth	220.8	236.6
Eff. Latitude	34.6	37.0
Eff. Longitude	234.9	248.6

TABLE D.19

Correlation Coefficients of Vertical Time Delay Residuals

Evaluation Condition 5

April 1969

Correlation Pair: Rosman ATS3 - Urbana ATS3

UT Hour Interval	$\delta\tau_v$ Alg. I	$\delta\tau_v$ Alg. II	$\delta\tau_v$ Alg. III	Number of Residual Pairs
[0, 1)	0.92578	0.95864	0.92389	39
[1, 2)	0.90207	0.94884	0.90169	39
[2, 3)	0.87555	0.94141	0.87593	38
[3, 4)	0.85331	0.91307	0.85335	36
[4, 5)	0.83596	0.90163	0.83515	38
[5, 6)	0.72912	0.87103	0.72569	39
[6, 7)	0.64894	0.85945	0.66163	37
[7, 8)	0.60540	0.86059	0.61830	37
[8, 9)	0.66268	0.88070	0.63270	38
[9,10)	0.66634	0.72591	0.65048	36
[10,11)	0.65231	0.77423	0.65263	34
[11,12)	0.76804	0.82481	0.75391	38
[12,13)	0.65650	0.76415	0.61154	36
[13,14)	0.70117	0.72275	0.65931	36
[14,15)	0.84803	0.84553	0.81070	36
[15,16)	0.87075	0.85854	0.84549	36
[16,17)	0.90559	0.91845	0.89427	36
[17,18)	0.89946	0.87922	0.87943	34
[18,19)	0.93089	0.93320	0.92927	35
[19,20)	0.93473	0.94429	0.93255	33
[20,21)	0.94504	0.95605	0.94418	34
[21,22)	0.93299	0.95179	0.93270	32
[22,23)	0.92778	0.96928	0.92723	36
[23,24)	0.91650	0.97916	0.91618	36

Nominal Value in Degrees for Month

	Rosman ATS3	Urbana ATS3
Elevation	47.8	40.9
Azimuth	162.3	156.4
Eff. Latitude	32.6	37.0
Eff. Longitude	278.1	273.4

TABLE D.20

Correlation Coefficients of Vertical Time Delay Residuals

Evaluation Condition 5

April 1969

Correlation Pair: Stanford ATS1 - Stanford ATS3

UT Hour Interval	$\delta\tau_v$ Alg. I	$\delta\tau_v$ Alg. II	$\delta\tau_v$ Alg. III	Number of Residual Pairs
(0, 1)	0.93977	0.85380	0.94229	85
(1, 2)	0.94376	0.91631	0.94545	86
(2, 3)	0.94006	0.95538	0.93974	85
(3, 4)	0.92604	0.90499	0.92692	79
(4, 5)	0.90655	0.90382	0.93102	84
(5, 6)	0.87271	0.89920	0.83635	87
(6, 7)	0.86461	0.89228	0.83346	84
(7, 8)	0.86002	0.93435	0.84618	83
(8, 9)	0.83395	0.93883	0.83184	77
(9,10)	0.83743	0.88724	0.79567	76
(10,11)	0.81012	0.88855	0.73958	76
(11,12)	0.78530	0.88637	0.69818	71
(12,13)	0.79214	0.91823	0.75877	74
(13,14)	0.79280	0.33786	0.93055	71
(14,15)	0.92229	0.96216	0.84723	65
(15,16)	0.90048	0.92848	0.84360	64
(16,17)	0.83382	0.84677	0.83408	72
(17,18)	0.82523	0.77408	0.87326	72
(18,19)	0.83890	0.77754	0.87648	73
(19,20)	0.84300	0.73964	0.87008	75
(20,21)	0.85837	0.72900	0.87816	74
(21,22)	0.87061	0.70635	0.89340	74
(22,23)	0.89216	0.71029	0.90905	71
(23,24)	0.90549	0.78109	0.92344	74

Nominal Value in Degrees for Month

	Stanford ATS1	Stanford ATS3
Elevation	37.9	22.9
Azimuth	220.8	117.3
Eff. Latitude	34.6	34.3
Eff. Longitude	234.9	244.5

TABLE D.21

Correlation Coefficients of Vertical Time Delay Residuals

Evaluation Condition 5

July 1969

Correlation Pair: Stanford ATS1 - Clark Lake ATS1

UT Hour Interval	$\delta\tau_v$ Alg. I	$\delta\tau_v$ Alg. II	$\delta\tau_v$ Alg. III	Number of Residual Pairs
[0, 1)	0.91517	0.90896	0.85109	42
[1, 2)	0.88735	0.90087	0.87940	39
[2, 3)	0.90767	0.93134	0.85087	40
[3, 4)	0.86235	0.88358	0.75910	41
[4, 5)	0.62018	0.81251	0.54842	41
[5, 6)	0.46142	0.72631	0.37431	39
[6, 7)	0.38519	0.79539	0.55053	30
[7, 8)	0.53334	0.73088	0.57095	30
[8, 9)	0.92500	0.89654	0.92563	21
[9,10)	0.91454	0.82443	0.89903	21
[10,11)	0.95127	0.90007	0.94674	22
[11,12)	0.95584	0.93666	0.95299	24
[12,13)	0.67821	0.77900	0.54551	25
[13,14)	0.85085	0.37531	0.90911	30
[14,15)	0.81672	0.78747	0.52312	32
[15,16)	0.90773	0.87937	0.83934	35
[16,17)	0.91189	0.88475	0.85143	40
[17,18)	0.93285	0.91832	0.91551	44
[18,19)	0.94716	0.92529	0.91857	41
[19,20)	0.93958	0.90317	0.97050	39
[20,21)	0.96158	0.94593	0.95094	42
[21,22)	0.96350	0.94562	0.91930	42
[22,23)	0.96722	0.95789	0.97961	41
[23,24)	0.94535	0.94041	0.90994	42

Nominal Value in Degrees for Month

	Stanford ATS1	Clark Lake ATS1
Elevation	38.1	37.6
Azimuth	220.4	229.8
Eff. Latitude	34.6	30.9
Eff. Longitude	234.9	240.2

TABLE D.22

Correlation Coefficients of Vertical Time Delay Residuals

Evaluation Condition 5

July 1969

Correlation Pair: Stanford ATS1 - Fort Collins ATS1

UT Hour Interval	$\delta\tau_v$ Alg. I	$\delta\tau_v$ Alg. II	$\delta\tau_v$ Alg. III	Number of Residual Pairs
[0, 1)	0.53855	0.60405	0.48738	66
[1, 2)	0.21069	0.37832	0.15722	45
[2, 3)	0.50904	0.54935	0.24477	40
[3, 4)	0.53682	0.52630	0.27330	54
[4, 5)	0.40843	0.45586	0.14874	68
[5, 6)	0.10844	0.32095	-0.15675	74
[6, 7)	-0.01535	0.35473	-0.19428	75
[7, 8)	0.09887	0.41491	-0.04885	81
[8, 9)	0.11446	0.45010	-0.07569	83
[9,10)	0.07267	0.45835	-0.02285	84
[10,11)	0.08203	0.51787	0.03603	82
[11,12)	0.06797	0.52005	-0.05014	78
[12,13)	0.05473	0.36485	-0.12477	77
[13,14)	0.10830	0.23369	-0.19971	76
[14,15)	0.46583	0.43898	0.19153	76
[15,16)	0.54207	0.41452	0.43584	76
[16,17)	0.64704	0.54986	0.63915	79
[17,18)	0.71092	0.64967	0.72853	80
[18,19)	0.77294	0.69369	0.72775	77
[19,20)	0.78478	0.73081	0.73044	76
[20,21)	0.77919	0.75860	0.77148	75
[21,22)	0.77737	0.77293	0.81352	77
[22,23)	0.78466	0.81374	0.81255	81
[23,24)	0.74600	0.81565	0.74628	80

Nominal Value in Degrees for Month

	Stanford ATS1	Fort Collins ATS1
Elevation	38.1	25.4
Azimuth	220.4	236.3
Eff. Latitude	34.6	37.0
Eff. Longitude	234.9	248.7

TABLE D.23

Correlation Coefficients of Vertical Time Delay Residuals

Evaluation Condition 5

July 1969

Correlation Pair: Rosman ATS3 - Urbana ATS3

UT Hour Interval	$\delta\tau_v$ Alg. I	$\delta\tau_v$ Alg. II	$\delta\tau_v$ Alg. III	Number of Residual Pairs
[0, 1)	0.76674	0.81496	0.71065	80
[1, 2)	0.77995	0.83158	0.73075	80
[2, 3)	0.83121	0.84192	0.75426	80
[3, 4)	0.73323	0.71431	0.60687	79
[4, 5)	0.70158	0.60920	0.54673	83
[5, 6)	0.65786	0.53779	0.55766	83
[6, 7)	0.66887	0.66072	0.61560	80
[7, 8)	0.60994	0.49554	0.45117	87
[8, 9)	0.55450	0.54458	0.37719	82
[9,10)	0.48936	0.54702	0.37671	82
[10,11)	0.53841	0.63172	0.37959	88
[11,12)	0.69170	0.72514	0.53576	87
[12,13)	0.73627	0.75396	0.67472	87
[13,14)	0.83672	0.82539	0.81144	83
[14,15)	0.82867	0.83304	0.80974	81
[15,16)	0.84175	0.82656	0.81588	82
[16,17)	0.84428	0.87845	0.82139	88
[17,18)	0.85820	0.91092	0.83849	86
[18,19)	0.85393	0.89224	0.83865	87
[19,20)	0.85460	0.89606	0.83791	83
[20,21)	0.84119	0.88781	0.81863	82
[21,22)	0.83837	0.88402	0.82599	79
[22,23)	0.84610	0.87317	0.79294	67
[23,24)	0.83046	0.88593	0.79070	79

Nominal Value in Degrees for Month

	Rosman ATS3	Urbana ATS3
Elevation	33.6	26.7
Azimuth	127.3	125.3
Eff. Latitude	32.5	36.8
Eff. Longitude	281.1	277.3

TABLE D.24

Correlation Coefficients of Vertical Time Delay Residuals

Evaluation Condition 5

October 1969

Correlation Pair: Stanford ATS1-Clark Lake ATS1

UT Hour Interval	$\delta\tau_v$ Alg. I	$\delta\tau_v$ Alg. II	$\delta\tau_v$ Alg. III	Number of Residual Pairs
[0, 1)	0.99007	0.97365	0.97068	42
[1, 2)	0.98236	0.98869	0.95237	42
[2, 3)	0.95949	0.98400	0.95953	42
[3, 4)	0.92699	0.96073	0.93556	39
[4, 5)	0.95085	0.97495	0.95935	37
[5, 6)	0.88822	0.97094	0.95189	36
[6, 7)	0.84978	0.94750	0.93691	39
[7, 8)	0.80638	0.94695	0.92767	36
[8, 9)	0.78266	0.94551	0.94760	26
[9,10)	0.73569	0.94211	0.94566	24
[10,11)	0.72884	0.90213	0.90594	21
[11,12)	0.80016	0.93064	0.90721	23
[12,13)	0.85673	0.92619	0.91702	29
[13,14)	0.80117	0.91836	0.92044	37
[14,15)	0.85890	0.76299	0.96291	42
[15,16)	0.68005	0.92351	0.94126	42
[16,17)	0.82293	0.85311	0.93654	38
[17,18)	0.94326	0.90738	0.95518	38
[18,19)	0.95259	0.97299	0.95044	39
[19,20)	0.96410	0.97487	0.93857	42
[20,21)	0.92583	0.93506	0.91062	42
[21,22)	0.96552	0.96524	0.92872	42
[22,23)	0.98134	0.95002	0.94566	37
[23,24)	0.98417	0.91113	0.95832	39

Nominal Value in Degrees for Month

	Stanford ATS1	Clark Lake ATS1
Elevation	38.3	37.9
Azimuth	219.9	229.4
Eff. Latitude	34.6	30.9
Eff. Longitude	235.0	240.3

TABLE D.25

Correlation Coefficients of Vertical Time Delay Residuals

Evaluation Condition 5

October 1969

Correlation Pair: Stanford ATS1 - Fort Collins ATS1

UT Hour Interval	$\delta\tau_v$ Alg. I	$\delta\tau_v$ Alg. II	$\delta\tau_v$ Alg. III	Number of Residual Pairs
[0, 1)	0.94390	0.86504	0.85526	74
[1, 2)	0.93363	0.89578	0.87357	72
[2, 3)	0.82730	0.85757	0.85411	72
[3, 4)	0.82968	0.85308	0.86865	72
[4, 5)	0.84588	0.89923	0.90254	72
[5, 6)	0.75661	0.83981	0.84753	69
[6, 7)	0.58350	0.66989	0.69142	69
[7, 8)	0.55273	0.75278	0.70424	75
[8, 9)	0.51570	0.76716	0.73215	75
[9,10)	0.35815	0.72709	0.74366	75
[10,11)	0.24700	0.71047	0.68837	71
[11,12)	0.35459	0.72343	0.67308	69
[12,13)	0.37106	0.73437	0.71860	69
[13,14)	0.12932	0.44684	0.57290	72
[14,15)	0.28574	0.30563	0.67378	76
[15,16)	0.73495	0.66471	0.63240	80
[16,17)	0.88759	0.64031	0.77130	77
[17,18)	0.92485	0.80416	0.83892	77
[18,19)	0.92948	0.84866	0.79444	78
[19,20)	0.93336	0.86555	0.73135	78
[20,21)	0.93073	0.89735	0.78431	78
[21,22)	0.94559	0.89165	0.81260	74
[22,23)	0.95458	0.82487	0.84935	77
[23,24)	0.96186	0.80289	0.89647	71

Nominal Value in Degrees for Month

	Stanford ATS1	Fort Collins ATS1
Elevation	38.3	25.6
Azimuth	219.9	235.9
Eff. Latitude	34.6	37.0
Eff. Longitude	235.0	248.8

TABLE D.26

Correlation Coefficients of Vertical Time Delay Residuals

Evaluation Condition 5

October 1969

Correlation Pair: Rosman ATS3 - Urbana ATS3

UT Hour Interval	$\delta\tau_v$ Alg. I	$\delta\tau_v$ Alg. II	$\delta\tau_v$ Alg. III	Number of Residual Pairs
[0, 1)	0.93251	0.94330	0.90439	32
[1, 2)	0.95587	0.95528	0.93703	27
[2, 3)	0.97053	0.96401	0.95525	27
[3, 4)	0.97412	0.96473	0.96451	32
[4, 5)	0.98680	0.98949	0.97616	29
[5, 6)	0.97239	0.97936	0.97798	29
[6, 7)	0.95915	0.97678	0.96470	29
[7, 8)	0.96246	0.98829	0.98067	30
[8, 9)	0.91202	0.97934	0.97235	29
[9,10)	0.87383	0.96368	0.96191	30
[10,11)	0.90226	0.97053	0.96071	30
[11,12)	0.85170	0.89442	0.94241	32
[12,13)	0.90566	0.96366	0.91269	35
[13,14)	0.86341	0.91505	0.93500	33
[14,15)	0.91689	0.91772	0.96755	33
[15,16)	0.86003	0.90511	0.92937	32
[16,17)	0.91574	0.94521	0.92767	36
[17,18)	0.91679	0.94502	0.91719	36
[18,19)	0.92138	0.94161	0.89293	36
[19,20)	0.95179	0.97099	0.93273	32
[20,21)	0.94722	0.97807	0.93169	36
[21,22)	0.88881	0.96455	0.92616	33
[22,23)	0.82323	0.95479	0.78296	35
[23,24)	0.83477	0.90505	0.79529	35

Nominal Value in Degrees for Month

	Rosman ATS3	Urbana ATS3
Elevation	33.0	26.4
Azimuth	126.6	124.9
Eff. Latitude	32.4	36.8
Eff. Longitude	281.2	277.4

APPENDIX E

TABLES OF CORRELATION COEFFICIENTS OF VERTICAL TIME DELAY – OVER ENTIRE EVALUATION INTERVAL

TABLE E.1

Correlation Coefficients of Vertical Time Delay Residuals
Over Entire
Evaluation Condition 1

	$\delta\tau_v$ Alg. I	$\delta\tau_v$ Alg. II	$\delta\tau_v$ Alg. III	Number of Residual Pairs
Correlation Pair: Stanford ATS3 - Stanford ATS1				
	0.87915	0.89689	0.88511	5334
Correlation Pair: Stanford ATS3 - Urbana ATS3				
	0.73917	0.68118	0.57075	4657
Correlation Pair: Urbana ATS3 - Sagamore Hill ATS3				
	0.83953	0.79823	0.80686	4540

TABLE E.2

Correlation Coefficients of Vertical Time Delay Residuals
Over Entire
Evaluation Condition 2

	$\delta\tau_v$ Alg. I	$\delta\tau_v$ Alg. II	$\delta\tau_v$ Alg. III	Number of Residual Pairs
Correlation Pair:	Stanford ATS3 - Stanford ATS1			
	0.88159	0.85537	0.87979	5527

TABLE E.3

Correlation Coefficients of Vertical Time Delay Residuals
Over Entire
Evaluation Condition 5

	$\delta\tau_v$ Alg. I	$\delta\tau_v$ Alg. II	$\delta\tau_v$ Alg. III	Number of Residual Pairs
Correlation Pair: Stanford ATS1 - Stanford ATS3				
	0.90284	0.82314	0.90038	1832
Correlation Pair: Stanford ATS1 - Clark Lake ATS1				
	0.93295	0.90137	0.89543	3763
Correlation Pair: Stanford ATS1 - Fort Collins ATS1				
	0.80925	0.71691	0.74504	6074
Correlation Pair: Rosman ATS3 - Urbana ATS3				
	0.86105	0.81425	0.87130	5637
Correlation Pair: Arecibo ATS3 - Cold Bay ATS1				
	0.03723	0.00581	-0.08283	1800

APPENDIX F

TABLES OF CUMULATIVE PROBABILITY DISTRIBUTION OF DAILY CORRELATION COEFFICIENTS

TABLE F.1

Cumulative Frequency Distribution of the Daily Correlation Coefficients of the Vertical Time Delay Residuals over Evaluation Condition 1

Correlation Pair: Stanford ATS3 - Stanford ATS1

Total Number of Correlation Coefficients: 85

Correlation Coefficient Interval	Cumulative Frequency Distribution (Percent)		
	$\delta\tau_v$ Alg. I	$\delta\tau_v$ Alg. II	$\delta\tau_v$ Alg. III
[-1,-.9)	0	0	0
[-1,-.8)	0	0	0
[-1,-.7)	0	0	0
[-1,-.6)	0	0	0
[-1,-.5)	0	0	0
[-1,-.4)	0	0	0
[-1,-.3)	0	0	0
[-1,-.2)	0	0	0
[-1,-.1)	0	0	0
[-1,0)	0	0	0
[-1,.1)	0	1.18	0
[-1,.2)	0	1.18	0
[-1,.3)	0	2.35	0
[-1,.4)	0	3.53	0
[-1,.5)	3.53	3.53	1.18
[-1,.6)	5.88	3.53	1.18
[-1,.7)	9.41	11.76	4.71
[-1,.8)	17.65	20.00	9.41
[-1,.9)	43.53	44.71	50.59
[-1,1]	[illegible]	[illegible]	100.00

TABLE F.2

"Cumulative Frequency Distribution of the Daily Correlation Coefficients of the Vertical Time Delay Residuals over Evaluation Condition 1

Correlation Pair: Stanford ATS3 - Urbana ATS3

Total Number of Correlation Coefficients: 76

Correlation Coefficient Interval	Cumulative Frequency Distribution (Percent) $\delta\tau_v$ Alg. I	$\delta\tau_v$ Alg. II	$\delta\tau_v$ Alg. III
[-1,-.9)	0	0	0
[-1,-.8)	0	1.32	0
[-1,-.7)	0	1.32	0
[-1,-.6)	0	1.32	0
[-1,-.5)	0	2.63	1.32
[-1,-.4)	0	3.95	1.32
[-1,-.3)	0	3.95	2.63
[-1,-.2)	0	5.26	2.63
[-1,-.1)	1.[illegible]	7.89	3.95
[-1,0)	3.95	7.89	5.26
[-1,.1)	3.95	11.84	10.53
[-1,.2)	6.58	13.16	17.11
[-1,.3)	9.21	17.11	23.68
[-1,.4)	9.21	31.58	31.58
[-1,.5)	14.47	39.47	38.16
[-1,.6)	23.68	46.05	55.26
[-1,.7)	32.89	61.84	65.79
[-1,.8)	53.95	78.95	81.58
[-1,.9)	89.47	92.11	94.74
[-1, 1]	100.00	100.00	100.00

TABLE F.3

Cumulative Frequency Distribution of the Daily Correlation Coefficients of the Vertical Time Delay Residuals over Evaluation Condition 1

Correlation Pair: Urbana ATS3 - Sagamore Hill ATS3

Total Number of Correlation Coefficients: 68

Correlation Coefficient Interval	Cumulative Frequency Distribution (Percent) $\delta\tau_v$ Alg. I	$\delta\tau_v$ Alg. II	$\delta\tau_v$ Alg. III
[-1,-.9)	0	0	0
[-1,-.8)	0	0	0
[-1,-.7)	0	0	0
[-1,-.6)	0	0	0
[-1,-.5)	0	0	0
[-1,-.4)	0	0	0
[-1,-.3)	0	0	0
[-1,-.2)	0	0	0
[-1,-.1)	0	1.47	0
[-1,0)	0	1.47	0
[-1,.1)	0	1.47	0
[-1,.2)	0	1.47	0
[-1,.3)	1.47	5.88	1.47
[-1,.4)	1.47	8.82	2.94
[-1,.5)	1.47	13.24	5.88
[-1,.6)	4.41	19.12	8.82
[-1,.7)	10.29	29.41	20.59
[-1,.8)	16.18	45.59	38.24
[-1,.9)	54.41	77.94	73.53
[-1, 1]	100.00	100.00	100.00

TABLE F.4

Cumulative Frequency Distribution of the Daily Correlation Coefficients of the Vertical Time Delay Residuals over Evaluation Condition 2

Correlation Pair: Stanford ATS3 - Stanford ATS1

Total Number of Correlation Coefficients: 88

Correlation Coefficient Interval	Cumulative Frequency Distribution (Percent) $\delta\tau_V$ Alg. I	$\delta\tau_V$ Alg. II	$\delta\tau_V$ Alg. III
[-1,-.9)	0	0	0
[-1,-.8)	0	0	0
[-1,-.7)	0	0	0
[-1,-.6)	0	0	0
[-1,-.5)	0	0	0
[-1,-.4)	0	0	0
[-1,-.3)	0	0	0
[-1,-.2)	0	0	0
[-1,-.1)	0	0	0
[-1,0)	0	1.14	0
[-1,.1)	0	1.14	0
[-1,.2)	0	1.14	0
[-1,.3)	0	2.27	0
[-1,.4)	0	3.41	0
[-1,.5)	3.41	3.41	1.14
[-1,.6)	5.68	5.68	1.14
[-1,.7)	9.09	11.36	4.55
[-1,.8)	17.45	20.45	11.36
[-1,.9)	42.05	54.55	46.59
[-1, 1]	100.00	100.00	100.00

TABLE F.5

Cumulative Frequency Distribution of the Daily Correlation Coefficients of the Vertical Time Delay Residuals over Evaluation Condition 5

Correlation Pair: Stanford ATS1 - Clark Lake ATS1

Total Number of Correlation Coefficients: 69

Correlation Coefficient Interval	Cumulative Frequency Distribution (Percent)		
	$\delta\tau_v$ Alg. I	$\delta\tau_v$ Alg. II	$\delta\tau_v$ Alg. III
[-1,-.9)	0	0	0
[-1,-.8)	0	0	0
[-1,-.7)	0	0	0
[-1,-.6)	0	0	0
[-1,-.5)	0	0	0
[-1,-.4)	0	0	0
[-1,-.3)	0	0	0
[-1,-.2)	0	0	0
[-1,-.1)	0	0	0
[-1,0)	0	0	0
[-1,.1)	1.45	0	1.45
[-1,.2)	1.45	0	1.45
[-1,.3)	1.45	0	1.45
[-1,.4)	2.90	1.45	1.45
[-1,.5)	4.35	2.90	2.90
[-1,.6)	5.80	5.80	5.80
[-1,.7)	10.14	8.70	7.25
[-1,.8)	15.94	15.94	21.74
[-1,.9)	[illegible]	34.7[illegible]	40.[illegible]
[-1, 1]	100.00	100.00	100.00

TABLE F.6

Cumulative Frequency Distribution of the Daily Correlation Coefficients of the Vertical Time Delay Residuals over Evaluation Condition 5

Correlation Pair: Stanford ATS1 - Fort Collins ATS1

Total Number of Correlation Coefficients: 95

Correlation Coefficient Interval	Cumulative Frequency Distribution (Percent) $\delta\tau_v$ Alg. I	$\delta\tau_v$ Alg. II	$\delta\tau_v$ Alg. III
[-1,-.9)	0	0	0
[-1,-.8)	0	0	0
[-1,-.7)	0	0	0
[-1,-.6)	0	0	0
[-1,-.5)	0	0	0
[-1,-.4)	0	0	0
[-1,-.3)	1.05	1.05	0
[-1,-.2)	2.11	1.05	0
[-1,-.1)	3.16	2.11	0
[-1,0)	7.37	5.26	2.11
[-1,.1)	10.53	7.37	4.21
[-1,.2)	13.68	9.47	5.26
[-1,.3)	17.89	12.63	5.26
[-1,.4)	26.32	15.79	8.42
[-1,.5)	32.63	20.00	14.74
[-1,.6)	36.84	30.53	25.26
[-1,.7)	46.32	45.26	42.11
[-1,.8)	55.79	58.95	67.37
[-1,.9)	81.05	87.37	88.42
[-1, 1]	100.00	100.00	100.00

TABLE F.7

Cumulative Frequency Distribution of the Daily Correlation Coefficients of the Vertical Time Delay Residuals over Evaluation Condition 5

Correlation Pair: Stanford ATS1 - Stanford ATS3

Total Number of Correlation Coefficients: 29

Correlation Coefficient Interval	Cumulative Frequency Distribution (Percent) $\delta\tau_v$ Alg. I	$\delta\tau_v$ Alg. II	$\delta\tau_v$ Alg. III
[-1,-.9)	0	0	0
[-1,-.8)	0	0	0
[-1,-.7)	0	0	0
[-1,-.6)	0	0	0
[-1,-.5)	0	0	0
[-1,-.4)	0	0	0
[-1,-.3)	0	0	0
[-1,-.2)	3.45	0	0
[-1,-.1)	3.45	0	3.45
[-1,0)	3.45	3.45	6.90
[-1,.1)	3.45	3.45	6.90
[-1,.2)	6.90	3.45	6.90
[-1,.3)	6.90	3.45	6.90
[-1,.4)	6.90	3.45	6.90
[-1,.5)	6.90	3.45	6.90
[-1,.6)	6.90	10.34	10.34
[-1,.7)	10.34	17.24	10.34
[-1,.8)	20.69	31.03	17.24
[-1,.9)	31.03	68.97	48.28
[-1, 1]	100.00	100.00	100.00

TABLE F.8

Cumulative Frequency Distribution of the Daily Correlation Coefficients of the Vertical Time Delay Residuals over Evaluation Condition 5

Correlation Pair: Rosman ATS3 - Urbana ATS3

Total Number of Correlation Coefficients: 85

Correlation Coefficient Interval	Cumulative Frequency Distribution (Percent)		
	$\delta\tau_v$ Alg. I	$\delta\tau_v$ Alg. II	$\delta\tau_v$ Alg. III
[-1,-.9)	0	0	0
[-1,-.8)	0	0	0
[-1,-.7)	0	0	0
[-1,-.6)	0	0	0
[-1,-.5)	0	0	0
[-1,-.4)	0	0	0
[-1,-.3)	0	0	0
[-1,-.2)	0	0	0
[-1,-.1)	0	0	0
[-1,0)	0	0	0
[-1,.1)	0	0	0
[-1,.2)	0	0	0
[-1,.3)	0	0	0
[-1,.4)	1.18	0	1.18
[-1,.5)	2.53	0	1.18
[-1,.6)	5.88	3.53	1.18
[-1,.7)	11.76	8.24	4.71
[-1,.8)	23.53	18.82	10.59
[-1,.9)	43.53	40.00	36.47
[-1, 1]	100.00	100.00	100.00

TABLE F.9

Cumulative Frequency Distribution of the Daily Correlation Coefficients of the Vertical Time Delay Residuals over Evaluation Condition 5

Correlation Pair: Arecibo ATS3 - Cold Bay ATS1

Total Number of Correlation Coefficients: 30

Correlation Coefficient Interval	Cumulative Frequency Distribution (Percent)		
	$\delta\tau_v$ Alg. I	$\delta\tau_v$ Alg. II	$\delta\tau_v$ Alg. III
[-1,-.9)	0	0	0
[-1,-.8)	0	0	0
[-1,-.7)	0	0	0
[-1,-.6)	6.67	3.33	6.67
[-1,-.5)	16.67	10.00	16.67
[-1,-.4)	20.00	13.33	23.33
[-1,-.3)	23.33	30.00	36.67
[-1,-.2)	26.67	36.67	50.00
[-1,-.1)	36.67	46.67	60.00
[-1,0)	40.00	66.67	70.00
[-1,.1)	50.00	73.33	76.67
[-1,.2)	56.67	83.33	83.33
[-1,.3)	66.67	93.33	90.00
[-1,.4)	73.33	96.67	93.33
[-1,.5)	80.00	100.00	96.67
[-1,.6)	93.33	100.00	100.00
[-1,.7)	96.67	100.00	100.00
[-1,.8)	100.00	100.00	100.00
[-1,.9)	100.00	100.00	100.00
[-1, 1]	100.00	100.00	100.00

APPENDIX G

BASIC IONOSPHERIC FORMULAE

Under free space (vacuum) conditions the satellite ranging signal would propagate at the speed of light, c , so that the time of propagation of the signal would be a direct measure of the satellite-to-navigator geometric range as

$$\tau(t) = \frac{\rho(t)}{c} \qquad (G.1)$$

where

$\rho(t)$ = satellite-navigator geometric range at time t

$\tau(t)$ = time of propagation of the ranging signal between satellite and navigator at time t

However, in the presence of the ionosphere, the interaction of the ranging signal with the medium results in variations of the signal velocity along the propagation path. In this case

$$\tau(t) = \int_{P(t)} \frac{ds}{v(\vec{r},t)} \qquad (G.2)$$

where

$P(t)$ = phase (optical) path between satellite and navigator at time t

$\vec{r}$ = position vector to a point on $P(t)$ from a geocentric coordinate system

$v(\vec{r},t)$ = magnitude of the velocity of the ranging signal at $\vec{r}$ and t

ds = differential element of arc along $P(t)$

In order to determine expressions for the ionospheric effects on the ranging signals, it is necessary to specify $v(\vec{r},t)$ in the ionosphere. There are three velocities of propagation associated with the propagation of electromagnetic energy: phase, group, and signal. The velocity of interest in any particular system is a function of the natures of both the measurement and the medium. In the present study, the velocity of interest is, strictly speaking,

the signal velocity [Brillouin, 1960]. However, at 1600 MHz, the absorption and dispersion of the signal should be small so that the group velocity would be a good approximation to the signal velocity. In the present study we will ignore absorptive effects and assume that the ranging signal propagates at the group velocity. The error involved in this assumption is small but is an open question that is in need of further study.

The group velocity of the ranging signal with carrier frequency f is derived from the phase refractive index, μ, of the ionosphere as

$$v(\vec{r},t) = \frac{c}{\mu(\vec{r},t)} + f \frac{\partial \mu(\vec{r},t)}{\partial f} \tag{G.3}$$

where $\mu(\vec{r},t)$ is given by the Appleton-Hartree equation [Kelso, 1964]. Ignoring absorptive effects

$$\mu_{o,e}(\vec{r},t) = \left[1 - \frac{f_N (r,t)}{f^2} \frac{1}{\alpha_{+,-}}\right]^{1/2} \tag{G.4}$$

where in rationalized mks units

$\mu_{o,e}(\vec{r},t)$ ≡ index of refraction at r and time t for either the ordinary or extraordinary wave for the two senses of circular polarization

f ≡ carrier frequency, Hz

$f_N(\vec{r},t)$ ≡ $\left[\dfrac{e^2}{4\pi^2 m\epsilon_o} N(\vec{r},t)\right]^{1/2}$

$N(\vec{r},t)$ ≡ electron density at $\vec{r}$ and t

e ≡ electron charge

m ≡ electron mass

ϵ_o ≡ permittivity of free space

$$\alpha_{+,-} \equiv 1 - \frac{(f_T/f)^2}{2(1-(f_N/f)^2)} \pm \left[\frac{(f_T/f)^4}{4(1-(f_N/f)^2)^2} + (f_L/f)^2\right]^{1/2}$$

$f_L \equiv f_H(\vec{r},t) \cos\theta$

$f_T \equiv f_H(\vec{r},t) \sin\theta$

$f_H(\vec{r},t) \equiv \frac{|e|\mu_o}{2\pi\ m} H(\vec{r},t)$, electron gyro-frequency

$H(\vec{r},t)$ ≡ magnetic field strength at $\vec{r}$ and t

$\theta(\vec{r},t)$ ≡ angle between propagation vector and magnetic field vector at $\vec{r}$ and t

μ_o ≡ permeability of free space

At ionospheric heights, the electron gyro-frequency, f_H , is of the order of 1.4 MHz, thus for carrier frequencies at L-band the effect of the magnetic field on the signal would be small. Neglecting the magnetic field effects, $\mu(\vec{r},t)$ simplifies to

$$\mu(\vec{r},t) = \left[1 - \frac{K}{f^2} N(\vec{r},t)\right]^{1/2} \qquad (G.5)$$

where

K = 80.6 in rationalized mks units.

Then from Eqs. (G.3) and (G.5) the group velocity of the ranging signal is given approximately as

$$v(\vec{r},t) \approx c \left[1 - \frac{K}{f^2} N(r,t)\right]^{1/2} \qquad (G.6)$$

In the ionosphere, the maximum values of $N(\vec{r},t)$ are of the order of 10^{12} electrons/m^3. Thus for frequencies of the order of 1600 MHz

$$f^2 \gg K\ N(\vec{r},t)$$

and from Ross [1965] it can be shown that when this is true that

$$P(t) \approx G(t)$$

Thus Eq. (G.2) is given to first order by

$$\tau(t) = \int_{G(t)} \left[1 + \frac{K}{2f^2c} N(r,t)\right] ds \qquad (G.7a)$$

or

$$\tau(r) = \frac{\rho(t)}{c} + \frac{1.34 \times 10^{-7}}{f^2} \int_{G(t)} N(\vec{r},t)\, ds \qquad (G.7b)$$

Eq. (G.7b) gives the time of propagation of the ranging signal between satellite and navigator, assuming group velocity.